

DYNAMICS AND THE GAUGE/GRAVITY
DUALITY

This work has been accomplished at the Institute for Theoretical Physics (ITFA) of the University of Amsterdam (UvA) and is financially supported by a Spinoza grant of the Netherlands Organization for Scientific Research (NWO).

© Balt van Rees, 2010

All rights reserved. Without limiting the rights under copyright reserved above, no part of this book may be reproduced, stored in or introduced into a retrieval system, or transmitted, in any form or by any means (electronic, mechanical, photocopying, recording or otherwise) without the written permission of both the copyright owner and the author of the book.

DYNAMICS AND THE GAUGE/GRAVITY DUALITY

ACADEMISCH PROEFSCHRIFT

ter verkrijging van de graad van doctor

aan de Universiteit van Amsterdam

op gezag van de Rector Magnificus

prof. dr. D.C. van den Boom

ten overstaan van een door het college voor promoties

ingestelde commissie,

in het openbaar te verdedigen in de Agnietenkapel

op dinsdag 7 september 2010, te 12.00 uur

door

BALTUS CORNELIS VAN REES

geboren te Leiden

PROMOTIECOMMISSIE

PROMOTOR

prof. dr. E.P.Verlinde

CO-PROMOTOR

dr. K. Skenderis

OVERIGE LEDEN

prof. dr. E.A. Bergshoeff

prof. dr. J. de Boer

prof. J. McGreevy

prof. dr. J. Smit

dr. M. Taylor

FACULTEIT DER NATUURWETENSCHAPPEN, WISKUNDE EN INFORMATICA

Publications

This thesis is based on the following publications:

- [1] K. Skenderis and B. C. van Rees
Real-time gauge/gravity duality
Phys. Rev. Lett. **101** (2008) 081601, arXiv:0805.0150 [hep-th].
- [2] K. Skenderis and B. C. van Rees
Real-time gauge/gravity duality: Prescription, Renormalization and Examples
JHEP **05** (2009) 085, arXiv:0812.2909 [hep-th].
- [3] B. C. van Rees
Real-time gauge/gravity duality and ingoing boundary conditions
Nucl. Phys. Proc. Suppl. **192-193** (2009) 193–196,
arXiv:0902.4010 [hep-th].
- [4] K. Skenderis and B. C. van Rees
Holography and wormholes in 2+1 dimensions
accepted for publication in *Com. Math. Phys.*, arXiv:0912.2090 [hep-th].
- [5] K. Skenderis, M. Taylor, and B. C. van Rees
Topologically Massive Gravity and the AdS/CFT Correspondence
JHEP **09** (2009) 045, arXiv:0906.4926 [hep-th].
- [6] K. Skenderis, M. Taylor, and B. C. van Rees
AdS boundary conditions and the Topologically Massive Gravity/CFT Correspondence
AIP Conference Proceedings **1196** (2009) 266–275, arXiv:0909.5617 [hep-th].



Contents

1	The gauge/gravity dualities	1
1.1	The AdS ₅ /CFT ₄ correspondence	2
1.2	General prescription	11
1.3	Field theory symmetries and Ward identities	14
1.4	Asymptotic behavior	20
1.5	Scalar field in AdS _{d+1}	26
1.6	Einstein gravity	33
2	Real-time gauge/gravity duality	43
2.1	QFT preliminaries	45
2.2	Prescription	49
2.3	Scalar field	54
2.4	Gravity	61
2.5	Conclusion	76
2.A	Real-time quantum field theory	77
3	Real-time correlation functions	83
3.1	Examples involving global AdS ₃	83
3.2	Poincaré coordinates	96
3.3	Higher-point correlation functions	104
3.4	Stationary black holes	106
3.5	Rotating black holes	120
3.6	Conclusion	125
4	Ingoing boundary conditions	127
4.1	Introduction	127
4.2	The real-time thermal dictionary	128
4.3	Ingoing boundary conditions	130
4.4	Higher-point correlation functions	132
4.5	Conclusion and discussion	134

5	Wormholes in 2+1 dimensions	137
5.1	Introduction and summary of results	137
5.2	Lorentzian wormholes	140
5.3	Euclidean wormholes	145
5.4	Holographic interpretation of Euclidean wormholes	148
5.5	Holographic interpretation of Lorentzian wormholes	154
5.6	Remarks	166
5.7	Outlook	168
5.A	Eternal black holes and filled tori	170
6	Coordinate systems for wormholes	173
6.1	Introduction and summary of results	173
6.2	Fenchel-Nielsen coordinates	175
6.3	The hyperbolic plane	178
6.4	Construction of a pair of pants	183
6.5	Domains for the charts	187
6.6	Coordinate systems and fatgraph description	196
7	Topologically massive gravity	209
7.1	Introduction	209
7.2	Setup and equations of motion	212
7.3	Aspects of the AdS/CFT dictionary	214
7.4	Asymptotic analysis for $\mu = 1$	216
7.5	Anomalies	225
7.6	Linearized analysis	229
7.7	Linearized analysis for general μ	238
7.8	Conclusions	244
7.A	Derivation of the equations of motion	245
7.B	Wick rotation	249
7.C	Linearized equations of motion in global coordinates	253
7.D	Some results from LCFT	254
7.E	Warped AdS	256
	Bibliography	259
	Summary	269
	Samenvatting	275
	Acknowledgements	281

Chapter 1

The gauge/gravity dualities

The various gravity/gauge theory dualities are among the most far-reaching recent developments in theoretical high-energy physics. These dualities claim that certain quantum theories of gravity in $(d + 1)$ -dimensional backgrounds are equivalent, or *dual*, to certain quantum field theories in d dimensions. (In many cases this quantum field theory is a gauge theory which led to the name ‘gauge/gravity duality’.) The dualities offer a completely new perspective on gravitational physics and in particular realize the idea of *holography* put forward in [7, 8]. Since typically the quantum field theory is strongly coupled when the dual gravity theory becomes weakly coupled and classical, these dualities also open up a window onto the strong-coupling dynamics of gauge theories. In recent times they have been applied to a variety of physical systems that range from high-energy phenomenology to condensed matter physics.

In this chapter we give a brief introduction to these dualities. A reasonable overview of all past and current developments would require a textbook on its own, so we shall have to omit a great number of topics and details. Our aim is to present enough material to convey a general picture and focus on those details that we need in the subsequent chapters of this thesis.

The outline of this chapter is as follows. We begin with a concrete example of a gauge/gravity duality where the gravity theory is type IIB string theory on $\text{AdS}_5 \times S^5$ and the dual gauge theory is the $\mathcal{N} = 4$ supersymmetric Yang-Mills theory. This example is intended to clarify the general ideas presented in later sections. In section 1.2 we discuss the basic structure common to all the gauge/gravity dualities. We then consider the Ward identities of the gauge theory in some detail in section 1.3 and discuss the necessary steps towards their realization in the

gravity theory in section 1.4. In section 1.5 we present an example computation of a field theory correlation function using the gravity theory. In the final section 1.6 we consider the realization in the gravity theory of the scale and diffeomorphism Ward identities.

1.1 The AdS₅/CFT₄ correspondence

In this section we discuss a concrete example of a gauge/gravity duality [9]. As we mentioned above, this section is intended to support the general ideas that we will subsequently present. We will necessarily be rather brief and refer the reader to the extensive literature, in particular the reviews [10, 11], for more details on this realization of the duality.

Our example concerns a duality between the $\mathcal{N} = 4$ supersymmetric Yang-Mills theory and type IIB string theory on AdS₅ × S⁵. The former turns out to be a *conformal field theory* (CFT) and our example is therefore called an *AdS/CFT correspondence*. It is in fact but one example of a more general class of AdS/CFT correspondences which all involve gravity theories in AdS_{d+1} spacetimes and d -dimensional CFT's.

1.1.1 Open versus closed strings

Consider a system of N coincident D3-branes in $\mathbb{R}^{1,9}$ in type IIB string theory. Let us take the branes to be extended along the x^i directions, with $i \in \{0, 1, 2, 3\}$ and with x^0 playing the role of time. On the six transverse dimensions we will pick spherical coordinates so they are spanned by an S⁵ plus a radial direction denoted y . The tension of the branes is given by

$$T = \frac{N}{g_s (2\pi)^3 \alpha'^2}, \quad (1.1)$$

where g_s is the string coupling constant. The IIB background geometry created by the branes is uniquely fixed by the translational and rotational symmetries, the energy density and five-form charge of the branes. It takes the following form:

$$ds^2 = f(y)^{-1/2} \eta_{ij} dx^i dx^j + f(y)^{1/2} (dy^2 + y^2 d\Omega_5^2) \quad f(y) = 1 + \frac{4\pi g_s N \alpha'^2}{y^4}, \quad (1.2)$$

with a constant dilaton $g_s = e^\Phi$ and axion C_0 and with a five-form flux:

$$F_5 = (1 + *_5) dx^0 \dots dx^3 df^{-1}. \quad (1.3)$$

In the metric (1.2) the branes are at $y = 0$ but they are completely redshifted away and have disappeared from view.

Let us now consider the low-energy limit of this system. A convenient way to obtain this limit is by sending $\alpha' \rightarrow 0$ while keeping the energies E of physical processes fixed. This way the dimensionless energies

$$\epsilon = \sqrt{\alpha'} E \tag{1.4}$$

indeed go to zero. In the metric (1.2) this limit implies that $f(y) \rightarrow 1$ for all nonzero y . Away from the branes we therefore recover the ten-dimensional flat space metric on which we have to consider low-energy excitations, which are described by IIB supergravity.

On the other hand we shall see that the behavior of the branes themselves can be described in two different ways, namely either in terms of open strings or in terms of closed strings. The fact that these are two descriptions of the same physical system will then lead to the AdS/CFT correspondence.

Open string description

The first way to describe the branes is in terms of open strings. At low energies the effective theory for the branes becomes a field theory, namely the $\mathcal{N} = 4$ super Yang-Mills (or SYM) theory with gauge group $U(N)$. This is a four-dimensional gauge theory with four chiral fermions and six real scalars, all transforming in the adjoint representation of the gauge group. The $\mathcal{N} = 4$ supersymmetry implies an $SU(4) \simeq \text{Spin}(6)$ group of global R-symmetries, for which the fermions transform in the fundamental and the scalars in the fundamental of $SO(6)$. The Lagrangian schematically has the form:

$$\begin{aligned} \mathcal{L} = & \frac{1}{g^2} \text{Tr} \left(\frac{1}{4} F_{\mu\nu} F^{\mu\nu} - \frac{1}{2} \mathcal{D}_\mu \Phi \mathcal{D}^\mu \Phi - i \bar{\psi} \bar{\sigma}^\mu \mathcal{D}_\mu \psi \right. \\ & \left. + \psi [\Phi, \psi] + \bar{\psi} [\Phi, \bar{\psi}] - \frac{1}{4} ([\Phi, \Phi])^2 \right) + \frac{\theta}{2\pi} \text{Tr} (F \wedge F), \end{aligned} \tag{1.5}$$

where \mathcal{D}_μ is the gauge covariant derivative and we suppressed spinor, gauge and $SU(4)$ indices. The only coupling constant g in the theory is given in terms of the string coupling constant g_s via $g^2 = g_s$. Furthermore, its θ angle is given in terms of the axion background value, $\theta = 2\pi C_0$. It turns out that the beta function for g vanishes to all orders in perturbation theory and it is generally believed that it vanishes non-perturbatively as well [12]. This implies that g is a physical parameter that is not transmuted into a scale. The resulting scale invariance of the theory can in fact be extended to the full conformal group and this makes the $\mathcal{N} = 4$ SYM theory a *conformal field theory* or CFT.

Since all fields transform in the adjoint representation of the $U(N) = SU(N) \times U(1)$ gauge group the overall $U(1)$ becomes free. In the brane picture this $U(1)$ multiplet essentially describes the motion of the center of mass of the brane. We may safely consider the brane system at rest and ignore it in what follows. One is then left with an $SU(N)$ theory.

Finally, there are in principle nonzero interactions between the ambient IIB supergravity modes and the $\mathcal{N} = 4$ theory, but these vanish as $\alpha' \rightarrow 0$ since the ten-dimensional Newton's constant $G_N \sim \alpha'^4$.

Closed string description

The second way to describe the brane system is in terms of closed strings. If we choose to use this description we have to take into account the gravitational redshift of the excitations in the geometry (1.2). The energy E of an excitation at a certain fixed y is redshifted at infinity to the value:

$$E_\infty = E f(y)^{-1/4}. \quad (1.6)$$

To take a low-energy limit in the closed-string description we again send the dimensionless energies $E_\infty \sqrt{\alpha'}$ to zero, which we may again implement by sending $\alpha' \rightarrow 0$. However from (1.6) we see that this does not necessarily imply that we have to send $E \sqrt{\alpha'}$ to zero since we may also send $f(y) \rightarrow \infty$. This in turn can be done by sending $y \rightarrow 0$ at the same time as $\alpha' \rightarrow 0$ while keeping the new coordinate

$$z = \frac{\alpha'}{y} \quad (1.7)$$

fixed. In this limit we find:

$$f(y) \rightarrow \frac{4\pi g_s N z^4}{\alpha'^2}. \quad (1.8)$$

After taking the limit, in terms of the coordinate z , we find the following metric:

$$ds^2 = \alpha' \left(\frac{1}{\sqrt{4\pi g_s N} z^2} \eta_{ij} dx^i dx^j + \sqrt{4\pi g_s N} \frac{dz^2}{z^2} + \sqrt{4\pi g_s N} d\Omega_5^2 \right). \quad (1.9)$$

This is precisely the $\text{AdS}_5 \times S^5$ product geometry where both factors have a radius of curvature

$$R^4 = 4\pi g_s N \alpha'^2. \quad (1.10)$$

(Notice that the Ricci scalar $\text{Ric} \sim 1/R^2$.) This curvature is supported by the five-form flux, which in the above limit takes the form:

$$F_5 \rightarrow -(1 + *_{10}) \frac{\alpha'^2}{\pi g_s N z^5} dx^0 \dots dx^3 dz. \quad (1.11)$$

The factor α' in front of the metric (1.9) makes the entire metric small. However this factor cancels in the worldsheet sigma model, for example for the bosonic part of the worldsheet action of a string in the above background we find:

$$\begin{aligned} S &= \frac{1}{2\pi\alpha'} \int d^2\sigma \sqrt{-h} (h^{\alpha\beta} G_{\mu\nu} \partial_\alpha X^\mu \partial_\beta X^\nu + \dots) \\ &= \frac{1}{2\pi} \int d^2\sigma \sqrt{-h} (h^{\alpha\beta} \tilde{G}_{\mu\nu} \partial_\alpha X^\mu \partial_\beta X^\nu + \dots), \end{aligned} \tag{1.12}$$

where $\tilde{G}_{\mu\nu} = G_{\mu\nu}/\alpha'$. We therefore obtain a finite theory in the low-energy limit. Indeed, we described above that all the excitations in the AdS₅ × S⁵ region have a low energy from the viewpoint of asymptotic observers. We may therefore forget about the smallness of α' altogether and consider excitations with arbitrary finite dimensionless energy $E\sqrt{\alpha'}$ on this background. In this description the ‘sum over histories’ becomes a sum over arbitrary backgrounds which are *asymptotically* of the AdS₅ × S⁵ form. This concept will be made more precise below.

Just as in the open string picture, the low-energy limit is again a *decoupling limit* in which the interactions with the low-energy excitations of the ambient flat geometry vanish. In the closed string description this follows from the fact that the redshift diverges as $y \rightarrow 0$ so only modes that have infinite energy in the AdS region can escape to infinity. Furthermore the closed strings in the bulk cannot probe the AdS region since it becomes of zero size, which for example can be concretely seen from the fact that the absorption cross section of the branes vanishes in the low-energy limit [9].

The AdS/CFT correspondence

We have given two different description of the low-energy dynamics of the brane system in its rest frame. In one description we recovered the $\mathcal{N} = 4$ SU(N) SYM theory (with coupling constants $g = g_s$ and $\theta = 2\pi C_0$) and in the other we found type IIB closed string theory on the AdS₅ × S⁵ background (with radius of curvature $R^4 = 4\pi g_s N \alpha'^2$ and dilaton $g_s = e^\Phi$ and axion C_0). One is therefore led to conjecture that these two theories are equivalent. This is precisely the content of the AdS/CFT correspondence we set out to derive.

The supergravity limit

In this work we will be exclusively working in the classical limit of the closed string theory, which for the case at hand implies that it reduces to classical IIB supergravity on AdS₅ × S⁵. This can only be a reliable approximation when the curvature radius of the geometry (1.10) is large in units of α' , which is when

$$g_s N \gg 1. \tag{1.13}$$

For example, the low-energy effective action for the gravitons schematically takes the form:

$$S = \frac{1}{2\kappa^2} \int d^{10}x (R + \alpha'^3 R^4 + \dots) \quad (1.14)$$

and substituting the background values of the curvature we find that the correction term $\alpha'^3 R^4$ is of order $(g_s N)^{-3/2}$. Furthermore, we should also suppress string loops so we require $g_s \ll 1$ (and therefore $N \gg 1$). Indeed, the ten-dimensional Newton's constant is given by

$$2\kappa^2 = (2\pi)^7 g_s^2 \alpha'^4, \quad (1.15)$$

and for small g_s we find that κ^2 is small in units of α' as well. In what follows we will often set $R^4 = 1$, which means that $\alpha'^2 = (4\pi g_s N)^{-1}$. In that case

$$\kappa^2 = \frac{4\pi^5}{N^2}. \quad (1.16)$$

Notice that the S^5 has now unit radius, so when we reduce over the sphere (as we will do in the next section) we see that the effective five-dimensional Newton's constant is again of order N^{-2} .

In the dual field theory the large N limit is actually the well-known 't Hooft limit [13] in which the so-called *planar* Feynman diagrams are dominant. In this limit the effective loop counting parameter for an $SU(N)$ gauge theory is $\lambda = g_s N$. Since according to (1.13) it is actually very big in the supergravity limit, we cannot at the same time use any perturbative approaches to the quantum field theory. This makes an explicit verification of the correspondence very hard, but on the other hand it does offer a unique opportunity to obtain results in a strongly coupled field theory from relatively straightforward computations in supergravity.

1.1.2 Bulk fields and boundary operators

The correspondence in particular implies that we can compute in two different ways the response of the brane system to probes like external closed strings. In the gauge theory these correspond to the insertion of certain local gauge-invariant operators, whereas they correspond to nontrivial boundary conditions for the fields in the $\text{AdS}_5 \times S^5$ geometry. One therefore expects a relation between the *fields* in the closed string theory and certain gauge-invariant *operators* in the gauge theory. Here we will present some details of this map in the aforementioned supergravity limit.

Symmetries and boundary operators

In this subsection we discuss the relevant class of gauge-invariant operators in the $\mathcal{N} = 4$ SYM theory. We begin with a discussion of the global symmetries in the theory, since it is natural to organize the operators in representations of these symmetries.

The symmetry algebra of $\mathcal{N} = 4$ SYM is built up as follows. The fact that the theory is conformal means that the usual Lorentz algebra $so(3, 1)$ is extended to the full conformal algebra $so(4, 2)$. There are four independent supersymmetries which rotate into each other under an $su(4) \simeq so(6)$ algebra of R-symmetries. We shall denote the corresponding charges as $Q_{\alpha a}$ with $\alpha \in \{1, 2\}$ a chiral spinor index and $a \in \{1, \dots, 4\}$ a fundamental $SU(4)$ index. The combination of the $so(4, 2) \simeq psu(2, 2)$ conformal symmetry and the $\mathcal{N} = 4$ supersymmetry generates a so-called *superconformal algebra* of symmetries. In this case we find that the full superconformal algebra is $psu(2, 2|4)$. Notice that we can act with the special conformal transformations on the $Q_{\alpha a}$ to get additional fermionic symmetries. Their charges are again chiral spinors and we shall denote them by $S_{\alpha a}$.

The field theory operators we consider are *composite*, which means that they are built up out of the fundamental fields:

$$\mathcal{D}_\mu, \Phi, \psi, F_{\mu\nu}. \quad (1.17)$$

Notice that we use the gauge covariant derivative \mathcal{D}_μ as an independent field rather than the gauge field A_μ itself since the former transforms homogeneously under gauge transformations. We obtain gauge-invariant combinations by taking a product of these fields, all evaluated at the same spacetime point, and taking a trace:

$$\mathcal{O}_I = \text{Tr} \left(\dots \mathcal{D}_\mu \dots \Phi \dots \psi \dots F_{\rho\sigma} \dots \right). \quad (1.18)$$

A composite operator is constructed from either a single such trace or a product of multiple traces. Such an operator still carries an arbitrary number of Lorentz and $SU(4)$ indices, which we summarized with a single index I .

The operators dual to the supergravity fields form a subclass of this set, namely the so-called single-trace *superconformal primary* operators and their descendants. The superconformal primary operators are the lowest dimension operators in a multiplet which implies that they must be annihilated by all the $S_{\alpha a}$. The single-trace ones take the form

$$\text{Tr} \left(\Phi^{\{I_1} \Phi^{I_2} \Phi^{I_3} \dots \Phi^{I_n\}} \right), \quad (1.19)$$

where the I_i are $SO(6)$ indices and $\{I_1 \dots I_n\}$ denotes the symmetrized traceless part. The fact that these operators take the above form follows essentially from

the fact that they cannot be the supersymmetry variation of other operators. The descendants in these representations are found by acting with the supercharges $Q_{\alpha a}$.

The superconformal primary operators are Lorentz scalars so all operators with nonzero spin in these representations have to be descendants obtained by acting with the supercharges $Q_{\alpha a}$ and $\bar{Q}_{\dot{\alpha} a}$. However the operators (1.19) are in fact 1/2 BPS and therefore annihilated by half of these supercharges. So out of the 16 independent real supercharges we can act with at most 8 on the above operators, or at most 4 with the same helicity. Therefore the helicities in this multiplet range between 0 and 2.

The final quantum number that labels their $psu(2, 2|4)$ representation is their *dilatation weight* or scaling dimension which is denoted as Δ . the scaling dimension of composite operators may in principle renormalize because of short-distance singularities. However the dilatation weight for the above operators is tied to their $su(4)$ representation labels and therefore does not renormalize. It is then simply the sum of the dimensions of the elementary fields out of which the operator is composed.

Symmetries and bulk fields

In this section we shall briefly discuss the relation between the above operators and supergravity fields on AdS_5 .

The bosonic field content of type IIB supergravity consists of the metric G , the dilaton Φ , the axion C_0 , two real antisymmetric two-forms C_2 and B_2 and a real antisymmetric four-form C_4 . In terms of the field strengths:

$$\begin{aligned} H_3 &= dB_2 \\ F_1 &= dC_0 \\ \tilde{F}_3 &= dC_2 - C_0 \wedge dB_2 \\ \tilde{F}_5 &= dC_4 - \frac{1}{2}C_2 \wedge dB_2 + \frac{1}{2}B_2 \wedge dC_2, \end{aligned} \tag{1.20}$$

the string frame action takes the form:

$$\begin{aligned} S &= \frac{1}{2\kappa^2} \int d^{10}x \sqrt{-G} e^{-2\Phi} \left(R + 4|d\phi|^2 - \frac{1}{2}|H_3|^2 \right) \\ &\quad - \frac{1}{4\kappa^2} \int d^{10}x \left(\sqrt{-G} (|F_1|^2 + |\tilde{F}_3|^2 + \frac{1}{2}|\tilde{F}_5|^2) + C_4 \wedge H_3 \wedge dC_2 \right). \end{aligned} \tag{1.21}$$

The five-form field strength is self-dual, $F_5 = *_{10}F_5$, which is an additional constraint that should be imposed separately from the field equation obtained from (1.21).

Let us now consider the $AdS_5 \times S^5$ solution whose metric was given in (1.9) and which solves the equations of motion derived from (1.21). (We use conventions where $\Phi = 0$ for the above solutions.) Its isometries form the group $SO(4, 2) \times SO(6)$ and we also find 32 independent Killing spinors. Their combined algebra is precisely the $psu(2, 2|4)$ we already discussed for the dual gauge theory. (To be precise the symmetries of the $AdS_5 \times S^5$ geometry are dual to the symmetries respected by the superconformal *vacuum* of the field theory.)

In the supergravity limit we may obtain a map between the fields introduced above (plus their fermionic superpartners) and the aforementioned class of 1/2 BPS superconformal multiplets in the dual field theory. To find this relation we have to put the fields in the appropriate representations, in particular we have to make manifest their $so(6) \simeq su(4)$ representation properties. This we can do by decomposing the fields into spherical harmonics on the S^5 part of the geometry. For example, for the dilaton Φ we may write a general field configuration as:

$$\Phi(x, y) = \sum_I \phi_I(x) Y^I(y). \quad (1.22)$$

Here x denotes the collective coordinates on the AdS_5 part of the geometry, y the coordinates on the S^5 part and the Y^I are a complete set of spherical harmonics on the S^5 , $\square_{S^5} Y^I = -k(I) Y^I$. From the decomposition (1.22) we obtain an infinite number of effective fields $\phi_I(x)$ in the AdS_5 geometry, one for each independent solution of the Laplacian on the S^5 . The fields $\phi_I(x)$ are by construction organized in $SO(6)$ representations. Let us now impose the lowest-order equations of motion, which would be the massless Klein-Gordon equation for Φ . We find:

$$0 = \square_{10} \Phi = (\square_{AdS_5} + \square_{S^5}) \Phi = \sum_I [\square_{AdS_5} \phi_I(x) - k(I) \phi_I(x)] Y^I(y). \quad (1.23)$$

We see that each of the ϕ_I satisfies an independent Klein-Gordon equation with increasing masses given by the eigenvalues $k(I)$ of the S^5 Laplacian.

The details of the S^5 reduction of the IIB supergravity fields were presented in [14]. We will not repeat them here, but suffice it to say that we find precisely one AdS_5 field for every one of the local single-trace 1/2 BPS gauge-invariant operators we mentioned above. In particular the fields again transform in short representations of $psu(2, 2|4)$ with helicities at most equal to two. As we shall see in more detail below, the scaling dimension Δ of these operators is determined directly in terms of the $k(I)$, so in terms of their effective mass on the AdS_5 part of the geometry. It precisely matches the spectrum on the gauge theory side.

Notice that in principle there is an infinite number of fields originating from the Kaluza-Klein decomposition of a single field. However we cannot trust the supergravity approximation if the fields fluctuate on the S^5 on distances smaller than

the Planck scale. This puts an upper bound on the number of fields we can reliably consider within supergravity. In the dual gauge theory there is a similar upper bound on the number of single-trace superconformal primaries since the fields are $su(N)$ matrices and if their length $n > N$ then one may show that the operators are no longer linearly independent. Within the regime of supergravity, then, the results are mutually consistent.

It is rather remarkable that the supergravity only ‘sees’ a fraction of the full set of gauge-invariant operators. It means in particular that, if the AdS/CFT correspondence is correct, the other operators should correspond to excitations with masses of order the string scale and therefore they should gain large anomalous dimensions at strong coupling. This is certainly possible: unlike the 1/2 BPS operators their dimensions are in general unprotected against quantum corrections.

1.1.3 Summary and generalizations

By describing the low-energy excitations of a system of D-branes in two different ways we have discovered a duality between a theory of gravity and a gauge theory. We have discussed the relation between the parameters of the two theories, found a matching of their global symmetry groups and discussed how the supergravity limit was dual to the planar, strong-coupling limit in the field theory. We also argued that a class of 1/2 BPS gauge-invariant operators is in one-to-one correspondence with supergravity fields. Notice that we have not yet presented a method for actually computing the field theory *observables*, *i.e.* the correlation functions of these operators, from the gravity side. Doing so will be the subject of the next section.

As we mentioned in the introduction to this chapter, this correspondence belongs to a much larger class of AdS/CFT correspondences. One may for example study the near-horizon limit of a variety of brane systems to obtain AdS_{d+1}/CFT_d dualities for other dimensions d as well. For each of these there is a compact manifold, equivalent to the S^5 for $d = 4$, which makes the total closed string background ten- or eleven-dimensional. One may also obtain generalizations by putting the branes in different background geometries which then result in different compact manifolds when one takes the decoupling limit. These correspond to different dual field theories with generally a different internal symmetry group. Another generalization concerns *deformations* of the theory by switching on nonzero sources, which would result in theories with nontrivial scale dependence. One may also consider nonzero *vacuum expectation values* of certain operators which can partially break the gauge symmetry. Finally, there are also *non-conformal* examples where the dual field theory is no longer conformal even in the UV. Although these dualities

are sometimes still called ‘AdS/CFT correspondences’, it is more appropriate to refer to these more general instances as ‘gauge-gravity dualities’.

It turns out that all these dualities have a very similar structure. In particular this is the case for the basic ‘dictionary’ that ‘translates’ observable quantities between the gauge theory and the gravity side and which we will present in the next section.

1.2 General prescription

In this section we shall be concerned with the main ingredient of the gauge/gravity duality, namely the general prescription to compute *observables* in the two theories. Since this prescription is to a large extent universal, *i.e.* independent of the specific theory under consideration, we shall from now on consider a *general* gauge/gravity duality between a d -dimensional field theory and a quantum theory of gravity for which $d + 1$ dimensions are noncompact.

More precisely our assumptions will be the following. First of all we will be working in a low-energy limit in which we suppose that we may reliably use classical gravity and which is dual to a strong-coupling (and planar) limit of some sorts in the dual field theory. Second, we suppose that a Kaluza-Klein reduction has been performed so we no longer have to explicitly consider the compact part of the closed string background geometry. We then work with an effective supergravity theory in $d + 1$ dimensions which we will assume to be a consistent truncation of the full supergravity theory. Third, we will suppose that there is an operator in the dual field theory corresponding to every bulk field we consider in this $(d + 1)$ -dimensional effective theory. Last, we will restrict ourselves to the cases where the closed string theory is defined on manifolds which are roughly speaking of the ‘asymptotically AdS’ form discussed above. As we shall see below this implies that the dual field theory is a CFT (and the dimensions of the operators we consider are protected) at least at asymptotically high energies.

1.2.1 Quantum field theory partition function

The field theory observables we will consider are the correlation functions of the local gauge-invariant operators \mathcal{O}_I . In the present context I is a general index labelling the different operators and it may include Lorentz indices as well. The correlation functions take the form:

$$\langle \mathcal{O}_{I_1}(x_1) \mathcal{O}_{I_2}(x_2) \dots \mathcal{O}_{I_n}(x_n) \rangle_{X,g}. \quad (1.24)$$

The subscripts X, g mean that the theory lives on a manifold X with a general metric g_{ij} which we take to be positive definite for now; in the next chapter we discuss the Lorentzian theories. Notice that the symbol $\langle \dots \rangle$ defines a certain state in the theory and the correlation functions depend implicitly on that state. For example, this state may include nonzero vacuum expectation values or operator insertions at infinity.

A convenient way to collect these correlation functions is to introduce sources $\phi_{(0)}^I(x)$ for every \mathcal{O}_I and write down the partition function:

$$Z_{\text{CFT}}[\phi_{(0)}, g_{ij}] = \langle \exp \left(- \int_{\mathcal{M}} d^d x \sqrt{g} \phi_{(0)}^I(x) \mathcal{O}_I(x) \right) \rangle_{X, g}. \quad (1.25)$$

Notice that when the sources are irrelevant the partition function makes sense only as a formal power series in these sources.

Upon functional differentiation of Z with respect to the sources and setting the sources to zero we obtain again the field theory correlation functions. To find the connected correlation functions we introduce:

$$W = \ln(Z), \quad (1.26)$$

from which we may obtain:

$$\langle \mathcal{O}_I(x) \mathcal{O}_J(y) \dots \rangle_{X, g} = \frac{-1}{\sqrt{g(x)}} \frac{\delta}{\delta \phi_{(0)}^I(x)} \frac{-1}{\sqrt{g(y)}} \frac{\delta}{\delta \phi_{(0)}^J(y)} \dots W \Big|_{\phi_{(0)}=0}. \quad (1.27)$$

Functional derivatives with respect to the inverse metric by definition generate insertions of the *energy-momentum tensor* T_{ij} of the theory,

$$\langle T_{ij}(x) \rangle_{X, g, \phi} = \frac{-2}{\sqrt{g(x)}} \frac{\delta W}{\delta g^{ij}(x)}. \quad (1.28)$$

Notice that this time we did not set the sources in W to zero which we indicated with the subscript ϕ on the left-hand side. We shall continue to use this subscript to indicate nonzero sources, but we will omit the subscripts X, g henceforth.

1.2.2 Relation to gravity

According to the gauge/gravity duality the operators \mathcal{O}_I should be in one-to-one correspondence with string theory fields Φ^I which are defined on a $(d+1)$ -dimensional manifold (M, G) . Since the corresponding sources $\phi_{(0)}^I$ represent external deformations of the system, it is natural that they correspond to the *boundary conditions* for the fields Φ^I . In particular the boundary conditions for the bulk

metric G should be defined in terms of the field theory metric g . Of course this can only be sensible when $\partial M = X$ which we therefore shall assume to be the case.

Once the boundary conditions for the gravity fields are fixed we can in principle perform a ‘stringy path integral’ on the closed string side. This would result in a partition function which depends on these boundary conditions,

$$Z_{\text{string}}[\phi_{(0)}, g_{ij}]. \quad (1.29)$$

The main statement of the gauge/gravity duality is that this partition function is *equal* to the field theory partition function:

$$Z_{\text{CFT}}[\phi_{(0)}, g_{ij}] = Z_{\text{string}}[\phi_{(0)}, g_{ij}]. \quad (1.30)$$

Upon functional differentiation with respect to the sources, this formula allows one to in principle compute arbitrary field theory correlation functions from the gravity theory.

Unfortunately, computing Z_{string} seems a formidable task as it presumably contains some path integral over arbitrary bulk field configurations Φ^I and bulk manifolds (M, G) that satisfy the boundary conditions. However, in the supergravity limit we can restrict ourselves to a saddle-point approximation on the gravity side. The string theory partition function is then expressed in terms of the on-shell supergravity action $I[\phi_{(0)}^I, g_{ij}]$, evaluated on the solution that is determined by these boundary data. We then find:

$$\boxed{W[\phi_{(0)}^I, g_{ij}] = -I[\phi_{(0)}^I, g_{ij}]} \quad (1.31)$$

in the supergravity limit. (In the case where multiple such solutions exist the dominant contribution comes from the solution with the smallest on-shell action.) The formula (1.31) is the main formula of this thesis. It was first presented in [15, 16]. Notice that upon functional differentiation of both sides with respect to the sources we find that we can compute correlation functions in a strongly coupled field theory using classical gravity!

In the remainder of this chapter we shall work out some of the details of equation (1.31). We begin by discussing the constraints that W must satisfy as a consequence of the symmetries of the field theory. We shall then consider the precise boundary behavior of the bulk fields and the relation to the field theory sources. We will see that the on-shell action I is actually always *infinite*, essentially because of the infinite volume of the AdS_{d+1} spacetime. These infinities should be removed with an appropriate renormalization procedure, the so-called *holographic renormalization*. We shall explain the details of this procedure in two examples.

Finally, we demonstrate how the resulting renormalized on-shell action satisfies the same constraints as W and can be used to compute field theory correlation functions.

Given the fact that all the field theory data is defined at the boundary of the $(d + 1)$ -dimensional spacetime, it is often said that the field theory ‘lives’ on the boundary of the spacetime. It is then called the *boundary* theory and the gravity theory is correspondingly called the *bulk* theory.

1.3 Field theory symmetries and Ward identities

If a field theory has a classical symmetry then we can check whether this symmetry also leaves the quantum partition function W invariant, provided we transform the sources appropriately. If so then this invariance leads to constraints on the form of W in the form of functional differential equations. In this section we work out some of these constraints.

1.3.1 Global internal symmetries

Let us first consider purely internal global symmetries of the theory that are not related to spacetime invariances. For example, consider a symmetry generated by a constant parameter ξ^I under which the infinitesimal transformation of the fundamental fields is $\Psi_I \rightarrow \Psi_I + \xi^J \delta_J \Psi_I$ and the corresponding transformation of the operators \mathcal{O}_I is given by $\xi^K M_{KI}{}^J \mathcal{O}_J$. When we make ξ^I position-dependent, the action changes by:

$$\delta_\xi S = \int d^d x \sqrt{g} (\nabla_i \xi^I) j_I^i, \quad (1.32)$$

where j_I^i is by definition the corresponding Noether current and ∇_i is the covariant derivative for the various spacetime indices on ξ^I . Since this transformation of the fields is merely a change of integration variable, W should be invariant under such a transformation (provided there are no anomalies). This translates into a functional differential equation for W . Namely, when we single out the source for j_I^i and call it A_i^I then we find that the transformation is equivalent to:

$$\begin{aligned} A_i^I &\rightarrow A_i^I + \nabla_i \xi^I \\ \phi_{(0)}^I &\rightarrow \phi_{(0)}^I + \phi_{(0)}^J \xi^K M_{KI}{}^J. \end{aligned} \quad (1.33)$$

The invariance of W is then seen to lead to the following identity:

$$0 = \delta_\xi W[A_i^a, \phi_{(0)}^I, g_{ij}] = \int d^d x \left(\nabla_i \xi^I \frac{\delta W}{\delta A_i^I} + \phi_{(0)}^I \xi^K M_{KI}{}^J \frac{\delta W}{\delta \phi_{(0)}^J} \right). \quad (1.34)$$

Since this should hold for any local ξ^I we obtain a constraint for W , namely

$$\nabla_i \frac{\delta W}{\delta A_i^K} - \phi_{(0)}^I M_{KI}{}^J \frac{\delta W}{\delta \phi_{(0)}^J} = 0. \quad (1.35)$$

We may alternatively phrase it in terms of correlation functions:

$$\nabla_i \langle j_K^i \rangle_\phi - \phi_{(0)}^I M_{KI}{}^J \langle \mathcal{O}_J \rangle_\phi = 0. \quad (1.36)$$

This is the *Ward identity* corresponding to the symmetry.

1.3.2 Diffeomorphism invariance

We will now discuss diffeomorphism invariance and the conservation of the energy-momentum tensor. To this end we consider an arbitrary infinitesimal diffeomorphism along a vector field ζ^i . The fundamental fields and the composite operators in the theory change according to their Lie derivative, and so do the sources and the metric: $\delta\phi_{(0)}^I = \mathcal{L}_\zeta \phi_{(0)}^I$ and $\delta g^{ij} = -\nabla^i \zeta^j - \nabla^j \zeta^i$. The change of W is then given by:

$$\delta_\zeta W = - \int d^d x 2(\nabla^i \zeta^j) \frac{\delta W}{\delta g^{ij}} + \int d^d x (\mathcal{L}_\zeta \phi_{(0)}^I) \frac{\delta W}{\delta \phi_{(0)}^I} \quad (1.37)$$

In principle one expects physical quantities to be independent of the coordinate system in which they are described and consequently one would always expect $\delta_\zeta W = 0$. However we will see in chapter 7 that in some cases W is *not* invariant under general coordinate transformations and we find:

$$\delta_\zeta W = \int d^d x \zeta^i \mathcal{A}_i. \quad (1.38)$$

Here \mathcal{A}_i is called the *diffeomorphism anomaly* of the theory.

In this chapter we will be concerned with theories for which the diffeomorphism anomaly vanishes. For concreteness let us restrict ourselves to the case where the nonzero $\phi_{(0)}^I$ are all scalars so that

$$\mathcal{L}_\zeta \phi_{(0)}^I = \zeta^i \partial_i \phi_{(0)}^I. \quad (1.39)$$

Substitution in (1.37) and demanding that $\delta_\zeta W = 0$ then leads to the following constraint:

$$2\nabla^i \frac{\delta W}{\delta g^{ij}} - (\partial_j \phi_{(0)}^I) \frac{\delta W}{\delta \phi_{(0)}^I} = 0, \quad (1.40)$$

which is equal to a conservation equation for T_{ij} ,

$$\nabla^i \langle T_{ij} \rangle_\phi - (\partial_j \phi_{(0)}^I) \langle \mathcal{O}_I \rangle_\phi = 0. \quad (1.41)$$

It is not hard to extend the above result for sources that carry vector or spinor indices.

Example

In the specific case where ζ^i is a Killing vector field we obtain $\delta g_{ij} = 0$ and in the absence of an anomaly (1.37) becomes:

$$0 = \int d^d x \sqrt{g} \phi_{(0)}^I \zeta^i \partial_i \langle \mathcal{O}_I \rangle_\phi. \quad (1.42)$$

Taking two further functional derivatives with respect to the source and setting all sources to zero afterwards results in:

$$0 = \left(\zeta^i(x) \frac{\partial}{\partial x^i} + \zeta^j(y) \frac{\partial}{\partial y^j} \right) \langle \mathcal{O}_I(x) \mathcal{O}_J(y) \rangle, \quad (1.43)$$

reflecting the translational invariance of the two-point function along the Killing vector field ζ^i .

1.3.3 Scale invariance

The final symmetry we discuss is scale invariance. In flat space classical scale invariance [17] is phrased as the invariance of the action under a combined coordinate rescaling:

$$x^i \rightarrow x^i + \lambda x^i, \quad (1.44)$$

plus a transformation of the fundamental fields Ψ_I as given by the *dilatation operator*:

$$\delta \Psi_I = i\lambda [D, \Psi_I] = -\lambda (x^i \partial_i \Psi_I + \Delta \Psi_I). \quad (1.45)$$

The transformation of the composite operators \mathcal{O}_I takes the same form, with Δ replaced by their corresponding scaling dimension.

We can alternatively describe the coordinate transformation (1.44) in terms of its action on the metric and the fundamental fields in the theory. The resulting change is again expressed in terms of a Lie derivative, this time along the specific vector field $\zeta^i = x^i$. We then obtain:

$$\delta_\lambda g_{ij} = \lambda (\partial_i x_j + \partial_j x_i) = 2\lambda g_{ij}. \quad (1.46)$$

and for the fundamental fields the combined transformation becomes:

$$\delta_\lambda \Psi_I = i\lambda [D, \Psi_I] + \lambda \mathcal{L}_\zeta \Psi_I. \quad (1.47)$$

When one writes out the Lie derivative for a generic tensor (or spinor) one finds that the first factor in the transformation (1.45) vanishes against a corresponding factor in the Lie derivative. Furthermore, the subsequent terms in the Lie derivative are of the form $\pm \nabla_j x^i = \pm \delta_j^i$ for each vector index on Ψ_I , with the positive

sign for lower vector indices and the negative sign for upper vector indices. The terms in the Lie derivative corresponding to the spinor indices on the fields vanish identically for this particular transformation. We thus obtain:

$$\delta_\lambda \Psi_I = -\lambda(\Delta - \tilde{s})\Psi_I, \quad (1.48)$$

where \tilde{s} is the number of lower minus the number of upper vector indices on the field Ψ_I . The composite operators again \mathcal{O}_I transform again in a similar way and the source-operator coupling therefore changes according to:

$$\delta_\lambda \left(\int d^d x \sqrt{g} \phi_{(0)}^I \mathcal{O}_I \right) = \lambda(-\Delta + \tilde{s} + d) \left(\int d^d x \sqrt{g} \phi_{(0)}^I \mathcal{O}_I \right), \quad (1.49)$$

where the extra d comes from the metric determinant. The action is by assumption invariant under this transformation, so to completely offset it we only have to shift

$$\delta \phi_{(0)}^I = \lambda(\Delta - \tilde{s} - d). \quad (1.50)$$

The combined variation of W is then given by:

$$\begin{aligned} \delta_\lambda W &= - \int d^d x \, 2\lambda g^{ij} \frac{\delta W}{\delta g^{ij}} + \int d^d x \, \lambda(\Delta - \tilde{s} - d) \phi_{(0)}^I \frac{\delta W}{\delta \phi_{(0)}^I} \\ &= \int d^d x \sqrt{g} \lambda g^{ij} \langle T_{ij} \rangle_\phi - \int d^d x \sqrt{g} \lambda(\Delta - \tilde{s} - d) \phi_{(0)}^I \langle \mathcal{O}_I \rangle_\phi \end{aligned} \quad (1.51)$$

and the above reasoning shows that it vanishes if there are no anomalies.

Let us make a distinction between *global* and *local* scale invariance, at the classical level for now. From (1.51) one observes that global scale invariance (in the absence of sources) requires $T_i^i = \nabla_i \mathcal{J}^i$ for some \mathcal{J}^i . However it may also happen that $T_i^i = 0$. In that case (1.51) shows that the invariance is extended to include local rescalings where λ can be an arbitrary function of x . This is called *Weyl* invariance. It turns out that the theories we shall consider are indeed Weyl invariant up to anomalies. We shall therefore from now on assume that $\lambda(x)$ is position-dependent.

Quantum scale dependence

The scale invariance found at the classical level generally does not extend to the quantum theory. Indeed, the regularization of the short-distance singularities always involves the introduction of a nontrivial scale and only in exceptional cases does this scale dependence completely disappear after the necessary counterterms are added and the regulator is removed. Let us therefore assume that the quantum partition function W also depends on an overall renormalization scale μ . Since μ is the only dimensionful parameter in the theory, a global scale transformation of the form presented above should be equivalent to a change in μ . This means that:

$$\mu \frac{\partial}{\partial \mu} W = - \int d^d x \, 2g^{ij} \frac{\delta W}{\delta g^{ij}} + \int d^d x \, (\Delta_I - \tilde{s} - d) \phi_{(0)}^I \frac{\delta W}{\delta \phi_{(0)}^I}. \quad (1.52)$$

For a general CFT the anomalous transformation property of W can be expressed as [18]:

$$\delta_\lambda W = \int d^d x \lambda \beta^I[\phi_{(0)}] \langle \mathcal{O}_I \rangle_\phi + \int d^d x \lambda \mathcal{A}_w[g_{ij}, \phi_{(0)}], \quad (1.53)$$

where \mathcal{A}_w is a local function of g_{ij} and $\phi_{(0)}$ and is called the *conformal anomaly* or the *Weyl anomaly* of the theory. The β^I are the beta functions of the theory, which may be nonzero for a CFT because of the presence of sources.

Let us demonstrate the relation between (1.53) and the ordinary renormalization group. To this end we consider the theory in flat space and set some of the relevant or marginal sources to a constant nonzero background value which we denote g^K . Let us furthermore suppose that \mathcal{A}_w vanishes for this configuration. Consider now an n -point correlation function obtained by functional differentiation of W . Combining (1.51), (1.52) and (1.53) we find its scale dependence:

$$\begin{aligned} & \left(\mu \frac{\partial}{\partial \mu} + \beta^I[g^K] \frac{d}{dg^I} \right) \langle \mathcal{O}_{I_1}(x_1) \mathcal{O}_{I_2}(x_2) \dots \mathcal{O}_{I_n}(x_n) \rangle \\ & + \sum_{i=1}^n \Gamma_{I_i}^J \langle \mathcal{O}_{I_1}(x_1) \dots \mathcal{O}_J(x_i) \dots \mathcal{O}_{I_n}(x_n) \rangle = 0, \end{aligned} \quad (1.54)$$

with

$$\Gamma_I^J = \frac{\partial \beta^J}{\partial \phi_{(0)}^I} [g^K]. \quad (1.55)$$

Equation (1.54) is the usual Callan-Symanzik equation. The beta functions are indeed given by the β^I and Γ_I^J is the matrix of anomalous dimensions.

Example

Consider a conformal Killing vector field ζ^i . After a diffeomorphism along ζ^i the metric changes by $\delta g_{ij} = \frac{2}{d} \nabla^k \zeta_k g_{ij}$. We can combine this diffeomorphism with a Weyl rescaling with $\lambda = -\frac{1}{d} \nabla^k \zeta_k$ such that eventually $\delta g_{ij} = 0$. The variation of the sources under the combined diffeomorphism plus local rescaling is then:

$$\delta \phi_{(0)}^I = \left(\mathcal{L}_\zeta - \frac{1}{d} (\nabla^k \zeta_k) (\Delta_I - \tilde{s} - d) \right) \phi_{(0)}^I. \quad (1.56)$$

Let us again consider the case where the \mathcal{O}_I are scalars, so $\mathcal{L}_\zeta \phi_{(0)}^I = \zeta^k \partial_k \phi_{(0)}^I$. In the absence of anomalies W should be invariant under this combined variation, which implies that:

$$\int d^d x \sqrt{g} \phi_{(0)}^I \left(\frac{\Delta}{d} (\nabla^k \zeta_k) + \zeta^k \partial_k \right) \langle \mathcal{O}_I \rangle_\phi = 0, \quad (1.57)$$

where we integrated by parts. This equation leads to the usual constraints on correlation functions along conformal Killing vector fields. For example in flat

space we may choose $\zeta^i = x^i$. By twice functionally differentiating (1.57) we find that the two-point function must satisfy:

$$0 = \left(x^i \frac{\partial}{\partial x^i} + y^j \frac{\partial}{\partial y^j} + \Delta_I + \Delta_J \right) \langle \mathcal{O}_I(x) \mathcal{O}_J(y) \rangle. \quad (1.58)$$

This is the familiar scaling behavior of a correlation function of primary operators.

Conformal anomalies

It is well-known [17] that (1.58) together with translation, Lorentz and special conformal invariance fixes the flat-space two-point function to be of the form:

$$\langle \mathcal{O}_I(x) \mathcal{O}_J(y) \rangle = \frac{G_{IJ} \delta_{\Delta_I, \Delta_J}}{|x - y|^{2\Delta}}, \quad (1.59)$$

where G_{IJ} is a constant and $\Delta = \Delta_I = \Delta_J$. In Fourier space we find that:

$$\int d^d x e^{-ikx} \frac{1}{|x|^{2\Delta}} = \frac{\pi^{(d+1)/2} \Gamma(d - 2\Delta)}{\Gamma(\Delta) \Gamma(-\Delta + (d + 1)/2)} |k|^{2\Delta - d}. \quad (1.60)$$

However this equation cannot be valid for the special values

$$\Delta = l + \frac{d}{2} \quad l \in \{0, 1, 2, \dots\}, \quad (1.61)$$

since for these values the right-hand side of (1.60) has a pole. This implies that for these values the function $|x|^{-2\Delta}$ is an ill-defined distribution and not a valid quantum field theory correlation function. The aforementioned Ward identities cannot be exactly true and there must be some anomaly such that the physical answer is not just the one we obtained above from symmetry arguments.

The anomaly can be found by subtracting the divergence in $|x|^{-2\Delta}$. We shall use dimensional regularization in which:

$$d = 2\Delta - 2l - \epsilon. \quad (1.62)$$

By expanding (1.60) in ϵ we find

$$\int d^d x e^{-ikx} \frac{1}{|x|^{2\Delta}} = c_l |k|^{2k} \left(\frac{2}{\epsilon} + \ln(|k|^2 \mu^{-2}) + \dots \right), \quad (1.63)$$

with

$$c_l = \frac{(-1)^{l+1} 2^{-2l} \pi^d}{\Gamma(l + 1) \Gamma(l + d/2)} \quad (1.64)$$

and we absorbed several terms in the definition of the renormalization scale μ . After subtracting the leading-order divergence we are left with a well-defined *renormalized* distribution of the form:

$$\mathcal{R} \frac{1}{|x|^{2l+d}} \equiv c_l \int \frac{d^d k}{(2\pi)^d} e^{ikx} |k|^{2l} \ln(|k|^2 \mu^{-2}) \quad (1.65)$$

Since we only subtracted an (infinite) contact term, this renormalized distribution agrees with the ordinary function away from $x = 0$. We note that such renormalized distributions would also be the outcome of standard perturbative quantum field theory computations.

Let us now return to the conformal anomaly. We can integrate back the two-point function for operators with a scaling dimension of the form (1.61) to find that the corresponding term in W must be of the form:

$$W = \frac{1}{2} \int d^d x \int d^d y \phi_{(0)}^I(x) \phi_{(0)}^J(y) G_{IJ} \mathcal{R} \frac{1}{|x-y|^{2l+d}} + O[(\phi_{(0)}^I)^3]. \quad (1.66)$$

From (1.65) we find the nontrivial scale dependence:

$$\mu \frac{\partial}{\partial \mu} W = - \int d^d x G_{IJ} c_l \phi_{(0)}^I(x) (-\square)^l \phi_{(0)}^J(x) + O[(\phi_{(0)}^I)^3], \quad (1.67)$$

so we obtain the corresponding conformal anomaly density:

$$\mathcal{A}_w(x) = -G_{IJ} c_l \phi_{(0)}^I(x) (-\square)^l \phi_{(0)}^J(x) + O[(\phi_{(0)}^I)^3]. \quad (1.68)$$

Notice that this is a flat-space result. As we shall see explicitly in section 1.6, nontrivial conformal anomalies also arise when we put the theory in curved space.

1.4 Asymptotic behavior

We shall now consider the gravity theory in more detail. As we discussed above, the bulk spacetime (M, G) must have some sort of asymptotically AdS form where the asymptotic (*i.e.* near-boundary) behavior of the bulk fields is given in terms of the field theory sources. In this section we shall define the precise notion of an ‘Asymptotically locally AdS spacetime’ and consider the proper specification of boundary data for the various bulk fields in such spacetimes.

One particular bulk field is the metric $G_{\mu\nu}$ itself and its boundary data should be given in terms of the field theory metric g_{ij} on X . We shall from now on denote this boundary metric as $g_{(0)ij}$ to indicate that it corresponds to field theory data, much like the $\phi_{(0)}^I$.

1.4.1 Example

As a first example we will demonstrate how to define the boundary data for a scalar field Φ propagating on a fixed AdS_{d+1} background. This spacetime has the metric

$$G_{\mu\nu} dx^\mu dx^\nu = \frac{dz^2}{z^2} + \frac{1}{z^2} \delta_{ij} dx^i dx^j \quad (1.69)$$

where the x^i span \mathbb{R}^d and $z > 0$. Its boundary is the d -dimensional plane at $z \rightarrow 0$, plus a point at $z \rightarrow \infty$ which compactifies this plane to a sphere. The point at infinity induces some subtleties which we may however safely ignore in this chapter. The boundary data for Φ is then defined solely on the plane at $z \rightarrow 0$. We will suppose that Φ satisfies the massive Klein-Gordon equation:

$$\square_G \Phi - m^2 \Phi = 0, \quad (1.70)$$

which in the metric (1.69) becomes:

$$z^2 \partial_z^2 \Phi + (1-d)z \partial_z \Phi + z^2 \delta^{ij} \partial_i \partial_j \Phi - m^2 \Phi = 0. \quad (1.71)$$

We will ignore the backreaction from the field on the spacetime.

Solving (1.71) for small z we find that the equation of motion has the asymptotic solution:

$$\Phi = \phi_{(0)}(x^k) z^{d-\Delta} + \dots + \phi_{(2\Delta-d)}(x^k) z^\Delta + \dots \quad (1.72)$$

with

$$\Delta = \frac{d}{2} + \frac{1}{2} \sqrt{d^2 + 4m^2} \quad (1.73)$$

and we ignored the special case $\Delta = d/2$. From (1.72) we see that for $\Delta \neq d$ the scalar field either diverges or vanishes near $z \rightarrow 0$ so we cannot specify standard Dirichlet boundary data. Rather the boundary data for Φ is determined by the specification of the *leading* term in the radial expansion, which is $\phi_{(0)}(x^k)$ for the case at hand. Indeed it is not hard to find a unique solution to (1.71) for general $\phi_{(0)}(x^k)$ so the Dirichlet problem phrased in this way is well-posed. As our notation already indicates we will interpret $\phi_{(0)}(x^k)$ as the source of the dual field theory operator. We shall furthermore see below that the scaling dimension of this operator is precisely the Δ defined in (1.73).

For the metric (1.69) we similarly see a divergence as $z \rightarrow 0$ so we should specify its boundary conditions also in terms of the leading term in a certain radial expansion. However in a theory of gravity there is *a priori* no distinguished radial coordinate in which we can expand and we therefore face an ambiguity in the specification of the boundary data. In the remainder of this section we will parametrize this ambiguity and demonstrate how it is in fact dual to the freedom to make Weyl rescalings in the boundary theory.

Reviews of the mathematical aspects discussed here can be found in [19, 20].

1.4.2 Conformally compact manifolds

We begin with a proper definition of the boundary of the spacetimes under consideration. To this end we suppose (M, G) is a *conformally compact* manifold-

with-metric, which is defined as follows. Let M be the interior of a manifold \bar{M} with boundary $\partial M = X$. Suppose there exists a smooth, non-negative *defining function* z on \bar{M} such that $z(\partial M) = 0$, $dz(\partial M) \neq 0$ and the metric

$$\tilde{G} = z^2 G \tag{1.74}$$

extends smoothly to a *non-degenerate* metric on \bar{M} . We then say that (M, G) is conformally compact and the choice of a defining function determines a *conformal compactification* of (M, G) . Notice that for example (1.69) defines such a conformally compact manifold with a defining function equal to the coordinate z .

The metric \tilde{G} induces a regular metric $g_{(0)}$ on X which however depends on the defining function. For example if we picked z as a defining function in (1.69) we would obtain δ_{ij} as the boundary metric, whereas if we picked $e^\sigma z$ for some function $\sigma(x^i)$, the boundary metric would be $e^{2\sigma} \delta_{ij}$. It follows that the pair (M, G) determines an equivalence class of boundary metrics on X , where two metrics are equivalent if they differ by a Weyl rescaling. Such an equivalence class is called a *conformal structure* on X . We shall denote the equivalence class of $g_{(0)}$ as $[g_{(0)}]$ and $(X, [g_{(0)}])$ is then called the *conformal infinity* or *conformal boundary* of (M, G) . This construction is same as the Penrose method of compactifying spacetime by introducing conformal infinity.

If we compute the Riemann tensor of G , we find that near ∂M it has the form:

$$R_{\mu\nu\rho\sigma} = -\tilde{G}^{\kappa\lambda} \nabla_\kappa z \nabla_\lambda z (G_{\mu\rho} G_{\nu\sigma} - G_{\nu\rho} G_{\mu\sigma}) + O(z^{-3}). \tag{1.75}$$

Notice that the leading term is order z^{-4} as G is order z^{-2} . Taking its trace we obtain that:

$$R = -D(D-1) \tilde{G}^{\kappa\lambda} \nabla_\kappa z \nabla_\lambda z + O(z). \tag{1.76}$$

If we now additionally impose that the spacetime has constant negative curvature

$$R = -D(D-1), \tag{1.77}$$

then we find to leading order:

$$\tilde{G}^{\kappa\lambda} \nabla_\kappa z \nabla_\lambda z = 1. \tag{1.78}$$

The Riemann curvature of such a metric thus approaches that of AdS space with cosmological constant $\Lambda = -(D-1)(D-2)/2$, for which one may check explicitly that $R_{\mu\nu\rho\sigma} = -G_{\mu\rho} G_{\nu\sigma} + G_{\nu\rho} G_{\mu\sigma}$ holds exactly. A conformally compact manifold whose metric also satisfies $R = -D(D-1)$ is therefore also called an *Asymptotically locally AdS* manifold. Notice that we added the word ‘local’ because we have not put any requirements on global issues like the topology of X , which may very well be different from the sphere at conformal infinity of global AdS.

1.4.3 Fefferman-Graham metric and Weyl rescalings

A main result of Fefferman and Graham [21] is that in a finite neighborhood of ∂M the metric of an AlAdS spacetime can always be cast in the form:

$$ds^2 = \frac{dz^2}{z^2} + \frac{1}{z^2} g_{ij} dx^i dx^j, \quad (1.79)$$

where the conformal boundary is at $z = 0$ and the metric g induces a regular metric at ∂M , so:

$$g_{ij}(x^k, z) = g_{(0)ij}(x^k) + \dots, \quad (1.80)$$

where the dots represent terms that vanish as $z \rightarrow 0$. Just as for the scalar field we interpret the leading term $g_{(0)ij}$ in the expansion (1.80) as the field theory metric.

The Fefferman-Graham expansion for a given AlAdS manifold is however not unique. Indeed, one may apply an infinitesimal coordinate transformation along a vector field ζ^μ given by:

$$\zeta^\mu \partial_\mu = -z\lambda \partial_z + \frac{1}{2} z^2 (\partial_i \lambda) g_{(0)}^{ij} \partial_j, \quad (1.81)$$

where λ is an arbitrary function of the boundary coordinates x^i . This coordinate transformation retains the Fefferman-Graham form of the metric (1.79), but it changes the boundary metric by a Weyl rescaling,

$$\delta g_{(0)ij} = 2\lambda g_{(0)ij}. \quad (1.82)$$

This Weyl rescaling freedom reflects the fact that a conformally compact manifold induces a conformal structure rather than a metric on the boundary. The choice for a specific representative $g_{(0)ij}$ within the class $[g_{(0)ij}]$ is equivalent to picking a specific Fefferman-Graham coordinate system.

Notice that the same diffeomorphism changes the leading-order term in the expansion (1.72) by:

$$\delta \phi_{(0)} = \lambda(\Delta - d)\phi_{(0)}. \quad (1.83)$$

The transformation of the field theory sources (1.82) and (1.83) is in fact precisely the one we found when we discussed scale invariance in section 1.3.3, see the equations (1.46) and (1.50). Weyl rescalings in the CFT are thus implemented by diffeomorphisms in an AlAdS metric [22, 23] and the freedom to change the Fefferman-Graham expansion is precisely dual to the freedom to perform local Weyl rescalings in the field theory. We will see below how these diffeomorphisms can induce conformal anomalies in the field theory as well.

We may also consider the case of constant λ for which the diffeomorphism along (1.81) reduces to a rescaling of the z coordinate. In the field theory we interpret

this as a rescaling of the renormalization scale, cf. equation (1.52). The coordinate z is therefore often said to be dual to the renormalization scale of the dual field theory, with small z corresponding to large μ , so the UV of the theory, and vice versa. We shall use this intuition below.

Notice finally that any field theory that is described by gravity in an AdS spacetime has this asymptotic Weyl invariance at least up to anomalies. This explains the statement made in the second paragraph of section 1.2 where we claimed that the field theory should behave like a CFT at least at high energies.

Summary

Let us summarize the results of this subsection. Within the class of gauge/gravity dualities we consider here the corresponding bulk spacetimes must have an AdS form. Near the boundary of such spacetimes the metric and other fields diverge. It is however always possible to pick a so-called Fefferman-Graham coordinate system with a distinguished radial coordinate z and to define the boundary data as the leading-order coefficient in the expansion of the fields in this coordinate z . We denoted these coefficients $\phi_{(0)}$ and $g_{(0)}$ above and they are interpreted as sources in the dual field theory. The Fefferman-Graham coordinate system is not unique but picking a different coordinate z corresponds to a Weyl rescaling in the dual field theory.

1.4.4 Holographic renormalization

With the boundary data specified we can try to find a bulk solution to the equations of motion and compute its on-shell action. Since the solution of the equations of motion is a function of $\phi_{(0)}$ and $g_{(0)}$, so is the corresponding on-shell action $I[\phi_{(0)}, g_{(0)}]$. According to (1.31) we may interpret it as the generating functional of connected correlation functions in the dual field theory.

However, the naive on-shell action is always infinite, essentially because of the infinite volume of AdS spacetimes. In order to obtain finite answers we need to regularize and then renormalize the computation of the on-shell action. This *holographic* renormalization procedure [24, 25, 26, 27, 28, 29] depends crucially on the asymptotic properties of an AdS metric and this is the place where the above framework finds a practical application.

The procedure of holographic renormalization is implemented as follows. The divergences in the on-shell action $I[\phi_{(0)}, g_{(0)}]$ all arise from integrals that diverge as we send the Fefferman-Graham coordinate $z \rightarrow 0$. To regulate these divergences one therefore introduces a cutoff by restricting the spacetime integrals to some

small but finite z_0 . The regulated on-shell action then contains a number of terms that would diverge as $z_0 \rightarrow 0$. These divergences are then cancelled by adding *counterterms* to the action, which are boundary terms defined at the cutoff surface $z = z_0$. These counterterms are chosen in such a way that the combined action is finite as one removes the cutoff. This results in a finite *renormalized* on-shell action which one may use to compute field theory correlation functions.

The precise counterterm action is far from arbitrary. First of all the counterterm action has to be a *boundary* action in order for the counterterms not to affect the bulk equations of motion. To maintain covariance under transformations of the boundary coordinates x^i these counterterms should furthermore be functionals of the *induced fields* on the slice given by $z = z_0$. They should also be *local* functionals of these fields in order not to change the nonlocal, dynamical, part of the on-shell action. Finally, in order to respect the variational principle for all finite values of z_0 the counterterms have to be defined in terms of the fields themselves and not involve their conjugate momenta, *i.e.* their radial derivatives. As a sidenote we remark that once the cutoff is removed the counterterms in fact precisely modify the variational principle such that it is appropriate for AlAdS spacetimes [30].

The precise counterterm action for AlAdS spacetimes depends on the bulk theory under consideration. On the other hand it does *not* depend on the specific solution to the equations of motion. Instead the counterterms are *universal* and make a given action finite for any solution to the corresponding equations of motion. This is dual to the statement that the renormalizability of the field theory can be demonstrated solely by analyzing its UV properties, *i.e.* independently of the specific form of the correlation functions.

Furthermore the procedure of holographic renormalization also leads to certain *constraints* which the renormalized on-shell action I must satisfy. These constraints precisely correspond to the field theory Ward identities of section 1.3. They are again independent of the specific form of the bulk solution which reflects the fact that the Ward identities are also a property of the UV of the dual field theory.

In the next sections we will present the holographic renormalization procedure in two simple examples. We will show how to find the counterterms that make the action finite and how the holographic Ward identities arise. We will also find an explicit solution to the equation of motion which we use to compute a two-point function in the boundary theory.

For a general introduction to holographic renormalization we refer to [31].

1.5 Scalar field in AdS_{d+1}

We will again consider the example of a free massive scalar field Φ in an AdS_{d+1} spacetime. Its action is given by:

$$S = \frac{1}{2} \int d^{d+1}x \sqrt{G} \left(\partial_\mu \Phi \partial^\mu \Phi + m^2 \Phi^2 \right). \quad (1.84)$$

We shall in this section use a new coordinate $r = -\log(z)$ in which the metric (1.69) becomes:

$$G_{\mu\nu} dx^\mu dx^\nu = dr^2 + \gamma_{ij} dx^i dx^j, \quad \gamma_{ij} = e^{2r} \delta_{ij}. \quad (1.85)$$

Notice that the conformal boundary of the spacetime is now at $r \rightarrow \infty$. In this coordinate the equation of motion (1.70) takes the form:

$$\ddot{\Phi} + d\dot{\Phi} + \square_\gamma \Phi - m^2 \Phi = 0, \quad (1.86)$$

where a dot denotes a radial derivative and $\square_\gamma = e^{-2r} \square_0$ with $\square_0 = \delta^{ij} \partial_i \partial_j$ the d -dimensional flat space Laplacian. We presented in equation (1.72) the leading-order form of the solution near the boundary. In the coordinate r it reads:

$$\Phi(r, x^i) = e^{(\Delta-d)r} \left(\phi_{(0)}(x^i) + \dots + e^{-(2\Delta-d)r} \phi_{(2\Delta-d)}(x^i) + \dots \right), \quad (1.87)$$

where we recall that $\Delta = \frac{1}{2}(d + \sqrt{d+4m^2})$ as given in (1.73). We shall assume that $\Delta > d/2$. Notice that there are asymptotically two independent solutions. We interpret the leading-order term $\phi_{(0)}(x)$ as the source in the dual field theory.

Asymptotic solution

Let us first expand the asymptotic solution to higher order. From the equation of motion we find that the subleading terms have the form of a power series:

$$\Phi = e^{(\Delta-d)r} \left(\phi_{(0)}(x^i) + e^{-2r} \phi_{(2)}(x^i) + \dots + e^{-2kr} \phi_{(2k)}(x^i) + \dots \right), \quad (1.88)$$

whose coefficients are given by:

$$\begin{aligned} \phi_{(2)} &= \frac{\square_0 \phi_{(0)}}{2(2\Delta - d - 2)} \\ \phi_{(2k)} &= \frac{\square_0 \phi_{(2k-2)}}{2k(2\Delta - d - 2k)}. \end{aligned} \quad (1.89)$$

For generic values of Δ this expansion continues indefinitely and a corresponding expansion exists for the second branch of the solution in (1.87). However if:

$$\Delta = l + \frac{d}{2} \quad l \in \{1, 2, 3, \dots\} \quad (1.90)$$

we find that equation (1.89) cannot be satisfied for $k = l$ and we have to modify the expansion:

$$\begin{aligned} \Phi = e^{(\Delta-d)r} & \left(\phi_{(0)}(x^i) + e^{-2r} \phi_{(2)}(x^i) + \dots + e^{-2kr} \phi_{(2k)}(x^i) + \dots \right. \\ & \left. + e^{-2lr} r \tilde{\phi}_{(2l)}(x^i) + e^{-2lr} \phi_{(2l)}(x^i) + \dots \right). \end{aligned} \quad (1.91)$$

We then find in addition to (1.89) the new relation for $k = l$:

$$\tilde{\phi}_{(2l)} = \frac{1}{l} \square_0 \phi_{(2l-2)} \quad (1.92)$$

and we also find that $\phi_{(2l)}$ is not determined by the asymptotic expansion. We shall see how it is determined in terms of $\phi_{(0)}$ once we find the full solution to the equations of motion below.

Notice that (1.90) implies that $m^2 = l^2 - d^2/4$. One often obtains precisely such masses by a Kaluza-Klein decomposition of the fields on the compact part of the geometry like we did in section 1.1.2. We will therefore focus on these cases from now on.

On-shell action and divergences

We now substitute the asymptotic solution (1.91) into the action (1.84). After an integration by parts we find that the bulk term vanishes by the equations of motion and the on-shell action reduces to a boundary term:

$$I = \frac{1}{2} \int_{r_0} d^d x \sqrt{\gamma} \Phi \dot{\Phi}. \quad (1.93)$$

This term would in principle be defined the surface $r \rightarrow \infty$ in the metric (1.85). However plugging in the above solution and using $\sqrt{\gamma} = e^{dr}$ we find:

$$\begin{aligned} I = \int_{r_0} d^d x e^{(2\Delta-d)r} & \left((\Delta - d) \phi_{(0)}^2 + e^{-2r} 2(\Delta - d - 1) \phi_{(0)} \phi_{(2)} + \dots \right. \\ & \left. - dr e^{-(2\Delta-d)r} \tilde{\phi}_{(2l)} \phi_{(0)} + (\tilde{\phi}_{(2l)} - d\phi_{(2l)}) \phi_{(0)} + \dots \right) \end{aligned} \quad (1.94)$$

and we find a number of *divergences* as we let $r \rightarrow \infty$. We therefore impose a cutoff and put the spatial integral in (1.93) at some large but finite r_0 . This regulates the divergences and ensures that the bare action is finite.

The divergent terms in (1.94) involve precisely all the terms that were determined by the radial expansion above. Indeed the first term involving the undetermined term $\phi_{(2l)}$ is precisely a finite term and is therefore unimportant as far as the construction of the counterterms is concerned. This explicitly demonstrates the

aforementioned statement that one does not need the full solution to the equations of motion to implement the holographic renormalization.

To cancel the divergences in (1.94) we have to define a *counterterm action* that we add to the above action such that the combined action is finite. As we mentioned above this has to be a local covariant functional of the induced values of the field at the cutoff surface, so of $\Phi(x, r_0)$.

We emphasize that adding such a counterterm action is *not* the same as simply crossing out the divergent terms in (1.94). Indeed in the latter case we would be defining the counterterms in terms of $\phi_{(0)}(x)$ which is manifestly not the same as $\Phi(x, r_0)$. To explicitly see the difference, consider for example the leading divergence. It is cancelled by the counterterm:

$$\begin{aligned}
 - \int_{r_0} d^d x \sqrt{\gamma} (\Delta - d) \Phi^2 = & - \int_{r_0} d^d x e^{(2\Delta-d)r} \left((\Delta - d) \phi_{(0)}^2 + \dots \right. \\
 & \left. + e^{-(2\Delta-d)r} 2(\Delta - d) \phi_{(0)} \phi_{(2l)} + \dots \right), \tag{1.95}
 \end{aligned}$$

which is indeed a proper local function of the induced values of the fields defined at the cutoff surface. By construction its radial expansion begins precisely with the divergence it is supposed to cancel, but there is also a finite piece which we shall see survives into the renormalized result. We would not obtain such a finite piece if we simply crossed out the divergences in (1.94). This latter method is therefore not only theoretically problematic but it leads to physically incorrect results as well.

The dilatation operator

There exist various systematic procedures to find the exact form of the counterterm action. The method we describe below follows [29] and relies on the following observation. Since the solution to the equations of motion is completely determined by the boundary data, so is the on-shell action I . For the *regulated* action these boundary data are the induced values of the bulk fields on the cutoff surface. For example, the on-shell action for the scalar field depends on the induced metric γ_{ij} and the boundary values of the scalar field Φ at this cutoff surface. We may therefore write:

$$I[\gamma_{ij}, \Phi] \tag{1.96}$$

This in particular implies that all the dependence on the cutoff is completely implicit in the dependence of I on the induced fields. The radial derivative of I is therefore given by a simple application of the chain rule:

$$\dot{I} = \int d^d x \dot{\gamma}_{ij} \frac{\delta I}{\delta \gamma_{ij}} + \int d^d x \Pi \frac{\delta I}{\delta \Phi} = 2 \int d^d x \gamma_{ij} \frac{\delta I}{\delta \gamma_{ij}} + \int d^d x \Pi \frac{\delta I}{\delta \Phi}. \tag{1.97}$$

Since the background metric is fixed we substituted its background value $\dot{\gamma}_{ij} = 2\gamma_{ij}$ and we also introduced $\Pi = \dot{\Phi}$. Notice that the dot in (1.97) denotes a derivative with respect to the cutoff. We shall henceforth denote the cutoff by r rather than r_0 since it is the only radial coordinate entering in this section.

From the expansion (1.91) we also know that

$$\Pi = (\Delta - d)\Phi + \dots \quad (1.98)$$

where the dots represent subleading terms as $r \rightarrow \infty$. We therefore find that:

$$\dot{I} = \delta_D I + \dots \quad (1.99)$$

with δ_D the *dilatation operator*:

$$\delta_D = 2 \int d^d x \gamma_{ij} \frac{\delta}{\delta \gamma_{ij}} + \int d^d x (\Delta - d)\Phi \frac{\delta}{\delta \Phi}. \quad (1.100)$$

Notice that it is appropriately named because when we send $r \rightarrow \infty$ it becomes precisely the field theory dilatation operator (1.51). It is now however a covariant operator which acts on arbitrary functionals of the fields Φ and γ_{ij} evaluated at the cutoff surface.

We now recall that

$$\Pi = \frac{1}{\sqrt{\gamma}} \frac{\delta I}{\delta \Phi}. \quad (1.101)$$

This result follows either from explicit variation of the action (1.84) or from general Hamilton-Jacobi theory where one treats the radial coordinate as the ‘time’ coordinate. Since I was a functional of γ_{ij} and Φ , then from (1.101) so is Π . Therefore the radial derivative acting on Π can also be written in the form (1.97):

$$\dot{\Pi} = 2 \int d^d x \gamma_{ij} \frac{\delta \Pi}{\delta \gamma_{ij}} + \int d^d x \Pi \frac{\delta \Pi}{\delta \Phi} \quad (1.102)$$

and again the radial derivative is asymptotically equal to the dilatation operator.

Eigenfunction expansion

The next step in the Hamiltonian holographic renormalization is to expand Π in *eigenfunctions* of the dilatation operator δ_D defined in (1.100). We write:

$$\Pi = \Pi_{(d-\Delta)} + \Pi_{(d-\Delta+2)} + \Pi_{(d-\Delta+4)} + \dots \quad (1.103)$$

where by definition

$$\delta_D \Pi_{(s)} = -s \Pi_{(s)}. \quad (1.104)$$

Notice that since the radial derivative is asymptotically equal to the dilatation operator we obtain that:

$$\dot{\Pi}_{(s)} = -s\Pi_{(s)} + \dots \quad (1.105)$$

However the organization in eigenfunctions of the dilatation operator is not precisely a radial expansion. Indeed, this expansion organizes the various divergences in Π in a *covariant* fashion, that is in terms of Φ rather than $\phi_{(0)}$.

From (1.98) we immediately find that $\Pi_{(d-\Delta)} = (\Delta - d)\Phi$ which is in fact how we obtained the leading-order weight $(d - \Delta)$ in (1.103). To find an expression for the subleading terms we use the equation of motion (1.86):

$$\dot{\Pi} + d\Pi - \square_\gamma \Phi - \Delta(\Delta - d)\Phi = 0. \quad (1.106)$$

We then replace $\dot{\Pi}$ with (1.102), substitute (1.103) for all instances of Π and use (1.104) to collect terms of equal dilatation weight. This results in the following expressions for the subleading terms:

$$\begin{aligned} \Pi_{(d-\Delta+2)} &= \frac{1}{2\Delta - d - 2} \square_\gamma \Phi \\ \Pi_{(d-\Delta+4)} &= \frac{-1}{(2\Delta - d - 4)(2\Delta - d - 2)^2} \square_\gamma^2 \Phi \\ \Pi_{(d-\Delta+2k)} &= \frac{c(k, \Delta, d)}{(2\Delta - d - 2k)} \square_\gamma^k \Phi \end{aligned} \quad (1.107)$$

where the coefficients $c(k, \Delta, d)$ can be determined recursively. The above expansion continues up to the terms with $k = l$, so the terms with weight $-\Delta$, where we find that the equation of motion (1.106) cannot be satisfied when we substitute the expansion (1.103). Just as for the radial expansion (1.91) we have to include an inhomogeneous term:

$$\Pi = \Pi_{(d-\Delta)} + \Pi_{(d-\Delta+2)} + \dots + \Pi_{(\Delta+2)} + r\tilde{\Pi}_{(\Delta)} + \Pi_{(\Delta)} + \dots \quad (1.108)$$

whose properties under dilatations take the form:

$$\delta_D(\Pi_{(\Delta)} + r\tilde{\Pi}_{(\Delta)}) = -\Delta(\Pi_{(\Delta)} + r\tilde{\Pi}_{(\Delta)}) + \tilde{\Pi}_{(\Delta)}. \quad (1.109)$$

Notice again the similarity between the dilatation operator and the radial derivative. By iterating the equations of motion we find that:

$$\tilde{\Pi}_{(\Delta)} = (-1)^l 2^{2l-2} \Gamma(l) \square_\gamma^{2l} \Phi, \quad (1.110)$$

whereas $\Pi_{(\Delta)}$ is not determined by this procedure.

Renormalized action and one-point function

We recall that the bare action (1.93) is given by:

$$I_{\text{bare}} = \frac{1}{2} \int_r d^d x \sqrt{\gamma} \Phi \Pi. \quad (1.111)$$

Substituting now the expansion (1.103) we directly find the divergences organized in a *covariant* expansion in Φ rather than in a radial expansion as given in (1.94). This means that we can directly cancel them with the counterterm action:

$$I_{\text{ct}} = -\frac{1}{2} \int_r d^d x \sqrt{\gamma} \Phi \left(\sum_{(d-\Delta) \leq s < \Delta} \Pi_{(s)} + r \tilde{\Pi}_{(\Delta)} \right) \quad (1.112)$$

and the renormalized action is given by:

$$I_{\text{ren}} = \lim_{r \rightarrow \infty} -\frac{1}{2} \int_r d^d x \sqrt{\gamma} \Phi \Pi_{\Delta}, \quad (1.113)$$

which is finite as $r \rightarrow \infty$.

Notice the presence of the explicit r in the last counterterm which is necessary to cancel the logarithmic divergence in (1.94). This explicit coordinate dependence leads to anomalous transformation properties under translations in the r direction. We mentioned in section 1.4.3 that these translations map to Weyl rescalings in the boundary theory and one may therefore expect a corresponding Weyl anomaly. This indeed turns out to be the case.

To find the anomaly we recall that the dilatation operator reduces to the global rescaling defined in (1.51) for $\lambda = 1$. We can therefore act with δ_D on the renormalized action and compare with (1.53) to find the corresponding anomaly \mathcal{A}_w . Using (1.109), (1.110) and (1.113) we obtain:

$$\delta_D I_{\text{ren}} = -\frac{1}{2} \lim_{r \rightarrow \infty} \int_r d^d x \sqrt{\gamma} \Phi \tilde{\Pi}_{(\Delta)} = \int d^d x (-1)^{l+1} 2^{2l-1} \Gamma(l) \phi_{(0)} \square_0^l \phi_{(0)}, \quad (1.114)$$

whose form precisely matches the conformal anomaly for operators of dimension (1.90) which we discussed in section 1.3.3. Notice that we obtained this anomaly without having to find a complete solution to the equations of motion: just as in the boundary theory it follows purely from the UV structure of the theory.

Correlation functions

From the renormalized action (1.113) we may obtain the one-point function in the presence of sources. Using (1.31) we find:

$$\langle \mathcal{O}(x^i) \rangle_{\phi} = \frac{1}{\sqrt{g_{(0)}}} \frac{\delta I_{\text{ren}}}{\delta \phi_{(0)}(x^i)} = \lim_{r \rightarrow \infty} \frac{e^{\Delta r}}{\sqrt{\gamma}} \frac{\delta}{\delta \Phi(x^i, r)} (I_{\text{bare}} + I_{\text{ct}}), \quad (1.115)$$

where the extra factor $e^{\Delta r}$ converts Φ to $\phi_{(0)}$ and γ to $g_{(0)}$ as $r \rightarrow \infty$. We may compute this explicitly by substituting the values for $\Pi_{(s)}$ and $\tilde{\Pi}_{(\Delta)}$ in (1.112) and using (1.101). We find:

$$\langle \mathcal{O}(x^i) \rangle_\phi = \lim_{r \rightarrow \infty} e^{\Delta r} \Pi_{(\Delta)}(r, x^i). \quad (1.116)$$

Substituting now (1.91) we obtain [27]:

$$\langle \mathcal{O}(x^i) \rangle_\phi = -2l\phi_{(2l)}(x^i) + C[\phi_{(0)}(x^i)], \quad (1.117)$$

where the $C[\phi_{(0)}]$ are local contact terms which are scheme-dependent.

In order to proceed from here we have to determine the full solution to the equation of motion (1.86) for given boundary data $\phi_{(0)}$. Indeed the full solution allows one to express $\phi_{(2l)}$ as a function of $\phi_{(0)}$ so we can differentiate (1.117) once more with respect to $\phi_{(0)}$ to obtain a nontrivial two-point function.

In Fourier space one easily obtains the two linearly independent solutions of (1.86). These are given in terms of modified Bessel functions:

$$e^{-(d/2)r} K_l(|k|e^{-r}) \quad e^{-(d/2)r} I_l(|k|e^{-r}) \quad (1.118)$$

For $r \rightarrow -\infty$ the solutions behave as:

$$\begin{aligned} e^{-(d/2)r} K_l(|k|e^{-r}) &= \sqrt{\frac{\pi e^{-(d-1)r}}{2|k|}} \exp(-|k|e^{-r})(1 + O(e^r)) \\ e^{-(d/2)r} I_l(|k|e^{-r}) &= \sqrt{\frac{e^{-(d-1)r}}{2\pi|k|}} \left[\exp(|k|e^{-r}) + \exp(-|k|e^{-r} - (l + \frac{1}{2})\pi i) \right] \\ &\quad \times (1 + O(e^r)) \end{aligned} \quad (1.119)$$

We see that the solution involving I_l blows up and therefore should be discarded. For large r we obtain:

$$e^{-(d/2)r} K_l(|k|e^{-r}) = \Gamma(l) \frac{2^{l+1} e^{-(d/2-l)r}}{|k|^l} (1 + O(e^{-r})) \quad (1.120)$$

The full solution to the equations of motion therefore takes the form:

$$\Phi(x, k) = \int \frac{d^d k}{(2\pi)^d} e^{ikx} \phi_{(0)}(k) \frac{|k|^l}{2^{l+1} \Gamma(l)} e^{-(d/2)r} K_l(|k|e^{-r}) \quad (1.121)$$

where K_l is the modified Bessel function of the second kind and we Fourier transformed the source $\phi_{(0)}$. One may expand the Bessel function to recover precisely

the expansion (1.91), including the inhomogeneous term. The full solution also determines the final term in (1.91):

$$\phi_{(2l)} = \int \frac{d^d k}{(2\pi)^d} e^{ikx} \phi_{(0)}(k) \frac{(-1)^{l-1}}{2^{2l} \Gamma(l) \Gamma(l+1)} |k|^{2l} \left(\log(|k|^2) - \log(4) + \frac{1}{2} \psi(l+1) - \gamma \right) \quad (1.122)$$

where $\psi(x) = d \ln \Gamma(x) / dx$ is the digamma function and γ the Euler-Mascheroni constant. We can plug this into (1.117) and differentiate once more with respect to $\phi_{(0)}$ to obtain:

$$\langle \mathcal{O}(k) \mathcal{O}(-k) \rangle = \frac{(-1)^{l+1}}{2^{2l} [\Gamma(l)]^2} |k|^{2l} \log(|k|^2 / \mu^2) + C(k^2) \quad (1.123)$$

where the C denote contact terms that we can safely ignore and we also introduced a scale μ on dimensional grounds. In position space we may use (1.65) to find:

$$\langle \mathcal{O}(x) \mathcal{O}(y) \rangle = \frac{2l \pi^{-d} \Gamma(l + d/2)}{\pi^{d/2} \Gamma(l)} \mathcal{R} \frac{1}{|x|^{2\Delta}} \quad (1.124)$$

We indeed reproduced the *renormalized* correlation function, which was to be expected from the anomalous conformal Ward identity we found above.

1.6 Einstein gravity

In this section we will work out the holographic renormalization for $(d+1)$ -dimensional Einstein gravity with a negative cosmological constant. The proper action functional is given by the Einstein-Hilbert term plus the Gibbons-Hawking boundary term:

$$S = \frac{1}{2\kappa^2} \int d^{d+1}x \sqrt{G} (-R + 2\Lambda) - \frac{1}{\kappa^2} \int d^d x \sqrt{\gamma} K. \quad (1.125)$$

This form of the action results in a well-defined variational principle if one keeps the metric fixed on a boundary that is at finite distance from the interior of the space [32]. We work in $(d+1)$ dimensions and will specialize to $d \leq 4$ below. The bulk metric is denoted $G_{\mu\nu}$, the boundary metric γ_{ij} and K_{ij} is the extrinsic curvature of the boundary. The equations of motion obtained from (1.125) are the Einstein equations:

$$R_{\mu\nu} - \frac{1}{2} R G_{\mu\nu} + \Lambda G_{\mu\nu} = 0 \quad (1.126)$$

and we use the following conventions for the curvatures:

$$R_{\mu\nu\rho}{}^\sigma = \partial_\nu \Gamma_{\mu\rho}^\sigma + \Gamma_{\mu\rho}^\lambda \Gamma_{\nu\lambda}^\sigma - (\mu \leftrightarrow \nu), \quad R_{\mu\rho} = R_{\mu\rho}{}^\sigma{}_\sigma. \quad (1.127)$$

In terms of the AdS radius of curvature ℓ one has $\Lambda = -\frac{1}{2}d(d-1)\ell^{-2}$. We will set $\ell = 1$ in what follows. Notice that one then obtains $R = -d(d+1)$ from the trace of (1.126).

AlAdS solution

We would like to renormalize the on-shell action for a solution to (1.126) which is AlAdS. In section 1.4.3 we described that near the conformal boundary the metric for such a solution can be put in the Fefferman-Graham form:

$$G_{\mu\nu}dx^\mu dx^\nu = dr^2 + \gamma_{ij}dx^i dx^j \quad \gamma_{ij}(r, x^k) = e^{2r}g_{(0)ij}(x^k) + \dots \quad (1.128)$$

In these coordinates the extrinsic curvature K_{ij} for a hypersurface of constant r takes the simple form:

$$K_{ij} = \frac{1}{2}\dot{\gamma}_{ij}, \quad (1.129)$$

where the dot denotes a radial derivative. The nonzero connection coefficients for the metric (1.128) are

$$\Gamma_{ij}^r = -K_{ij}, \quad \Gamma_{rj}^i = K_j^i, \quad \Gamma_{jk}^i[G] = \Gamma_{jk}^i[\gamma], \quad (1.130)$$

and the Einstein equations become:

$$\begin{aligned} 0 &= R - K^2 + K_{ij}K^{ij} + d(d-1) \\ 0 &= \nabla_i K_j^i - \nabla_j K \\ 0 &= \partial_r(K_j^i) + K K_j^i - R_j^i - d\delta_j^i. \end{aligned} \quad (1.131)$$

Here and below we write R_{ij} and ∇_i for the curvature and the covariant derivative associated with the metric γ_{ij} . Similarly indices are always raised with γ^{ij} unless indicated otherwise.

We may use the equations (1.131) to obtain an asymptotic expansion of the metric. For example for the first subleading term we find:

$$\gamma_{ij} = e^{2r} \left(g_{(0)ij} + e^{-2r} g_{(2)ij} + \dots \right) \quad (1.132)$$

with, for $d > 2$,

$$g_{(2)ij} = \frac{1}{d-2} \left(R_{(0)ij} - \frac{1}{2(d-1)} R_{(0)} g_{(0)ij} \right), \quad (1.133)$$

where $R_{(0)ij}$ is the Ricci tensor for the metric $g_{(0)ij}$. Notice that this term is a *local* function of the boundary data $g_{(0)ij}$. Iterating this procedure one finds that all the subleading terms up until $g_{(d)ij}$ are locally determined by $g_{(0)ij}$, but at order e^{-dr} the procedure breaks down and one finds that $g_{(d)ij}$ is not (completely) determined by the asymptotic solution to the equations of motion. Furthermore, for d even and greater than two one also has to insert a term of the form $\tilde{g}_{(d)ij} r e^{-dr}$ in the asymptotic expansion. The resulting asymptotic structure is then very similar to

that of the scalar field presented in the equations (1.89) and (1.91) above. Furthermore, just as for the scalar field we will see below that the nonlocally determined term $g_{(d)ij}$ will eventually enter in the one-point function (as in equation (1.117)) and that the inhomogeneous term $\tilde{g}_{(d)ij}$ is related to a conformal anomaly (as in equation (1.114)).

Divergences and constraint equations

Let us now analyze the divergences in the on-shell action. Using the above expressions for the bulk curvature and cosmological constant one finds that the on-shell action reduces to:

$$I = \frac{d}{\kappa^2} \int d^{d+1}x \sqrt{G} - \frac{1}{\kappa^2} \int d^d x \sqrt{\gamma} K. \quad (1.134)$$

Upon substitution of the Fefferman-Graham expansion one finds a number of divergences. For example, from (1.128) and (1.129) one finds at leading order:

$$I_{\text{bare}} = \frac{1-d}{\kappa^2} \int_{r_0} d^d x \left(\sqrt{g_{(0)}} e^{dr} + \dots \right), \quad (1.135)$$

where we introduced a cutoff at a large but finite r_0 to regulate the divergences.

The divergences should be cancelled with a suitable counterterm action which can be obtained as follows. Just as for the scalar field we begin by introducing the conjugate momentum as the variation of the on-shell action:

$$\pi^{ij} = \frac{2\kappa^2}{\sqrt{\gamma}} \frac{\delta I}{\delta \gamma_{ij}}. \quad (1.136)$$

From (1.125) one may easily compute it to be:

$$\pi^{ij} = K^{ij} - K \gamma^{ij}, \quad (1.137)$$

which can be inverted to $K_{ij} = \pi_{ij} + \pi_k^k \gamma_{ij} / (d-1)$. In terms of π^{ij} the first equation in (1.131) then becomes:

$$R + \pi_j^i \pi_i^j - \frac{(\pi_k^k)^2}{d-1} + d(d-1) = 0 \quad (1.138)$$

If one then substitutes (1.136) this equation becomes a functional differential equation for I which is precisely the Hamilton-Jacobi equation for the on-shell gravity action. We will shortly see how this single equation is sufficient to completely determine the divergent part of the on-shell action.

Dilatation weight expansions

Let us again introduce the *dilatation operator* which we introduced in (1.100) above. In this case the metric is the only dynamical field and the dilatation operator therefore takes the form:

$$\delta_D = 2 \int d^d x \gamma_{ij} \frac{\delta}{\delta \gamma_{ij}}. \quad (1.139)$$

Just as in the previous section we notice that the regulated on-shell action I as well as the conjugate momentum π^{ij} are functionals of the boundary metric γ_{ij} alone. By a repetition of the discussion around equation (1.99) one may conclude that the action of the dilatation operator on these quantities is therefore asymptotically equal to taking a radial derivative. To isolate the divergent pieces it is then again convenient to use an expansion in eigenfunctions of the dilatation operator.

Notice that we may always write the on-shell action as an integral over the cutoff surface:

$$I = \frac{1}{2\kappa^2} \int d^d x \sqrt{\gamma} \lambda \quad (1.140)$$

for some (a priori complicated) function $\lambda[\gamma_{ij}]$. We will now expand λ in eigenfunctions of the dilatation operator. Using (1.135) and the fact that $\sqrt{\gamma} = e^{dr} \sqrt{g(0)} + \dots$ we see that the leading-order weight of λ has to be zero. We therefore write:

$$\lambda = \lambda_{(0)} + \lambda_{(2)} + \dots \quad (1.141)$$

with by definition:

$$\delta_D \lambda_{(s)} = -s \lambda_{(s)} \quad (1.142)$$

and from (1.135) we immediately find $\lambda_{(0)} = 2(1-d)$. We shall shortly see that one needs to add inhomogeneous terms to the expansion (1.141) when d is even, just as in equation (1.108) for the conjugate momentum of the scalar field.

Let us now consider the expansion of π^{ij} . Notice that since γ_{ij} has weight two we find that lowering or raising an index on a tensor increases or decreases its dilatation weight by two, respectively. We will choose to expand π_j^i in eigenfunctions of the dilatation operator. To leading order one finds from (1.137) that

$$\pi_j^i = (1-d) \delta_i^j + \dots, \quad (1.143)$$

so the corresponding expansion for π_j^i also begins with a term of weight zero. (This is consistent with (1.136) and the fact that λ also begins with a term of weight zero.) We therefore write:

$$\pi_j^i = \pi_{(0)j}^i + \pi_{(2)j}^i + \dots, \quad (1.144)$$

with again:

$$\delta_D \pi_{(s)j}^i = -s \pi_{(s)j}^i \quad (1.145)$$

and with the leading-order term:

$$\pi_{(0)j}^i = (1-d) \delta_j^i. \quad (1.146)$$

We will explain below that it again becomes necessary to add an inhomogeneous term to the expansion for certain values of d .

Computation of the expansion coefficients

We can now explicitly construct all the divergent terms in the expansion (1.141) using the constraint equation (1.138). Just as for the scalar field all these terms will be algebraically determined and the resulting expressions will be local and covariant functions of the boundary metric γ_{ij} .

The first step is to realize that for any variation of γ_{ij} we may use (1.136) and (1.140) to find:

$$\sqrt{\gamma} \pi^{ij} \delta \gamma_{ij} = \delta(\sqrt{\gamma} \lambda) \quad (1.147)$$

at least up to a total divergence. We may however use the total divergence ambiguity in λ to make sure that the above equation holds exactly, see [29] for details. We may then set $\delta = \delta_D$ and find that

$$2\pi_k^k = (d + \delta_D) \lambda \quad (1.148)$$

and upon substitution of the above expansions for λ and π_j^i we obtain:

$$\lambda_{(s)} = \frac{2}{d-s} \pi_{(s)k}^k. \quad (1.149)$$

We may furthermore obtain $\pi_{(s)j}^i$ from substitution of the expansions in (1.136). This results in:

$$\sqrt{\gamma} \pi_{(s)j}^i = \gamma_{jk} \frac{\delta}{\delta \gamma_{ik}} \int d^d x \sqrt{\gamma} \lambda_{(s)}. \quad (1.150)$$

Notice that we may substitute (1.149) into (1.150) to recover $\pi_{(s)j}^i$ completely by knowing only its trace, at least for $s \neq d$. This allows for a recursive solution of (1.138) as we now illustrate by performing the first few steps.

First of all, at dilatation weight zero equation (1.138) reduces to an equation that is trivially satisfied upon substitution of (1.146). At dilatation weight two we use (1.146) to obtain:

$$2\pi_{(2)k}^k = -R \quad (1.151)$$

and using (1.149):

$$\lambda_{(2)} = -\frac{1}{d-2} R, \quad (1.152)$$

at least for $d \neq 2$. Furthermore, from (1.150) we find:

$$\pi_{(2)ij} = \frac{1}{d-2}(R_{ij} - \frac{1}{2}R\gamma_{ij}), \quad (1.153)$$

again for $d \neq 2$.

Next, at dilation weight 4 we obtain:

$$\begin{aligned} \pi_{(4)k}{}^k &= \frac{(\pi_{(2)k}{}^k)^2}{2(d-1)} - \frac{1}{2}\pi_{(2)j}{}^i\pi_{(2)i}{}^j \\ &= -\frac{1}{8(d-2)^2}\left(\frac{d}{d-1}R^2 + 4R_j^i R_i^j\right), \end{aligned} \quad (1.154)$$

and for $d \neq 2, 4$ we may again use (1.149) to find

$$\lambda_{(4)} = -\frac{1}{4(d-4)(d-2)^2}\left(\frac{d}{d-1}R^2 + 4R_j^i R_i^j\right) \quad (1.155)$$

and so on.

In general the above procedure breaks down at dilatation weight $s = d$. For odd d we find that $\pi_{(d)k}{}^k = 0$ and that $\lambda_{(d)}$ is undetermined by this procedure. For even d the expansions for λ and π_j^i given above need to be modified to:

$$\begin{aligned} \pi_j^i &= \pi_{(0)j}{}^i + \dots + r\tilde{\pi}_{(d)j}{}^i + \pi_{(d)j}{}^i + \dots \\ \lambda &= \lambda_{(0)} + \dots + r\tilde{\lambda}_{(d)} + \lambda_{(d)} + \dots \end{aligned} \quad (1.156)$$

with:

$$\delta_D(r\tilde{\pi}_{(d)j}{}^i + \pi_{(d)j}{}^i) = -dr\tilde{\pi}_{(d)j}{}^i - d\pi_{(d)j}{}^i + \tilde{\pi}_{(d)j}{}^i \quad (1.157)$$

and similarly for $\lambda_{(d)}$ and $\tilde{\lambda}_{(d)}$. Repeating then the above procedure we find first of all that $\pi_{(s)j}{}^i$ and $\lambda_{(s)}$ are unmodified for $s < d$. Furthermore, for $s = d$ we find from (1.138) the traces of the new terms, namely $\tilde{\pi}_{(d)k}{}^k = 0$ and $\pi_{(d)k}{}^k$ is the same as above. Using (1.148) one also obtains that

$$\tilde{\lambda}_{(d)} = \pi_{(d)k}{}^k \quad (1.158)$$

and $\lambda_{(d)}$ is again undetermined. Finally we use (1.150) to obtain:

$$\tilde{\pi}_{(d)j}{}^i = \frac{1}{\sqrt{\gamma}}\gamma_{jk}\frac{\delta}{\delta\gamma_{ik}}\int d^d x\sqrt{\gamma}\pi_{(d)k}{}^k, \quad (1.159)$$

but since $\lambda_{(d)}$ is undetermined we cannot determine $\pi_{(d)j}{}^i$ from (1.150).

Let us consider explicitly the dimensions $d = 2$ and $d = 4$. For $d = 2$ we find

$$\tilde{\lambda}_{(2)} = \pi_{(2)k}{}^k = -\frac{1}{2}R, \quad (1.160)$$

and then from (1.159) one obtains

$$\tilde{\pi}_{(2)j}{}^i = 0, \quad (1.161)$$

since the metric variation of the topological invariant $\int d^2x \sqrt{\gamma} R$ vanishes completely. For $d = 4$ we obtain:

$$\tilde{\lambda}_{(4)} = \pi_{(4)k}{}^k = -\left(\frac{1}{24}R^2 + \frac{1}{8}R_j^i R_i^j\right), \quad (1.162)$$

which we may substitute in (1.150) to find an expression for $\tilde{\pi}_{(4)j}{}^i$ that we shall not write down here.

Counterterms and renormalization

The counterterm action is given by the terms with positive dilatation weight. Remembering that the metric determinant has weight d , we find for odd dimensions that

$$I_{\text{ct}} = -\frac{1}{2\kappa^2} \int d^d x \sqrt{\gamma} (\lambda_{(0)} + \lambda_{(2)} + \dots + \lambda_{(d-1)}) \quad (1.163)$$

and for even dimensions that

$$I_{\text{ct}} = -\frac{1}{2\kappa^2} \int d^d x \sqrt{\gamma} (\lambda_{(0)} + \lambda_{(2)} + \dots + r\tilde{\lambda}_{(d)}). \quad (1.164)$$

For all dimensions the renormalized on-shell action is given by:

$$I_{\text{ren}} = \lim_{r \rightarrow \infty} (I_{\text{bare}} + I_{\text{ct}}) = \lim_{r \rightarrow \infty} \frac{1}{2\kappa^2} \int d^d x \sqrt{\gamma} \lambda_{(d)}, \quad (1.165)$$

and we immediately obtain the renormalized one-point function of the energy-momentum tensor as:

$$\begin{aligned} \langle T_{ij}(x) \rangle_{g_{(0)}} &= \frac{2}{\sqrt{g_{(0)}(x)}} \frac{\delta}{\delta g_{(0)}^{ij}(x)} I_{\text{ren}} \\ &= \lim_{r \rightarrow \infty} \frac{-e^{(d-2)r}}{\kappa^2 \sqrt{\gamma(x)}} \frac{\delta}{\delta \gamma_{ij}(x)} \int d^d x \sqrt{\gamma} \lambda_{(d)} \\ &= - \lim_{r \rightarrow \infty} e^{(d-2)r} \frac{1}{\kappa^2} \pi_{(d)ij}, \end{aligned} \quad (1.166)$$

where we added a subscript $g_{(0)ij}$ on the left-hand side to indicate the nontrivial curved background metric. An explicit expression for $\pi_{(d)ij}$ can be found by using the Fefferman-Graham expansion. For example for $d = 2$ we have:

$$\gamma_{ij} = e^{2r} g_{(0)ij} + g_{(2)ij} + \dots \quad (1.167)$$

and

$$\begin{aligned}
 \pi_{(2)ij} &= \pi_{ij} - \pi_{(0)ij} + \dots \\
 &= K_{ij} - K\gamma_{ij} + \gamma_{ij} + \dots \\
 &= -g_{(2)ij} + g_{(0)ij} \text{tr}(g_{(0)}^{-1}g_{(2)}) + \dots
 \end{aligned} \tag{1.168}$$

where the dots represent terms that vanish as $r \rightarrow \infty$. Furthermore we may use the fact that $\pi_{(2)k}^k = -\frac{1}{2}R = -\frac{1}{2}e^{-2r}R_{(0)} + \dots$ to find that $\text{tr}(g_{(0)}^{-1}g_{(2)}) = -\frac{1}{2}R_{(0)}$. Our final result for $d = 2$ is then [27]:

$$\langle T_{ij} \rangle_{g_{(0)}} = \frac{1}{2\kappa^2}(2g_{(2)ij} + R_{(0)}g_{(0)ij}). \tag{1.169}$$

We will use this result in the upcoming chapters.

Ward identities and anomalies

In section 1.3 we formulated the conformal Ward identities in terms of the trace of the one-point function of the energy-momentum tensor. In particular, from (1.51) and (1.53) we find that in the absence of any other sources:

$$\mathcal{A}_w[g_{(0)}] = \langle T_i^i \rangle_{g_{(0)}}. \tag{1.170}$$

Explicit expressions can be found by taking the trace of (1.166) and substituting the above results for $\pi_{(d)k}^k$. We obtain [24, 25]:

$$\begin{aligned}
 \langle T_i^i \rangle_{g_{(0)}} &= -\frac{1}{\kappa^2} \lim_{r \rightarrow \infty} e^{dr} \pi_{(d)k}^k \\
 &= \begin{cases} 0 & d \text{ odd} \\ \frac{1}{2\kappa^2} R_{(0)} & d = 2 \\ \frac{1}{\kappa^2} \left(\frac{1}{24} R_{(0)}^2 + \frac{1}{8} R_{(0)j}^i R_{(0)i}^j \right) & d = 4 \end{cases}
 \end{aligned} \tag{1.171}$$

The final expressions were first obtained in [24]. They satisfy the Wess-Zumino consistency conditions and are therefore valid conformal anomalies. Notice that the asymptotic analysis was sufficient to find these holographic Weyl anomalies and we did not need to completely solve the equations of motion, in agreement with the general discussion of section 1.4.4.

For $d = 2$ we may recover the standard Virasoro central charge which in our conventions can be obtained from $\langle T_i^i \rangle_{g_{(0)}} = \frac{c}{24\pi}R$. We find:

$$c = \frac{12\pi}{\kappa^2} = \frac{3\ell}{2G_N}, \tag{1.172}$$

where we reinstated the AdS radius of curvature ℓ and used $\kappa^2 = 8\pi G_N$. This result agrees with [33]. Notice that the supergravity limit only applies when gravity

is weak and the AdS radius is large, so only when $c \gg 1$. This is the two-dimensional analogue of the large N limit discussed in section 1.1.

Finally we may also obtain the diffeomorphism Ward identity. This identity follows from the second equation of (1.131) which may be rewritten as:

$$\nabla_i \pi_j^i = 0 \tag{1.173}$$

Substituting now the expansion in terms of the dilatation operator we find that this directly leads to the conservation of the energy-momentum tensor:

$$\nabla_{(0)i} \langle T_j^i \rangle_{g_{(0)}} = 0, \tag{1.174}$$

where $\nabla_{(0)i}$ is the covariant derivative with respect to $g_{(0)ij}$. This is precisely (1.41) in the absence of sources. Notice again that the asymptotic analysis was sufficient to obtain this Ward identity.

Chapter 2

Real-time gauge/gravity duality

Since the advent of the AdS/CFT correspondence [9, 15, 16] a considerable amount of work has been devoted to developing holographic dualities leading to a very precise understanding of the ‘holographic dictionary’ that translates between bulk and boundary quantities. We sketched some aspects of this dictionary in the previous chapter and refer to the reviews [10, 11, 31] for more details. So far this dictionary was however always formulated in a purely ‘Euclidean’ regime, *i.e.* when the boundary theory is Wick-rotated and the corresponding bulk solution involves a positive-definite metric as well. While this suffices for many applications, there are also many reasons for obtaining a general *real-time dictionary* which can be used directly for Lorentzian signature backgrounds.

Indeed there is a wide range of applications for such a real-time prescription. To mention a few: one would like to understand better holography for time dependent backgrounds, to have a holographic description of non-equilibrium QFT and to be able to compute correlators in non-trivial states. Such a development would also be useful for applications of holography to modelling the dynamics of the quark-gluon plasma or condensed-matter systems, see [34, 35, 36] for reviews.

From a more theoretical perspective, one would like to understand better the interplay between causality and holography. Since bulk and boundary lightcones are different, it is not *a priori* clear that a bulk computation will produce the correct causal structure for boundary correlators, for example the correct $i\epsilon$ insertions. Conversely, one can ask how the bulk causal structure emerges from

boundary correlators. A related question is to understand how black hole horizons are encoded in boundary correlators. More generally one would like to study holographically the process of gravitational collapse.

In this chapter we develop a precise real-time gauge/gravity dictionary. Our formalism is applicable at the same level of generality as the corresponding Euclidean prescription and therefore constitutes an integral part of the definition of the holographic correspondence. More precisely, our setup is valid for all QFTs that have a holographic dual and is applicable for the holographic computation of arbitrary correlation functions of gauge-invariant operators in non-trivial states. Furthermore, the prescription is fully holographic, *i.e.* only boundary data and regularity in the interior are needed for the computations, and within the supergravity approximation all information is encoded in classical bulk dynamics.

There have been several earlier works discussing holography in Lorentzian signature, including [37, 38, 39, 40, 41, 42, 43, 44, 45, 46, 47]. One set of these papers is based on semi-classical quantization of the bulk fields around a classical bulk solution. For example, a case often discussed is that of the quantization of a free scalar field in AdS and the computation of the associated boundary 2-point function. Such results are clearly difficult to extend to cases where bulk interactions are essential because of the difficulty in quantizing the bulk gravitational theory. For example, higher point functions, correlators of the stress energy tensor and holographic RG flows are outside the remit of these works. Moreover, for the computation of the correlators in the supergravity limit one should not have to consider the quantization of the bulk theory at all – classical bulk dynamics should suffice.

A Lorentzian prescription that has been used widely in the literature is that of Son and Starinets [40]. This prescription leads to the computation of retarded 2-point functions and is based on imposing specific ‘ingoing’ boundary conditions in the interior of the spacetime. It leads to correct results (provided the infinities have been subtracted correctly) but is somewhat unsatisfactory from the holographic point of view, because it presumes the existence of a horizon in the bulk spacetime and ignores certain surface terms in the on-shell action. These issues can however be overcome once one embeds the prescription of [40] in our more general framework, as we explain in detail in chapter 4.

The remainder of this chapter is structured as follows. We begin with a review of real-time quantum field theory in section 2.1. Afterwards we present in section 2.2 the real-time gauge/gravity prescription. The holographic renormalization and computation of correlators in our prescription is discussed in detail for a scalar field in section 2.3 and for gravity in section 2.4. An appendix to this chapter contains further real-time quantum field theory results. In the next chapter we

apply the prescription to several concrete examples.

2.1 QFT preliminaries

In this section we review some aspects of real-time quantum field theory. In particular we discuss the specification of the initial and final states and the in-in formalism for non-equilibrium processes. The results in this section will be the springboard for the gauge/gravity prescription we present in the next section. For more details on real-time quantum field theory we refer to [48, 49, 50, 51].

2.1.1 Vacuum amplitudes

An essential ingredient for the computation of real-time correlation functions is the proper specification of the initial and final state. In this section we review how this is implemented for vacuum-to-vacuum amplitudes.

Consider a d -dimensional quantum field theory (QFT) defined on a Lorentzian spacetime with coordinates (t, \vec{x}) and with a set of fundamental fields collectively denoted as $\varphi(t, \vec{x})$. It is a standard result that the path integral on a segment $-T < t < T$ with the fields constrained to equal $\varphi_-(\vec{x})$ at $t = -T$ and $\varphi_+(\vec{x})$ at $t = T$ produces the transition amplitude $\langle \varphi_+, T | \varphi_-, -T \rangle$. This amplitude can be used as a building block for the vacuum amplitudes. Namely one multiplies this expression with the vacuum wave functions $\langle 0 | \varphi_+, T \rangle$ and $\langle \varphi_-, -T | 0 \rangle$ and integrates over $\varphi_+(\vec{x})$ and $\varphi_-(\vec{x})$ to produce the amplitude $\langle 0, -T | 0, T \rangle$. (As we review below, one may switch on sources between $-T$ and T in order to obtain nontrivial amplitudes as well.) The vacuum wave functions can be computed using a path integral corresponding to an infinite evolution in *imaginary* time. Indeed, such an infinite evolution, starting for example at $-T$, corresponds to a transition amplitude $\lim_{\beta \rightarrow \infty} \langle \varphi_-, -T | e^{-\beta H} | \Psi \rangle$ for some state $|\Psi\rangle$. By inserting a complete set of energy eigenstates one finds that taking the limit projects onto the vacuum wave function $\langle \varphi_-, -T | 0 \rangle$, times a factor $\langle 0 | \Psi \rangle$ which does not depend on φ_- and therefore only contributes to the overall normalization. We similarly obtain $\langle 0 | \varphi_+, T \rangle$ from an infinite evolution in imaginary time starting at $t = T$. The insertion of these wave functions is therefore equivalent to extending the fields in the path integral to live along a contour in the complex time plane as sketched in figure 2.1a.

These wave function insertions ultimately lead to the standard $i\epsilon$ factors in correlation functions. Namely one can deform the contour to a straight line that runs almost parallel to the real axis with only a slight downward slope in the complex

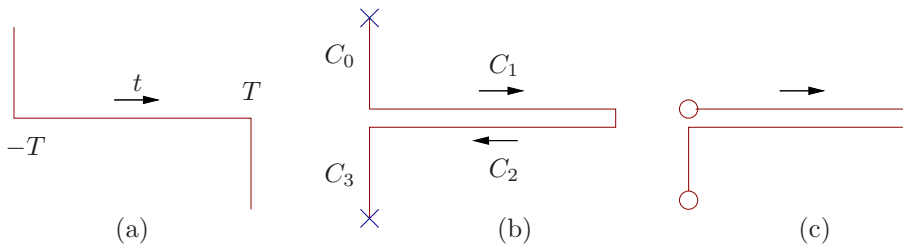


Figure 2.1: (a) Vacuum-to-vacuum contour. (b) In-in contour. (c) Real-time thermal contour. The circles reflect points that should be identified. The horizontal segments are on top of each other in the complex time plane, although they are separated in the figure.

time plane. This deformation does not affect the aforementioned projection onto the ground state. The downward slope in the contour is equivalent to replacing $t \rightarrow t(1 - i\epsilon)$. In appendix 2.A we review that this is precisely the correct $i\epsilon$ factor for Feynman propagators and also present a simple example where one may explicitly compute the vacuum wave functions.

2.1.2 In-in formalism

Let us now consider real-time correlation functions in nontrivial states, for example

$$\langle \Psi | \mathcal{O}(t) | \Psi \rangle = \langle \Psi | e^{i\hat{H}t} \mathcal{O} e^{-i\hat{H}t} | \Psi \rangle \quad (2.1)$$

for some state $|\Psi\rangle$ which is not an eigenstate of the Hamiltonian \hat{H} . The expression on the right-hand side demonstrates that we not only have to evolve the state $|\Psi\rangle$ forward in time before we insert the operator, but afterwards we also have to evolve *back* in time before we insert the final wave function. This results in the in-in or ‘closed time path’ formalism of [52, 53, 54, 55]. Extending the contour to go beyond the point t , say to some point t' , and then back again amounts to an insertion of the identity operator in the form $\exp[i\hat{H}(t' - t)] \exp[-i\hat{H}(t' - t)]$. Such an extension of the contour will not change the overall amplitude.

In the previous subsection we used the Euclidean path integral to create the vacuum state which is then fed into the Lorentzian path integral as the initial and final state. More generally, one can use the Euclidean path integral to generate other states that can serve as initial/final states for the Lorentzian path integral. Indeed, in the context of a conformal field theory on \mathbb{R}^d the relation between Euclidean path integrals and states is the basis for the operator-state correspondence: inserting a local operator \mathcal{O} , say at the origin of \mathbb{R}^d , and then performing the path integral over the interior of the sphere S^{d-1} that surrounds the origin results in

the corresponding quantum state $|\Psi_{\mathcal{O}}\rangle$ on S^{d-1} . In particular, the vacuum state is generated by inserting the identity operator.

We are thus led to a prescription for computing real-time correlation functions in a given initial state involving a closed time contour as sketched in figure 2.1b. In the figure, the vertical pieces C_0, C_3 represent Euclidean path integrals, with the crosses representing operator insertions. As described in the previous paragraph, these segments create the chosen initial state $|\Psi\rangle$ at a certain time. To compute real-time correlation functions one evolves this state forward and backward in time following the horizontal segments C_1 and C_2 and inserts operators on these segments.

The in-in formalism can also be applied to quantum field theory at a finite temperature T . The expectation values of gauge-invariant operators then become traces,

$$\langle \mathcal{O}(t) \rangle_{\beta} = \text{Tr}(\hat{\rho} \mathcal{O}(t)), \quad (2.2)$$

with $\hat{\rho} = \exp(-\beta \hat{H})$ the thermal density matrix and $\beta = 1/T$. By a repetition of the above arguments leading to the in-in contour, one finds that for real-time thermal correlators one can use the closed time path contour in figure 2.1c. The vertical segment now represents the thermal density matrix and has length β . The circles indicate points that should be identified and reflect the fact that thermal correlators satisfy appropriate periodicity conditions in imaginary time (bosonic/fermionic variables are periodic/antiperiodic). As in the discussion in the previous paragraph, one can compute real-time correlation functions by inserting operators on the horizontal segments. Other density matrices, for example a thermal density matrix with chemical potentials, may be obtained in a similar manner.

Besides the examples in figure 2.1 one may also consider more general deformations of the contour in the complex time plane. In fact, one may deform the contour into any other direction in complex coordinate space. Such deformations are allowed as long as the contour does not run upward in the complex time plane, since the spectrum of the operator $\exp(-i\hat{H}\Delta t)$ is bounded only for $\text{Im}(\Delta t) \leq 0$. Similar restrictions apply for deformations in other directions in complex coordinate space. In general, the ‘metric’ along such a deformed contour would be complex.

2.1.3 Generating functional

For all of the contours defined above one can write a generating functional of correlation functions of gauge-invariant operators in nontrivial states with the

following path integral representation:

$$Z_{\text{QFT}}[\phi_{(0)}^I; C] = \int_C [\mathcal{D}\varphi] \exp \left(i \int_C dt \int d^{d-1}x \sqrt{-g_{(0)}} \left(\mathcal{L}_{\text{QFT}}[\varphi] - \phi_{(0)}^I \mathcal{O}_I[\varphi] \right) \right). \quad (2.3)$$

Here φ denotes again collectively all QFT fields, $\phi_{(0)}^I$ are sources that couple to gauge invariant operators \mathcal{O}_I and $g_{(0)ij}$ is the spacetime metric (and also the source for the stress energy tensor T_{ij}). The path integral is defined for fields living on the contour C in the complex time plane. Therefore, we think of t as an *complex* time coordinate and $\int_C dt$ is then a contour integral. The partition function also depends on the shape of this contour.

For the piecewise horizontal and vertical contours like those in figure 2.1 one may split up the integral along C into a sum of integrals corresponding to the different segments of the contour. Let us exemplify this using the contour of figure 2.1b. The vertical segments C_0 and C_3 in the contour are associated with Euclidean path integrals, as discussed above. In these segments we can parametrize the contour using $t = -i\tau$ with τ a real coordinate along C and this substitution indeed results in the usual signs for a Euclidean path integral. (We demonstrate this in an example in appendix 2.A.) The segments C_1 and C_2 in figure 2.1b form a closed time path. It can be parametrized using a ‘contour time’ coordinate t_c that increases monotonically along the contour. In the segment C_1 we can simply set $t = t_c$, where now t_c ranges from 0 to T (where T may be ∞), and we can integrate along C_2 using $t = 2T - t_c$, with $T < t_c < 2T$. Notice that $dt = -dt_c$ on C_2 , which gives rise to an extra sign for the action on this segment.

For more general contours one finds an equivalent result. Instead of using a single complex t coordinate as in (2.3) one may always choose to parametrize the contour using real coordinates like τ and t_c . The action in (2.3) then reduces to the Euclidean action along the vertical segments of the contour and to the Lorentzian action along the horizontal segments, with an extra minus sign for backward-going horizontal segments.

Contour time-ordering

Upon functional differentiation with respect to the sources one may obtain correlation functions from the path integral (2.3). From the usual slicing arguments that lead to the path-integral representation it follows that the operators in these correlation functions are *contour-time-ordered*. That is, if we pick a real contour time parameter t_c that increases monotonically along the entire contour, then the operators in the correlation functions obtained from a path integral along this contour are ordered from small to large t_c .

To see the implications of contour time-ordering let us consider two-point functions for the in-in contour in figure 2.1b. Suppose that the source $\phi_{(0)}$ in (2.3) is nonzero only along the Lorentzian segments C_1 and C_2 . We parametrize this segment using the contour time coordinate t_c introduced above. The source-operator coupling can then be split in two parts and the partition function is defined as:

$$Z[\phi_{(0)[1]}, \phi_{(0)[2]}] = \langle \exp \left(-i \int_0^T dt_c d^{d-1} x \phi_{(0)[1]} \mathcal{O}_{[1]} + i \int_T^{2T} dt_c d^{d-1} x \phi_{(0)[2]} \mathcal{O}_{[2]} \right) \rangle, \quad (2.4)$$

where a subscript in square brackets denotes the segment on which the field lives. (We will adopt such a notation throughout this work.) The expectation values of course depend on the ensemble or state that is specified at $t = 0$, but we will not write this explicitly.

Via functional differentiation one obtains four possible two-point functions,

$$\langle \mathcal{T}_c \mathcal{O}_{[i]}(t, x) \mathcal{O}_{[j]}(t', x') \rangle = (-1)^{\delta_{ij}} \frac{\delta^2 Z}{\delta \phi_{(0)[i]}(t, x) \delta \phi_{(0)[j]}(t', x')} \Big|_{\phi_{(0)[1]} = \phi_{(0)[2]} = 0}, \quad (2.5)$$

with \mathcal{T}_c denoting contour-time-ordering. Along the first segment contour-time-ordering coincides with normal time-ordering,

$$\langle \mathcal{T}_c \mathcal{O}_{[1]}(t, x) \mathcal{O}_{[1]}(t', x') \rangle = \langle \mathcal{T} \mathcal{O}(t, x) \mathcal{O}(t', x') \rangle. \quad (2.6)$$

Along the second, backward-running segment, contour-time-ordering coincides with anti-time ordering, denoted by $\bar{\mathcal{T}}$,

$$\langle \mathcal{T}_c \mathcal{O}_{[2]}(t, x) \mathcal{O}_{[2]}(t', x') \rangle = \langle \bar{\mathcal{T}} \mathcal{O}(t, x) \mathcal{O}(t', x') \rangle. \quad (2.7)$$

If one puts one argument on the forward contour and the other on the backward contour, the latter one will always be later in contour time than the former and we get the Wightman functions:

$$\begin{aligned} \langle \mathcal{T}_c \mathcal{O}_{[1]}(t, x) \mathcal{O}_{[2]}(t', x') \rangle &= \langle \mathcal{O}_{[2]}(t', x') \mathcal{O}_{[1]}(t, x) \rangle = \langle \mathcal{O}(t', x') \mathcal{O}(t, x) \rangle, \\ \langle \mathcal{T}_c \mathcal{O}_{[2]}(t, x) \mathcal{O}_{[1]}(t', x') \rangle &= \langle \mathcal{O}_{[2]}(t, x) \mathcal{O}_{[1]}(t', x') \rangle = \langle \mathcal{O}(t, x) \mathcal{O}(t', x') \rangle. \end{aligned} \quad (2.8)$$

Notice that the in-in path is therefore suitable to obtain vacuum-to-vacuum Wightman functions from a path integral as well.

2.2 Prescription

We are now ready to present the real-time gauge/gravity prescription. In the previous section we discussed that the computation of real-time correlation functions requires a proper specification of the initial and final state, which is often

implemented via a contour in the complex time plane. In particular, for vacuum amplitudes the specification of the contour led to the proper $i\epsilon$ insertions in the correlation functions. Our starting point in the holographic description is that this contour dependence should be reflected in the bulk string theory, and in the low energy approximation it should be part of the supergravity description. Within the saddle-point approximation, our prescription is to associate supergravity solutions with QFT contours, or, more figuratively, to ‘fill in’ the *entire* QFT contour with a bulk solution. We have sketched several examples of such a construction in figure 3.1 on page 85.

One can think of the field theory contour C as a d -dimensional subspace of a complexified boundary spacetime. In most cases, as we saw above, this would be a line in the complexified time plane times a real space, $\mathbb{R} \times \Sigma^{d-1}$. The corresponding bulk solution should have C as its conformal boundary and the bulk fields Φ^I should satisfy boundary conditions parametrized by fields $\phi_{(0)}^I(t, \vec{x})$ living on C . In particular this holds for the bulk metric $G_{\mu\nu}$ whose boundary values should be given in terms of the boundary metric $g_{(0)ij}$ on the various segments of the contour. Since the signature of $G_{\mu\nu}$ is the same as that of $g_{(0)ij}$, we see that horizontal segments of C will be filled in with Lorentzian solutions, while vertical segments will be filled in with Euclidean solutions.¹ We denote the total bulk manifold consisting of all these segments as M_C . The signature of the metric on M_C then jumps at certain ‘corner’ hypersurfaces where the solution corresponding to a vertical segment meets with a horizontal one. These hypersurfaces end on the corners of the contour. Below we show how appropriate *matching conditions* control the behavior of the fields at these hypersurfaces.

Note that the bulk manifold is *not* necessarily of the form $\mathbb{R} \times X^d$ with $\partial X^d = \Sigma^{d-1}$. Instead, we can have more general bulk solutions that may ‘interpolate’ between various parts of the contour. An important example is the eternal BTZ black hole we consider below.

Given such a solution M_C that fills in the entire field theory contour C , the next step in the prescription is to compute the corresponding on-shell supergravity action. We may again write it as a single integral along a contour in complexified coordinate space:

$$I[\phi_{(0)}; C] = \int_{M_C} d^{d+1}x \sqrt{-G} \mathcal{L}_{\text{bulk}}^{\text{on-shell}} \quad (2.9)$$

Just as in field theory one may pass from the complex coordinate t to a real contour time variable τ or t_c . The vertical segments of the contour then involve the

¹We use the word ‘Euclidean’ for solutions that are obtained after some form of Wick rotation in the equations of motion. Normally the metric on these solutions is positive definite and they should be more properly called ‘Riemannian’. We will see in later sections, however, that the ‘Euclidean’ solutions can also involve a complex metric.

Euclidean on-shell action and horizontal segments the Lorentzian on-shell action, with factors of i and signs becoming standard in this description. Notice that this discussion does not require that t_c and τ extend globally on M , as the asymptotic analysis suffices to fix all signs.

The partition function of the quantum field theory is then given by a formula analogous to (1.31), namely:

$$Z_{QFT}[\phi_{(0)}; C] = \exp(iI[\phi_{(0)}; C]). \quad (2.10)$$

The sources $\phi_{(0)}$ that are localized in the conformal boundary of the Euclidean part of the solution are associated with the initial and final state, whereas sources on the conformal boundary of the Lorentzian solution lead to n -point functions upon differentiation.

Equation (2.10) is a bare relation, since both the bare QFT partition function and the bare on-shell supergravity action are divergent. We described in chapter 1 the procedure of holographic renormalization which is needed to render a Euclidean on-shell supergravity action finite. In section 2.2.2 we will describe how this procedure can be extended to on-shell actions integrated along a contour as in (2.10).

Notice that the Euclidean bulk solution which is associated with the initial state on the QFT side can also be thought of as providing a Hartle-Hawking wave function [56] for the bulk theory. Thus our prescription is not only QFT inspired but also in line with standard considerations on wave functions in quantum gravity, see also [39, 44] for related discussions. There has been considerable discussion in the literature over the choice of contour in the Euclidean path integrals and the reality conditions of the the semi-classical saddle point evaluation, see for example [57]. In our case, the bulk reality conditions are dictated by the boundary theory and, in particular, for a generic complex boundary contour the bulk manifold would have a complex metric (but in all cases the boundary correlators would satisfy standard reality conditions).

2.2.1 Corners

Piecewise straight contours have corners, where either a horizontal and a vertical segment meet or two horizontal segments join. These corners extend to hypersurfaces S in the bulk. The signature of the metric changes at the hypersurface corresponding to a corner of a horizontal and a vertical segment, but otherwise it remains unchanged. Modulo subtleties at the boundary of S , which we discuss in the next section, we impose the following two matching conditions at S :

1. We impose continuity of the fields across S . That is, we require the induced metric, the values of the scalars, and induced values of the other fields to be continuous;
2. If the contour passes from a segment M_- to M_+ , then we impose appropriate continuity of the conjugate momenta across S :

$$\pi_- = \eta\pi_+, \tag{2.11}$$

where π_{\pm} denote collectively the conjugate momenta of all fields on the two sides M_{\pm} of S (defined using a real time coordinate like t_c or τ), and $\eta = -i$ when we consider a Euclidean to a Lorentzian corner like for example from C_0 to C_1 in figure 2.1b, whereas $\eta = -1$ if we have a (non-trivial) Lorentzian to Lorentzian corner as from C_1 to C_2 in figure 2.1b. In all cases, the matching condition is equivalent to

$$\hat{\pi}_+ = \hat{\pi}_-, \tag{2.12}$$

where $\hat{\pi}$ is defined using the complex time variable t . In other words, if we use analytic continuation of the fields in the complex t coordinate to smooth out the corner by bending the contour, then the matching conditions dictate that the solution would be at least C^1 . In chapter 3 we illustrate with examples how these matching conditions determine the bulk solution for a given contour.

The on-shell supergravity action can be regarded as the saddle point approximation of the ‘bulk path integral’ which can also be used to justify the matching conditions in the following way. Recall that a path integral for fields living on a certain manifold can always be split in two by cutting the manifold in two halves and imposing boundary conditions for the fields on the cut surface. Afterwards, one can glue the pieces back together by imposing the same boundary condition on either side and then integrate over these boundary conditions.

The saddle-point approximation can similarly be performed in steps. After cutting the manifold, one first finds a saddle-point approximation on either side with arbitrary initial data at the cut surface. This replaces the partial path integrals on either side by an on-shell action which in particular depends on the initial data. Then, one imposes continuity of the initial data, which is the first matching condition, and performs a second saddle-point approximation with respect to the initial data. Since the first variation of an on-shell action with respect to boundary data yields the conjugate momentum, this second saddle-point precisely yields (2.11). The matching conditions should then be viewed as an equation determining the initial data. One may verify that the signs come out right, too.

2.2.2 Holographic renormalization

The fundamental holographic relation (2.10) is a bare relation because both sides are divergent: there are UV divergences on the QFT side and IR infinite volume divergences on the gravitational side. So appropriate renormalization is needed to make this relation well-defined. Below we will show that the procedure of holographic renormalization for the spaces under consideration is *a priori* more complicated, but that none of these complications enter in the final result. Therefore formulas like for example (1.117) on page 32 for the holographically computed one-point functions remain valid in the context of our real-time prescription as well. As the precise derivation of this result is not essential for the rest of the paper, the reader may wish to skip the remainder of this chapter on a first reading and proceed directly to the examples of chapter 3.

As we explained in the previous chapter, the holographic renormalization in the Euclidean case is done by introducing a set of local covariant boundary counterterms which render the on-shell action finite. In the Lorentzian setup, in addition to the infinities due to the non-compactness of the radial direction, there are also new infinities because of the non-compactness of the time direction. Correspondingly, in checking the variational problem one now has to deal both with boundary terms at spatial infinity and also at timelike infinity. Thus, in generalizing the Euclidean analysis to the Lorentzian case there are two issues to be discussed. First, one has to check that the Euclidean analysis that leads to the radial counterterms goes through when we move from Euclidean to Lorentzian signature. This is indeed the case because all steps involved in the derivation of the radial counterterms are algebraic and hold irrespectively of the signature of spacetime. The second issue one needs to analyze are the infinities due to the non-compactness of the time directions and the new boundary terms at timelike infinity. One possible approach to this issue would be to analyze the asymptotic structure of the solutions near timelike infinity, which as far as we know has not been performed. Our prescription bypasses this problem by gluing in Euclidean AdS manifolds near timelike infinity. This effectively pushes the asymptotic region to the (radial) boundary of the Euclidean AdS manifold, whose asymptotic structure is well known.

What remains to analyze is whether there are any problems at the ‘corners’, *i.e.* at the hypersurfaces where the Lorentzian and Euclidean solutions are joined. In principle, there can be new corner divergences which would require new counterterms. In the next two sections we show that such corner divergences are absent in two examples: a free massive scalar field in a fixed background and pure gravity. We expect such corner divergences to be absent in general.

2.3 Scalar field

This section serves to illustrate the holographic renormalization for the prescription (2.10), and we will therefore adopt the simplest possible setting. As indicated in figure 2.2, we consider here a single corner where the contour makes a right angle, passing from a vertical segment to a horizontal segment. The ‘space’ part of the boundary manifold is taken to be \mathbb{R}^{d-1} . In the absence of sources, we explain below how this contour can be ‘filled’ with empty AdS_{d+1} , with a metric that jumps along a spacelike hypersurface from Euclidean to Lorentzian. On this background, we consider a massive scalar field which propagates freely and without backreaction and we compute the renormalized one-point function of the dual operator.

2.3.1 Background manifold

For the bulk manifold under consideration, we take one copy M_1 of empty Lorentzian AdS_{d+1} in the Poincaré coordinate system (r, x^i) with the metric

$$ds^2 = dr^2 + e^{2r} \eta_{ij} dx^i dx^j, \quad (2.13)$$

and one copy M_0 of empty Euclidean AdS in similar coordinates and metric

$$ds^2 = dr^2 + e^{2r} \delta_{ij} dx^i dx^j. \quad (2.14)$$

We will take x^0 to be the time coordinate, denoting it by t on M_1 and τ on M_0 . We use the notation x^a for the other boundary coordinates, so for example $x^i = (t, x^a)$ on M_1 , and we also introduce $x^A = (r, x^a)$. The conformal boundaries of the spacetimes lie at $r \rightarrow \infty$ and are denoted $\partial_r M_1$ and $\partial_r M_0$.

Next, we perform the gluing and the matching. To this end, we cut off the spacetimes across the surface $t = 0$ and $\tau = 0$ such that $t > 0$ and $\tau < 0$, and glue them together along the cut surface which we call $\partial_t M$. This surface is the extension of the corner in the boundary to the bulk. The induced metric on $\partial_t M$ is the same on both sides,

$$h_{AB} dx^A dx^B = dr^2 + e^{2r} \delta_{ab} dx^a dx^b, \quad (2.15)$$

and the extrinsic curvature \mathcal{K}_{AB} vanishes on both sides. Therefore, both the conjugate momentum $\pi_{AB} = \mathcal{K} h_{AB} - \mathcal{K}_{AB}$ as well as the induced metric h_{AB} are continuous across $\partial_t M$ and all the matching conditions of section 2.2.1 are satisfied for this background. (We elaborate on the matching conditions for gravity in the next subsection.) The unit normals to $\partial_t M$ on either side are given by

$$n_{[1]\mu} dx^\mu = -e^r dt, \quad n_{[0]\mu} dx^\mu = e^r d\tau, \quad (2.16)$$

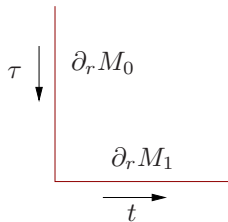


Figure 2.2: A single corner in the contour in the complex time plane. We use this part of a field theory contour to illustrate the holographic renormalization.

where we used subscripts in square brackets to indicate whether we are on M_1 or on M_0 .

Notice that the contour of figure 2.2 is not complete, since there is no out state specified at the right end of the contour. This should be remedied, for example by gluing a Euclidean segment at $t = T$ which would result in the vacuum-to-vacuum contour of figure 2.1a. In the bulk, this incompleteness means that we should also glue another solution to some ‘final’ hypersurface lying in M_1 . To obtain the contour of figure 2.1a, for example, one should glue in half a Euclidean solution M_2 . With \mathbb{R}^{d-1} as the spacelike manifold, this would result in a spacetime as sketched in figure 3.4a on page 98.

In this section we will focus on a single corner. We will therefore omit any contributions from such an M_2 , as well as some terms defined on the final matching surface for M_1 . Since the matching between M_1 and M_2 is a word-for-word repetition of the matching between M_0 and M_1 , these terms can be easily reinstated.

2.3.2 Scalar field setup

In the background we just described we consider a scalar field Φ of mass m , dual to a scalar operator \mathcal{O} of dimension Δ such that $m^2 = \Delta(\Delta - d)$. We will consider the case where $\Delta = d/2 + k$ with $k \in \{1, 2, 3, \dots\}$, and sometimes we will specialize to $k = 2$. The actions for Φ on M_1 and M_0 are respectively given by:

$$\begin{aligned} S_1 &= \frac{1}{2} \int_{M_1} \sqrt{-G} (-\partial_\mu \Phi \partial^\mu \Phi - m^2 \Phi^2), \\ S_0 &= \frac{1}{2} \int_{M_0} \sqrt{G} (\partial_\mu \Phi \partial^\mu \Phi + m^2 \Phi^2). \end{aligned} \tag{2.17}$$

Suppose Φ is a solution on M_0 and M_1 of the equations of motion derived from these actions, with asymptotic value corresponding to the radial boundary data

and furthermore satisfies the aforementioned matching conditions (which we discuss in more detail below) on the gluing surface. Our aim is then to compute the corresponding on-shell action,

$$iS_1 - S_0, \quad (2.18)$$

while using the method of holographic renormalization to make it finite. As we mentioned above, equation (2.18) can alternatively be written as:

$$\frac{i}{2} \int_C dt \int dr d^{d-1}x \sqrt{-G} (-\partial_\mu \Phi \partial^\mu \Phi - m^2 \Phi^2), \quad (2.19)$$

with a path C in the complex time plane as in figure 2.2, which goes down at first (yielding $-S_0$ after substituting $t = -i\tau$) and then makes a corner and lies along the real t axis. We will not use this notation in this example, but it will be relevant when we consider gravity below.

Let us repeat the essential ingredients of the holographic renormalization for the scalar field in Euclidean signature which we presented in section 1.5. The holographic renormalization relies on the fact that the solution Φ can (both on M_0 and on M_1) be written as a Fefferman-Graham expansion:

$$\Phi = e^{(k-d/2)r} (\phi_{(0)} + e^{-2r} \phi_{(2)} + \dots + e^{-2kr} [\phi_{(2k)} + \tilde{\phi}_{(2k)} \log e^{-2r}] + \dots). \quad (2.20)$$

In this expansion, the radial boundary data is given by specification of $\phi_{(0)}(x^i)$. As one can verify using the equation of motion for Φ , the coefficients $\phi_{(2n)}$ with $2n < 2k$, as well as $\tilde{\phi}_{(2k)}$, are *locally* determined by $\phi_{(0)}$. For example, for $k \neq 1$, we find

$$\phi_{(2)} = \frac{\square \phi_{(0)}}{4(k-1)}, \quad (2.21)$$

with \square the Laplacian of the boundary metric on $\partial_r M$, which in the case at hand is either η_{ij} or δ_{ij} . Similarly, all coefficients $\phi_{(2n)} \propto \square^n \phi_{(0)}$ for $n < k$ and $\tilde{\phi}_{(2k)} \propto \square^k \phi_{(0)}$, all with some k -dependent coefficients. The coefficient $\phi_{(2k)}$ is normally nonlocally determined by $\phi_{(0)}$, but in our case it also depends on the initial data that one may specify at $\partial_t M$. As we demonstrated in equation (1.117) in the previous chapter, in Euclidean backgrounds without corners this coefficient (times a factor $-2k$) is precisely the renormalized one-point function. Below, we show this is still the case in Lorentzian signature and in the presence of corners.

2.3.3 Matching conditions

Let us first discuss the matching conditions of subsection 2.2.1 for the scalar field. Consider two solutions Φ_1 and Φ_0 on M_1 and M_0 that satisfy the given radial

boundary data, but have arbitrary initial data. The first matching condition is continuity of Φ across $\partial_t M$, that is:

$$\Phi_0(\tau = 0, r, x^a) = \Phi_1(t = 0, r, x^a) \quad (2.22)$$

for all r and x^a .

To derive the second matching condition, we compute the on-shell action for Φ_0 and Φ_1 satisfying the equation of motion and the first condition (2.22). This action is divergent and we regulate it by cutting off the radial integrals at some large but finite r_0 . We then consider the variation of the regulated version of the total action (2.18) as we vary the initial data $\Phi(t = 0, r, x^a)$ and obtain

$$\delta(iS_1 - S_0) = \int_{\partial_t M} \sqrt{h} e^{-r} (-i\partial_t \Phi_1 - \partial_\tau \Phi_0) \delta\Phi_1, \quad (2.23)$$

where we used that $\delta\Phi_1 = \delta\Phi_0$ by (2.22). As explained in section 2.2, we then request that the total action is also at an extremum with respect to the initial data. The second matching condition thus becomes:

$$i\partial_t \Phi_1 + \partial_\tau \Phi_0 = 0 \quad \text{on } \partial_t M. \quad (2.24)$$

As we mentioned before (and as one may check easily using $t = -i\tau$), this second matching condition can be read as C^1 -continuity in the complex time plane of Φ across the corner. In the remainder of this section, whenever we write C^n -continuity, we always mean continuity in the complex time plane.

Now let us substitute the Fefferman-Graham expansion (2.20) of Φ_1 and Φ_2 in the matching conditions (2.22) and (2.24). The matching conditions imply the C^1 -continuity of all coefficients $\phi_{(2l)}$, which, in turn, implies higher-order continuity of the source $\phi_{(0)}$. For example, the first matching condition for $\phi_{(2)}$ becomes, via (2.21),

$$\square_{[1]} \phi_{(0)[1]} = \square_{[0]} \phi_{(0)[0]} \quad \text{on } \partial_t M, \quad (2.25)$$

which shows that $\phi_{(0)}$ has to be at least C^2 -continuous across the matching surface. Notice that this is again continuity in the complex time plane, since $\square_{[1]}$ is not equal to $\square_{[0]}$. Next, the second matching condition applied to $\phi_{(2)}$ actually implies C^3 -continuity for $\phi_{(0)}$:

$$i\partial_t \square_{[1]} \phi_{(0)[1]} + \partial_\tau \square_{[0]} \phi_{(0)[0]} = 0. \quad (2.26)$$

A similar story holds for the subsequent terms. Since the highest number of derivatives is always in $\tilde{\phi}_{(2k)} \propto \square^k \phi_{(0)}$, applying the second matching condition to this term results eventually in a C^{2k+1} -continuity condition for $\phi_{(0)}$ in the complex time plane. Below, we will see the relevance of these high-order continuity conditions.

A comment considering this smoothness condition for $\phi_{(0)}$ is in order. Namely, this continuity condition essentially follows from the requirement of the existence of a Fefferman-Graham expansion at the matching surface. In that light, this higher-order smoothness condition for $\phi_{(0)}$ is not surprising, since without it the Fefferman-Graham expansion would fail even in the case without a corner. Although it would be interesting to study what happens for discontinuous boundary data, such an investigation can be undertaken independently of the presence of corners and shall not be pursued here.

2.3.4 Holographic renormalization

The on-shell action (2.18), evaluated on the solution that satisfies the matching conditions, is of the form:

$$\begin{aligned}
 iS_1 - S_0 = & -\frac{i}{2} \int_{\partial_r M_1} \sqrt{-\gamma} \Phi_1 \partial_r \Phi_1 - \frac{1}{2} \int_{\partial_r M_0} \sqrt{\gamma} \Phi_0 \partial_r \Phi_0 \\
 & - \frac{1}{2} \int_{\partial_t M} \sqrt{h} [-i\Phi_1 \partial_t \Phi_1 + \Phi_0 \partial_\tau \Phi_0].
 \end{aligned} \tag{2.27}$$

The contributions from $\partial_t M$, *i.e.* the second line in (2.27), vanish by virtue of the matching conditions. Recall that we are omitting the contribution from any ‘final’ surface for M_1 , which will however by the same mechanism cancel against a matching solution.

The remainder of the action is defined on the cutoff surface $r = r_0$ and it would diverge if $r_0 \rightarrow \infty$. Therefore, a counterterm action has to be added before removing the cutoff. Since the radial terms in (2.27) have a familiar form, one can use precisely the same procedure of holographic renormalization as in section 1.5 to find the counterterm action. In particular, we found the counterterm action (1.112) for a scalar field with general k . Let us focus on the case $k = 2$, for which

$$S_{\text{ct}} = \frac{1}{2} \int_{\partial_r M} \sqrt{|\gamma|} \left((k - \frac{d}{2}) \Phi^2 + \frac{\Phi \square_\gamma \Phi}{2(1-k)} + \frac{1}{4} \Phi \square_\gamma^2 \Phi \log e^{-r} \right) \tag{2.28}$$

is the explicit counterterm action. The first two terms are actually valid for any $k \geq 2$ and we used the notation \square_γ for the Laplacian of the induced metric γ at $r = r_0$. In our case, we simply have $\square_\gamma = e^{-2r} \square_0$, both on M_1 and on M_0 . Taking care of the signs, we find that

$$iS_1 - S_0 + iS_{\text{ct},1} + S_{\text{ct},0} \tag{2.29}$$

is finite as $r_0 \rightarrow \infty$. We see that the usual procedure of holographic renormalization yields a finite on-shell action and possible initial or final terms (which might have caused corner divergences) are absent exactly by the matching conditions.

2.3.5 One-point functions

One-point functions are computed by taking variational derivatives of the on-shell action with respect to the boundary data. Let us compute the one-point function $\langle \mathcal{O}_{[1]}(x) \rangle$, where the subscript indicates that x lies on $\partial_r M_1$. In QFT on a background with a Lorentzian metric $g_{(0)ij}$, the coupling between a source $\phi_{(0)}$ and an operator \mathcal{O} in the partition function is as in (2.3). Therefore, the one-point function is

$$\langle \mathcal{O}_{[1]}(x) \rangle = \frac{i}{\sqrt{-g_{(0)}}} \frac{\delta}{\delta \phi_{(0)[1]}(x)} Z[\phi_{(0)}]. \quad (2.30)$$

In our case, the partition function $Z[\phi_{(0)}]$ is given by the renormalized on-shell supergravity action. The easiest way to take care of the divergences is by taking the functional derivative before removing the regulator, resulting in:

$$\langle \mathcal{O}_{[1]}(x) \rangle = \lim_{r_0 \rightarrow \infty} \frac{i e^{(k+d/2)r_0}}{\sqrt{-\gamma}} \frac{\delta}{\delta \Phi_1(x, r_0)} \left[i S_1 - S_0 + i S_{ct,1} + S_{ct,0} \right], \quad (2.31)$$

where the extra factor $e^{(k+d/2)r_0}$ converts Φ to $\phi_{(0)}$ and γ to $g_{(0)}$ as $r_0 \rightarrow \infty$.

In performing this computation, we see that the presence of corners gives rise to corner terms, which arise from the integration by parts that is necessary in varying the counterterm action (2.28). For example, for the variation of the second term in (2.28) we obtain:

$$\begin{aligned} \delta \left(\frac{1}{2} \int_{\partial_r M} \sqrt{|\gamma|} \frac{\Phi \square_\gamma \Phi}{2(1-k)} \right) = \\ \int_{\partial_r M} \sqrt{|\gamma|} \frac{\delta \Phi \square_\gamma \Phi}{2(1-k)} + \frac{1}{2} \int_{C_1} \sqrt{|\sigma|} \frac{e^{-2r} (\partial_t \Phi \delta \Phi - \Phi \partial_t \delta \Phi)}{2(1-k)}. \end{aligned} \quad (2.32)$$

The second term on the right hand side is a corner contribution. However, a similar corner term arises in $S_{ct,0}$, and in the total action (2.29) these two corner terms cancel each other precisely by the matching conditions.

The subsequent terms in the counterterm action are all of the form $\sqrt{\gamma} \Phi \square_\gamma^n \Phi$ for $n < k$, plus a log term of the form $\sqrt{\gamma} \Phi \square_\gamma^k \Phi \log e^{-r_0}$. After the integration by parts, these all give corner terms as well, which involve a higher number of derivatives of Φ . More precisely, the corner expressions that one obtains from such terms are of the form

$$\int_C \sqrt{\gamma} e^{-2r} \Phi \partial_t \square_\gamma^{n-1} \Phi, \quad (2.33)$$

and equivalent terms with some of the derivatives shifted to the first Φ .

Let us now systematically show that all such terms cancel against a matching solution, using the higher-order smoothness of $\phi_{(0)}$ that we derived before. First of

all, recall that the matching conditions imply that $\phi_{(0)}$ should actually be C^{2k+1} -continuous. This in turn means that $\phi_{(2)}$ is C^{2k-1} continuous, $\phi_{(4)}$ is C^{2k-3} -continuous, etc., up to $\tilde{\phi}_{(2k)}$ and $\phi_{(2k)}$, which are just C^1 -continuous. Substituting this in the Fefferman-Graham expansion (2.20), we see that Φ is not only C^1 -continuous by the matching conditions, but also C^3 -continuous up to terms of order $e^{-(k+d/2)r}$, and C^5 continuous up to terms of order $e^{(-k-d/2+2)r}$, etc.

We now rewrite the leading piece of (2.33) as

$$\int_C e^{(k+d/2-2n)r} \sqrt{g_{(0)}} \phi_{(0)} (\partial_t \square_0^{n-1} \Phi) + \dots \quad (2.34)$$

A complete cancellation of this term between M_1 and M_0 takes place if Φ is C^{2n-1} -continuous up to and including terms of order $e^{-(k+d/2-2n)r}$. However, the previous argument shows that C^{2n-1} -continuity for Φ holds up to terms of order $e^{-(k+d/2-2n+4)r}$, and the continuity condition is satisfied indeed, for all $n < k$. Therefore, as $r_0 \rightarrow \infty$, the terms coming from M_0 and M_1 cancel indeed and no corner contributions to the one-point functions arise. A similar argument shows that there is no problem with the log term with $n = k$ either.

Having shown the absence of corner contributions in (2.31), one finds that the expression for the one-point function becomes of the standard form, given for example for $k = 2$ by:

$$\langle \mathcal{O}_{[1]}(x) \rangle = \lim_{r_0 \rightarrow \infty} e^{k+d/2r_0} \left[\partial_r \Phi(x) - \left(k - \frac{d}{2}\right) \Phi(x) - \frac{\square_\gamma \Phi(x)}{2(1-k)} - \frac{1}{2} \square_\gamma^2 \Phi(x) \log e^{-2r} \right]_{r=r_0}. \quad (2.35)$$

Substitution of the expansion (2.20) yields:

$$\langle \mathcal{O}_{[1]}(x) \rangle = -2k \phi_{(2k)[1]}(x), \quad (2.36)$$

which is precisely the same result as (1.117) in section 1.5. Equation (2.36) is actually valid for all nonzero k .

Finally, consider the one-point function on M_2 , where we should use the Euclidean version of the source-operator coupling, $-\int \sqrt{g_{(0)}} \phi_{(0)[0]} \mathcal{O}_{[0]}$. Repeating the above procedure, we find again exactly the same result as in (1.117):

$$\langle \mathcal{O}_{[0]}(x) \rangle = -2k \phi_{(2k)[0]}(x). \quad (2.37)$$

Since $\phi_{(2k)}(x)$ is continuous across the matching surface by the first matching condition, and since localized corner terms are absent, the one-point function is continuous across the corner as well.

2.4 Gravity

For gravity the procedure requires modification and becomes more involved. We therefore begin with an outline of the steps taken below.

The first step is to establish the variational principle for the Einstein-Hilbert action for a manifold whose boundary has corners. Recall that in the Euclidean setup a well-defined variational problem requires the addition of the boundary counterterms [30] and the variational derivatives w.r.t. boundary data lead to the boundary correlators. In the Lorentzian setup the variational derivatives w.r.t. initial and final data are also important and lead to matching conditions. The analysis of the variational problem is done in subsection 2.4.2. We will find that there is a need for a special corner term.

The next step is to understand how to glue the various pieces together. Given a corner in the boundary contour there should exist a corresponding bulk hypersurface across which the various bulk pieces are matched. So we need to understand the possible bulk extensions of the boundary contour. This is analyzed in subsection 2.4.3 where we show that the extensions are parametrized by a single function $f(r, x^a)$ with a certain asymptotic expansion.

Using these results we then derive the matching conditions in subsection 2.4.4 and find their implications for the radial expansion of the bulk fields near the corner in 2.4.5. These are all the data we need to analyze whether there are any new contributions to the on-shell action and the one-point function from the matching surfaces. This is done for the on-shell action in subsection 2.4.6 and for the 1-point functions in subsection 2.4.7. We find that there are possible contributions from each segment but the matching conditions imply complete cancellation between the contributions of the two pieces that one glues to each other.

The upshot of the discussion is therefore very similar to the scalar field: we will show that no localized corner terms arise and that the one-point function of the stress energy tensor is (appropriately) continuous across the corner.

2.4.1 Setup

As we mentioned earlier, we consider manifolds M_C consisting of a number of segments M_j where the metric is Lorentzian or Euclidean. To simplify the computation of the on-shell action for these spacetimes, we use the notation involving the complex coordinate t as discussed in section 2.2. In this notation the Einstein-

Hilbert action S_j for each separate segment M_j is *always* written as

$$S_j = \frac{1}{2\kappa^2} \int_{M_j} d^{d+1}x \sqrt{-G}(R - 2\Lambda), \quad (2.38)$$

where $\kappa^2 = 8\pi G_{d+1}$ and $\Lambda = -d(d-1)/(2\ell^2)$ with ℓ the AdS radius. Throughout this chapter, we set $\ell = 1$. In (2.38) the square root is defined with a branch cut just above the real axis. For example, we obtain a Euclidean metric using $t = e^{-i\pi/2}\tau$, so $\sqrt{-G} = \sqrt{e^{-i\pi}|G|}$ which with our choice of branch cut becomes $-i\sqrt{|G|}$. This leads to $iS = -S_E$ with $S_E = \int \sqrt{|G|}(-R + 2\Lambda)$ the correct Euclidean action. Similarly, for a Lorentzian metric on a backward-going contour we obtain an extra minus sign since we are on the other branch of the square root. (To see this, notice that the time coordinate t_c on this segment is given by $t = e^{i\pi}t_c$. If G, G_c denote the metric determinant in the t, t_c coordinate system, respectively, then $G_c = e^{2\pi i}G$, and we make a full turn indeed.) The advantage of this formalism is that the total Einstein-Hilbert action S_{EH} for M_C becomes

$$iS_{EH} = iS_0 + iS_1 + \dots \quad (2.39)$$

for all vertical or horizontal segments M_0, M_1, \dots . We see that all the signs are absorbed in the volume element. This action for M_C needs to be supplemented with various surface terms which we define in due course.

Although we will not discuss this in detail, this prescription can be extended to general complex metrics, allowing for the ‘filling’ of more general QFT contours that are not just built up from horizontal and vertical segments in the complex time plane. In such cases the bulk metric $G_{\mu\nu}$ may be complex, but it should always be non-degenerate for the scalar curvature to be well-defined. Allowing for a complex metric implies that one has to allow for complex diffeomorphisms as well, for example to bring the metric to a Fefferman-Graham form. Complex diffeomorphisms are discussed in some detail in [57]. For such cases, our choice for the branch cut in the volume element is then precisely consistent with the requirement that a QFT contour cannot go upward in the complex time plane.

2.4.2 Finite boundaries

In equation (2.39), we split the on-shell action for M_C as a sum over the various segments M_i . Just as for the scalar field, we will find the matching conditions via a saddle-point approximation which involves taking functional derivatives of the on-shell action with respect to the initial and final data. This only works if we have a well-defined variational principle for each segment separately, which is what we investigate in this subsection.

Consider a single Asymptotically locally AdS (AlAdS) manifold M with a (possibly complex) metric $G_{\mu\nu}$ and two ‘initial’ and ‘final’ boundaries which we denote here as $\partial_{\pm}M$. The manifold M also has a radial conformal boundary, which we denote as ∂_rM , and the corners where $\partial_{\pm}M$ meets ∂_rM are denoted as C_{\pm} . We pick coordinates (r, x^i) on M , with $x^i = (t, x^a)$, and we will also use $x^A = (r, x^a)$. The conformal boundary is again at $r \rightarrow \infty$. We regulate the computation of the on-shell action by imposing $r < r_0$. In this subsection we consider the variational principle in the case where one keeps r_0 finite throughout.

A well-defined variational principle for Dirichlet boundary conditions in the presence of corners requires the Einstein-Hilbert action to be supplemented not only with the usual Gibbons-Hawking boundary terms on ∂_rM and $\partial_{\pm}M$, but also with special corner terms defined on C_{\pm} [58, 59, 60]. To find these corner terms, we choose coordinates such that ∂_rM is given by $r = r_0$ and $\partial_{\pm}M$ by $t = t_{\pm}$. The metric near the corners can be put in the following two ADM-forms:

$$\begin{aligned} G_{\mu\nu}dx^{\mu}dx^{\nu} &= (\hat{H}^2 + \hat{H}_i\hat{H}^i)dr^2 + 2\hat{H}_i dx^i dr + \hat{\gamma}_{ij}dx^i dx^j, \\ \hat{\gamma}_{ij}dx^i dx^j &= (-\hat{M}^2 + \hat{M}_a\hat{M}^a)dt^2 + 2\hat{M}_a dx^a dt + \sigma_{ab}dx^a dx^b, \end{aligned} \quad (2.40)$$

as well as

$$\begin{aligned} G_{\mu\nu}dx^{\mu}dx^{\nu} &= (-M^2 + M_A M^A)dt^2 + 2M_A dx^A dt + h_{AB}dx^A dx^B, \\ h_{AB}dx^A dx^B &= (H^2 + H_a H^a)dr^2 + 2H_a dx^a dr + \sigma_{ab}dx^a dx^b. \end{aligned} \quad (2.41)$$

Relating the two metrics, we find

$$\begin{aligned} H^2 &= \frac{\hat{H}^2 M^2}{M^2 + (M^r)^2 \hat{H}^2} & \hat{H}_t &= M_r \\ \hat{M}^2 &= M^2 - (M^r)^2 H^2 & -\frac{M^r}{M^2} &= \frac{\hat{H}^t}{\hat{H}^2}. \end{aligned} \quad (2.42)$$

For a real Lorentzian metric M^2 and \hat{M}^2 are positive, whereas they are negative for a Euclidean metric. We will henceforth assume that σ , the determinant of σ_{ab} , is real and positive. This will simplify the discussion and is sufficient for all the examples below.

The standard Gibbons-Hawking-York surface terms involve the extrinsic curvature ${}^{\pm}\mathcal{K}_{AB}$ of $\partial_{\pm}M$ and \hat{K}_{ij} of ∂_rM , which we will define using the (possibly complex) unit normals,

$$\begin{aligned} \partial_rM : \hat{n}_{\mu}dx^{\mu} &= \frac{\sqrt{-G}}{\sqrt{-\hat{\gamma}}} dr \rightarrow \hat{K}_{ij} = \frac{\sqrt{\hat{H}^2 \hat{M}^2}}{2\sqrt{\hat{M}^2 \hat{H}^2}} (\hat{D}_i \hat{H}_j + \hat{D}_j \hat{H}_i - \partial_r \hat{\gamma}_{ij}), \\ \partial_{\pm}M : {}^{\pm}n_{\mu}dx^{\mu} &= \pm \frac{\sqrt{-G}}{\sqrt{h}} dt \rightarrow {}^{\pm}\mathcal{K}_{AB} = \pm \frac{\sqrt{H^2 M^2}}{2\sqrt{H^2 M^2}} (D_A M_B + D_B M_A - \partial_t h_{AB}). \end{aligned} \quad (2.43)$$

Adding the Gibbons-Hawking-York terms, we define the bare action as:

$$S_b = \frac{1}{2\kappa^2} \left[\int d^{d+1}x \sqrt{-G} (R - 2\Lambda) + 2 \int_{\partial_{\pm} M} d^d x \sqrt{h} {}^{\pm}\mathcal{K} + 2 \int_{\partial_r M} d^d x \sqrt{-\hat{\gamma}} \hat{K} \right], \quad (2.44)$$

where here and below the summation over $\partial_{\pm} M$ is implicit and we use the conventions given above for the square roots. For a real Lorentzian metric all the above terms are real, but for a real Euclidean metric all terms in (2.44) are purely imaginary (because $\sqrt{-G}$ and $\sqrt{-\hat{\gamma}}$ are then imaginary, from which it follows that ${}^{\pm}n_{\mu} dx^{\mu}$ and therefore ${}^{\pm}\mathcal{K}$ are imaginary as well). As one may verify explicitly, in the latter case our choice of branch cut for the square roots in the volume elements implies that $iS_b = -S_E$ with S_E the Euclidean action with the correct Gibbons-Hawking-York terms.

In the case of corners, (2.44) is not the correct action to use for Dirichlet boundary conditions. This is because we cannot perform a diffeomorphism at the corner mixing t and r without changing the definition of the two slices and therefore \hat{H}_t , M_r , M^2 and \hat{H}^2 are no longer pure gauge at the corner. With this in mind, the variation of the bare action (2.44) is given by the equations of motion, the conjugate momenta for all the various boundaries, plus a corner term

$$\delta S_b = \frac{1}{2\kappa^2} \int_{C_{\pm}} d^{d-1}x \sqrt{\sigma} \delta X_{\pm} + \dots, \quad (2.45)$$

with X given implicitly by

$$\delta X_{\pm} = \pm 2 \frac{\sqrt{H^2 M^2}}{M^2} \delta M^r. \quad (2.46)$$

To find an explicit form of X_{\pm} , we have to integrate δX for fixed \hat{M}^2 and H^2 , using the relations (2.42). If the metric is completely real and H^2 and \hat{M}^2 are positive, then we find

$$\delta X_{\pm} = \pm 2 \delta \operatorname{arcsinh} \left(\frac{H M^r}{\hat{M}} \right), \quad (2.47)$$

whereas if \hat{M}^2 is negative and H^2 and M^r are positive we get

$$\delta X_{\pm} = \mp 2i \delta \arccos \left(\frac{H M^r}{\sqrt{-\hat{M}^2}} \right). \quad (2.48)$$

We can rewrite these expressions in a covariant form using the unit normals defined in (2.43). Their inner product is given by:

$${}^{\pm}n^{\mu} \hat{n}_{\mu} = \pm \frac{\sqrt{H^2}}{\sqrt{\hat{M}^2}} M^r. \quad (2.49)$$

For real M^2 , $\sqrt{H^2}$ and \hat{M}^2 , we can therefore write without branch cut ambiguities:

$$X_{\pm} = \begin{cases} 2 \operatorname{arcsinh}(\pm n^{\mu} \hat{n}_{\mu}) & \hat{M}^2 > 0 \\ -2i \operatorname{arcsin}(i \pm n^{\mu} \hat{n}_{\mu}) & \hat{M}^2 < 0. \end{cases} \quad (2.50)$$

In the more general case, the required corner term has the same structure but one needs to be careful about the branch cuts. Notice that X is defined up to a local piece, for example a constant.

Following [58, 59, 60], we aim for a variational principle that is well-defined for a fixed induced metric on the boundaries, *i.e.* for fixed $\hat{\gamma}_{ij}$ and h_{AB} . In that case, we should add a corner term to cancel the unwanted variation δX in (2.45). Such a corner term is given by

$$S_{C_{\pm}} = -\frac{1}{2\kappa^2} \int_{C_{\pm}} d^{d-1}x \sqrt{\sigma} X_{\pm}. \quad (2.51)$$

Adding corner terms to the action (2.44) defines an improved (but still bare) action S_I ,

$$\begin{aligned} S_I &= S_b + S_{C_{\pm}} \\ &= \frac{1}{2\kappa^2} \left[\int d^{d+1}x \sqrt{-G} (R - 2\Lambda) + 2 \int_{\partial_{\pm} M} d^d x \sqrt{h} \pm \mathcal{K} \right. \\ &\quad \left. + 2 \int_{\partial_r M} d^d x \sqrt{-\hat{\gamma}} \hat{K} - \int_{C_{\pm}} d^{d-1}x \sqrt{\sigma} X_{\pm} \right], \end{aligned} \quad (2.52)$$

whose variation is of the form

$$\begin{aligned} \delta S_I &= \frac{1}{2\kappa^2} \left[\int_{\partial_r M} \sqrt{-\hat{\gamma}} (\hat{\gamma}^{ij} \hat{K} - \hat{K}^{ij}) \delta \hat{\gamma}_{ij} + \int_{\partial_{\pm} M} \sqrt{h} (h^{AB} \pm \mathcal{K} - \pm \mathcal{K}^{AB}) \delta h_{AB} \right. \\ &\quad \left. - \int_{C_{\pm}} d^{d-1}x \delta(\sqrt{\sigma}) X_{\pm} \right], \end{aligned} \quad (2.53)$$

which is the correct variation for Dirichlet boundary conditions indeed. We will henceforth use this improved action as the bare action and drop the subscript I .

2.4.3 Fefferman-Graham coordinates

The above discussion was valid for a general spacetime whose boundary has corners. Since we are interested in AlAdS spacetimes where the metric diverges near the radial boundary, we will run into divergences as we let $r_0 \rightarrow \infty$. To investigate these divergences, we pick a coordinate system in which the metric is of the Fefferman-Graham form,

$$ds^2 = dr^2 + \gamma_{ij} dx^i dx^j, \quad (2.54)$$

with the radial expansion

$$\gamma_{ij} = e^{2r}(g_{(0)ij} + e^{-2r}g_{(2)ij} + \dots + e^{-dr}[g_{(d)ij} + \tilde{g}_{(d)ij} \log e^{-2r}] + \dots). \quad (2.55)$$

As we explained in section 1.6, from the Einstein equations we find that all coefficients $g_{(2n)ij}$ with $2n < d$, as well as $\tilde{g}_{(d)ij}$, are locally determined by $g_{(0)ij}$ and involve up to $2n$ or d derivatives of $g_{(0)ij}$. The term $g_{(d)ij}$ is not locally determined (except for its trace and its divergence) and this term directly enters in the one-point function of the stress energy tensor (see equation (1.169) for $d = 2$ and [27] for the explicit expressions in other dimensions).

The disadvantage of the Fefferman-Graham form of the metric is that one can generally no longer pick a coordinate t such that the surfaces $\partial_{\pm}M$ are given by slices of constant t . On the other hand, one can use the leftover gauge freedom to make sure that $\partial_{\pm}M$ are asymptotically given by:

$$\partial_{\pm}M : t = f_{\pm}(r, x^a), \quad (2.56)$$

with

$$\lim_{r \rightarrow \infty} f_{\pm}(r, x^a) = t_{\pm} \quad (2.57)$$

and t_{\pm} constants. We will discuss the asymptotic behavior of f_{\pm} more precisely below.

Let us consider a single initial or final boundary. Dropping for now the subscript \pm , we write an ADM-decomposition of γ_{ij} near the corner:

$$\gamma_{ij}dx^i dx^j = (-N^2 + N^a N_a)dt^2 + 2N_a dt dx^a + \tau_{ab} dx^a dx^b. \quad (2.58)$$

We may pick boundary Gaussian normal coordinates centered at the corner, so that $N_a \sim O(1)$. Furthermore, $N^2 = e^{2r}N_{(0)}^2 + N_{(2)}^2 + \dots$ and $\tau_{ab} = e^{2r}\tau_{(0)ab} + \tau_{(2)ab} + \dots$. We can relate this ADM-decomposition to the double ADM-decomposition (2.41) of the previous subsection by introducing a new coordinate

$$t' = t - f(r, x^a), \quad (2.59)$$

after which the initial slice is given by $t' = 0$. In the new coordinates, the metric is of the form (2.41), with t replaced by t' , and with the components

$$\begin{aligned} -M^2 + M_A M^A &= -N^2 + N_a N^a \\ M_r &= (-N^2 + N_a N^a) \partial_r f \\ M_a &= N_a + (-N^2 + N_c N^c) \partial_a f \\ H^2 + H_a H^a &= 1 + (-N^2 + N_a N^a) (\partial_r f)^2 \\ H_a &= (-N^2 + N_c N^c) \partial_a f \partial_r f + N_a \partial_r f \\ \sigma_{ab} &= \tau_{ab} + (-N^2 + N_c N^c) \partial_a f \partial_b f + N_a \partial_b f + N_b \partial_a f, \end{aligned} \quad (2.60)$$

where indices are raised with the appropriate metric. We use these equations below to write down a radial expansion of the components on the left-hand side in terms of the Fefferman-Graham expansion and a radial expansion of f .

For AlAdS spacetimes the Dirichlet boundary data are given by $g_{(0)ij}$ and h_{AB} . Asymptotically, $g_{(0)ij}$ determines a Fefferman-Graham radial coordinate as well as the subleading coefficients up to $g_{(d)ij}$ in the Fefferman-Graham expansion of the metric. Of course, the initial and final metric h_{AB} should be such that $\partial_{\pm}M$ can be embedded in the asymptotic metric dictated by $g_{(0)ij}$ and this condition constrains the asymptotic form of h_{AB} . To be precise, h_{AB} should have a radial expansion that is compatible with the last three equations in (2.60) for a certain f . However, as long as f is unspecified, h_{AB} is not to any order determined in terms of $g_{(0)ij}$.

We remark that the last three lines in (2.60) signify constraints on h_{AB} only. Therefore, they are different from the usual constraints on the initial data in a Hamiltonian formalism of general relativity, which also involve the extrinsic curvature. These usual constraints are satisfied if the extrinsic curvature of the initial slice is computed using the embedding of the initial slice as a hypersurface in the solution. Therefore, they are automatically satisfied if we compute the extrinsic curvature using the first three lines of (2.60). Since this is how we compute the extrinsic curvature below, we will not worry about these constraints.

2.4.4 Gluing and matching conditions

In the previous subsections, we found an improved action (2.52) and discussed the Fefferman-Graham expansion for a single AlAdS spacetime with corners. We now take two of such spacetimes and glue them together along the initial and final hypersurfaces $\partial_{\pm}M$.

We will denote the two segments by M_0 and M_1 and we glue ∂_+M_0 to ∂_-M_1 , which we from now on we denote as ∂_tM . The corner, *i.e.* the intersection of ∂_tM with ∂_rM_0 and ∂_rM_1 , is denoted by C . As before, a subscript (sometimes in square brackets) indicates the manifold under consideration. We make no assumptions about the signature of the metric on M_0, M_1 and in fact the metric may even be complex. We write the total action as

$$iS_0 + iS_1, \tag{2.61}$$

with the individual actions given by (2.52). We recall that we use the conventions of subsection 2.4.1, so extra factors of i might be included in the volume elements and extrinsic curvatures. As we did for the scalar field, we will henceforth ignore

the contribution from other segments than M_0 and M_1 as well as the contribution to the on-shell actions of M_0 and M_1 that may arise from other matching surfaces.

Let us now find the precise matching conditions that the metrics on M_0 and M_1 have to satisfy near $\partial_t M$. The first matching condition is continuity of the initial and final Dirichlet data. For gravity, this becomes continuity of the induced metric:

$$h_{[0]AB} = h_{[1]AB}. \quad (2.62)$$

The second matching condition is obtained from the variation of the on-shell regularized action with respect to the data on $\partial_t M$. Let us first suppose the variation vanishes at the corner C . In that case, we read off from (2.53) that the second matching condition becomes:

$$\mathcal{K}_{[0]AB} + \mathcal{K}_{[1]AB} = 0. \quad (2.63)$$

We can also consider a variation that does not vanish at C , for which (2.53) shows that

$$(X_{[1]} + X_{[0]})\delta(\sqrt{\sigma}) = 0, \quad (2.64)$$

where we included the $\delta(\sqrt{\sigma})$ because of the following reason. Notice that this is a corner matching condition which is therefore not valid to all orders in r . However, since $\sqrt{\sigma} \sim e^{(d-1)r}$, (2.64) is actually divergent as $r_0 \rightarrow \infty$. Therefore, it only vanishes completely if the X 's match to high order in their radial expansion. If there are no log terms, then we find

$$X_{[1]} + X_{[0]} = O(e^{-dr}). \quad (2.65)$$

Equation (2.65) is the corner analogue of the bulk matching condition (2.63). Notice that such a corner condition was absent when we discussed the scalar field discussed above. Its implications will be investigated in the next subsection.

We showed before that \mathcal{K}_{AB} and X are imaginary for a Euclidean metric. Therefore, although it is not transparent in our notation, the matching conditions (2.63) and (2.65) do contain factors of i when joining a Lorentzian to a Euclidean metric.

2.4.5 Imposing the matching conditions

For the scalar field, the matching conditions were crucial in demonstrating the cancellation of corner divergences and the absence of localized corner contributions to the one-point function. A similar cancellation will occur for gravity, but imposing the three matching conditions (2.62), (2.63) and (2.65) will not be as straightforward as for the scalar field.

In this subsection we shall impose the matching conditions order by order in a radial expansion of h_{AB} , \mathcal{K}_{AB} and X . We start with a detailed analysis of the leading-order terms in the matching conditions. We then discuss continuity in the complex time plane of the boundary metric. Just as for the scalar field, the higher-order continuity is related to the continuity of the subleading terms in the Fefferman-Graham expansion of the bulk metric. Afterwards, we show that our leading-order results extend to the higher-order terms as well.

Leading order matching conditions

We will work in the Fefferman-Graham coordinates, with the matching surface $\partial_t M$ given by (2.56). Without loss of generality, we assume that the corner is given by $t = 0$ on $\partial_r M_1$ and $\tau = 0$ on $\partial_r M_0$, so $\lim_{r \rightarrow \infty} f(r, x^a) = 0$ on either side. We suppose that f behaves asymptotically as

$$f = e^{-r} f_{(1)}(x^a) + \dots \quad (2.66)$$

This is generally the leading asymptotic behavior of f , since any slower falloff near $r \rightarrow \infty$ would yield a non-spacelike induced metric on $\partial_t M$ in a real Lorentzian spacetime. Substituting the expansion (2.66) and the leading-order terms in the ADM-decomposition (2.58) of γ_{ij} in (2.60), we find the leading behavior of H^2 , M^2 and M^r . The inner product between the unit normals, given in (2.49), becomes to leading order:

$$\pm n^\mu \hat{n}_\mu = \mp \frac{\sqrt{N_{(0)}^2} f_{(1)}}{\sqrt{1 - N_{(0)}^2 f_{(1)}^2}}. \quad (2.67)$$

Since continuity of X_\pm follows from continuity of $\pm n^\mu \hat{n}_\mu$, the corner matching condition (2.65) becomes to leading order:

$$\sqrt{N_{(0)[0]}^2} f_{(1)[0]} = \sqrt{N_{(0)[1]}^2} f_{(1)[1]}, \quad (2.68)$$

where we reinstated the subscripts to indicate the manifold under consideration.

Let us work out the consequences of this condition. Recall that we absorbed factors of i in the square roots of the metric determinant, and therefore (2.68) is not necessarily a relation between real quantities. For example, if we match a Lorentzian to a Euclidean solution, then $N_{(0)}^2$ changes sign across the corner and the square root on the Euclidean side of (2.68) becomes imaginary. On the other hand, the square root on the Lorentzian side is real, and so is $f_{(1)}$ since we use real coordinates. This means that in that case we must have:

$$f_{(1)[0]} = f_{(1)[1]} = 0, \quad (2.69)$$

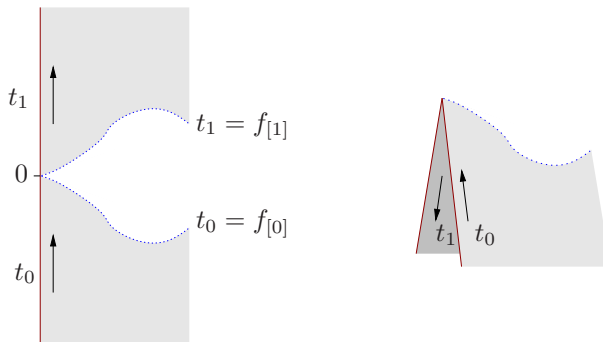


Figure 2.3: On the left, the dotted lines represent two bulk hypersurfaces given by $t = f$ in the vicinity of a corner in the boundary contour at $t = 0$. On the right, we see that around a full turn in the boundary contour it is natural to expect that $f_{[1]} = -f_{[0]}$.

which more generally holds in all cases for which the phase of $N_{(0)}^2$ is discontinuous across the corner. Actually, this phase is only continuous when we match two solutions with the same signature (recall that we chose boundary coordinates in which $N_{a(0)} = 0$). This happens either if we have no corner at all, or if the corner makes a 180-degree turn. In the first case, we can pick boundary coordinate systems in which $N_{(0)}^2$ is continuous across the corner and (2.68) becomes simply

$$f_{(1)[0]} = f_{(1)[1]} . \quad (2.70)$$

Since we just artificially split a spacetime in two parts, it is natural that there is no further constraint on f . The case in which the corner makes a full turn is slightly more involved. First of all, the two boundary segments ending on the corner must be straight horizontal lines in the complex time plane, since the boundary contour cannot go up in this plane. We may again assume that $N_{(0)}^2$ is continuous across the corner, but that does not mean that the square roots in (2.68) are. Namely, one of the segments is backward-going in the complex time plane and in subsection 2.4.1 we already mentioned that the square root for a backward-going contour results in a minus sign. The matching condition for a full turn therefore becomes

$$f_{(1)[0]} = -f_{(1)[1]} . \quad (2.71)$$

This implies that, at least at this order, we can freely move the hypersurface $\partial_t M$ up and down in the bulk, as long as we move it by the same amount on both components and keep the location of the corner fixed. We have sketched this in figure 2.3.

We have worked out the leading order term in the corner matching condition in three cases, corresponding to three different corners. We emphasize that our

formalism of subsection 2.4.1 allowed us to summarize all three cases in the single equation (2.68). We will see below that the subleading behavior of f is constrained in an analogous way.

As a sidenote, let us also compute the leading order term in the radial expansion of the second matching condition (2.63). If we use (2.43) to expand the trace of the extrinsic curvature ${}^{\pm}\mathcal{K}_{AB}$ the leading order term becomes:

$${}^{\pm}\mathcal{K} = \pm d \frac{\sqrt{N_{(0)}^2} f_{(1)}}{\sqrt{1 - N_{(0)}^2 f_{(1)}^2}}. \quad (2.72)$$

The trace part of (2.63) therefore results to leading order again in (2.68). It is plausible that for AlAdS spacetimes the corner matching condition (2.65) follows from (2.63) and does not need to be imposed separately. This would be related to the fact that the asymptotics of the bulk metric are completely determined by the Fefferman-Graham data, but a more complete analysis is required to settle this issue completely. This will not be attempted here and we will instead continue to treat (2.65) as an additional condition.

Continuity in the complex time plane

Just as for the scalar field, the Fefferman-Graham expansion relates subleading terms in the matching conditions to higher-order continuity in the complex time plane of the sources. Before proceeding with the subleading terms in the matching conditions, let us therefore first discuss the notion of smoothness in the complex time plane for the boundary metric.

Consider a contour in the complex time plane with a corner. We will define C^k -smoothness for the boundary metric as the condition that the k 'th order t -derivatives of the metric components exist and are continuous at the at the corner of the contour. Although this is a natural definition, in our notation a complication arises because we do not work directly with a complex time coordinate on for example the vertical segments. Instead, we rather use a contour time like t_c or τ which is real on a particular segment of the contour and for such parametrizations the continuity condition has a different form. We may find this new form by regarding these local parameters as related to t via a *complex* diffeomorphism, for example $t = -i\tau$ or $t = 2T - t_c$. If we use these parameters to express continuity of the metric, then we need to take care of the transformation properties under the diffeomorphism as well. For example, C^0 continuity of $g_{(0)ij}$ across the corner of figure 2.2, where $t = -i\tau$, becomes the condition that at the corner

$$g_{(0)[0]\tau\tau} = -g_{(0)[1]tt}, \quad g_{(0)[0]\tau a} = -i g_{(0)[1]ta}, \quad g_{(0)[0]ab} = g_{(0)[1]ab}. \quad (2.73)$$

Similarly, C^1 continuity in the complex time plane becomes

$$\partial_\tau(g_{(0)[0]ab}) = -i\partial_t(g_{(0)[1]ab}), \quad \partial_\tau(g_{(0)[0]\tau\tau}) = i\partial_t(g_{(0)[1]tt}). \quad (2.74)$$

The extension to higher orders and other components is analogous. As an example, take $ds_{[0]}^2 = d\tau^2 + \delta_{ab}dx^a dx^b$ and $ds_{[1]}^2 = -dt^2 + \delta_{ab}dx^a dx^b$. Although there is an apparent discontinuity in the metric components, with our definitions the metric is C^∞ at the corner.

We will from now on *assume* that the boundary metric at the corner is C^d continuous in the complex time plane. The reason for this smoothness condition is the same as that for the scalar field: it guarantees the existence of a Fefferman–Graham expansion of the metric at the corner, and the locally determined coefficients in this expansion are then automatically continuous across the corner as well. Since we continue to use real coordinates like τ , we will always need to supplement the continuity condition with the transformation under the complex diffeomorphism.

Higher order matching conditions

We showed above that the leading order matching conditions imply that $f_{(1)}$ usually vanishes, except in special cases when $N_{(0)}^2$ does not change across the corner. In this subsection, we show that the matching conditions and the C^d continuity of the boundary metric fix the higher-order terms in f to behave just as $f_{(1)}$, at least up to terms that vanish faster than e^{-dr} .

We first assume that the leading order term in f is:

$$f(r, x^a) = e^{-nr} f_{(n)}(x^a). \quad (2.75)$$

One may easily check that in this case

$$\pm n^\mu \hat{n}_\mu = \mp \sqrt{N_{(0)}^2} f_{(n)} e^{(1-n)r} + \dots \quad (2.76)$$

and a repetition of the previous analysis shows that, for $n \leq d$, the leading order term in (2.65) becomes equivalent to

$$\sqrt{N_{(0)[0]}^2} f_{(n)[0]} = \sqrt{N_{(0)[1]}^2} f_{(n)[1]}. \quad (2.77)$$

Therefore, if the phase of $\sqrt{N_{(0)}^2}$ is discontinuous across the corner, we find that not only $f_{(1)}$ but all terms up to and including order e^{-dr} in $f(r, x^a)$ vanish as well.

If $N_{(0)}^2$ is continuous, then $f_{(1)}$ does not necessarily vanish, equation (2.75) no longer holds, and the above derivation for the subleading terms is no longer valid.

However, the C^d continuity of the boundary metric implies that the locally determined terms in the Fefferman-Graham expansion (2.55) are continuous across the matching surface as well and the metric is thus the same to high order on either side (up to the complex diffeomorphism discussed above). A discontinuity in (2.55) may appear at the earliest for the nonlocally determined term $g_{(d)ij}$, which is at overall order $e^{(2-d)r}$ in the radial expansion of the bulk metric. By substituting this radial expansion in the fourth equation in (2.60), and using the continuity to all orders of $H^2 + H_a H^a$, we find that f has to be continuous across the corner up to and including terms of order e^{-dr} . (Notice that the fourth equation in (2.60) is invariant under $f \leftrightarrow -f$, but we fixed the overall sign already at leading order.)

This finishes our discussion about imposing the matching conditions: the previous two paragraphs show that f ‘matches’ up to and including terms of order e^{-dr} for all three cases. Up to this order, we find that $f_{[0]} = -f_{[1]}$ for a full turn, that $f_{[0]}$ and $f_{[1]}$ both vanish for any other corner, and that $f_{[0]} = f_{[1]}$ if there is no corner at all. In the next subsection, we will use these conditions to demonstrate the absence of localized (divergent) corner contributions to the on-shell action, in order to eventually show the continuity of the one-point function of the stress energy tensor around the corner.

2.4.6 Computation of the on-shell action

The bare on-shell action (2.52) has the usual Gibbons-Hawking-York contribution from $\partial_t M$ as well as an extra corner contribution. However, the matching conditions directly imply that these terms cancel between the two spacetimes. The total action (2.61) becomes:

$$\begin{aligned}
 iS_0 + iS_1 &= \frac{i}{2\kappa^2} \int_{M_0} d^{d+1}x \sqrt{-G}(R - 2\Lambda) + \frac{i}{\kappa^2} \int_{\partial_r M_0} d^d x \sqrt{-\gamma} K \\
 &+ \frac{i}{2\kappa^2} \int_{M_1} d^{d+1}x \sqrt{-G}(R - 2\Lambda) + \frac{i}{\kappa^2} \int_{\partial_r M_1} d^d x \sqrt{-\gamma} K. \quad (2.78)
 \end{aligned}$$

This action can be renormalized with the usual radial counterterms which we found explicitly in section 1.6, except for a subtlety involving the bulk integrals in this action. Namely, the t -integrals do not run between fixed endpoints, say $t = 0$ and $t = T$, but now rather end on $t = f_{\pm}(r, x^a)$. The usual radial counterterms, however, assume an r -independent limit on the bulk integral and the radial counterterms may not exactly cancel all divergences.

We will now show that these extra divergences also cancel between the two matching solutions. To first order, the cancellation can be shown very explicitly. Namely,

if f is of the form (2.66), then we can radially expand the volume element as:

$$\begin{aligned} \int_{M_0} \sqrt{-G} d^{d+1}x &= \int^{r_0} dr \int dx^a \int_{f(r,x^a)} dt \sqrt{N^2 \sigma} \\ &= \int^{r_0} dr \left[\int dx^a \int_{f(r_0,x^a)} dt \sqrt{N^2 \sigma} - e^{(d-1)r} \int dx^a f_{(1)} \sqrt{N_{(0)}^2 \sigma_{(0)}} + \dots \right]. \end{aligned} \quad (2.79)$$

The first term has an r -independent lower limit on the t -integral and so all divergences in this term are dealt with by integrating the usual radial counterterms also until $f(r_0, x^a)$. The second term is not cancelled by counterterms and may lead to new divergences. However, in (2.78) a similar term comes from the expansion of the action S_1 for M_1 and by the corner matching condition (2.68) the terms exactly cancel each other. Notice that an extra sign on M_1 arises because we expand the upper rather than the lower limit of the t -integral.

For higher orders, we recall that f is continuous or vanishing up to and including terms of order e^{-dr} . Using also the higher-order continuity of the bulk metric, a continuation of the expansion (2.79) shows that the corrections cancel up to finite terms. This means that no extra divergences arise from the discrepancy between the limits of the t -integration.

Having eliminated all possible sources of corner divergences, we may conclude that the usual radial counterterms are sufficient to make the total on-shell action finite. For example, in $d = 4$ we can easily construct the explicit counterterm action from the discussion of section 2.4. It takes the form:

$$S_{\text{ct}} = \frac{1}{2\kappa^2} \int d^d x \sqrt{-\gamma} \left(3 + \frac{1}{4} R + \frac{1}{4} \log e^{-r_0} \left[\frac{1}{4} R^{ij} R_{ij} - \frac{1}{6} R^2 \right] \right), \quad (2.80)$$

where the curvatures are those of the boundary metric γ_{ij} at $r = r_0$. This counterterm action is valid for all signatures if we define $\sqrt{-\gamma}$ in the same way as $\sqrt{-G}$ above, *i.e.* with the branch cut above the positive real axis.

2.4.7 Continuity of the one-point function

We have shown that the on-shell action can be holographically renormalized with the usual counterterms in the presence of corners. It remains to show that the one-point function is appropriately continuous around the corners as well.

The renormalized one-point function of the stress energy tensor is obtained by varying the renormalized on-shell action with respect to radial boundary data. As for the scalar field, the integration by parts in the variation of a counterterm action like (2.80) may result in localized corner contributions to the one-point

function. However, a similar analysis as for the scalar field shows that the higher-order continuity of the boundary metric in the complex time plane ensures that such contributions again cancel between two matching solutions.

Let us explicitly show the cancellation of the first corner term that arises from the integration by parts of the radial counterterms, which originates from the second term in (2.80). This is just an Einstein-Hilbert like term and it cancels against the matching solution if the extrinsic curvature of the corner, which we denote $K_{(0)ab}$, is continuous across the corner:

$$K_{(0)[0]ab} + K_{(0)[1]ab} = 0. \quad (2.81)$$

Cancellation of the next term gives a higher-order continuity condition. Explicitly, the variation of these terms gives

$$\begin{aligned} \delta \int_{\partial_r M} d^d x \sqrt{-\gamma} \left[\frac{R_{ij} R^{ij}}{(d-2)^2} - \frac{dR^2}{4(d-1)(d-2)} \right] &= \int_{\partial_r M} d^d x \sqrt{-\gamma} (\dots) \delta \gamma_{ij} \\ &+ \int_C d^{d-1} x \sqrt{\sigma} \left[n_i P^{ij} (\nabla^l \delta \gamma_{lj} - \gamma^{kl} \nabla_j \delta \gamma_{kl}) + (\nabla_i P^{ij}) (n_j \gamma^{kl} \delta \gamma_{kl} - n^k \delta \gamma_{kj}) \right], \end{aligned} \quad (2.82)$$

where

$$P^{ij} = -\frac{dR\gamma^{ij}}{4(d-1)(d-2)} + \frac{R^{ij}}{(d-2)^2} \quad (2.83)$$

and n^i is an appropriately defined unit normal for the corner as a submanifold of $\partial_r M$. From (2.82) we explicitly see that the higher-order continuity condition involves up to three derivatives of the metric in $d = 4$.

By the absence of initial or corner contributions, the holographic expression for the one-point function of the stress-energy tensor is completely analogous to the Euclidean case. We may therefore repeat the result (1.166) of section 1.6, namely

$$\langle T_{ij} \rangle_{g_{(0)}} = - \lim_{r \rightarrow \infty} e^{(d-2)r} \frac{1}{\kappa^2} \pi_{(d)ij}, \quad (2.84)$$

where $\pi_{(d)ij}$ is the term of dilatation weight d in the expansion of the radial canonical momentum in eigenfunctions of the dilatation operator. Upon substitution of the radial expansion one finds that the one-point function is expressed directly in terms of $g_{(d)ij}$ and terms that are determined locally by $g_{(0)ij}$. For example, in $d = 2$ we obtained (1.169) and in $d = 4$ we find up to scheme-dependent terms that

$$\langle T_{ij} \rangle = \frac{2}{\kappa^2} \left(g_{(4)ij} - \frac{1}{8} [(\text{Tr } g_{(2)})^2 - \text{Tr } g_{(2)}^2] - \frac{1}{2} (g_{(2)}^2)_{ij} + \frac{1}{4} g_{(2)ij} \text{Tr } g_{(2)} \right), \quad (2.85)$$

see [27] for the exact expressions in other dimensions.

Since by assumption all locally determined terms in the Fefferman-Graham expansion of the metric are continuous, continuity of the one-point function will follow from continuity of $g_{(d)ij}$ across the corner. Fortunately, the continuity of $g_{(d)ij}$ follows directly if we substitute the expansion (2.55) in the last equation of (2.60). The left-hand side in this equation is continuous to all orders by the first matching condition. On the other side, we know that f is continuous up to and including terms of order e^{-dr} , and we know that all $g_{(2n)ij}$ with $2n < d$ as well as $\tilde{g}_{(d)ij}$ are continuous since they are locally determined by $g_{(0)ij}$. Collecting terms of overall order $e^{(2-d)r}$ then establishes that $g_{(d)ij}$ has to be continuous as well. (As shown in [30], there is no diffeomorphism freedom at this order if we fix a boundary coordinate system and a boundary metric, so continuity of $g_{(d)ab}$ implies continuity of $g_{(d)ij}$ indeed.) We have thus established that the vev of the stress-energy tensor is continuous across the corner (in the sense discussed in subsection 2.4.5).

We end this section with a remark about the function $f(r, x^a)$. Recall that we could in some cases freely specify this function at the corner, provided it was the same on both sides (possibly up to a sign). On the other hand, this function has no place in the QFT, and therefore holographically computed QFT correlators should be independent of f . Our prescription passes this test, since the one-point function we obtain is indeed independent of f .

2.5 Conclusion

We have presented a general prescription to holographically compute real-time correlation functions within the supergravity approximation. The main challenge in developing such a real-time prescription, relative to Euclidean methods, was to understand in detail how to deal with initial data. Our prescription is a direct ‘holographic lift’ of QFT real-time techniques to the gravitational setting, namely there is a gravitational counterpart of all QFT steps involved in such computations. In more detail, in QFT one typically chooses a contour in the complex time plane which usually consists of a sequence of horizontal (real) and vertical (imaginary) segments, the latter being related to the choice of density matrix or initial/final state. On the gravitational side, we construct solutions that directly correspond to such QFT contours. Typically, horizontal segments are associated with Lorentzian solutions and vertical segments with Euclidean solutions, with appropriate matching conditions imposed on the joining surface. The Euclidean parts encode the initial and final state in the field theory and this is reflected in the bulk, where they can be thought of as Hartle-Hawking wave functions [56]. We will see in the next chapter how these wave functions also provide the necessary initial and final data for the perturbations around a given supergravity background.

For the prescription to well defined, one must establish that one can remove all infinities through a process of (holographic) renormalization. Relative to the Euclidean discussion, new infinities can appear at timelike infinity. In our setup the analysis boils down to analyzing possible new contributions from the joining surfaces. We show that no new counterterms are needed and the holographic 1-point functions are continuous across the matching surface. The continuity of the 1-point functions is an important consistency condition of the entire setup: as mentioned above, the Euclidean parts of the solution are directly related to the initial/final state but as is also well known the 1-point functions encode the same information, too.

As a sidenote, the holographic nature of the prescription also nicely shows up in the following issue that we encountered when demonstrating the renormalization. Starting from a boundary state defined at a boundary Cauchy surface, say the surface $t = t_0$, one can extend this surface to the bulk, $t = f(r, \vec{x})$ with $f(r, \vec{x}) \rightarrow t_0$ as $r \rightarrow \infty$, but clearly there is a certain amount of freedom of how this is done, parametrized by the subleading behavior of $f(r, \vec{x})$. These extensions are not part of the boundary theory, so the renormalized theory should be independent of them. We explicitly find that possible dependence on $f(r, \vec{x})$ drops out indeed.

Having set up the prescription, we will in the next chapter move on to demonstrate how to apply it in a variety of examples that each illustrate different points.

2.A Real-time quantum field theory

In this appendix we discuss some aspects of real-time quantum field theory relevant for our discussion. The material presented here is not new and it is included to make this work self-contained.

2.A.1 Vacuum wave function insertions

In this section we will analyze how the vacuum wave function insertions in the path integral lead to $i\epsilon$ insertions. In the main text, we mentioned how the wave functions can be obtained as path integrals along vertical segments in the complex time plane, leading ultimately to a contour as in figure 2.1a. Let us begin by an explicit computation of these wave functions in a relatively simple case.

Computation of the wave functions

We will consider a real free massive boson on flat Minkowski space $\mathbb{R}^{1,d-1}$. As explained in the main text, the initial wave function $\langle \phi_-, -T | 0 \rangle$ is computed via the projection:

$$\lim_{\beta \rightarrow \infty} \langle \phi_-, -T | e^{-\beta \hat{H}} | \Psi \rangle = \langle \phi_-, -T | 0 \rangle \langle 0 | \Psi \rangle. \quad (2.86)$$

For simplicity, we shift the time coordinate such that $-T \rightarrow 0$ and we will take $|\Psi\rangle = |\phi_\beta, i\beta\rangle$ for some spatial field configuration $\phi_\beta(x)$.

Since we take the field to be free, the path integral is Gaussian and can be computed exactly. Let $\hat{\phi}(t, x)$ be the solution to the Euclidean equation of motion satisfying $\hat{\phi}(i\beta, x) = \phi_\beta(x)$ and $\hat{\phi}(0, x) = \phi_-(x)$. We then obtain

$$\langle \phi_-, 0 | 0 \rangle = \lim_{\beta \rightarrow \infty} \mathcal{N} e^{-S_E[\hat{\phi}]}, \quad (2.87)$$

with \mathcal{N} a normalization that does not depend on ϕ_- and S_E the Euclidean on-shell action for the boson. The Lorentzian action for the boson is:

$$S_L[\phi] = \frac{1}{2} \int dt d^{d-1}x \left(-\eta^{\mu\nu} \partial_\mu \phi \partial_\nu \phi - m^2 \phi^2 \right) \quad (2.88)$$

and we find after substitution of $t = -i\tau$ that $iS_L \rightarrow -S_E$ with the Euclidean action given by:

$$S_E[\phi] = \frac{1}{2} \int_{-\beta}^0 d\tau \int d^{d-1}x \left(\delta^{\mu\nu} \partial_\mu \phi \partial_\nu \phi + m^2 \phi^2 \right). \quad (2.89)$$

where we also set the limits of the τ integrals to the appropriate values. On-shell this action reduces to a surface integral,

$$\langle \phi_-, 0 | 0 \rangle = \lim_{\beta \rightarrow \infty} \mathcal{N} \exp \left(-\frac{1}{2} \int d^{d-1}x [\hat{\phi}(\tau, x) \partial_\tau \hat{\phi}(\tau, x)]_{\tau=-\beta}^0 \right). \quad (2.90)$$

Finding $\hat{\phi}$ is not hard and in the limit $\beta \rightarrow \infty$ we find that all dependence on ϕ_β can be absorbed in a shift of \mathcal{N} and we recover the usual Gaussian wave function [49], written in Fourier space as

$$\langle \phi_-, 0 | 0 \rangle = \mathcal{N}' \exp \left(-\frac{1}{2} \int \frac{d^{d-1}k}{(2\pi)^{d-1}} \phi_-(k) \omega_k \phi_-(-k) \right), \quad (2.91)$$

with $\omega_k = \sqrt{k^2 + m^2}$. The conjugate final wave function $\langle 0 | \phi_+, T \rangle$ can be computed using the same procedure, leading to exactly the same result.

If interactions are switched on, the wave functions receive corrections. However, as long as these interactions can be switched off adiabatically for large times, the

corrections can also be ignored in the limit $t_i, t_f \rightarrow \infty$. The analogous case in thermal field theory, which we discuss below, is briefly discussed in [51, section 2.4.1]. For massless field theories there are subtleties, but these considerations are not directly relevant for us and they will not be discussed here. A computation of the ground state wave function for electromagnetism and linearized gravity can be found in [61].

Effect of the wave function insertions

Let us now show how the wave function insertions determine $i\epsilon$ -insertions in the propagator. To this end, we introduce a source J for ϕ and compute

$$Z[J] = \langle 0 | e^{-i \int J \phi} | 0 \rangle. \quad (2.92)$$

We suppose that the source vanishes smoothly at the endpoints $t = \pm T$ of the Lorentzian segment. Again via the usual slicing arguments, the path-integral representation one obtains is

$$\begin{aligned} Z[J] = \int [\mathcal{D}\phi] \exp \left(iS[\phi] - i \int dt d^{d-1}x J \phi - \frac{1}{2} \int \frac{d^{d-1}k}{(2\pi)^{d-1}} \phi_-(k) \omega_k \phi_-(-k) \right. \\ \left. - \frac{1}{2} \int \frac{d^{d-1}k}{(2\pi)^{d-1}} \phi_+(k) \omega_k \phi_+(-k) \right), \end{aligned} \quad (2.93)$$

where $\phi_{\pm}(k)$ is the Fourier transform of $\phi(\pm T, x)$ with respect to the spatial coordinates. Notice that the boundary values for the path integral $\int [\mathcal{D}\phi]$ are not fixed.

To compute the path integral, we shift the integrand $\phi = \chi + \psi$, where χ satisfies $\square\chi - m^2\chi = J$ and ψ is the new integration variable. Notice that χ is not uniquely defined unless we specify some boundary conditions. To find these, notice that the aim of this shift is to get all the factors involving J and χ to come out in front of the path integral, resulting in

$$Z[J] = \mathcal{N} \exp \left(- \frac{i}{2} \int d^d x \chi J \right), \quad (2.94)$$

from which we would directly obtain the propagator as is shown below. However, an analysis of the boundary terms shows that such a factorization only occurs if one imposes additionally the two extra constraints:

$$\begin{aligned} -i \int d^{d-1}x \psi_-(x) \partial_t \chi(-T, x) - \int \frac{d^{d-1}k}{(2\pi)^{d-1}} \psi_-(-k) \omega_k \chi_-(k) = 0, \\ +i \int d^{d-1}x \psi_+(x) \partial_t \chi(T, x) - \int \frac{d^{d-1}k}{(2\pi)^{d-1}} \psi_+(-k) \omega_k \chi_+(k) = 0, \end{aligned} \quad (2.95)$$

which should hold for all values of ψ_{\pm} . These conditions provide the boundary conditions for χ . Since the source vanishes at the endpoints, χ is homogeneous for $t = \pm T$, and therefore has a Fourier expansion involving only modes of the form $e^{\mp i\omega_k t + ikx}$. The boundary conditions that one derives from these constraints are then simply that $\chi(-T, x)$ should contain only negative frequencies (*i.e.* modes of the form $e^{-i\omega t + ikx}$ with $\omega < 0$) and $\chi(T, x)$ should contain only positive frequencies. But this uniquely fixes χ to be of the form

$$\chi = \int dt' d^{d-1}x' \Delta_F(t-t', x-x') J(x'), \quad (2.96)$$

with Δ_F the Feynman propagator,

$$\Delta_F(t, x) = \int \frac{dt d^{d-1}x}{(2\pi)^d} \frac{e^{-i\omega t + ikx}}{-\omega^2 + k^2 - m^2 - i\epsilon}. \quad (2.97)$$

As one may verify by contour deformation, one indeed obtains only positive/negative frequencies to the future/past of the source.

We can now take the limit $T \rightarrow \infty$. Assuming that the source and any perturbatively added interactions vanish slowly at late times, the propagator and the wave functions are unmodified and all that is left are the $i\epsilon$ -insertions which enter in the perturbative expansion, which is precisely what we wanted to show.

Different (equivalent) arguments that translate wave functions to $i\epsilon$ insertions can be found in the textbooks [49] and [48]. In the main text we already discussed the method of [48] where the contour of figure 2.1a is deformed to a straight line that runs almost parallel to the real time axis, from $-T(1 - i\epsilon)$ to $T(1 - i\epsilon)$, with $T \rightarrow \infty$. The projection property is left unchanged and this way one still obtains vacuum-to-vacuum amplitudes. The contour should always go downward or horizontal in the complex time plane so that the operator $\exp(-i\hat{H}\Delta t)$ remains finite.

Finally, notice that the saddle-point χ is actually a *complex* solution, although we started with a real scalar field and a real source $J(x)$. This can be viewed as a contour deformation in field space before taking the saddle-point approximation. Such a deformation is very explicit when one discretizes the path integral. Nevertheless, the usual hermiticity constraints of n -point functions are still satisfied. The fact that a saddle-point approximation may involve complex fields holds for gravity as well. In the context of holography, it is the hermiticity of the boundary stress energy tensor and its correlators that restricts the allowed complex metrics.

2.A.2 Analyticity properties of two-point functions

In this section, we briefly review the analytic properties of two-point functions and corresponding $i\epsilon$ -insertions.

We start with the Wightman function

$$\langle \psi(x)\psi(0) \rangle, \quad (2.98)$$

which is analytic in the lower half of the complex t plane [62]. The Wightman function can be obtained by the replacement $-i\tau = t - i\epsilon$ in the Euclidean correlator, because then the poles along the real t axis are shifted into the upper half of the complex t plane. Its Fourier transform,

$$\int dt d^{d-1}x e^{i\omega t - ikx} \langle \psi(x)\psi(0) \rangle, \quad (2.99)$$

vanishes for negative frequencies, since we can close the contour for the t -integral via the lower half plane. Positivity of the spectral density also implies that the Fourier transform is a real and positive distribution for positive frequencies [62]. The Fourier transform thus maps a function (or distribution) that is analytic in a upper or lower half plane to a function that vanishes on the right or the left real axis.

Next, the time-ordered two-point function is defined as

$$\langle \mathcal{T}\psi(x)\psi(0) \rangle = \theta(t)\langle \psi(x)\psi(0) \rangle + \theta(-t)\langle \psi(0)\psi(x) \rangle, \quad (2.100)$$

which can be obtained from the Euclidean correlator by the replacement $-i\tau = t - i\epsilon t$. Its poles are shifted into the upper half of the complex t plane for $\text{Re } t > 0$ and in the lower half plane for $\text{Re } t < 0$. To obtain the Fourier transform, we close the contour in the appropriate half plane in the complex time plane. Picking up the poles, we find a sum over positive frequencies for $t > 0$ and one over negative frequencies for $t < 0$. This implies that we need the usual Feynman contour around the poles to define the inverse Fourier transform. One may replace $\omega \rightarrow \omega + i\epsilon\omega$ in the Fourier-space expression to explicitly indicate such a contour. Obviously

$$-(\omega + i\epsilon\omega)^2 = -\omega^2 - i\epsilon \quad (2.101)$$

and for example the propagator (2.97) indeed has the required analyticity properties.

Finally, the retarded two-point function is defined as:

$$\Delta_R(x', x) = -i\theta(x' - x)\langle [\mathcal{O}(x'), \mathcal{O}(x)] \rangle. \quad (2.102)$$

Causality of the field theory determines that it vanishes completely outside the future lightcone. We may write it as an inverse Fourier transform:

$$\Delta_R(x, 0) = \frac{1}{(2\pi)^d} \int d\omega d^{d-1}k e^{-i\omega t + ikx} \Delta_R(\omega, k). \quad (2.103)$$

Notice that $\Delta_R(x, 0)$ vanishes for $t < 0$. Since we can then close the ω integral in (2.103) in the upper half plane, we find that $\Delta_R(\omega, k)$ must be analytic in the upper half of the complex frequency plane. Finally, the advanced two-point function is the reversed retarded two-point function:

$$\Delta_A(x, x') = \Delta_R(x', x). \quad (2.104)$$

It therefore vanishes outside of the past lightcone and is analytic in the lower half of the complex frequency plane.

Chapter 3

Real-time correlation functions

In this chapter we consider a number of concrete applications of the real-time gauge/gravity prescription. The examples below are meant to illustrate the applicability of the prescription for computing time-ordered, retarded or Wightman correlation functions in a variety of backgrounds directly from the bulk theory. Notice that such correlation functions sometimes differ only by the form of their $i\epsilon$ insertions (or other analyticity properties). Although such factors of $i\epsilon$ are often inserted by hand, in QFT they can be obtained from a formal derivation which was briefly discussed in appendix 2.A. Any first-principles real-time gauge/gravity prescription should therefore also be able to correctly determine these $i\epsilon$ insertions via bulk computations. The examples below show that our prescription indeed produces $i\epsilon$ insertions that are always in agreement with field theory expectations (as described in appendix 2.A), which provides a nontrivial check of the prescription.

3.1 Examples involving global AdS_3

For the first set of examples we will consider a two-dimensional CFT with a holographic dual defined on a cylinder with metric

$$ds^2 = -dt^2 + d\phi^2 \tag{3.1}$$

and a contour for the CFT which consists of the ϕ circle times a path C in the complex time plane, with C being piecewise horizontal or vertical. The discussion

can be extended straightforwardly to a CFT in d dimensions, but we restrict ourselves to $d = 2$ for now. Various possibilities for C are indicated on the left of figure 3.1. We will compute the two-point function for operators inserted on all three of the contours drawn in figure 3.1.

As we mentioned in section 2.2 in the previous chapter, the general idea is to ‘fill in’ the entire field theory contour with bulk spaces. In the case when all sources vanish along C , one can fill each horizontal segment of C with a segment of empty Lorentzian AdS_3 and each vertical segment with a segment of Euclidean AdS_3 . The metric on the Lorentzian segments is of the form:

$$ds^2 = -(r^2 + 1)dt^2 + \frac{dr^2}{r^2 + 1} + r^2 d\phi^2 \quad (3.2)$$

and the Euclidean metric can be obtained by the replacement $t = -i\tau$. In this metric, surfaces of constant t or τ have vanishing extrinsic curvature and the induced metric is independent of the signature of the spacetime metric. Therefore, the matching conditions for gravity are satisfied if we glue the Euclidean and Lorentzian segments together along such surfaces. The complete bulk solution M_C consisting of Lorentzian and Euclidean segments glued together along these constant t or τ surfaces therefore satisfies all the matching conditions and can be taken as a filling for the given contour. We have drawn such fillings schematically on the right of figure 3.1. Note that these ‘piecewise AdS’ spacetimes may not be the only bulk solutions for the given class of contours, a point which we will come back to when we discuss black holes.

By switching on boundary sources, we can perturb such backgrounds, with the provision that the matching conditions are satisfied for the perturbations as well. In the two examples below, we will add a massive scalar field in the bulk and compute a contour time-ordered two-point function of the dual operator. We will work in the approximation in which the scalar field is free and propagates without backreaction.

3.1.1 Generalities

Before considering specific contours, we first discuss some generalities regarding the solutions to the Klein-Gordon equation that are valid for each Lorentzian and Euclidean segment separately.

We start from the action

$$S = \frac{1}{2} \int d^{d+1}x \sqrt{-G} (-\partial_\mu \Phi \partial^\mu \Phi - m^2 \Phi^2), \quad (3.3)$$

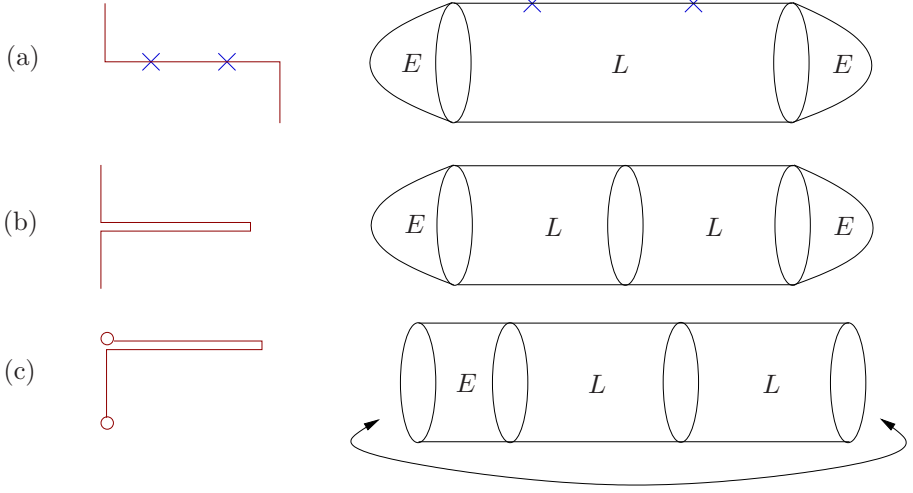


Figure 3.1: On the left, various contours in the complex time plane. The vertical segments in the first two contours should be thought of as extending to infinity, yielding a vacuum state on the corner. The circles in the third contour should be identified; it is then a thermal contour. The crosses represent an example of the operator insertions we consider. On the right, we sketch the spacetimes consisting of piecewise Euclidean (E) and Lorentzian (L) AdS_3 that fill the given contours. One should impose matching conditions on the hypersurfaces between the segments.

with $d = 2$ and the metric $G_{\mu\nu}$ given by (3.2). As usual, we have $m^2 = \Delta(\Delta - 2)$ with $\Delta - 1 = l \in \{1, 2, \dots\}$. The mode solutions to the Klein-Gordon equation are of the form

$$e^{-i\omega t + ik\phi} f(\omega, \pm k, r), \quad (3.4)$$

with

$$f(\omega, k, r) = C_{\omega kl} (1+r^2)^{\omega/2} r^k F((\omega+k+1+l)/2, (\omega+k+1-l)/2; k+1; -r^2), \quad (3.5)$$

where F is a hypergeometric function and $C_{\omega kl}$ is a normalization factor chosen such that the coefficient of the leading term as $r \rightarrow \infty$ equals 1. For large r the solution behaves as

$$f(\omega, k, r) = r^{l-1} + \dots + r^{-l-1} \alpha(\omega, k, l) [\ln(r^2) + \beta(\omega, k, l)] + \dots \quad (3.6)$$

with

$$\begin{aligned} \alpha(\omega, k, l) &= \frac{((\omega+k+1-l)/2)_l ((\omega-k+1-l)/2)_l}{l!(l-1)!}, \\ \beta(\omega, k, l) &= -\psi((\omega+k+1+l)/2) - \psi((-\omega+k+1-l)/2), \end{aligned} \quad (3.7)$$

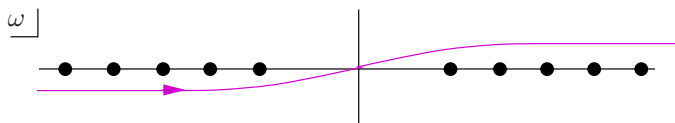


Figure 3.2: The dots represent poles in complex frequency space and a contour should be specified to avoid those poles.

where $(a)_n = \Gamma(a+n)/\Gamma(a)$ is the Pochhammer symbol and $\psi(x) = d \ln \Gamma(x)/dx$ is the digamma function. In the expansion (3.6) we omitted terms of lower powers of r and some terms polynomial in ω and k (which would lead to contact terms in the 2-point functions given below).

For $r \rightarrow 0$, which is in the interior of the spacetime, the hypergeometric function in (3.5) is approximately one and only the solutions with $k > 0$ remain regular. The admissible mode solutions therefore take the form:

$$e^{-i\omega t + ik\phi} f(\omega, |k|, r), \quad (3.8)$$

and we will only use these modes in what follows.

Let us now construct a bulk-boundary propagator out of these modes, which is a solution to the bulk equations of motion which tends to a delta-function source on the boundary. Since the leading coefficient in (3.6) equals one in Fourier space, such a bulk-boundary propagator can be obtained by a simple integral over ω and a sum over k of these modes. However if the frequency equals

$$\omega = \omega_{nk}^\pm \equiv \pm(2n + |k| + 1 + l), \quad n \in \{0, 1, 2, \dots\}, \quad (3.9)$$

then the digamma functions become singular and the term $\alpha(\omega, |k|, l)\beta(\omega, |k|, l)$ in the radial expansion of the modes has a pole. To obtain a well-defined bulk-boundary propagator, one needs to specify a contour in ω -space around these poles, for example the contour sketched in figure 3.2. Notice that at this point the choice for a specific contour is completely arbitrary. The difference between two contours would be a sum over residues:

$$\begin{aligned} g(\omega_{nk}, k, r) &= \oint_{\omega_{nk}} d\omega f(\omega_{nk}, k, r) \\ &= r^{-l-1} \alpha(\omega_{nk}, k, l) \left(\oint_{\omega_{nk}} d\omega \beta(\omega, k, l) \right) + \dots \\ &= r^{-l-1} 4\pi i \alpha(\omega_{nk}, |k|, l) + \dots, \end{aligned} \quad (3.10)$$

where the contour integral is defined as counterclockwise for ω_{nk}^- and clockwise for ω_{nk}^+ , so that $g(\omega_{nk}^+, |k|, r) = g(\omega_{nk}^-, |k|, r)$ and $\alpha(\omega_{nk}^+, |k|, l) = \alpha(\omega_{nk}^-, |k|, l)$. We

see that the poles only occur at normalizable order in the radial expansion of the modes (indeed, the first terms in this expansion are always local so they cannot contain poles in frequency space). The modes $g(\omega_{nk}, |k|, r)$ are therefore called the *normalizable modes*.

These normalizable modes can in fact be added at will (so not just as residues) to any solution without changing the leading term in the radial expansion of the solution. The most general solution (without specifying any initial or final data) therefore involves an arbitrary sum over these modes. For general boundary data $\phi_{(0)}(t, \phi)$ it is thus of the form

$$\begin{aligned} \Phi(t, \phi, r) = & \frac{1}{4\pi^2} \sum_{k \in \mathbb{Z}} \int_C d\omega \int d\hat{t} \int d\hat{\phi} e^{-i\omega(t-\hat{t})+ik(\phi-\hat{\phi})} \phi_{(0)}(\hat{t}, \hat{\phi}) f(\omega, |k|, r) \\ & + \sum_{\pm} \sum_{k \in \mathbb{Z}} \sum_{n=0}^{\infty} c_{nk}^{\pm} e^{-i\omega_{nk}^{\pm} t + ik\phi} g(\omega_{nk}, |k|, r), \end{aligned} \quad (3.11)$$

with so far arbitrary coefficients c_{nk}^{\pm} (provided the sum converges). For convenience, let us fix the contour C to be of the Feynman form sketched in figure 3.2, since any different contour can also be implemented by changing the normalizable modes. As we show in detail below, the initial and final data, so the other segments and matching conditions, will eventually completely fix the c_{nk}^{\pm} .

Below, we will often make use of the following observation. To the past of all the sources we have $t - \hat{t} < 0$ in (3.11) and the contour of the ω -integral can be closed in the upper half of the complex frequency plane. The choice for a Feynman contour implies that we pick up the poles at the negative frequencies only, which we repeat are just the normalizable modes. The solution can then be fully written as a sum over normalizable modes,

$$\begin{aligned} \Phi = & \frac{1}{4\pi^2} \sum_{n=0}^{\infty} \sum_{k \in \mathbb{Z}} e^{-i\omega_{nk}^- t + ik\phi} \phi_{(0)}(\omega_{nk}^-, k) g(\omega_{nk}, |k|, r) \\ & + \sum_{\pm} \sum_{k \in \mathbb{Z}} \sum_{n=0}^{\infty} c_{nk}^{\pm} e^{-i\omega_{nk}^{\pm} t + ik\phi} g(\omega_{nk}, |k|, r), \end{aligned} \quad (3.12)$$

which is to be expected by completeness of the normalizable modes. Similarly, to the future of all the sources, we can deform the contour in the lower half plane and pick up the residues at the positive frequencies.

Next, consider the solution on the Euclidean segments. The metric on these segments takes the form:

$$ds^2 = (r^2 + 1)d\tau^2 + \frac{dr^2}{r^2 + 1} + r^2 d\phi^2. \quad (3.13)$$

One can obtain the Euclidean mode solutions by a replacement of the form $t = -i\tau$ in the Lorentzian mode solutions. We will set all sources to zero along the Euclidean segments, so the solutions there will always consist of normalizable modes only:

$$\Phi_E(\tau, \phi, r) = \sum_{\pm} \sum_{k \in \mathbb{Z}} \sum_{n=0}^{\infty} d_{nk}^{\pm} e^{-\omega_{nk}^{\pm} \tau + ik\phi} g(\omega_{nk}, |k|, r), \quad (3.14)$$

with to be determined coefficients d_{nk}^{\pm} . Note that, if a contour extends all the way to $\tau \rightarrow \infty$, then we also require finiteness of the solution in this limit. This corresponds to the absence of any sources at this point. Such a condition directly implies that all the d_{nk}^- are zero, whereas the d_{nk}^+ are still unconstrained. The converse statement holds for a contour extending to $\tau \rightarrow -\infty$. Notice that if the bulk had been the entire Euclidean AdS space then τ would extend to both plus and minus infinity and therefore *all* the d_{nk}^{\pm} would be zero, corresponding to the fact that with zero sources the unique regular solution on Euclidean AdS is identically equal to zero. In our case the sources are zero but we only consider a segment (or half) of the space, so solutions that would be excluded are now allowed because they are only singular at the other part of the space.

This finishes the introduction of the solutions on the various segments; we will now consider specific contours and demonstrate how the matching conditions determine the coefficients of the normalizable modes.

3.1.2 Time-ordered two-point function

Let us consider the contour in figure 3.1a. According to standard QFT results the path integral with operators inserted on the crosses in the figure should result in a time-ordered two-point function. We shall now see how this can be reproduced using the gauge/gravity dictionary.

As indicated on the right of figure 3.1a, the contour is ‘filled’ with a Lorentzian solution (with the metric (3.2)) which is sandwiched between two Euclidean ‘caps’ (whose metric is given in (3.13)). We pick a time coordinate t on the Lorentzian segment which runs from 0 to T . The Euclidean time coordinates are denoted τ and we have $-\infty < \tau < 0$ on the ‘initial cap’ and $0 < \tau < \infty$ on the ‘final cap’.

In the previous subsection we discussed how the most general solution on the Lorentzian segment takes the form (3.11) where we fixed the contour C to be of the form sketched in figure 3.2. Similarly the most general solution on the Euclidean segments takes the form (3.14) with all $d_{nk}^+ = 0$ for the initial cap and all $d_{nk}^- = 0$ for the final cap. The undetermined coefficients c_{nk}^{\pm} and d_{nk}^{\pm} are not

determined by the radial boundary data alone and parametrize the freedom to add an arbitrary normalizable solution.

Let us now impose the matching conditions discussed in section 2.2.1. Without loss of generality we may suppose that near the matching surface at $t = 0$ and $t = T$ the sources vanish smoothly. The Lorentzian solution near these surfaces can then be written as a sum over normalizable modes as in (3.12). For the case at hand we find:

$$\begin{aligned}\Phi_L(t \sim 0, \phi, r) &= \frac{1}{4\pi^2} \sum_{n=0}^{\infty} \sum_{k \in \mathbb{Z}} e^{-i\omega_{nk}^- t + ik\phi} \phi_{(0)}(\omega_{nk}^-, k) g(\omega_{nk}, |k|, r) \\ &\quad + \sum_{\pm} \sum_{k \in \mathbb{Z}} \sum_{n=0}^{\infty} c_{nk}^{\pm} e^{-i\omega_{nk}^{\pm} t + ik\phi} g(\omega_{nk}, |k|, r), \quad (3.15) \\ \Phi_L(t \sim T, \phi, r) &= \frac{1}{4\pi^2} \sum_{n=0}^{\infty} \sum_{k \in \mathbb{Z}} e^{-i\omega_{nk}^+ t + ik\phi} \phi_{(0)}(\omega_{nk}^+, k) g(\omega_{nk}, |k|, r) \\ &\quad + \sum_{\pm} \sum_{k \in \mathbb{Z}} \sum_{n=0}^{\infty} c_{nk}^{\pm} e^{-i\omega_{nk}^{\pm} t + ik\phi} g(\omega_{nk}, |k|, r).\end{aligned}$$

We begin with the matching near the initial surface $\tau = t = 0$. The first matching is the continuity equation:

$$\Phi_L(t = 0, \phi, r) = \Phi_E(\tau = 0, \phi, r). \quad (3.16)$$

Substituting (3.15) and (3.14) with all $d_{nk}^+ = 0$ we find an equality between two sums over normalizable modes. However since the different modes $g(\omega_{nk}, |k|, r)$ are orthogonal (up to the symmetry $g(\omega_{nk}^+, k, r) = g(\omega_{nk}^-, k, r)$) one can in fact equate the coefficients of the various modes. The first matching condition then results in:

$$\frac{1}{4\pi^2} \phi_{(0)}(\omega_{nk}^-, k) + c_{nk}^- + c_{nk}^+ = d_{nk}^-. \quad (3.17)$$

The second matching condition involves matching the conjugate momenta in such a way that we obtain C^1 continuity in the complex time plane. Using $t = -i\tau$ we directly obtain that for the initial surface one should demand:

$$-i\partial_t \Phi_L(t = 0, \phi, r) = \partial_{\tau} \Phi_E(\tau = 0, \phi, r). \quad (3.18)$$

Substituting the solutions we find

$$-\frac{1}{4\pi^2} \omega_{nk}^- \phi_{(0)}(\omega_{nk}^-, k) - \omega_{nk}^- c_{nk}^- - \omega_{nk}^+ c_{nk}^+ = -\omega_{nk}^- d_{nk}^-, \quad (3.19)$$

which we may combine with (3.17) to find that $c_{nk}^+ = 0$. Similarly one may check

that the matching conditions at $t = T$ lead to:

$$\begin{aligned} \frac{1}{4\pi^2} \phi_{(0)}(\omega_{nk}^+, k) e^{-i\omega_{nk}^+ T} + c_{nk}^- e^{-i\omega_{nk}^- T} &= d_{nk}^+ \\ \omega_{nk}^+ \frac{1}{4\pi^2} \phi_{(0)}(\omega_{nk}^+, k) e^{-i\omega_{nk}^+ T} + \omega_{nk}^- c_{nk}^- e^{-i\omega_{nk}^- T} &= \omega_{nk}^+ d_{nk}^+, \end{aligned} \quad (3.20)$$

which in turn determine $c_{nk}^- = 0$ and then also all the d_{nk}^\pm follow directly from the above equations. Therefore the bulk solution on all the segments is completely fixed by the matching conditions. We remark that, had we chosen any other contour C in (3.11), we would have found nonzero values of some of the c_{nk}^\pm , effectively throwing us back to the Feynman contour of figure 3.2.

According to the prescription (2.10) the one-point function in the presence of sources is just as in Euclidean signature given by a functional differentiation of the on-shell action with respect to the source:

$$\langle \mathcal{O}(x) \rangle_\phi = \frac{-1}{\sqrt{-g_{(0)}}} \frac{\delta}{\delta \phi_{(0)}} I_{\text{ren}}[\phi_{(0)}; C] \quad (3.21)$$

with $I_{\text{ren}}[\phi_{(0)}; C]$ the renormalized on-shell action integrated along the contour of figure 3.1a. As we demonstrated in section 2.3, the gluing of different solutions does not affect the usual prescription that this renormalized one-point function is given by the renormalized radial conjugate momentum. In particular, analogous to (1.117) in Euclidean signature, we obtained (2.36) for a one-point function inserted along a Lorentzian segment. For the case at hand this results (up to contact terms) in:

$$\langle \mathcal{O}(x) \rangle_\phi = -2l\phi_{(2l)} = \frac{l}{4\pi^2 i} \sum_k \int_C d\omega \phi_{(0)}(\omega, k) e^{-i\omega t + ik\phi} \alpha(\omega, |k|, l) \beta(\omega, |k|, l), \quad (3.22)$$

where $\phi_{(2l)}$ is the term of order r^{-1-l} in the radial expansion of the solution and the right-hand side is obtained by substituting the expansion (3.6) into (3.11) with all the $c_{nk}^\pm = 0$. After a second functional differentiation we find that the time-ordered two-point function is given by:

$$\langle 0|T\mathcal{O}(t, \phi)\mathcal{O}(0, 0)|0 \rangle = \frac{l}{4\pi^2} \sum_k \int_C d\omega e^{-i\omega t + ik\phi} \alpha(\omega, |k|, l) \beta(\omega, |k|, l). \quad (3.23)$$

The dependence of the bulk solution on the contour C directly enters in the boundary two-point function and this is how we indeed recover the standard Feynman prescription leading to time-ordered QFT correlators. We emphasize again that the contour C was completely fixed by the matching to the caps. The frequency integral along C is equivalent to integrating over the real axis while shifting

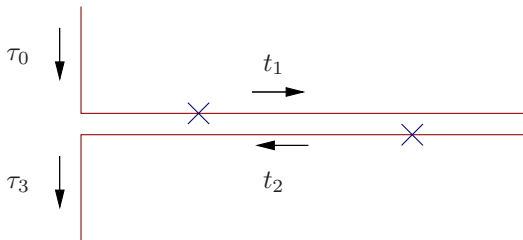


Figure 3.3: The in-in contour we use to compute a Wightman function. We choose a time coordinates that increases in the direction of the arrows.

$\omega \rightarrow \omega(1+i\epsilon)$. The Fourier transform in (3.23) can then be performed by deforming the contour and picking up the residues. We obtain:

$$\langle 0|T\mathcal{O}(t, \phi)\mathcal{O}(0, 0)|0\rangle = \frac{l^2/(2^{l+1}\pi)}{[\cos(t - i\epsilon t) - \cos(\phi)]^{l+1}}. \quad (3.24)$$

This is the expected form for a time-ordered two-point function on a cylinder. As we will see below, the normalization coefficient agrees with the standard AdS/CFT normalization of 2-point functions as well.

3.1.3 Wightman functions

Our next example is the computation of a vacuum-to-vacuum two-point function using an in-in formalism. As explained in section 2.1, the in-in formalism in particular allows for the computation of Wightman functions directly from a path integral. In our case, we can do the same holographically.

Let us therefore consider the contour sketched in figure 3.1b, given again in figure 3.3. It runs from $i\infty$ to 0, then to T (with T real and positive), then back to the origin and then to $-i\infty$. As we outlined above and sketched on the right of figure 3.1b, for such a contour we consider a filling that consists of two Lorentzian AdS₃ spacetimes between two Euclidean AdS₃ caps. These four space(time)s will be denoted as M_i , with i running from 0 to 3. We will use a subscript i also on other quantities to distinguish on which of the M_i they are defined. Sometimes, in order to avoid confusion with other subscripts, we will put this subscript in square brackets, writing for example $c_{[i]}$.

This time we will use real contour-time coordinates. We then split the contour-integrated action in (2.9) into the following combination:

$$-\int_{-\infty}^0 d\tau_0 L_E(\Phi_0) + i \int_0^T dt_1 L_L(\Phi_1) - i \int_T^{2T} dt_2 L_L(\Phi_2) - \int_0^\infty d\tau_3 L_E(\Phi_3), \quad (3.25)$$

with the Lagrangians

$$\begin{aligned} L_L(\Phi) &= \frac{1}{2} \int d^2x \sqrt{|G|} (-\partial_\mu \Phi \partial^\mu \Phi - m^2 \Phi^2), \\ L_E(\Phi) &= \frac{1}{2} \int d^2x \sqrt{|G|} (\partial_\mu \Phi \partial^\mu \Phi + m^2 \Phi^2). \end{aligned} \quad (3.26)$$

We use a contour time coordinate on every segment M_i whose direction is indicated in figure 3.3. We glue the surface given by $\tau_3 = 0$ to that given by $t_2 = 2T$, and similarly the surfaces $t_1 = T$ to $t_2 = T$ and $t_1 = 0$ to $\tau_0 = 0$.

A full list of matching conditions is now given by continuity of the fields, plus continuity of their derivatives with appropriate signs. These signs are easily found by equating the conjugate momenta obtained from functional differentiation of the on-shell actions as we showed in section 2.3. One obtains:

$$\begin{aligned} -\partial_{\tau_0} \Phi_0(\tau_0 = 0) - i\partial_{t_1} \Phi_1(t_1 = 0) &= 0 \\ +i\partial_{t_1} \Phi_0(t_2 = T) + i\partial_{t_2} \Phi_2(t_2 = T) &= 0 \\ -i\partial_{t_2} \Phi_2(\tau_2 = 2T) + \partial_{\tau_3} \Phi_3(\tau_3 = 0) &= 0. \end{aligned} \quad (3.27)$$

We will consider the case of a nonzero source $\phi_{(0)[1]}$ only on the conformal boundary of M_1 . In that case Φ_1 is given by (cf. (3.11)):

$$\begin{aligned} \Phi_1(t_1, \phi, r) &= \frac{1}{4\pi^2} \sum_{k \in \mathbb{Z}} \int_C d\omega \int_{M_1} d\hat{t} \int d\hat{\phi} e^{-i\omega(t_1 - \hat{t}) + ik(\phi - \hat{\phi})} \phi_{(0)[1]}(\hat{t}, \hat{\phi}) f(\omega, |k|, r) \\ &\quad + \sum_{\pm} \sum_{k \in \mathbb{Z}} \sum_{n=0}^{\infty} c_{[1]nk}^{\pm} e^{-i\omega_{nk}^{\pm} t_1 + ik\phi} g(\omega_{nk}, |k|, r), \end{aligned} \quad (3.28)$$

with C again a Feynman contour and to be determined coefficients $c_{[1]nk}^{\pm}$. We again take the source to vanish near $t_1 = 0$ and $t_1 = T$ so near these hypersurfaces we may (just as in the previous example) perform the ω -integral and write the solution as a sum over normalizable modes:

$$\begin{aligned} \Phi_1(t_1 \sim 0, \phi, r) &= \frac{1}{4\pi^2} \sum_{n=0}^{\infty} \sum_{k \in \mathbb{Z}} e^{-i\omega_{nk}^- t_1 + ik\phi} \phi_{(0)[1]}(\omega_{nk}^-, k) g(\omega_{nk}, |k|, r) \\ &\quad + \sum_{\pm} \sum_{k \in \mathbb{Z}} \sum_{n=0}^{\infty} c_{[1]nk}^{\pm} e^{-i\omega_{nk}^{\pm} t_1 + ik\phi} g(\omega_{nk}, |k|, r), \quad (3.29) \\ \Phi_1(t_1 \sim T, \phi, r) &= \frac{1}{4\pi^2} \sum_{n=0}^{\infty} \sum_{k \in \mathbb{Z}} e^{-i\omega_{nk}^+ t_1 + ik\phi} \phi_{(0)[1]}(\omega_{nk}^+, k) g(\omega_{nk}, |k|, r) \\ &\quad + \sum_{\pm} \sum_{k \in \mathbb{Z}} \sum_{n=0}^{\infty} c_{[1]nk}^{\pm} e^{-i\omega_{nk}^{\pm} t_1 + ik\phi} g(\omega_{nk}, |k|, r). \end{aligned}$$

Since there is no source on the other segments, the solutions Φ_0 , Φ_2 and Φ_3 are all just sums over normalizable modes. For Φ_2 we obtain:

$$\Phi_2(t_2, \phi, r) = \sum_{\pm} \sum_{k \in \mathbb{Z}} \sum_{n=0}^{\infty} c_{[2]nk}^{\pm} e^{-i\omega_{nk}^{\pm} t_2 + ik\phi} g(\omega_{nk}, |k|, r). \quad (3.30)$$

For M_0 we can again only allow for modes of the form $e^{+|\omega|\tau_0}$, since τ_0 extends to $-\infty$. Similarly, since $\tau_3 \rightarrow \infty$ on M_3 , the modes there are of the form $e^{-|\omega|\tau_3}$. We thus find that

$$\begin{aligned} \Phi_0(\tau_0, \phi, r) &= \sum_{k \in \mathbb{Z}} \sum_{n=0}^{\infty} c_{[0]nk} e^{\omega_{nk}^+ \tau_0 + ik\phi} g(\omega_{nk}, |k|, r), \\ \Phi_3(\tau_3, \phi, r) &= \sum_{k \in \mathbb{Z}} \sum_{n=0}^{\infty} c_{[3]nk} e^{-\omega_{nk}^+ \tau_3 + ik\phi} g(\omega_{nk}, |k|, r). \end{aligned} \quad (3.31)$$

We will now impose the matching conditions and use again the orthogonality of the normalizable modes $g(\omega_{nk}, |k|, r)$ to impose this condition ‘mode-wise’. The first matching between M_1 and M_0 , which is $\Phi_1(t_1 = 0, \phi, r) = \Phi_0(\tau_0 = 0, \phi, r)$, then yields

$$c_{[0]nk} = \frac{1}{4\pi^2} \phi_{(0)[1]}(\omega_{nk}^-, k) + c_{[1]nk}^+ + c_{[1]nk}^-, \quad (3.32)$$

and the second matching condition, which is the first equation in (3.27), becomes

$$-\omega_{nk}^+ c_{[0]nk} - \frac{1}{4\pi^2} \omega_{nk}^- \phi_{(0)[1]}(\omega_{nk}^-, k) - \omega_{nk}^+ c_{[1]nk}^+ - \omega_{nk}^- c_{[1]nk}^- = 0. \quad (3.33)$$

Recalling that $\omega_{nk}^+ = -\omega_{nk}^-$ and combining the two matching conditions, we find that

$$c_{[1]nk}^+ = 0, \quad (3.34)$$

which is the statement that there are no positive frequencies to the past of the sources.

Similarly, from the matching conditions between M_2 and M_3 , one deduces

$$c_{[2]nk}^+ = 0, \quad (3.35)$$

so on M_2 we can only allow for negative frequencies with respect to t_2 . Then, from the matching condition between M_1 and M_2 , we see that frequencies should be inverted on M_2 : positive frequencies on M_1 become negative frequencies on M_2 (with respect to t_2) and vice versa. Therefore, on M_1 there can only be positive frequencies close to $t_1 = T$. Indeed, working out the details results in

$$c_{[1]nk}^- = 0, \quad (3.36)$$

which, combined with (3.34), completely fixes the $c_{[1]nk}^\pm$ on M_1 to be zero. We obtain again the Feynman prescription for the bulk-boundary propagator on M_1 , which is reassuring: using the in-in instead of the in-out formalism should not have changed our result of the previous subsection and indeed we found that it did not.

The solution is now completely fixed and one may compute all of the $c_{[2]nk}^\pm$ and the $c_{[0]nk}$ and $c_{[3]nk}$ using the matching conditions. For the Wightman function, we will only be interested in the solution on M_2 for a source on M_1 , so we will only need the $c_{[2]nk}^\pm$. Equation (3.35) already fixed half of them, and the first matching condition between M_1 and M_2 yields

$$c_{[2]nk}^- = \frac{1}{4\pi^2} \phi_{(0)[1]}(\omega_{nk}^+, k) e^{-2i\omega_{nk}^+ T}. \quad (3.37)$$

With the solutions determined, consider the one-point functions. Just as in the previous example we use the result of section 2.3 which states that the renormalized one-point function in the presence of sources is given by the renormalized radial conjugate momentum, leading specifically to the equations (2.36) and (2.37). For the case under consideration, we thus obtain

$$\langle \mathcal{O}_{[i]}(x) \rangle = \frac{i}{\sqrt{-g_{(0)}}} \frac{\delta}{\delta \phi_{(0)[i]}} (-S_0 + iS_1 - iS_2 - S_3 + S_{ct}) = -2l\phi_{(2l)[i]}(x), \quad (3.38)$$

with $\phi_{(2l)[i]}$ the term of order r^{-l-1} in the radial expansion of Φ_i .

We are in particular interested in the Wightman function. Using the QFT result of section 2.1 we find that we may obtain it as:

$$\begin{aligned} \langle \mathcal{O}(x)\mathcal{O}(x') \rangle &= \langle T_C \mathcal{O}_{[2]}(x)\mathcal{O}_{[1]}(x') \rangle \\ &= \frac{i}{\sqrt{-g_{(0)}}} \frac{\delta}{\delta \phi_{(0)[1]}(x')} \langle \mathcal{O}_{[2]}(x) \rangle \\ &= -2li \frac{\delta \phi_{(2l)[2]}(x)}{\delta \phi_{(0)[1]}(x')}. \end{aligned} \quad (3.39)$$

With the solution Φ_2 we found above, we obtain

$$\phi_{(2l)[2]}(x) = \frac{i}{\pi} \sum_{k \in \mathbb{Z}} \sum_{n=0}^{\infty} \alpha(\omega_{nk}, |k|, l) e^{-i\omega_{nk}^+(2T-t_2)+ik\phi} \int_{M_1} dt d\hat{\phi} e^{i\omega_{nk}^+ \hat{t} - ik\hat{\phi}} \phi_{(0)[1]}(\hat{t}, \hat{\phi}). \quad (3.40)$$

Using $t = 2T - t_2$ and taking the functional derivative, we get:

$$\langle \mathcal{O}(x)\mathcal{O}(x') \rangle = \frac{2l}{\pi} \sum_{n \geq 0} \sum_{k \in \mathbb{Z}} e^{-i\omega_{nk}^+(t-t')+ik(\phi-\phi')} \alpha(\omega_{nk}^+, |k|, l). \quad (3.41)$$

This expression satisfies some standard checks that are expected for a Wightman function, namely it vanishes for $\omega < 0$ and the coefficients are real and positive definite, see appendix 2.A. Evaluating the summations, we find

$$\langle \mathcal{O}(x)\mathcal{O}(x') \rangle = \frac{l^2/(2^l\pi)}{[\cos(t-i\epsilon) - \cos(\phi)]^{l+1}}, \quad (3.42)$$

which has poles when $t - i\epsilon$ is real, so it is analytic in the lower half plane, also as expected.

3.1.4 Thermal AdS

Let us now consider the thermal contour indicated in figure 3.1c. We again take t_1 to run from 0 to T on M_1 , t_2 to run from T to $2T$ on M_2 , and τ to run from 0 to β on M_3 . The novelty here is that we glue the part with $\tau = \beta$ to the surface with $t_1 = 0$ in order to obtain a thermal state. The action splits into:

$$i \int_0^T dt_1 L_L[\Phi_1] - i \int_T^{2T} dt_2 L_L[\Phi_2] - \int_0^\beta d\tau L_E[\Phi_3]. \quad (3.43)$$

Again, we consider a source living only on M_1 and solve the Klein-Gordon equation. The general expressions for Φ_1 and Φ_2 (without specification of initial and final data) are exactly the same as before and are given by the equations (3.28) and (3.30). We can also use the expressions (3.29) for Φ_1 when $t \sim 0$ or $t \sim T$. Since the τ coordinate on the Euclidean segment has a finite range we may allow for both positive and negative frequencies on this segment. The most general purely normalizable Euclidean solution is then:

$$\Phi_3(\tau, \phi, r) = \sum_{\pm} \sum_{k \in \mathbb{Z}} \sum_{n=0}^{\infty} c_{[3]nk}^{\pm} e^{\omega_{nk}^{\pm} \tau + ik\phi} g(\omega_{nk}, |k|, r). \quad (3.44)$$

The full list of matching conditions is now

$$\begin{aligned} \Phi_1(t_1 = T) &= \Phi_2(t_2 = T) & \partial_t \Phi_1(t_1 = T) &= -\partial_t \Phi_2(t_2 = T) \\ \Phi_2(t_2 = 2T) &= \Phi_3(\tau = 0) & i\partial_t \Phi_2(t_2 = 2T) &= \partial_\tau \Phi_3(\tau = 0) \\ \Phi_1(t_1 = 0) &= \Phi_3(\tau = \beta) & -i\partial_t \Phi_1(t_1 = 0) &= \partial_\tau \Phi_3(\tau = \beta), \end{aligned}$$

which, after some algebraic manipulations, results in

$$c_{[1]nk}^{\pm} = \frac{1}{4\pi^2} \phi_{(0)[1]}(\omega_{nk}^{\pm}, k) \frac{1}{e^{\beta\omega_{nk}^{\pm}} - 1}. \quad (3.45)$$

The nonzero $c_{[1]nk}^\pm$ directly enter into the two-point function and we get

$$\begin{aligned} \langle T\mathcal{O}_{[1]}(x')\mathcal{O}_{[1]}(x)\rangle_\beta &= \frac{l}{2\pi^2i} \sum_{k\in\mathbb{Z}} \int_C d\omega e^{-i\omega(t-t')+ik(\phi-\phi')} \alpha(\omega, |k|, l) \beta(\omega, |k|, l) \\ &+ \frac{2l}{\pi} \sum_{\pm} \sum_{k\in\mathbb{Z}} \sum_{n=0}^{\infty} \frac{\alpha(\omega_{nk}, |k|, l)}{e^{\beta|\omega_{nk}^\pm|} - 1} e^{-i\omega_{nk}^\pm(t-t')+ik(\phi-\phi')}, \end{aligned} \quad (3.46)$$

with the subscript β indicating the temperature. As in the ‘free-field’ approximation, we find the sum of the zero-temperature Feynman propagator and a heat-bath contribution. Also, notice the symmetry $x \leftrightarrow x'$. After rewriting the thermal contributions as geometric series, one readily finds that this expression becomes

$$\langle T\mathcal{O}(x)\mathcal{O}(x')\rangle_\beta = \sum_{n\in\mathbb{Z}} \frac{l^2/(2^l\pi)}{[\cos(t - i\epsilon t + in\beta) - \cos(\phi)]^{l+1}}, \quad (3.47)$$

which satisfies the KMS condition, so it corresponds to a thermal two-point function indeed. It is a sum over images of the zero temperature result, reflecting the fact that Euclidean thermal AdS is obtained by identifications in the time direction of Euclidean global AdS.

One can actually arrive more directly at (3.47) by using the relation between thermal AdS and global AdS to first obtain the Euclidean correlator by a sum over images and then analytically continue to real-time. This was the way (3.47) was obtained earlier in [63]. Of course, the $i\epsilon$ insertions then have to be fixed by hand. The emphasis in this and the previous examples is on the fact that we can unambiguously arrive at equations like (3.47), including the correct $i\epsilon$ insertions, by employing a Lorentzian signature gauge/gravity dictionary and without assuming any special properties of the background under consideration.

3.2 Poincaré coordinates

For our next example we consider a CFT in d -dimensional Minkowski ($Mink_d$) spacetime. As is well known, Minkowski spacetime is conformally isometric to an open region of the Einstein static universe, $\mathbb{R} \times S^{d-1}$. Thus the correlators for the CFT in Minkowski spacetime can be obtained from those of the Einstein universe (as we demonstrate for $d = 2$ in subsection 3.2.5). We explained in section 1.4.3 that boundary Weyl transformations are a specific class of bulk diffeomorphisms and therefore a similar procedure can be done holographically.

Nevertheless, it is still interesting to directly compute the correlators in Minkowski spacetime, not least because this is the typical background for most QFT computations. Furthermore, for a CFT on $Mink_d$ to be exactly equivalent to the theory

on $\mathbb{R} \times S^{d-1}$ the boundary conditions of all QFT fields at infinity of $Mink_d$ must be the ones dictated by the theory on $\mathbb{R} \times S^{d-1}$. One may however wish to study the QFT on $Mink_d$ with fields satisfying different boundary conditions at infinity. For example, the ground state of a conformally coupled scalar ϕ on $\mathbb{R} \times S^{d-1}$ has necessarily $\langle \phi \rangle = 0$ because of the curvature coupling of the scalar. The same theory on $Mink_d$ however allows for ground states with non-vanishing $\langle \phi \rangle$, since in this case the curvature coupling vanishes. In such cases the nonzero scalar vev spontaneously breaks conformal invariance. This is described in the bulk by domain wall spacetimes containing additional bulk fields capturing the vevs of gauge invariant operators. One can extend the methods described here to apply to the computation of real-time correlators along holographic RG flows, extending the Euclidean computations in [64, 65], but we shall not discuss this in detail here.

Instead we will compute vacuum-to-vacuum amplitudes for the CFT without vevs. To this end, we consider the field theory path of figure 2.1a, but with \mathbb{R}^{d-1} as the spacelike part of the boundary manifold. We can compactify the entire contour by adding a single point, resulting in the boundary geometry shown in figure 3.4a. The Lorentzian segment is cut off at finite initial and final times $t = \pm T$. Below we holographically compute a time-ordered two-point function for a CFT in this background.

3.2.1 Bulk spacetime

As before, the first step is to find a suitable bulk manifold that fills in the contour.

We begin with the Lorentzian segment of the contour. In the absence of any sources and vevs, it is filled in with a segment of empty AdS_{d+1} in Poincaré coordinates:

$$ds^2 = \frac{dz^2 - dt^2 + d\vec{x}^2}{z^2}. \quad (3.48)$$

The Poincaré coordinate system covers only a part of all of AdS_{d+1} , as indicated in figure 3.4b. We will however cut off the bulk manifold along the hypersurfaces $t = \pm T$ and therefore we will not need the rest of the AdS_{d+1} spacetime anyway. The Lorentzian segment with the above metric and $-T < t < T$ will be referred to as M_1 below.

The two Euclidean segments can be filled with Euclidean AdS_{d+1} , whose metric can be obtained from (3.48) by the replacement $t = -i\tau$. We again need only a part of these spaces and cut off the Euclidean solutions along hypersurfaces of constant τ . More precisely, we call M_0 the Euclidean manifold with the metric

$$ds^2 = \frac{dz^2 + d\tau_0^2 + d\vec{x}^2}{z^2} \quad (3.49)$$

and $\tau_0 < 0$. Similarly, we take M_2 the Euclidean manifold with the $\tau_2 > 0$ and the same metric (3.49) with the replacement $\tau_0 \rightarrow \tau_2$.

Next, we glue the three components together by gluing the surface given by $\tau_0 = 0$ on M_0 to the surface $t = -T$ on M_1 , and the surface $\tau_2 = 0$ to the surface $t = T$ on M_1 . One may easily verify that the matching conditions for gravity are satisfied, since the induced metric on surfaces of constant t or τ is the same and these surfaces are totally geodesic. We conclude that the combination of M_0 , M_1 and M_2 satisfies all the holographic boundary data as well as all the matching conditions, and so it can serve as the background around which we study perturbations below.

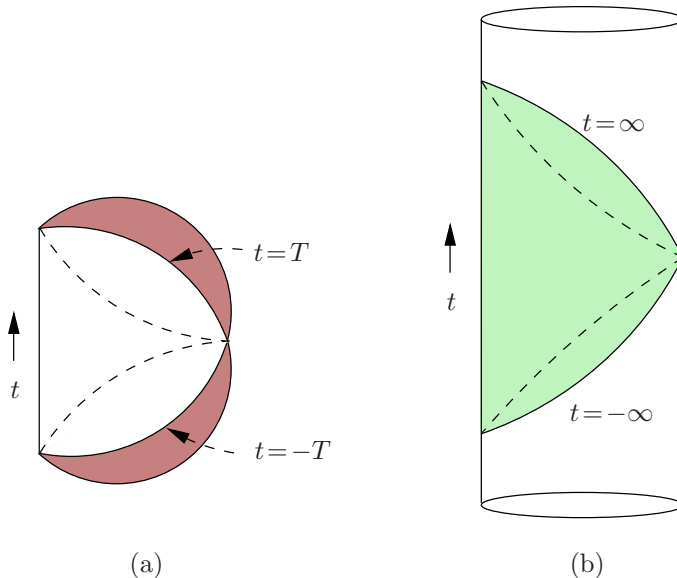


Figure 3.4: (a) The geometry used for the computation of the two-point function in $Mink_d$. The Lorentzian manifold is cut off at slices given by $t = \pm T$, to which the darker shaded Euclidean caps are glued. (b) The Poincaré coordinate system covers only a part of AdS_{d+1} . Both the global AdS time and the Poincaré time run upward. The planes $t = \pm\infty$ bound the coordinate system.

3.2.2 Solutions

We will again obtain a time-ordered two-point function of a scalar operator of conformal weight $\Delta = \frac{d}{2} + l$, with $l \in \{1, 2, \dots\}$, which is dual to a bulk scalar field of mass $m^2 = \Delta(\Delta - d)$. As we did in the previous examples, we take the scalar field to propagate freely and without backreaction.

On M_1 the action for the scalar field is again (3.3), this time with the metric (3.48). Solutions to the equations of motion satisfy the Klein-Gordon equation:

$$z^{d+1}\partial_z(z^{-d+1}\partial_z\Phi) + z^2\Box_0\Phi - m^2\Phi = 0. \quad (3.50)$$

We already discussed the solutions to this equation in Euclidean signature in section 1.5. Let us now revisit this analysis for a Lorentzian signature metric. After separation of variables we find modes labeled by (ω, \vec{k}) :

$$e^{-i\omega t + i\vec{k}\cdot\vec{x}} z^{d/2} K_l(qz), \quad e^{-i\omega t + i\vec{k}\cdot\vec{x}} z^{d/2} I_l(qz). \quad (3.51)$$

For spacelike momenta $q^2 = -\omega^2 + \vec{k}^2 > 0$, these modes are unambiguously defined. For timelike momenta $q^2 < 0$, we have to consider possible branch cuts. First of all, we put the square root in defining $q = \sqrt{q^2}$ just above the negative real axis. We indicate this by using

$$q_\epsilon = \sqrt{-\omega^2 + \vec{k}^2 - i\epsilon}. \quad (3.52)$$

Second, K_l has a branch cut along the negative real axis, which is however unimportant since $|\arg(q_\epsilon z)| \leq \pi/2$. Finally, I_l has no branch cut since l is an integer.

To select the right solution on M_1 , we should look at the asymptotics. They take the form:

$$\begin{aligned} z^{d/2} K_l(qz \rightarrow 0) &= \Gamma(l) \frac{z^{d/2-l}}{2^{l+1} q^l} + \dots \\ z^{d/2} I_l(qz \rightarrow 0) &= \frac{1}{\Gamma(l+1)} \frac{z^{d/2+l}}{2^l q^{-l}} + \dots \\ z^{d/2} K_l(qz \rightarrow \infty) &= \sqrt{\frac{\pi z^{d-1}}{2q}} e^{-qz} + \dots \\ z^{d/2} I_l(qz \rightarrow \infty) &= \sqrt{\frac{z^{d-1}}{2\pi q}} [e^{qz} + e^{-qz - (l+\frac{1}{2})\pi i}] + \dots \end{aligned} \quad (3.53)$$

For spacelike momenta $q^2 > 0$ we find that finiteness as $z \rightarrow \infty$ selects $z^{d/2} K_l(qz)$ as the only correct solution, just as in section 1.5. On the other hand, for timelike momenta no linear combination of the solutions remains finite as $z \rightarrow \infty$, which means that any solution that does remain finite as $z \rightarrow \infty$ should be obtained as an infinite sum over the modes. Furthermore, from the asymptotics as $z \rightarrow 0$, we find that the modes $z^{d/2} K_l(q_\epsilon z) \sim z^{d/2-l}$ correspond to sources on the conformal boundary, whereas the $z^{d/2} I_l(q_\epsilon z) \sim z^{d/2+l}$ are the normalizable modes.

For timelike momenta $q_\epsilon z = -i|q|z$ and we will henceforth rewrite the modified Bessel function of the first kind using $I_l(-i|q|z) = e^{-i\pi l/2} J_l(|q|z)$. Although we

could also have rewritten $K_l(-i|q|z) = (i\pi e^{i\pi/2}/2)H_n^{(1)}(|q|z)$, we do not do so below, since $z^{d/2}K_l(q_\epsilon z)$ is needed for both spacelike and timelike momenta. We emphasize that $K_l(q_\epsilon z)$ is unambiguously defined for all real q^2 .

Next, consider the manifolds M_0 and M_2 , both with the Euclidean metric (3.49) and $0 < \tau < \infty$ and $-\infty < \tau < 0$, respectively. Although we will mainly work in position space below, we will for completeness present the mode solutions here as well. First of all, the mode solutions on M_0 and M_2 are obtained by the usual substitution $t \rightarrow -i\tau$ in the Lorentzian modes (3.51). Since we will not switch on any sources on these segments, the solutions on M_0 and M_2 need to be purely normalizable. As we just showed, this implies that only the modes $z^{d/2}J_l(|q|z)$ with $q^2 < 0$ are allowed. Furthermore, since no operators are inserted at the points $\tau \rightarrow \pm\infty$, we will also request finiteness of the solution in this limit. This implies a restriction to negative frequencies on M_0 and to positive frequencies on M_2 . More explicitly, the solutions on these segments are built up from the modes

$$\begin{aligned} e^{|\omega|\tau_0 + i\vec{k}\cdot\vec{x}} z^{d/2} J_l(|q|z) & \quad \text{on } M_0, \\ e^{-|\omega|\tau_2 + i\vec{k}\cdot\vec{x}} z^{d/2} J_l(|q|z) & \quad \text{on } M_2, \end{aligned} \tag{3.54}$$

with $-\omega^2 + \vec{k}^2 < 0$. Since the individual modes diverge as $z \rightarrow \infty$, we should again sum an infinite number of these modes in order to get a solution that vanishes also at this point.

3.2.3 Bulk-boundary propagator

The next step is to compute a bulk-boundary propagator, which we denote by $X(t, \vec{x}, z)$. We will consider the propagator for a source on the conformal boundary of M_1 only. Let us first investigate the solution on M_1 . Inspired by the Euclidean bulk-boundary propagator, we may try:

$$X_1(t, \vec{x}, z) = \frac{1}{(2\pi)^d} \int_C d\omega \int d\vec{k} e^{-i\omega t + i\vec{k}\cdot\vec{x}} \frac{2^{l+1} q_\epsilon^l}{\Gamma(l)} z^{d/2} K_l(q_\epsilon z). \tag{3.55}$$

The $i\epsilon$ -prescription is equivalent to a Feynman contour C in the ω -plane around the branch cuts which we show in figure 3.5. The expression (3.55) is not obviously convergent as $z \rightarrow \infty$. However, we can perform the Fourier transform by closing and deforming the contour. The $i\epsilon$ -prescription tells us which branch cuts we pick up and the corresponding position-space expression is equal to

$$X_1(t, \vec{x}, z) = i\Gamma(l)\Gamma(l + \frac{d}{2})\pi^{-\frac{d}{2}} \frac{z^{l+\frac{d}{2}}}{(-t^2 + \vec{x}^2 + z^2 + i\epsilon)^{l+d/2}}, \tag{3.56}$$

which clearly converges for large z .

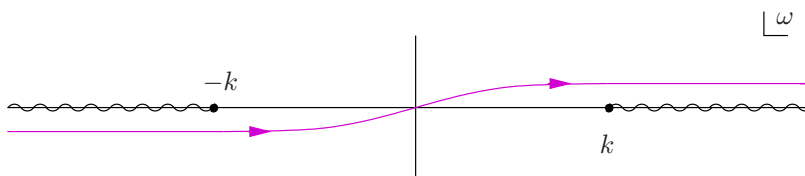


Figure 3.5: The contour around the branch cuts (wavy lines) in the complex frequency plane used to define a bulk-boundary propagator.

As in the previous section, this bulk-boundary propagator is not unique without imposing initial and final conditions. Indeed, one may always add a normalizable solution, which we will denote as $Y(t, \vec{x}, z)$. Notice that we know that normalizable solutions on M_1 exist from our discussion of the previous section, where we used global coordinates. In the previous subsection we found that $Y(t, \vec{x}, z)$ must be a linear combination of the modes $z^{d/2} I_l(q_\epsilon z)$ with $q^2 < 0$, which we write as

$$Y_1(t, \vec{x}, z) = \frac{1}{(2\pi)^d} \int d\omega \int dk e^{-i\omega t + i\vec{k} \cdot \vec{x}} \theta(-q^2) c_{[1]}(\omega, \vec{k}) z^{d/2} J_l(|q|z), \quad (3.57)$$

with further constrains on $c_{[1]}(\omega, \vec{k})$ by requesting finiteness for $z \rightarrow \infty$ that we will not work out here. To reiterate, without initial or final conditions such normalizable solutions can be added at will to our suggested bulk-boundary propagator (3.55), so the normalizable solutions parametrize the ambiguity in the bulk-boundary propagator. In particular, any different $i\epsilon$ -prescription than the one we fixed above can be implemented by changing these $c_{[1]}(\omega, \vec{k})$.

3.2.4 Matching

With the solutions on M_1 specified, let us now discuss the matching. We will show that the matching conditions imply that $X_1(t, \vec{x}, z)$ is the right bulk-boundary propagator and that no normalizable solution can be added since $Y_1(t, \vec{x}, z)$ can never be matched to a regular and normalizable solution on M_0 and M_2 .

We begin with the matching conditions between M_0 , M_1 and M_2 :

$$\begin{aligned} \Phi_1(t_1 = T, \vec{x}, z) &= \Phi_2(\tau = 0, \vec{x}, z) & i\partial_{t_1} \Phi_1(t_1 = T, \vec{x}, z) + \partial_\tau \Phi_2(\tau = 0, \vec{x}, z) &= 0 \\ \Phi_1(t_1 = -T, \vec{x}, z) &= \Phi_2(\tau = 0, \vec{x}, z) & -i\partial_{t_1} \Phi_1(t_1 = T, \vec{x}, z) - \partial_\tau \Phi_2(\tau = 0, \vec{x}, z) &= 0. \end{aligned} \quad (3.58)$$

Let us now show that we can find solutions X_0 and X_2 on M_0 and M_2 that can be matched to X_1 . This is straightforward in position space, where we can verify

that the expressions

$$\begin{aligned} X_0(\tau_0, \vec{x}, z) &= i\Gamma(l)\Gamma(l + \frac{d}{2})\pi^{-\frac{d}{2}} \frac{z^{\frac{d}{2}+l}}{(-(-T - i\tau_0)^2 + \vec{x}^2 + z^2 + i\epsilon)^{l+d/2}}, \\ X_2(\tau_2, \vec{x}, z) &= i\Gamma(l)\Gamma(l + \frac{d}{2})\pi^{-\frac{d}{2}} \frac{z^{\frac{d}{2}+l}}{(-(T - i\tau_2)^2 + \vec{x}^2 + z^2 + i\epsilon)^{l+d/2}}, \end{aligned} \quad (3.59)$$

satisfy the equations of motion on all of M_0, M_2 and are normalizable. Furthermore, they actually satisfy the matching conditions as well. To see this, notice that the $(+i\epsilon)$ -insertions in the denominators of (3.59) are not necessary for nonzero τ , but they are necessary to ensure that (3.59) are well-defined (distributions) on the initial and final hypersurfaces given by $\tau_0 = 0$ and $\tau_2 = 0$. With the given $i\epsilon$ -insertions, we can compare (3.59) to (3.56) and one readily verifies that the matching conditions are satisfied.

Let us now show that one could not have picked any other $i\epsilon$ -insertions ($-i\epsilon, +i\epsilon t$, etc.) on the Lorentzian side. If we would have done so, the matching conditions would directly dictate a corresponding change in (3.59). However, such a change in the Euclidean solutions is not allowed, because any other $i\epsilon$ -insertion in (3.59) would give a singularity in either X_0 or in X_2 . For example, if we would replace the $+i\epsilon$ with $-i\epsilon$ on M_2 , then X_2 would be singular at $\tau_2 = \epsilon/2T$, around the point given by $\vec{x}^2 + z^2 = T^2$ and thus this solution should be discarded. We conclude that the $i\epsilon$ -insertion in (3.56) is the only one that moves the singularity everywhere away from the contour.

It remains to show that (3.56) is the indeed the unique bulk-boundary propagator by demonstrating that there are no matching Euclidean solutions for the normalizable solution (3.57). Using the normalizable modes we found above, the solution on M_0 should necessarily be of the form

$$Y_0(\tau_0, \vec{x}, z) = \int d\omega \int d\vec{k} e^{i\omega\tau_0 + i\vec{k}\cdot\vec{x}} \theta(-q^2) c_{[0]}(|\omega|, \vec{k}) z^{d/2} J_l(|q|z), \quad (3.60)$$

for some coefficients $c_{[0]}(|\omega|, \vec{k})$. A similar expression holds for the solution on M_2 :

$$Y_2(\tau_2, \vec{x}, z) = \int d\omega \int d\vec{k} e^{-i\omega\tau_2 + i\vec{k}\cdot\vec{x}} \theta(-q^2) c_{[2]}(|\omega|, \vec{k}) z^{d/2} J_l(|q|z). \quad (3.61)$$

Consider now the matching conditions, for example the continuity condition between M_1 and M_2 :

$$Y_1(T, \vec{x}, z) = Y_2(\tau_0 = 0). \quad (3.62)$$

Although this is an equality between two integrals, the modes $z^{d/2} J_l(|q|z)$ are orthogonal,

$$\int_0^\infty dz z^{-1} J_l(|q|z) J_l(|q'|z) = c\delta(|q| - |q'|), \quad (3.63)$$

with c a constant. We can therefore equate the integrands (up to $\omega \leftrightarrow -\omega$), which results in

$$c_{[1]}(\omega, \vec{k}) + c_{[1]}(-\omega, \vec{k}) = c_{[0]}(|\omega|, \vec{k}). \quad (3.64)$$

The other matching conditions can be imposed in a similar way and they ultimately determine $c_{[1]}(\omega, \vec{k}) = c_{[0]}(\omega, \vec{k}) = c_{[2]}(\omega, \vec{k}) = 0$. There is thus no normalizable solution and the bulk-boundary propagator $X(t, \vec{x}, z)$ is unique.

3.2.5 Two-point function

As for the computation of the time-ordered two-point function, the only difference with the Euclidean case are the $i\epsilon$ -insertions in the bulk-boundary propagator, which in Fourier space corresponds to the replacement $q \rightarrow q_\epsilon$. Just as for AdS_{d+1} in global coordinates, these enter directly in the two-point function which, up to contact terms, is then given by:

$$\langle T\mathcal{O}(q)\mathcal{O}(-q) \rangle = \frac{i(-1)^l}{2^{2l-1}\Gamma(l)^2} q_\epsilon^{2l} \log(q_\epsilon/\mu). \quad (3.65)$$

As expected, its analytic continuation to Euclidean signature coincides precisely with the renormalized Euclidean two-point function (1.123). The $i\epsilon$ insertion we obtained holographically corresponds again to the Feynman contour of figure 3.5 around the branch cuts, signifying time-ordering indeed. In position space, we find

$$\begin{aligned} \langle T\mathcal{O}(x)\mathcal{O}(0) \rangle &= \frac{1}{(2\pi)^d} \frac{i(-1)^l}{2^{2l-1}\Gamma(l)^2} \int e^{-i\omega t + i\vec{k}\cdot\vec{x}} q_\epsilon^{2l} \log(q_\epsilon/\mu) \\ &= \frac{2\Gamma(l+d/2)}{\pi^{d/2}\Gamma(l)} \mathcal{R} \frac{1}{(-t^2 + \vec{x}^2 + i\epsilon)^{l+\frac{d}{2}}}, \end{aligned} \quad (3.66)$$

and the $i\epsilon$ -insertion agrees with [66].

Normalization

Let us compare the normalization of the time-ordered two-point function on the cylinder with that on two-dimensional Minkowski space. We start from the time-ordered two-point function on the cylinder given in (3.24):

$$\langle T\mathcal{O}(x)\mathcal{O}(0) \rangle = \frac{l^2/(2^l\pi)}{[\cos(t - i\epsilon t) - \cos(\phi)]^{l+1}}, \quad ds^2 = -dt^2 + d\phi^2,$$

and apply the coordinate transformation $t = u - v$, $\phi = u + v$, after which we find

$$\langle T\mathcal{O}(x)\mathcal{O}(0) \rangle = \frac{l^2/(2^{2l+1}\pi)}{[\sin(u - i\eta)\sin(v + i\eta)]^{l+1}}, \quad ds^2 = 4dudv,$$

where now $\eta = \epsilon(u - v)$. We then Weyl transform and use covariance of the two-point function:

$$\langle T\mathcal{O}(x)\mathcal{O}(0) \rangle = \frac{2l^2/\pi}{[\tan(u - i\eta)\tan(v + i\eta)]^{l+1}}, \quad ds^2 = \frac{dudv}{\cos^2(u)\cos^2(v)},$$

where we should remember that the two-point function is multiplied by two Weyl factors; one evaluated at x and one at 0 . For $-\pi/2 < u, v < \pi/2$, we can rewrite the denominator using

$$\tan(u - i\eta)\tan(v + i\eta) = \tan(u)\tan(v) + i\epsilon(u - v)[\tan(u) - \tan(v)] = \tan(u)\tan(v) + i\epsilon'$$

with ϵ' positive and constant. Finally, using $x + y = \tan(u)$ and $x - y = \tan(v)$, we obtain

$$\langle T\mathcal{O}(x)\mathcal{O}(0) \rangle = \frac{2l^2/\pi}{[-y^2 + x^2 + i\epsilon']^{l+1}}, \quad ds^2 = -dy^2 + dx^2,$$

and the normalization is indeed the same as in (3.66) evaluated at $d = 2$.

3.3 Higher-point correlation functions

In this subsection, we briefly discuss how real-time higher-point correlation functions can be computed with our prescription. We take an interacting scalar field with potential

$$V(\Phi) = \frac{1}{2}m^2\Phi^2 + \frac{\lambda}{3}\Phi^3 + \dots \quad (3.67)$$

so that the equation of motion becomes:

$$\square\Phi - m^2\Phi - \lambda\Phi^2 = 0. \quad (3.68)$$

This equation can be solved perturbatively. We first compute the sequence:

$$\begin{aligned} \square\Phi_{\{0\}} - m^2\Phi_{\{0\}} &= 0, \\ \square\Phi_{\{1\}} - m^2\Phi_{\{1\}} &= \lambda\Phi_{\{0\}}^2, \\ \square\Phi_{\{2\}} - m^2\Phi_{\{2\}} &= \lambda\Phi_{\{1\}}^2, \\ &\dots \end{aligned} \quad (3.69)$$

where $\Phi_{\{0\}}$ satisfies the radial boundary data and $\Phi_{\{i\}}$ with $i \geq 1$ vanish asymptotically. The full solution is then obtained as:

$$\Phi = \Phi_{\{0\}} + \Phi_{\{1\}} + \Phi_{\{2\}} + \dots \quad (3.70)$$

To compute the series $\Phi_{\{i\}}$, we need to compute the bulk-bulk propagator Z . This propagator satisfies

$$(\square_G - m^2)Z(x, x') = \frac{-1}{\sqrt{-G}}\delta^{d+1}(x - x') \quad (3.71)$$

and vanishes asymptotically. In terms of $Z(x, x')$, we find:

$$\Phi_{\{i+1\}}(x) = \lambda \int_M d^{d+1}x' \sqrt{-G} Z(x, x') \Phi_{\{i\}}^2(x'). \quad (3.72)$$

In our case, the bulk manifold M splits into multiple parts and we need to integrate the bulk-bulk propagator against $\Phi_{\{i\}}$ on the various segments. The bulk-bulk propagator therefore also splits in multiple components depending the segment that x and x' lie on. We will indicate this by a subscript. For example, $Z_{[12]}(x, x')$ denotes the bulk-bulk propagator with x on M_1 and x' on M_2 . Equation (3.72) then becomes:

$$\Phi_{[j]\{i+1\}}(x) = \lambda \sum_k \int_{M_k} d^{d+1}x' \sqrt{-G} Z_{[jk]}(x, x') \Phi_{[k]\{i\}}^2(x'), \quad (3.73)$$

with the sum over all of the components M_k . Of course, $Z_{[jk]}$ is homogeneous on M_j if $j \neq k$. Also, we will explicitly see below that $Z_{[jk]}(x, x') = Z_{[kj]}(x', x)$.

Let us now find this matrix of bulk-bulk propagators. These bulk-bulk propagators need to satisfy the matching conditions, since then so will all the $\Phi_{\{i\}}$ and consequently also Φ . (Our derivation of the matching conditions for a scalar field in section 3.1 was independent of the potential $V[\Phi]$, so the matching conditions are unchanged by the interaction terms.) For concreteness, consider the bulk spacetime of the previous subsection, with a Lorentzian segment M_1 sandwiched between two Euclidean segments M_0 and M_2 . The matching conditions become important when we move x from, say M_1 to M_0 while keeping x' fixed. For example, we get

$$\begin{aligned} Z_{[11]}(t_1 = -T, \vec{x}, z; t'_1, \vec{x}', z') &= Z_{[01]}(\tau_0 = 0, \vec{x}, z; t'_1, \vec{x}', z'), \\ -i\partial_t Z_{[11]}(t_1 = -T, \vec{x}, z; t'_1, \vec{x}', z') - \partial_\tau Z_{[01]}(\tau_0 = 0, \vec{x}, z; t'_1, \vec{x}', z') &= 0, \end{aligned} \quad (3.74)$$

just as in (3.58), and all the other matching conditions are similar.

The uniqueness of the bulk-bulk propagator is clear from the previous subsection, where we showed that there is no normalizable homogeneous solution that satisfies the matching conditions. As for existence, the bulk-bulk propagator for Lorentzian AdS in Poincaré coordinates is already known, see for example [11] and the references therein, where one may find that

$$Z_{[11]}(x, x') = Z[\xi_{11}], \quad (3.75)$$

with ξ_{11} an AdS-invariant function,

$$\xi_{11} = \frac{(z - z')^2 - (t - t')^2 + (\vec{x} - \vec{x}')^2 + i\epsilon}{z^2 + z'^2 - (t - t')^2 + (\vec{x} - \vec{x}')^2} \quad (3.76)$$

and Z given by

$$Z[\xi_{11}] = \frac{2^{-\Delta}\Gamma(\Delta)}{\pi^{d/2}\Gamma(\Delta - \frac{d}{2})\Gamma(2\Delta - d)} \left(1 - \xi_{11}\right)^\Delta F\left(\frac{\Delta}{2}, \frac{\Delta + 1}{2}; \Delta - \frac{d}{2} + 1; [1 - \xi_{11}]^2\right), \quad (3.77)$$

with $F(a, b; c; z)$ the hypergeometric function and $m^2 = \Delta(\Delta - d)$. This solution is regular except when $\xi_{11} \rightarrow 0$. Analytically continuing t, t' to M_0 or M_2 by the replacement $t = -T - i\tau_0$ or $t = T - i\tau_2$ yields other ξ_{ij} , and the $i\epsilon$ -insertions again ensure that these ξ_{ij} satisfy the matching conditions when either x or x' moves from one segment to the other. So if we define

$$Z_{[ij]}(x, x') = Z[\xi_{ij}], \quad (3.78)$$

then the various $Z_{[ij]}$ satisfy (3.71), the matching conditions, and vanish asymptotically. Therefore, the full matrix of bulk-bulk propagators can be obtained by this analytic continuation. Just as for the bulk-boundary propagator, the matching conditions uniquely fix the $i\epsilon$ -insertions to be those in equation (3.76).

Again, these $i\epsilon$ -insertions enter directly into the higher-point correlation functions. These are obtained as usual by further functional differentiation of the renormalized one-point function. For example, for a time-ordered vacuum-to-vacuum three-point function with all three arguments on M_1 we obtain

$$\langle T\mathcal{O}(x_1)\mathcal{O}(x_2)\mathcal{O}(x_3)\rangle = (2\Delta - d) \frac{\delta^2\phi_{(2\Delta-d)}(x_1)}{\delta\phi_{(0)}(x_2)\delta\phi_{(0)}(x_3)} \Big|_{\phi_{(0)}=0}, \quad (3.79)$$

with $\phi_{(2\Delta-d)}$ the coefficient of the normalizable mode (of order z^Δ) in the z -expansion of Φ , and the source $\phi_{(0)}$ should be set to zero after the functional differentiation. Given the bulk solution, the procedure to obtain these correlation functions is therefore just as for Euclidean metrics, except for the replacement $t \rightarrow t - i\epsilon t$ (so $-t^2 \rightarrow -t^2 + i\epsilon$).

3.4 Stationary black holes

The thermal contour drawn in figure 3.1c admits another possible bulk solution, which corresponds to an eternal black hole. In this section, we will use this filling to compute the time-ordered two-point function for an operator dual to a free scalar field moving in the black hole background. We will again work in $d = 2$, so

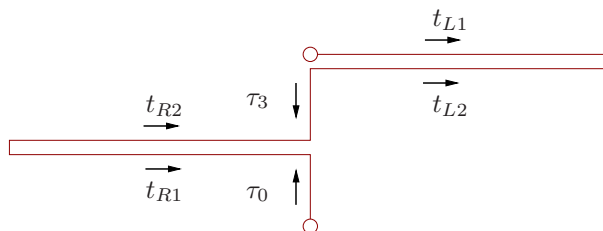


Figure 3.6: The contour we use for the black hole. The circles should be identified.

the bulk spacetime is the static three-dimensional BTZ black hole. The rotating black hole will be discussed in the next subsection.

Below, we will actually use the deformed contour of figure 3.6 rather than the contour of figure 3.1c. As we will see shortly, this has the advantage of ‘opening up’ the second boundary of the black hole spacetime as well. In the next subsection, we describe a bulk manifold that fills in this deformed contour. Afterwards, we proceed by switching on a scalar field and holographically compute correlation functions.

3.4.1 Bulk spacetime

Consider the eternal Lorentzian massive non-rotating BTZ black hole, whose Penrose diagram is given in figure 3.7a. The black hole splits into four parts, which we denote by L, R, F and P. On either part the metric is

$$ds^2 = -(r^2 - r_+^2)dt^2 + \frac{dr^2}{(r^2 - r_+^2)} + r^2 d\phi^2. \quad (3.80)$$

If necessary, we will use a subscript like L or R to indicate the corresponding part of the spacetime. Notice that time runs backward on R. The mass and temperature of the black hole are given by

$$M = \frac{r_+^2}{8G_3}, \quad T = \frac{r_+}{2\pi}. \quad (3.81)$$

(Recall that we set the AdS radius to one, $\ell^2 = 1$.) To simplify the notation, we make the coordinate transformation

$$t = \frac{t'}{r_+}, \quad r = r' r_+, \quad \phi = \frac{\phi'}{r_+}, \quad (3.82)$$

after which the metric reads

$$ds^2 = -(r^2 - 1)dt^2 + \frac{dr^2}{(r^2 - 1)} + r^2 d\phi^2, \quad (3.83)$$

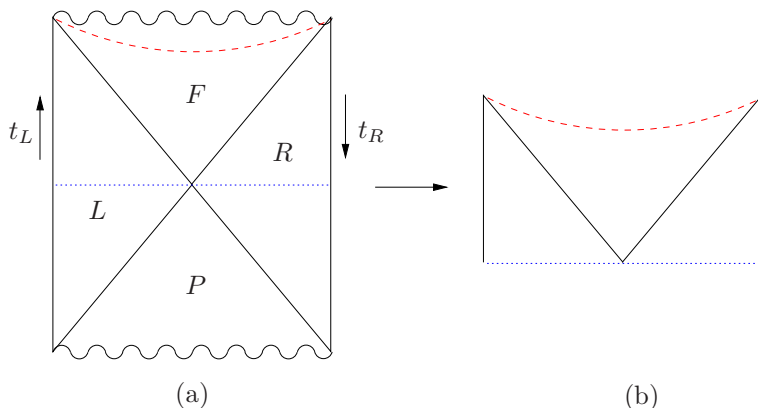


Figure 3.7: (a) The Penrose diagram for the eternal BTZ black hole. The arrows indicate the direction of time. In the diagram, every point represents a circle. The horizons, which are the solid diagonal lines, separate the spacetime in four regions labelled by L , R , F and P . (b) We cut off the spacetime along the dotted lines and keep the part in between them.

where we have dropped the primes. Note that the periodicity of ϕ has now changed to

$$\phi \sim \phi + 2\pi r_+. \quad (3.84)$$

At the very end of the computation we will return to standard conventions.

To use this spacetime as a filling for (a part of) the contour of figure 3.6, we first have to cut it off along an initial slice, which we take to be the $t_L = t_R = 0$ slice, as well as a final slice, which we choose to be the $r_F = \hat{r}$ slice, with $\hat{r} < 1$ a constant. These segments are the (blue) dotted and the (red) dashed lines of figure 3.7a, respectively. As is shown in figure 3.7b, we keep the segment in between these surfaces. Notice that $t_L > 0$ but $t_R < 0$ on this segment. We will need two copies of the segment, which we denote by M_1 and M_2 .

Next, consider the Euclidean solution with the metric

$$ds^2 = (r^2 - 1)d\tau^2 + \frac{dr^2}{(r^2 - 1)} + r^2 d\phi^2 \quad (3.85)$$

and with periodicities

$$\tau \sim \tau + 2\pi, \quad \phi \sim \phi + 2\pi r_+. \quad (3.86)$$

Topologically, this solution is $D_2 \times S^1$, with D_2 a two-dimensional disk and the S^1 is parametrized by ϕ . As shown in figure 3.8, we will cut it in half along the hypersurface given by $\tau = 0$ and $\tau = \pi$, and keep the part given by $0 < \tau < \pi$.

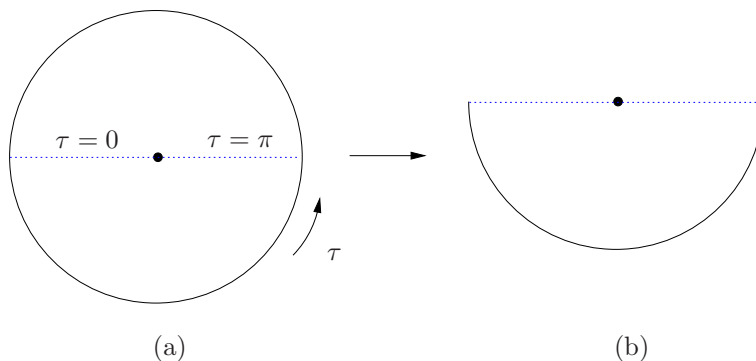


Figure 3.8: (a) The Euclidean BTZ black hole, where again every point represents a circle. Euclidean time τ runs as indicated. (b) We cut off the spacetime along the dotted line given by $\tau = 0$ and $\tau = \pi$ and keep the lower part.

We will again need two copies of this part, which we denote as M_0 and M_3 . In figure 3.8b, we have drawn these spacetimes as half a disk.

We now glue the four manifolds together as shown in figure 3.9. Notice that M_0 is glued to M_1 such that the part with $\tau = 0$ is glued to the part with $t_L = 0$, and the part with $\tau = \pi$ is glued to the part with $t_R = 0$. The same holds for the gluing between M_2 and M_3 .

Let us verify that the matching conditions for gravity are satisfied. First of all, the fact that M_1 and M_2 are identical means that the matching conditions for gravity are trivially satisfied along their gluing surface, which is the (red) dashed line in figure 3.9. In fact, we could have glued M_1 and M_2 along any spacelike bulk hypersurface extending all the way to the two radial boundaries (and disjoint from the surfaces $t_L = t_R = 0$), and the matching conditions would still be satisfied.

For the matching between the Euclidean and the Lorentzian segments, one may directly see from the metrics (3.83) and (3.85) that any surface of constant t or τ has the same induced metric. One may also use reflection and translation symmetry to find that the extrinsic curvature of such slices must vanish. Therefore, the matching conditions for gravity are satisfied for this gluing, too. Finally, by passing to a coordinate system that is regular everywhere at the gluing surface, one may verify that there are no problems at the coordinate singularity at $r = 1$, either.

The manifold sketched in figure 3.9 is similar to a construction presented in [39], where the initial state for an eternal Lorentzian black hole was given by half a Euclidean black hole. However the real-time prescription where dual states are represented by Euclidean manifolds can only be made precise if one includes a *sec-*

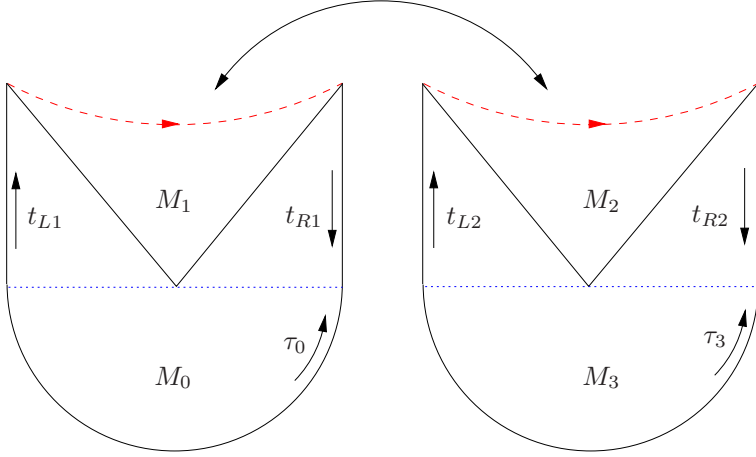


Figure 3.9: The four components M_0 , M_1 , M_2 and M_3 are glued together to create a manifold that fills the contour of figure 3.6. The direction of the various time coordinates is the same as in figure 3.6.

ond copy of the manifold of [39] and glues it to the first copy along some late-time hypersurface, leading precisely to the construction in figure 3.9. In field theory, this second copy corresponds to the backward-going segments of the contour and the specification of the *final* rather than the initial state. The two copies are in this case identical, precisely because the initial and final field theory states are identical as well.

Let us now turn to the matching conditions for a scalar field. The overall action (3.3) can be split into a separate piece for each segment:

$$iS_1 - iS_2 - S_0 - S_3. \quad (3.87)$$

Continuity and the saddle-point approximation for the combination of actions (3.87) determines the matching conditions to be:

$$\begin{aligned} \Phi_1(r = \hat{r}) &= \Phi_2(r = \hat{r}) & i\partial_r\Phi_1(r = \hat{r}) - i\partial_r\Phi_2(r = \hat{r}) &= 0 \\ \Phi_1(t_L = 0) &= \Phi_0(\tau = 0) & -i\partial_t\Phi_1(t_L = 0) + \partial_\tau\Phi_0(\tau = 0) &= 0 \\ \Phi_1(t_R = 0) &= \Phi_0(\tau = \pi) & i\partial_t\Phi_1(t_R = 0) - \partial_\tau\Phi_0(\tau = \pi) &= 0 \\ \Phi_2(t_L = 0) &= \Phi_3(\tau = 0) & i\partial_t\Phi_2(t_L = 0) + \partial_\tau\Phi_3(\tau = 0) &= 0 \\ \Phi_2(t_R = 0) &= \Phi_3(\tau = \pi) & -i\partial_t\Phi_2(t_R = 0) - \partial_\tau\Phi_3(\tau = \pi) &= 0. \end{aligned} \quad (3.88)$$

Incidentally, one may have wondered why the second set of horizontal line segments in figure 3.6 points to the left rather than to the right. This can be seen from the matching conditions (3.88): as one may verify they correspond to C^1 continuity

in the complex time plane only if the contour has the shape of figure 3.6. One may also verify that a replacement $t_{R2} \rightarrow -t_{R2}$ has no effect on the *shape* of the contour.

3.4.2 Mode solutions

We can now turn to the computation of two-point functions. We start by finding mode solutions to the Klein-Gordon equation,

$$\square_G \Phi - m^2 \Phi = 0, \quad (3.89)$$

on the various components. As usual, $m^2 = \Delta(\Delta - 2)$ and we assume $\Delta = 1 + l$ with $l \in \{1, 2, \dots\}$. In Lorentzian signature, we find two possible solutions, which we denote by ψ_{\pm} ,

$$\psi_{\pm} = e^{-i\omega t + ik\phi} f(\pm\omega, k, r), \quad (3.90)$$

with a radial part given by

$$\begin{aligned} f(\omega, k, r) &= C_{\omega kl} \left(1 - \frac{1}{r^2}\right)^{i\omega/2} r^{-l-1} \\ &\times F\left(\frac{i}{2}(\omega - k) + \frac{1}{2}(1 + l), \frac{i}{2}(\omega + k) + \frac{1}{2}(1 + l); i\omega + 1; 1 - \frac{1}{r^2}\right), \end{aligned} \quad (3.91)$$

with $F(a, b; c; z)$ a hypergeometric function and

$$C_{\omega kl} = \frac{\Gamma(\frac{i}{2}(\omega + k) + \frac{1}{2}(1 + l))\Gamma(\frac{i}{2}(\omega - k) + \frac{1}{2}(1 + l))}{\Gamma(i\omega + 1)\Gamma(l)} \quad (3.92)$$

chosen such that the coefficient of the leading behavior of $f(\pm\omega, k, r)$ as $r \rightarrow \infty$ equals one. The asymptotic expansion of the modes is given by

$$\psi_{\pm} = e^{-i\omega t + ik\phi} \left(r^{l-1} + \dots + \alpha(\pm\omega, k, l) r^{-l-1} [\ln(r^2) + \beta(\pm\omega, k, l)] + \dots \right), \quad (3.93)$$

with

$$\begin{aligned} \alpha(\omega, k, l) &= (-1)^l \frac{(\frac{i}{2}(\omega + k) + \frac{1}{2}(1 - l))_l (\frac{i}{2}(\omega - k) + \frac{1}{2}(1 - l))_l}{l!(l-1)!}, \\ \beta(\omega, k, l) &= -\psi\left(\frac{i}{2}(\omega + k) + \frac{1}{2}(1 + l)\right) - \psi\left(\frac{i}{2}(\omega - k) + \frac{1}{2}(1 + l)\right) + \text{local}, \end{aligned} \quad (3.94)$$

where the local terms we omitted from $\beta(\omega, k, l)$ originate from the expansion of the prefactor $(1 - 1/r^2)^{i\omega/2}$ up to the relevant order. Such local terms lead to contact terms in the two-point function and will be omitted. The similarity between the modes (3.91) and (3.5) is not accidental: one may verify that the backgrounds with the metrics (3.83) and (3.2) are related by analytic continuation

in complex (t, r, ϕ) -space, and so are the corresponding mode solutions in these backgrounds. Since the behavior of the modes in the interior of the spacetime is different, we will not use this fact here.

Near the horizon both modes oscillate infinitely rapidly. To see this, we transform to Poincaré coordinates, given by

$$\tanh(t) = -\frac{y}{x}, \quad r^2 = \frac{x^2 - y^2 + z^2}{z^2}, \quad e^{2\phi} = x^2 - y^2 + z^2, \quad (3.95)$$

which brings the metric to the form

$$ds^2 = \frac{1}{z^2}(dx^2 - dy^2 + dz^2). \quad (3.96)$$

With this definition the future and past horizons on the L quadrant are mapped to $x = -y$ and $x = y$, respectively. Taking the near-horizon limit $x \pm y \rightarrow 0$, we find

$$\psi_{\pm} = C_{\omega kl} \exp\left(\mp \frac{i\omega}{2} \ln(x \pm y)^2 + i(k \mp \omega)\phi\right)(1 + \dots). \quad (3.97)$$

We can create modes that are well-defined almost everywhere on the Lorentzian segments via analytic continuation across the horizons, in the way specified by Unruh [67, 68], see also [41]. Depending on whether we analytically continue from L to R via the lower or the upper half of the complex y plane, an extra factor of $e^{\pi\omega}$ or $e^{-\pi\omega}$ should be added to the L mode to produce an R mode. Since this is the case for both ψ_+ and ψ_- , we find four different combinations:

$$\begin{aligned} \phi_{++} &= \begin{cases} e^{-i\omega t + ik\phi} f(\omega, k, r) & \text{on L} \\ e^{-i\omega t + ik\phi + \pi\omega} f(\omega, k, r) & \text{on R} \end{cases} \\ \phi_{+-} &= \begin{cases} e^{-i\omega t + ik\phi} f(\omega, k, r) & \text{on L} \\ e^{-i\omega t + ik\phi - \pi\omega} f(\omega, k, r) & \text{on R} \end{cases} \\ \phi_{-+} &= \begin{cases} e^{-i\omega t + ik\phi} f(-\omega, k, r) & \text{on L} \\ e^{-i\omega t + ik\phi + \pi\omega} f(-\omega, k, r) & \text{on R} \end{cases} \\ \phi_{--} &= \begin{cases} e^{-i\omega t + ik\phi} f(-\omega, k, r) & \text{on L} \\ e^{-i\omega t + ik\phi - \pi\omega} f(-\omega, k, r) & \text{on R.} \end{cases} \end{aligned} \quad (3.98)$$

These modes form a complete set both on L and on R, and can thus be used to decompose any solution. In particular, solutions that are regular at the horizons can be obtained as an infinite sum over these modes.

Finally, on the Euclidean solutions M_0 and M_3 , the mode solutions are as usual obtained by the replacement $t \rightarrow -i\tau$ in the ψ_{\pm} . In this case, there is no need

for an analytic continuation, and we find two rather than four solutions, which we denote by ϕ_{\pm} :

$$\phi_{\pm} = e^{\omega\tau + ik\phi} f(\pm\omega, k, r). \quad (3.99)$$

Going through the same arguments as before, one finds that these modes also oscillate infinitely fast near the horizon.

3.4.3 No normalizable solution

Let us now show the absence of a normalizable solution satisfying the matching conditions. This would imply uniqueness of any solution satisfying given radial boundary data.

We begin on M_1 where we write

$$Y_1 = \sum_k \int d\omega (c_{[1]++}\phi_{++} + c_{[1]+-}\phi_{+-} + c_{[1]-+}\phi_{-+} + c_{[1]--}\phi_{--}), \quad (3.100)$$

with the $c_{[1]\pm\pm}$ some functions of ω and k . Notice that the sum is over $r+k \in \mathbb{Z}$ to comply with the periodicity (3.84). The solution looks different in the various regions. Using (3.98) we obtain

$$\begin{aligned} Y_{1,L} &= \sum_k \int d\omega e^{-i\omega t + ik\phi} [(c_{[1]++} + c_{[1]+-})f(\omega) + (c_{[1]-+} + c_{[1]--})f(-\omega)], \\ Y_{1,R} &= \sum_k \int d\omega e^{-i\omega t + ik\phi} [(c_{[1]++}e^{\pi\omega} + c_{[1]+-}e^{-\pi\omega})f(\omega) \\ &\quad + (c_{[1]-+}e^{\pi\omega} + c_{[1]--}e^{-\pi\omega})f(-\omega)], \end{aligned} \quad (3.101)$$

where here and below we suppress the k, r arguments from $f(\omega, k, r)$ for notational simplicity. By substituting the asymptotic behavior (3.93) of the modes, we find that Y_1 is normalizable on both L and R if

$$\begin{aligned} c_{[1]++} + c_{[1]--} + c_{[1]+-} + c_{[1]-+} &= 0, \\ (c_{[1]++} + c_{[1]-+})e^{\pi\omega} + (c_{[1]+-} + c_{[1]--})e^{-\pi\omega} &= 0. \end{aligned} \quad (3.102)$$

Similarly, on M_2 we consider

$$Y_2 = \sum_k \int d\omega (c_{[2]++}\phi_{++} + c_{[2]+-}\phi_{+-} + c_{[2]-+}\phi_{-+} + c_{[2]--}\phi_{--}) \quad (3.103)$$

and the same argument as above leads to the the same conditions (3.102) but with $c_{[1]\pm\pm}$ replaced by $c_{[2]\pm\pm}$. Besides satisfying the same radial boundary data, the matching conditions between M_1 and M_2 imply that Y_1 and Y_2 also have the same

initial data on the matching surface. Since the solution on either M_1 or M_2 is uniquely specified by boundary and initial data, we find that $c_{[2]\pm\pm} = c_{[1]\pm\pm}$.

On the Euclidean parts M_0 and M_3 the solution should be a linear combination of the Euclidean modes (3.99). We write it as

$$\begin{aligned} Y_0 &= \sum_k \int d\omega e^{\omega\tau_0 - ik\phi} [c_{[0]+}f(\omega) + c_{[0]-}f(-\omega)], \\ Y_3 &= \sum_k \int d\omega e^{\omega\tau_3 - ik\phi} [c_{[3]+}f(\omega) + c_{[3]-}f(-\omega)]. \end{aligned} \quad (3.104)$$

As for Y_1 and Y_2 , the demand for normalizability implies

$$c_{[0]+} + c_{[0]-} = 0, \quad c_{[3]+} + c_{[3]-} = 0. \quad (3.105)$$

We now impose the matching conditions (3.88) between the Euclidean and the Lorentzian solution. Using the orthogonality of the normalizable modes, this leads to algebraic relations between the individual coefficients $c_{[i]\pm}$ and $c_{[j]\pm\pm}$. In particular, the matching conditions between M_0 and M_1 determine

$$c_{[1]+-} = 0, \quad (3.106)$$

while those between M_2 and M_3 fix

$$c_{[1]-+} = 0. \quad (3.107)$$

Using (3.102) we conclude that all the $c_{[1]\pm\pm} = 0$ and thus no normalizable solution exists.

3.4.4 Bulk-boundary propagator

We will now find the bulk-boundary propagator for a delta-function source at $(\hat{t}, \hat{\phi})$ on the L part of M_1 . Since we have just shown the absence of any normalizable solution, any bulk-boundary propagator that satisfies the matching conditions is guaranteed to be unique. Let us therefore make an educated guess and consider a solution X_1 on M_1 that contains only the modes ϕ_{++} and ϕ_{--} :

$$X_1 = \frac{1}{4\pi^2 r_+} \sum_k \int d\omega e^{i\omega\hat{t} - ik\hat{\phi}} (a_{[1]++}\phi_{++} + a_{[1]--}\phi_{--}), \quad (3.108)$$

with new coefficients $a_{[1]\pm\pm}$ which are to-be determined functions of ω and k . Again, to comply with the periodicity of ϕ given in (3.84), we need $r_+k \in \mathbb{Z}$ as well as the extra prefactor of $1/r_+$ to normalize the boundary delta function.

Notice that we already split off a factor $e^{i\omega\hat{t}-ik\hat{\phi}}$ from $a_{[1]++}$ and $a_{[1]--}$. On the two regions R and L, our ansatz takes the following form:

$$X_{1,L} = \frac{1}{4\pi^2 r_+} \sum_k \int d\omega e^{-i\omega(t-\hat{t})+ik(\phi-\hat{\phi})} [a_{[1]++} f(\omega) + a_{[1]--} f(-\omega)], \quad (3.109)$$

$$X_{1,R} = \frac{1}{4\pi^2 r_+} \sum_k \int d\omega e^{-i\omega(t-\hat{t})+ik(\phi-\hat{\phi})} [a_{[1]++} e^{\pi\omega} f(\omega) - a_{[1]--} e^{-\pi\omega} f(-\omega)].$$

As we mentioned above, we put a delta-function source on $(\hat{t}, \hat{\phi})$ on the conformal boundary of L and no sources on the conformal boundary of R. Substituting the asymptotics (3.93), such boundary conditions for X_1 lead to

$$\begin{aligned} a_{[1]++} + a_{[1]--} &= 1, \\ a_{[1]++} e^{\pi\omega} + a_{[1]--} e^{-\pi\omega} &= 0. \end{aligned} \quad (3.110)$$

Notice that these conditions already fix the solution on M_1 to be:

$$a_{[1]++} = \frac{-1}{e^{2\pi\omega} - 1}, \quad a_{[1]--} = \frac{e^{2\pi\omega}}{e^{2\pi\omega} - 1}. \quad (3.111)$$

In passing, we mention that it is not manifest that X_1 is finite at the horizons. To check this, one substitutes the near-horizon expansion (3.97) of the modes and then computes the ω -integral by contour deformation. One finds that an $i\epsilon$ -insertion is necessary to ensure convergence and to regulate the lightcone singularity. (A subtle point is that the $a_{[1]++}$ and $a_{[1]--}$ both have a pole at $\omega = 0$, but the residues cancel each other so the contour can be freely deformed around this singularity.) The sum over k can be computed using similar methods as we employ for the two-point function below and the computation then shows that after the $i\epsilon$ insertion X_1 is regular at all the horizons indeed. Notice that the light-cone singularity is expected; we found a similar singularity when we wrote down the position-space expression (3.56) in Poincaré coordinates. It can be removed by integrating the delta function on the boundary against a smooth source.

Let us now verify that we can find normalizable solutions on M_0 , M_2 and M_3 such that the matching conditions are satisfied, so that X_1 is indeed the bulk-boundary propagator on M_1 . We start with the matching solution X_0 on M_0 . It should be a linear combination of the modes ϕ_{\pm} ,

$$X_0 = \frac{1}{4\pi^2 r_+} \sum_k \int d\omega e^{\omega\tau+ik\phi} e^{i\omega\hat{t}-ik\hat{\phi}} (a_{[0]+} f(\omega) + a_{[0]-} f(-\omega)). \quad (3.112)$$

Let us consider the following coefficients:

$$a_{[0]+} = a_{[1]++}, \quad a_{[0]-} = -a_{[1]++} = a_{[1]--} - 1, \quad (3.113)$$

with $a_{[1]\pm\pm}$ as given above. As one may directly verify by substituting the asymptotic behavior (3.93) (now with $t = -i\tau$), the solution X_0 is normalizable since $a_{[0]_+} + a_{[0]_-} = 0$. Notice furthermore that $0 < \tau < \pi$ on M_0 . Therefore, despite the factor $e^{\omega\tau}$, the ω -integral is still convergent along the real axis on M_0 , because $a_{[0]\pm} \sim e^{-2\pi\omega}$ for large positive ω .

To verify that the matching conditions are satisfied between M_0 and M_1 , notice that the difference between the Euclidean and the Lorentzian solution on L,

$$X_{1,L}(t=0) - X_0(\tau=0) = \frac{1}{4\pi^2 r_+} \sum_k \int d\omega e^{i\omega\hat{t} - ik\hat{\phi}} \phi_{--} = 0 \quad (3.114)$$

since $\hat{t} > 0$, so one can deform the contour in the upper half of the complex ω -plane where ϕ_{--} has no poles even at normalizable order. (Actually, near the horizon, it is the oscillating behavior of radial part of the modes that determines where to deform the contour to. Since this is still the upper half plane, the difference vanishes there as well.) A similar argument shows that the second matching condition on L as well as the both matching conditions on R are also satisfied.

Next we consider the solution on M_2 ,

$$X_2 = \frac{1}{4\pi^2 r_+} \sum_k \int d\omega e^{-i\omega t_2 + ik\phi} e^{i\omega\hat{t} - ik\hat{\phi}} (a_{[2]_{++}}\phi_{++} + a_{[2]_{+-}}\phi_{+-} + a_{[2]_{-+}}\phi_{-+} + a_{[2]_{--}}\phi_{--}). \quad (3.115)$$

Since the radial boundary data on M_1 and M_2 are now different, we cannot use the argument used earlier for the normalizable solution Y to argue that $a_{[2]\pm\pm}$ is the same as $a_{[1]\pm\pm}$ and we have to compute $a_{[2]\pm\pm}$.

To begin with, notice that the matching between M_1 and M_2 takes places on the F component of the black hole as indicated in figure 3.7. Starting from the L quadrant one must cross the future horizon but not the past horizon to arrive at the F quadrant. Therefore, the modes ϕ_{++} and ϕ_{+-} , which become singular at the future horizon, acquire an additional factor of $e^{\pm\pi\omega}$ as we move from L to F. However, the modes ϕ_{-+} and ϕ_{--} become singular only at the past horizon and do not get such a factor. These factors should be included both on M_1 and M_2 and show up in the matching conditions:

$$a_{[2]_{+-}}e^{-\pi\omega} + a_{[2]_{++}}e^{\pi\omega} = a_{[1]_{+-}}e^{-\pi\omega} + a_{[1]_{++}}e^{\pi\omega} = \frac{-e^{\pi\omega}}{e^{2\pi\omega} - 1}, \quad (3.116)$$

$$a_{[2]_{-+}} + a_{[2]_{--}} = a_{[1]_{-+}} + a_{[1]_{--}} = \frac{e^{2\pi\omega}}{e^{2\pi\omega} - 1}.$$

These two equations, together with those arising from normalizability on both sides of M_2 , completely fix the $a_{[2]\pm\pm}$ to be:

$$\begin{aligned} a_{[2]++} &= 0, & a_{[2]+-} &= \frac{-e^{2\pi\omega}}{e^{2\pi\omega} - 1}, \\ a_{[2]-+} &= 0, & a_{[2]--} &= \frac{e^{2\pi\omega}}{e^{2\pi\omega} - 1}, \end{aligned} \tag{3.117}$$

and we have found a normalizable solution X_2 on M_2 that matches to the solution X_1 on M_1 .

Finally, we need to verify that we can obtain a normalizable solution X_3 on M_3 that matches to X_2 . Since X_2 , in contrast with X_1 , is already fully normalizable, X_3 can be easily obtained by a simple analytic continuation of the solution on X_2 . Just as for M_0 , one may again verify that the ω -integral in X_3 is convergent along the real axis, that X_3 is normalizable and that the matching conditions are satisfied.

Thus, the bulk-boundary propagator X_1 can be matched to normalizable solutions on all segments. Since there are no solutions that are everywhere normalizable, we have obtained *the* bulk-boundary propagator for the black hole filling of the contour of figure 3.6. The same bulk-boundary propagator was actually written down in [41], where it was obtained by imposing boundary conditions at the horizon which are natural from considerations of quantum field theory in curved space [68]. We have now derived that this is indeed the correct bulk-boundary propagator for the real-time gauge/gravity dictionary.

3.4.5 Two-point functions

In this subsection we will compute the time-ordered and Wightman function for real times. By looking at figure 3.6, we find that we need operator insertions on the L component of either M_1 or M_2 , because these segments lie along the real time axis. To simplify the notation we omit the subscript L, which should be understood in all formulas in this subsection.

As we explained in section 2.3, the one-point function in the presence of sources is again just the normalizable component $\phi_{(2l)}$ of the bulk-boundary propagator, times a factor $-2l$ which is fixed by holographic renormalization. Completely analogous to the analysis in section 3.1, this normalizable component $\phi_{(2l)}$ can be read off by substituting (3.93) in the solution $X_{1,L}$ or $X_{2,L}$. The two-point

function computation is again completely analogous, and we find

$$\begin{aligned} \langle T\mathcal{O}(x)\mathcal{O}(x') \rangle &= \langle T_C\mathcal{O}_{[1]}(x)\mathcal{O}_{[1]}(x') \rangle = \frac{li}{2\pi^2 r_+} \sum_k \int d\omega e^{-i\omega(t-t') + ik(\phi-\phi')} \times \\ & [a_{[1]++}\alpha(\omega, k, l)\beta(\omega, k, l) + a_{[1]--}\alpha(-\omega, k, l)\beta(-\omega, k, l)]. \end{aligned} \quad (3.118)$$

We recognize the structure of a time ordered propagator at finite temperature [51]. Such a propagator is of the form

$$\Delta(\omega, k) = -n(\omega)\Delta_A(\omega, k) + (1 + n(\omega))\Delta_R(\omega, k), \quad (3.119)$$

with $n(\omega)$ the Bose-Einstein distribution,

$$n(\omega) = \frac{1}{e^{\beta\omega} - 1}, \quad (3.120)$$

and Δ_R and Δ_A are the retarded and advanced thermal propagators, which should be analytic functions in the respectively upper and the lower half of the complex ω plane, see appendix 2.A. Since $\beta = 2\pi$ in our coordinates, we find $a_{[1]++} = -n(\omega)$. The structure of (3.118) thus agrees with expectations.

To obtain a position-space expression, choose $t' = 0$ and $t > 0$. This allows us to perform the ω -integral by deforming the contour to the lower half plane and picking up the poles. These poles come from $\beta(-\omega, k, l)$ and from the a_{++} and the a_{--} . The former have poles at the quasinormal frequencies,

$$\omega = \omega_{nk}^\pm \equiv -i(2n + l + 1) \pm k, \quad (3.121)$$

and the latter have poles at $\omega = -im$ with $m \in \{1, 2, \dots\}$ (the apparent pole at $\omega = 0$ in α_{++} and α_{--} has zero residue).

Afterwards, we compute the sum over k as follows. We first use Poisson resummation to replace the sum by an integral and a sum over images $\phi \sim \phi + 2\pi r_+ p$ with $p \in \mathbb{Z}$. The integral can again be done via contour deformation, replacing it by an infinite sum over residues as well. One then finds that the sum over the poles at $\omega = -im$ vanishes and we are left with the sum involving the quasinormal frequencies only,

$$\begin{aligned} \frac{(-1)^{l+1}2l}{\pi\Gamma(l)\Gamma(l+1)r_+} \sum_{\pm} \sum_{n=0}^{\infty} \sum_{m=1}^{\infty} (\pm 1) e^{-i(2n+l+1\pm m)(t-i\epsilon t) + im\phi} \times \\ \frac{\Gamma(1+n+l\pm m)\Gamma(1+n+l)}{\Gamma(1+n\pm m)\Gamma(1+n)}, \end{aligned} \quad (3.122)$$

where the $i\epsilon$ factor is uniquely fixed by requesting convergence away from contact points and we suppressed the aforementioned sum over images. This expression

can be evaluated without too much difficulty and adding the sum over images (remembering that the Poisson resummation yields an extra factor of r_+), we finally get

$$\langle T\mathcal{O}(x)\mathcal{O}(0) \rangle = \sum_{m \in \mathbb{Z}} \frac{l^2/(2^l \pi)}{[-\cosh(t - i\epsilon t) + \cosh(\phi + 2m\pi r_+)]^{l+1}}. \quad (3.123)$$

This computation was done using the metric in (3.83) where the mass of the BTZ entered through the periodicity of the angular coordinate (3.84). To restore standard conventions, we now perform the diffeomorphism $t \rightarrow r_+ t$ and $\phi \rightarrow r_+ \phi$ followed by a Weyl transformation so that the boundary background metric is $ds^2 = -dt^2 + d\phi^2$ with $\phi \sim \phi + 2\pi$. Implementing these transformations in the two-point function we obtain

$$\langle T\mathcal{O}(x)\mathcal{O}(0) \rangle = \sum_{m \in \mathbb{Z}} \frac{(2\pi T)^{4l+4} l^2 / (2^l \pi)}{[-\cosh(2\pi T t - i\epsilon t) + \cosh(2\pi T(\phi + 2m\pi))]^{l+1}}, \quad (3.124)$$

where we reinstated the temperature T given in (3.81). This correlator satisfies the KMS condition and is a sum over images in the ϕ direction. It was obtained earlier via an analytic continuation of the Euclidean correlator in [69]. As discussed in more detail in [63], it is related to the thermal AdS two-point function by a double analytic continuation. This can directly be seen from (3.123), where the substitution $t \rightarrow i\hat{\phi}$ and $\phi \rightarrow i\hat{t}$ yields precisely (3.47) (up to $i\epsilon$ insertions which then have to be inserted by hand). This is the real-time manifestation of the fact that Euclidean thermal AdS₃ and Euclidean BTZ, which are both filled tori, are related by an S transformation of the boundary torus.

Let us also write down the Wightman function, which can be obtained following the same steps as in section 3.1.3:

$$\begin{aligned} \langle \mathcal{O}(x)\mathcal{O}(x') \rangle &= \langle T_C \mathcal{O}_{[2]}(x)\mathcal{O}_{[1]}(x') \rangle = \frac{-li}{2\pi^2 r_+} \sum_k \int d\omega e^{-i\omega(t-t') + ik(\phi-\phi')} \times \\ & [a_{[2]_{+-}} \alpha(\omega, k, l) \beta(\omega, k, l) + a_{[2]_{--}} \alpha(-\omega, k, l) \beta(-\omega, k, l)]. \end{aligned} \quad (3.125)$$

We can again obtain a position-space expression by closing the contour and picking up the poles, which results in

$$\langle \mathcal{O}(x)\mathcal{O}(0) \rangle = \sum_{m \in \mathbb{Z}} \frac{(2\pi T)^{4l+4} l^2 / (2^l \pi)}{[-\cosh(2\pi T t - i\epsilon) + \cosh(2\pi T(\phi + 2m\pi))]^{l+1}}. \quad (3.126)$$

Finally, the retarded two-point function is of the form

$$i\Delta_R(x, 0) \equiv \theta(x) \langle [\mathcal{O}(x), \mathcal{O}(0)] \rangle = \langle T\mathcal{O}(x)\mathcal{O}(0) \rangle - \langle \mathcal{O}(0)\mathcal{O}(x) \rangle. \quad (3.127)$$

From the above expressions, we find that it is analytic in the upper half of the complex ω -plane and vanishes for $t < 0$. Actually, it has support only on the forward lightcone, which agrees with QFT expectations. Notice also that there is no need to insert $i\epsilon$'s in the frequency-space expressions, since the poles in the complex frequency plane all have non-zero imaginary part. Such behavior however cannot arise in a CFT with a discrete energy spectrum, at least at finite N , where one expects that retarded correlators have poles on the real axis. Reconciling this behavior with expectations from the AdS/CFT correspondence is still an open issue; we refer to [39, 63] for discussions of this point.

Let us finally remark that the retarded two-point function (3.127) can also be shown to be related to purely ingoing boundary conditions at the horizon [41], leading eventually to a recipe as presented in [40]. The derivation of this recipe from the current perspective is presented in more detail in the next chapter.

3.5 Rotating black holes

In the previous examples, we started with a CFT contour and obtained a corresponding bulk solution by the condition that it ‘filled’ this contour. In this section we will do the converse. We will start from a Lorentzian solution and look for Euclidean solutions that can be matched to it. This then leads to a specific CFT contour corresponding to the combined solution.

Let us discuss the practical use of this procedure. As discussed in section 2.1, the parts of the solution associated with vertical segments of the contour are directly related to the initial and final state or density matrix of the field theory. The same information is in principle also encoded in the asymptotics of the solution, since from those one can compute the holographic 1-point functions and from them in principle one can reconstruct the dual state. Typically, it is not very easy to extract the dual state starting from the vevs. The real-time methods discussed here present a new tool, namely given a Lorentzian solution one looks for Euclidean solutions that can be matched to it. One then uses this information to infer the holographic interpretation of the solution.

In this subsection we illustrate how this is done using the rotating BTZ black hole [70, 71]. This discussion readily generalizes to higher dimensional rotating AdS-Kerr black holes [72, 73, 74]. As one may expect, the contour turns out to be a thermal contour with a chemical potential for angular momentum. Furthermore, this example illustrates a number of additional issues as it provides a concrete example of the use of a complex metric.

3.5.1 Lorentzian solution

The metric for the three-dimensional rotating BTZ black hole [70, 71] is given by

$$ds^2 = -(r^2 - r_+^2 - r_-^2)dt^2 + r^2 d\phi^2 + 2r_+ r_- dt d\phi + \frac{r^2 dr^2}{(r^2 - r_+^2)(r^2 - r_-^2)}, \quad (3.128)$$

with ϕ periodic,

$$\phi \sim \phi + 2\pi. \quad (3.129)$$

The mass, angular momentum and temperature of the black hole are related to r_+ and r_- via

$$M = \frac{r_+^2 + r_-^2}{8G_3}, \quad J = \frac{r_+ r_-}{4G_3}, \quad T = \frac{r_+^2 - r_-^2}{2\pi r_+}. \quad (3.130)$$

It is convenient to use $(\hat{t}, \hat{\phi}, \hat{r})$ coordinates:

$$\begin{aligned} \hat{t} &= r_+ t + r_- \phi, \\ \hat{\phi} &= r_- t + r_+ \phi, \\ \hat{r}^2 &= \frac{r^2 - r_-^2}{r_+^2 - r_-^2}. \end{aligned} \quad (3.131)$$

Then the metric becomes

$$ds^2 = -(\hat{r}^2 - 1)d\hat{t}^2 + \frac{d\hat{r}^2}{\hat{r}^2 - 1} + \hat{r}^2 d\hat{\phi}^2, \quad (3.132)$$

with the periodicity condition

$$(\hat{t}, \hat{\phi}) \sim (\hat{t} + 2\pi r_-, \hat{\phi} + 2\pi r_+), \quad (3.133)$$

with r_- and r_+ real, and we consider $0 \leq |r_-| < r_+$ but not the extremal case where $|r_-| = r_+$.

We consider an *eternal* rotating BTZ black hole with two radial boundaries. The rotating BTZ black hole has a Penrose diagram that can be extended indefinitely to the future and the past, across the various horizons [71]. We will however cut off the spacetime along a spacelike hypersurface extending from one radial boundary to another, just as for the static BTZ example of the previous subsection. We thus explicitly avoid these extra regions and the singularities.

3.5.2 Euclidean solution

To find a boundary contour corresponding to this spacetime, we will first look for a Euclidean solution that is to be matched to the Lorentzian solution across some

initial hypersurface. Usually, in passing to the Euclidean version of a rotating black hole we not only make the replacement $t = -i\tau$, but also analytically continue the angular momentum parameter (which is J or r_- in our case) to imaginary values. This way, the Euclidean metric one obtains is real. We will however show that the matching conditions are only satisfied for a complex Euclidean metric, given in coordinates (τ, r, φ) by

$$ds^2 = (r^2 - r_+^2 - r_-^2)d\tau^2 + r^2d\varphi^2 - 2ir_+r_-d\tau d\varphi + \frac{r^2dr^2}{(r^2 - r_+^2)(r^2 - r_-^2)}, \quad (3.134)$$

with coordinate ranges we make precise below. We now discuss this metric in more detail. First of all, the Einstein equations are still satisfied for the complex metric, since they are satisfied for any real or complex r_- . Second, a coordinate singularity arises at the horizons. Insisting on a nondegenerate metric, a (complex) coordinate transformation near the horizon shows that the necessary periodicity in Euclidean time that avoids such a singularity is

$$(\tau, \varphi) \sim \left(\tau + \frac{2\pi r_+}{r_+^2 - r_-^2}, \varphi + \frac{2\pi i r_-}{r_+^2 - r_-^2} \right), \quad (3.135)$$

which notably involves a translation in the imaginary φ direction. To comply with this periodicity, we will take the Euclidean manifold M_0 to be defined as follows. We first introduce $M_{\mathbb{C}}$ by extending the coordinates (τ, r, φ) to complex values, with the periodicities as above. The metric (3.134) should then be seen as a nondegenerate holomorphic $(2,0)$ -tensor on $M_{\mathbb{C}}$. Within $M_{\mathbb{C}}$, we take M_0 to be the submanifold given by real τ and r , but $\text{Im}(\varphi) = \tau(r_-/r_+)$. Notice that M_0 has three real dimensions. The metric restricts to M_0 as a complex tensor and the volume element is a three-form which we can integrate along M_0 . If we introduce

$$\hat{\varphi} = \varphi - \frac{ir_-}{r_+}\tau, \quad (3.136)$$

then τ, r and $\hat{\varphi}$ are real on M_0 and therefore constitute an ordinary real coordinate system on M_0 . In these coordinates the periodicity becomes

$$(\tau, \hat{\varphi}) \sim \left(\tau + \frac{2\pi r_+}{r_+^2 - r_-^2}, \hat{\varphi} \right) \quad (3.137)$$

and $\hat{\varphi} \sim \hat{\varphi} + 2\pi$ as well. However, the *boundary* metric in $(\tau, \hat{\varphi})$ coordinates is no longer diagonal. Since this will complicate the analysis below, we continue to use the complex φ coordinate instead.

3.5.3 Matching

Let us now glue the ‘Euclidean’ and the Lorentzian manifolds together. We will first match the manifolds along a slice of constant t or τ away from the horizon.

Afterwards, we will deal with the subtleties introduced by the horizon.

We begin with the first matching condition. On the Lorentzian side, we find that the induced metric on a slice of constant t is given by:

$$h_{AB}dx^A dx^B = r^2 d\phi^2 + \frac{r^2 dr^2}{(r^2 - r_+^2)(r^2 - r_-^2)}. \quad (3.138)$$

On the Euclidean side, we find exactly the same metric on a slice of constant τ , with the replacement $\phi \rightarrow \varphi$, and therefore the first matching condition is satisfied. Let us now discuss the matching of the canonical momenta. On the Lorentzian side the extrinsic curvature (defined as usual with a real outward pointing unit normal) is

$${}^L\mathcal{K}_{AB}dx^A dx^B = \frac{2r_+r_-}{\sqrt{(r^2 - r_+^2)(r^2 - r_-^2)}} drd\phi \quad (3.139)$$

and on the Euclidean side we obtain

$${}^E\mathcal{K}_{AB}dx^A dx^B = \frac{2ir_+r_-}{\sqrt{(r^2 - r_+^2)(r^2 - r_-^2)}} drd\phi. \quad (3.140)$$

A short computation then shows that the second matching condition is satisfied as well, including the factor of i . Finally, the ‘corner’ matching condition which we discussed in section 2.4 is also satisfied.

Notice that a complex metric is already needed in the first matching condition, *i.e.* the continuity equation for the induced metric h_{AB} . Had we continued r_- to imaginary value on the Euclidean side so that the bulk metric is real, the induced metrics on the matching surface would not be the same (because the factor $1/(r^2 - r_-^2)$ in (3.138) would become $1/(r^2 + r_-^2)$). The fact that the metric is complex is therefore not directly related to the factor of i appearing in the matching conditions for the conjugate momenta.

The matching conditions should also be satisfied at the horizons. Based on the example of the static BTZ black hole, one may consider using half a period of the Euclidean solution and matching the surface given by $\tau = 0$ to $t_L = 0$ and the surface given by $\tau = \pi r_+/(r_+^2 - r_-^2)$ to $t_R = 0$. However, moving from $\tau = 0$ to $\tau = \pi r_+/(r_+^2 - r_-^2)$ on M_0 also involves an extra shift in the complex φ direction. Therefore, a correct matching can be obtained by setting $\phi_L = \varphi$ on the matching surface at L, and $\phi_R = \varphi + \pi i r_-/(r_+^2 - r_-^2)$ at R. One may then verify that the matching condition are satisfied at the horizon by transforming to a coordinate system that is nonsingular at the horizon. Since ∂_φ is a Killing vector, the gravity matching conditions for the background were insensitive to the extra twist in φ .

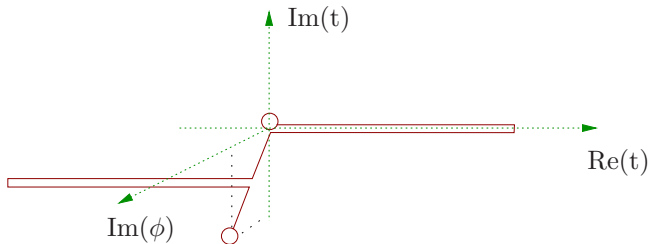


Figure 3.10: The contour for the boundary CFT that corresponds to a rotating black hole does not only lie in the complex t plane, but also extends into the complex ϕ plane. The circles should be identified.

However, for a scalar field the first matching condition becomes

$$\begin{aligned} \Phi_0(\tau = 0, \varphi = 0, r) &= \Phi_{1,L}(t_L = 0, \phi = 0, r), \\ \Phi_0\left(\tau = \frac{\pi r_+}{r_+^2 - r_-^2}, \varphi = \frac{\pi i r_-}{r_+^2 - r_-^2}, r\right) &= \Phi_{1,R}(t_R = 0, \phi = 0, r). \end{aligned} \quad (3.141)$$

which is clearly sensitive to the twist in φ .

We have shown that (half of) M_0 with the metric (3.134) can be matched to the Lorentzian rotating BTZ black hole. We can therefore also glue two Euclidean and two Lorentzian spacetimes in the same manner as shown in figure 3.9 for the BTZ black hole. Analyzing then the boundary of this combination of spacetimes, we can finally read off the boundary contour corresponding to the rotating BTZ black hole: it is the contour of figure 3.10. This is the same contour as in figure 3.6, except that the vertical segments involve a shift in the imaginary ϕ (or φ) direction of total magnitude $2\pi r_- / (r_+^2 - r_-^2)$. Let us now interpret this result in field theory.

First of all, notice that the *boundary* metric on the vertical segments is already complex, as can be verified by using real coordinates for the boundary of M_0 via the coordinate transformation (3.136). This is in fact consistent with the anticipated result that this contour corresponds to a CFT at finite temperature and with non-zero chemical potential for angular momentum. Namely, for such an ensemble the density matrix is

$$\rho = \exp(-\beta(H + \mu P_\phi)), \quad (3.142)$$

where H is the Hamiltonian and P_ϕ is a translation in ϕ . At the level of the path integral, such an ensemble corresponds to a contour that not only evolves in the imaginary time but also in the imaginary ϕ direction. From the periodicity (3.135), we immediately read off:

$$\beta = \frac{2\pi r_+}{r_+^2 - r_-^2} \quad \mu = \frac{r_-}{r_+}. \quad (3.143)$$

Of course, if one works purely in Euclidean time, one may also analytically continue μ , r_- and J and then both the boundary and the bulk metric would be real. Our aim here was to develop a real-time formalism and this led to complex metrics both in the boundary theory and in the bulk spacetime.

Let us finish this section with a brief comment on the use of complex (but non-degenerate) metrics in quantum gravity. First, it has been argued in the past (see for example [57]) that use of complex metrics after Wick rotation might be essential for a path integral over metrics. Second, saddle-point approximations often involve a deformation of the integration contour to a point in the complex plane, even if the integral originally is along the real axis. One particularly elementary example where this happens is a discretized vacuum-to-vacuum path integral for the harmonic oscillator, where the initial and final vacuum wave functions require such a contour deformation. Finally, complete reality of the bulk metric can no longer be maintained when one studies perturbations, as the $i\epsilon$ insertions that follow from our prescription necessarily yield a complex graviton propagator.

3.6 Conclusion

In this chapter we holographically computed a number of real-time correlation functions using the prescription that we presented in chapter 2. The first two examples involved the holographic computation of a vacuum time-ordered and Wightman function. Although their functional form was already known, we were able to compute both of them completely holographically, without analytic continuation or insertion of $i\epsilon$ factors by hand; instead, our computation provided for all the right signs and $i\epsilon$ insertions. We then computed a two-point function in real-time thermal AdS. In this computation, we used the same Lorentzian background but different initial data, which highlights the importance of properly defining the initial and final boundary conditions.

The prescription can be used to compute higher-point functions as well and we explicitly demonstrated how to do such computations in an AdS background. This discussion straightforwardly extends to any other Asymptotically (locally) AdS bulk spacetime. It is worth mentioning that our prescription resulted in a bulk-bulk propagator which is already of quantum-mechanical nature (*i.e.* Feynman rather than retarded). This shows that the bulk fields are path-integral quantized and the Euclidean caps provide the proper initial and final states. The prescription thus naturally incorporates QFT in curved space and it is not necessary to quantize perturbations by hand again.

A real-time thermal contour can also be ‘filled’ with an eternal black hole space-

time. Despite the presence of singularities and horizons, we demonstrated how the initial and final conditions could again be unambiguously specified via Euclidean caps. This procedure extends to rotating black holes, where the analytic continuation is more subtle. In our case, the reality conditions of the bulk fields and factors of i that arise in passing from real to imaginary time agree with QFT arguments, where the situation is well-understood. In particular, this procedure led to a complex bulk (and boundary) metric in the case of a rotating black hole.

The correlators we computed in the various examples were largely known from earlier work, where they were obtained using special properties of the backgrounds and analytic continuation. The emphasis here was on the coherent derivation of these results using the new real-time prescription: statistical factors and appropriate $i\epsilon$ insertions in 2-point functions all follow uniquely from solving the matching conditions.

Chapter 4

Ingoing boundary conditions

In the introduction to chapter 2 we briefly discussed a prescription presented in [40] for holographically computing retarded two-point functions. In this brief chapter we explain how this specific prescription can be embedded into the general real-time gauge/gravity prescription of the previous chapters.

4.1 Introduction

In the previous chapters we presented a prescription involving the real-time analogue of the standard Euclidean gauge/gravity dictionary. We have seen that this real-time dictionary is necessarily more involved than the continuation of the fundamental formula (1.31), as it becomes necessary to specify initial and final field theory states and initial and final supergravity data on the right-hand side. As we showed in detail in chapter 2, the map between field theory states and supergravity data directly yielded a prescription for the computation of any real-time correlation function from a holographic background, just as concrete and generally valid as (1.31) in Euclidean signature.

Although the problem of initial data in the gauge/gravity duality was never fully addressed before, specific prescriptions did exist in special cases. In particular, the authors of [40] used a black hole argument to specify the initial and final bulk data in the case of retarded real-time thermal correlation functions: their prescription is to use ‘purely ingoing’ boundary conditions for the supergravity fields at a bulk horizon. It was later shown in [41] that these conditions are related to ‘natural’ boundary conditions discussed earlier in the black hole literature [75, 67] and

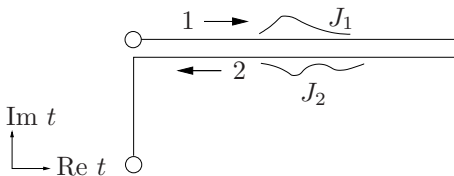


Figure 4.1: A real-time thermal contour in the complex time plane. The circles should be identified. The two Lorentzian segments are labelled 1 and 2 on which we have sources J_1 and J_2 , respectively. Although these segments are separated in the figure they lie on top of each other in the complex time plane.

that (with such boundary conditions understood) the prescription follows from taking functional derivatives of the on-shell action, although the authors did not take into account contributions to the on-shell action from timelike infinity, which are generically non-zero. Nevertheless the recipe of [40, 41] turned out to yield consistent results (provided the infinities have been subtracted correctly, see below) and is by now widely used.

However, adhering only to this specific recipe would leave several questions unanswered. For example, in general one expects the field theory state (or rather ensemble) to determine all the initial conditions, including any boundary conditions for bulk fluctuations. The prescription in [40, 41], on the other hand, presumes the existence of a horizon and uses specific behavior of the bulk fields there. How is this related to field theory data? More specifically, can we change the state somewhat and obtain different (‘non-natural’) boundary conditions as well? Furthermore, as mentioned above there are additional contributions in the on-shell action from initial and final surfaces within the setup of [40, 41]. If the prescription is therefore to be obtained by taking functional derivatives of an on-shell action as suggested in [41], why can these surface contributions be ignored?

In this chapter we apply the general real-time prescription of chapter 2 to the holographic computation of retarded thermal correlation functions and show that it reduces almost precisely to the recipe of [40]. In the process, all the questions raised in the previous paragraph can be answered as well. In the last sections we discuss the generalization to higher-point functions and some general lessons about the prescription.

4.2 The real-time thermal dictionary

Consider a field theory at finite temperature $T = 1/\beta$. The dynamics of the corresponding gas or plasma is described by *real-time thermal correlation functions*.

These correlators can be obtained [51] from a path integral along a contour in the complex time plane as sketched in figure 4.1, with sources J_1 and J_2 (for an operator \mathcal{O}) on the two horizontal segments of the contour. We will in this chapter focus on the *retarded* two-point function of the operator \mathcal{O} . The relevance of the retarded correlator is that it describes the *linear response* of the system to an external perturbation. To see this, notice that a perturbation can be described as a deformation of the theory such that the Hamiltonian \hat{H} changes to $\hat{H} + \int J\mathcal{O}$. In the in-in formalism this deformation should be present on both contours, so we need to set $J_1 = J_2 = J$. Expanding then in J , we obtain the first-order response to the one-point function on C_1 :

$$\begin{aligned}
 \delta_J \langle \mathcal{O}(x') \rangle &= \int_C dx J(x) \frac{\delta}{\delta J(x)} \langle \mathcal{O}_{[1]}(x') \rangle_J \\
 &= -i \int_0^T dt_1 J(x) \langle \mathcal{T}_c \mathcal{O}_{[1]}(x) \mathcal{O}_{[1]}(x') \rangle + i \int_0^T dt_2 J(x) \langle \mathcal{T}_c \mathcal{O}_{[2]}(x) \mathcal{O}_{[1]}(x') \rangle \\
 &= -i \int_0^T dt J(x) \langle \mathcal{T} \mathcal{O}(x) \mathcal{O}(x') \rangle + i \int_T^0 dt \langle \mathcal{O}(x) \mathcal{O}(x') \rangle \\
 &= \int_0^T dt J(x) \Delta_R(x', x), \tag{4.1}
 \end{aligned}$$

where we used the notation of section 2.1 and we suppressed the spatial integrations. The object $\Delta_R(x, x')$ is the retarded two-point function,

$$\Delta_R(x', x) = -i\theta(x' - x) \langle [\mathcal{O}(x'), \mathcal{O}(x)] \rangle, \tag{4.2}$$

which vanishes outside the future lightcone. The response is thus causal, as expected.

Now let us apply the real-time gauge/gravity prescription for this specific field theory configuration. The prescription instructs us to fill in the *entire* field theory contour with bulk spacetimes. Consider therefore first the vertical segment in figure 4.1 and suppose that it can be filled in with a Euclidean black hole solution (see the previous chapter for the case of thermal AdS). Topologically, this fills the imaginary time circle with a disk (plus some transverse space which is unimportant here). To add in the Lorentzian segments, we slice open the Euclidean black hole solution by making a cut in the disk, say at Euclidean time $\tau = 0$ up to the center of the disk. To the two cut surfaces we glue two copies of a segment of an eternal Lorentzian black hole solution which we will call M_1 and M_2 . We finally glue M_1 and M_2 together along some late-time surface. The total space is sketched in figure 4.2. (In the final section we further comment on this space and its relation with the construction of section 3.4.)

As usual, the sources J_1, J_2 on the boundary contour correspond to boundary data for the supergravity fields and switching them on causes perturbations on

the background of figure 4.2. According to the real-time gauge/gravity prescription these perturbations propagate from one segment to the other via certain *matching conditions* that essentially guarantee C^1 continuity of the fields across the gluing. (We recall that the precise conditions can be derived from a saddle-point approximation.) Notice that the matching conditions can often be met by analytic continuation of the bulk solution, in which case they provide for the correct $i\epsilon$ insertions. The procedure for black holes is however more involved and we refer to the computations in section 3.4 for details about the computations that follow.

4.3 Ingoing boundary conditions

As we are interested in computing retarded correlation functions from (4.1), we will have to consider a bulk perturbation on the background of figure 4.2 with $J_1 = J_2$. We will now show that precisely in these cases, the real-time gauge/gravity prescription yields ingoing boundary conditions for the bulk fields. As an example, consider a free bulk scalar field Φ with mass m satisfying the bulk Klein-Gordon equation. For brevity, only the solution on M_1 will be written down below.

We assume that we can use separation of variables in t , the angular (or other transverse) coordinates $\vec{\varphi}$ and the radial coordinate r . One then finds four mode solutions,

$$e^{-i\omega t} Y_l(\vec{\varphi}) \phi_{\pm\pm}(\omega, l, m^2, r),$$

with Y_l some basis of harmonic functions on the transverse space. These modes are either purely ingoing (ϕ_{-+} and ϕ_{--}) or purely outgoing (ϕ_{++} and ϕ_{+-}); the second \pm indicates the different possible analytic continuations across the horizons

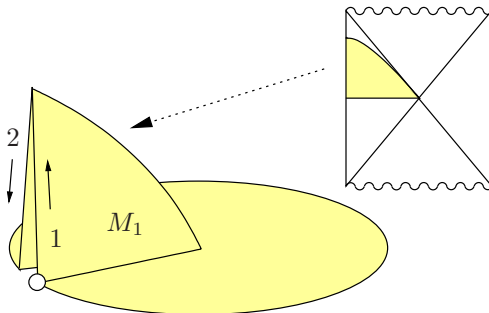


Figure 4.2: The Euclidean segment of the contour is filled in with a disk; the two Lorentzian segments with two copies of a part of an eternal black hole.

which we do not need here. Any solution Φ can be expanded in these modes with certain coefficients $a_{\pm\pm}(\omega, l)$:

$$\Phi(t, \vec{\varphi}, r) = \sum_l \int d\omega e^{-i\omega t} Y_l(\vec{\varphi}) \times (a_{++}\phi_{++} + a_{+-}\phi_{--} + a_{-+}\phi_{-+} + a_{--}\phi_{--}). \quad (4.3)$$

Now consider the solution corresponding to a delta-function source at $(t, \vec{\varphi}) = 0$ on $\partial_r M_1$ and denote the corresponding solution on M_1 as $\Delta_{[11]}$. If the modes are appropriately normalized, then according to equation (3.111) on page 115 we find that $\Delta_{[11]}$ has the form (4.3) with the coefficients:

$$\begin{aligned} a_{[11]++} &= (1 - e^{\beta\omega})^{-1} & a_{[11]+-} &= 0 \\ a_{[11]-+} &= 0 & a_{[11]--} &= (1 - e^{-\beta\omega})^{-1}. \end{aligned}$$

These $a_{[11]\pm\pm}$ are uniquely determined by demanding normalizability along the radial boundary of the entire manifold of figure 4.2 (except of course at the origin of $\partial_r M_1$), combined with the matching conditions between the segments. This solution precisely satisfies the ‘natural’ boundary conditions of [41].

Let us now move the delta-function source to the origin of $\partial_r M_2$. The perturbation propagates to M_1 via the matching conditions, where we denote the corresponding solution as $\Delta_{[21]}$. :

$$\begin{aligned} a_{[21]++} &= (e^{\beta\omega} - 1)^{-1} & a_{[21]+-} &= 0 \\ a_{[21]-+} &= (1 - e^{\beta\omega})^{-1} & a_{[21]--} &= 0, \end{aligned}$$

which are obtained in the same way as the $a_{[11]}$.

With obvious modifications, $\Delta_{[11]}$ and $\Delta_{[21]}$ can be made into bulk-boundary propagators. We can then integrate them against a source J_1 on $\partial_r M_1$ and another source J_2 on $\partial_r M_2$. Adding the two solutions gives the *unique* solution for given J_1 and J_2 that satisfies the matching conditions. In particular, if $J_1 = J_2$ then the bulk solution Φ_1 on M_1 becomes:

$$\begin{aligned} \Phi_1 &= \int_{\partial_r M_1} J_1 \Delta_{[11]} + \int_{\partial_r M_2} J_2 \Delta_{[12]} \\ &= \int_{\partial_r M} J (\Delta_{[11]} + \Delta_{[12]}). \end{aligned} \quad (4.4)$$

The last line is important, as it shows that the coefficients of Φ_1 are alternatively given by a *new* bulk-boundary propagator which is found by adding the two propagators given above. It has the coefficients

$$a_{[1]\pm\pm} = a_{[11]\pm\pm} + a_{[12]\pm\pm} \quad (4.5)$$

and we find that all the outgoing modes $a_{[1]_{\pm}}$ vanish. Therefore, the free-field bulk solution for $J_1 = J_2$ satisfies purely ingoing boundary conditions.

This solves two of the above puzzles: the choice between natural or ingoing conditions is determined by field theory, namely by switching on the source J_2 as well. We can also change the ensemble by adding sources on the Euclidean segment; the gluing and matching ensure that this indeed leads to ‘non-natural’ conditions at the horizon.

On-shell action and correlation functions

Let us now compute a retarded correlator. The real-time gauge/gravity instructs us to use (2.10) where the right-hand side splits into a sum of the on-shell supergravity actions for all the segments in figure 4.2. The action for each segment contains initial and final surface terms that arise from the integration by parts in both the radial and the time coordinates. However, it is precisely by virtue of the matching conditions that all these terms cancel between adjacent segments, which nicely resolves the final question of the introduction as well.

Using a Fefferman-Graham radial coordinate r , we find that Φ_1 has an expansion near $\partial_r M_1$ of the form:

$$\Phi_1 = J(x)r^{\Delta-d} + \dots + \phi_{(2\Delta-d)}(x)r^{-\Delta} + \dots \quad (4.6)$$

with $x = (t, \vec{\varphi})$ and $m^2 = \Delta(\Delta - d)$. After renormalization (see sections 1.5 and 2.3) and differentiation, the dual one-point function of an operator on $\partial_r M_1$ in the presence of sources is given by the normalizable term,

$$\langle \mathcal{O}(x) \rangle = -(2\Delta - d)\phi_{(2\Delta-d)}(x), \quad (4.7)$$

plus possible contact terms. We can then use (4.1) to obtain the retarded two-point function

$$\Delta_R(x, x') = -(2\Delta - d) \frac{\delta\phi_{(2\Delta-d)}(x)}{\delta J(x')},$$

with $\phi_{(2\Delta-d)}$ the normalizable term in the purely ingoing solution Φ_1 . Up to the normalization which arises from the holographic renormalization, this is precisely the prescription of [40, 41].

4.4 Higher-point correlation functions

The previous discussion applied to two-point functions only. In this section, we will show that ingoing boundary conditions can be used to compute specific three- and higher-point correlation functions as well.

Higher-point correlators cannot be computed holographically from a free-field analysis and the full, nonlinear bulk field equations have to be considered instead. These can be solved perturbatively, for example by using a bulk-bulk propagator. For a background as in figure 4.2, which consists of multiple segments, such a bulk-bulk propagator has to be defined for the entire manifold as we showed in section 3.3. Its form is again uniquely determined by demanding normalizability along the entire radial boundary, combined with the matching conditions between the segments.

As an example, consider the corrections arising from a nonlinear term $\sim \lambda\Phi^2$ in the Klein-Gordon equation. Let us again focus on the bulk solution Φ_1 on M_1 and consider only the case $J_1 = J_2$.

Following the arguments in section 3.3, the first-order correction to Φ_1 is obtained by integrating the bulk-bulk propagator against the square of the free-field solution on all the segments. For $J_1 = J_2$, the free-field solution is causal (like the boundary response) and in particular vanishes on the Euclidean segment, so we may restrict the integration to M_1 and M_2 only. An argument along the same lines as above then shows that this integral over M_1 and M_2 can be rewritten as a *single* integral over M_1 with a *new* bulk-bulk propagator, namely precisely one that satisfies purely ingoing boundary conditions.

Therefore, as far as Φ_1 is concerned, we may forget about the backward-going segment M_2 altogether and use purely ingoing boundary conditions for the bulk-bulk propagator instead. This result extends to all orders in λ and also holds if one uses for example a derivative expansion, as long as the bulk perturbation is causal.

On the other hand, M_2 is important for the boundary theory, since we need the full boundary contour to understand precisely which correlators we are computing. In particular, the solution near $\partial_r M_2$ shows that purely ingoing bulk solutions actually correspond to $J_1 = J_2$ on the boundary.

As an example, consider a holographically computed three-point function:

$$\Delta(x, x', x'') = (2\Delta - d) \frac{\delta^2 \phi_{(2\Delta-d)}(x)}{\delta J(x'') \delta J(x')}, \quad (4.8)$$

with $\phi_{(2\Delta-d)}(x)$ again the normalizable component of Φ_1 , which is now a purely ingoing (approximate) solution to the nonlinear field equations. To find the precise field theory expression for $\Delta(x, x', x'')$, we need to expand the right-hand side of (4.1) to quadratic order in $J = J_1 = J_2$. Following [51], the quadratic term is:

$$\delta_J \langle \mathcal{O}(x) \rangle = \dots - \int d^d x' \int d^d x'' \Delta_{RR}(x, x', x'') J(x') J(x'') + \dots \quad (4.9)$$

with Δ_{RR} the retarded three-point function,

$$\Delta_{RR} = \theta(t - t')\theta(t - t'')\langle [[\mathcal{O}(x), \mathcal{O}(x')], \mathcal{O}(x'')] \rangle.$$

Therefore, the three-point function (4.8) computed using purely ingoing boundary conditions is:

$$\Delta(x, x', x'') = \Delta_{RR}(x, x', x'') + \Delta_{RR}(x, x'', x').$$

This argument readily generalizes to higher-point functions.

4.5 Conclusion and discussion

We have shown that the real-time gauge/gravity prescription reduces to the ingoing prescription of [40, 41] when $J_1 = J_2$, *i.e.* when one computes retarded correlation functions. We also discussed which higher-point Lorentzian correlation functions are computed with ingoing boundary conditions. Along the way, the questions raised in the introduction were answered as well.

The above example illustrates that a bulk solution for the *entire* field theory contour is both necessary and sufficient to make the real-time dictionary just as precise as its imaginary-time counterpart.

Let us finally discuss some details of the construction sketched in figure 4.2. This construction is similar but not equal to the manifold sketched in figure 3.9 on page 110 in the previous chapter. In fact the two constructions are related by a deformation of the late-time hypersurface where the two Lorentzian segments are matched together. Indeed, by deforming this surface in figure 3.9 downward (towards the Euclidean segments) we can make the region beyond the horizon disappear entirely and end up with precisely the construction of figure 4.2. We showed in section 2.4 that this deformation freedom is a general feature of the real-time gauge/gravity prescription and does not affect the holographically computed correlation functions.

The freedom to deform the late-time hypersurface is reminiscent of field theory, where it is not necessary to path integrate further than the latest operator insertion either. It shows that one does not need to compute the complete real-time development of a spacetime to compute real-time correlators. For instance, there is no need to include the singularity or new asymptotic regions beyond a possible inner horizon. No significance is attached to any horizon either, as the final surface may be deformed freely through such horizons. In particular, any construction invoking membranes at the horizon would be at most an effective (but interesting) description.

One may think that the deformation freedom contradicts the fact that the entire spacetime is encoded in boundary correlators. This contradiction disappears if one realizes that the boundary correlators in principle have the power to resolve the field theory states. In the bulk, these states completely determine the Euclidean segments which in turn provide sufficient initial data to reconstruct the Lorentzian spacetime as well. The spacetime is therefore encoded completely in the boundary correlators, although sometimes only in an indirect way.

Chapter 5

Wormholes in 2+1 dimensions

In the previous chapters we have outlined a prescription for the computation of real-time correlation functions using the gauge/gravity duality. This prescription extends the fundamental AdS/CFT dictionary (1.31) to backgrounds with Lorentzian signature. In this chapter we apply the real-time gauge/gravity prescription to a class of three-dimensional Lorentzian ‘wormhole’ spacetimes that were found and studied in [76, 77]. Our main motivation is to illustrate various global issues that arise in real-time holography, in particular the holographic encoding of the bulk spacetime.

5.1 Introduction and summary of results

The wormholes of [76, 77] are global solutions of 2+1 dimensional gravity with a negative cosmological constant. Three dimensional gravity is an ideal setup to study global issues in holography because of the absence of local degrees of freedom. In the holographic context one finds that the general solution of the bulk Einstein equations with a cosmological constant in the Fefferman-Graham gauge can be explicitly obtained for general Dirichlet boundary conditions specified by an arbitrary boundary metric [78]. In contrast to the higher dimensional case, where in general the Fefferman-Graham expansion contains an infinite number of terms, in three dimensions the series terminates (see (5.28) below) and all coefficients can be expressed explicitly in terms of the boundary metric and boundary stress

energy tensor. What is left to be done is to impose regularity in the interior and this step requires global analysis¹.

One way to think about the wormholes of [76, 77] is as generalized eternal BTZ black holes. Whereas the spatial slices of an eternal BTZ black hole have a cylindrical topology, in the wormholes the spatial slices are general two-dimensional Riemann surfaces with boundary. We sketch an example of a wormhole in figure 5.1.

These spacetimes have a number of different asymptotic regions, which we will call outer regions in this chapter, one for each boundary component of the Riemann surface. The outer regions are separated by horizons and there is a non-trivial topology behind the horizons. The wormholes are locally just AdS_3 and should therefore have a holographic interpretation. Each outer region, however, is isometric to the static BTZ black hole and it would seem as though holographic data, which are obtained from the behavior of the solution near the conformal boundary, do not contain enough information to completely describe the wormhole spacetime. This follows from a simple counting argument. The spacetimes are uniquely determined given a Riemann surface of genus g with m boundaries. Such a Riemann surface is determined by $6g - 6 + 3m$ parameters. Each of the outer regions however depends on only one parameter, the mass of the BTZ black hole, so the holographic data from the m outer regions would seem to provide only m parameters. We will shortly describe how the real-time dictionary resolves this puzzle.

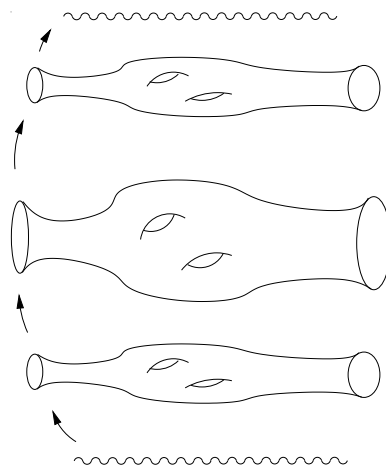


Figure 5.1: A wormhole spacetime with two outer regions corresponding to a Riemann surface of genus 2 with 2 boundary components.

There are corresponding Euclidean solutions which have been discussed in [79]. These spaces are *handlebodies*, *i.e.* closed surfaces of genus g filled in with hyperbolic three-space. These are also generalizations of BTZ whose Euclidean counterpart is a solid torus, *i.e.* a handlebody of genus 1. For these spacetimes a fairly straightforward application of the Euclidean gauge/gravity prescription

¹Note also that the Fefferman-Graham coordinates are in general well-defined only in a neighborhood of the boundary and they may not cover the entire spacetime.

shows there is no corresponding puzzle: the holographic one-point function captures the non-trivial topology and in particular does contain enough parameters to completely describe these spaces. This indicates that it is the real-time issues that are crucial in understanding holography for the Lorentzian wormholes.

We will indeed find that once we properly apply the real-time gauge/gravity prescription of chapter 2 there is a direct and unambiguous holographic interpretation of the entire Lorentzian wormhole spacetimes. The real-time prescription relies on gluing to a given Lorentzian spacetime Euclidean spaces that provide the initial and final states. A class of such Euclidean spaces are the handlebodies described above, but we emphasize that there are also other choices one can make. Once the complete spacetime has been specified (with the Euclidean parts representing initial/final states included), the holographic one-point functions do carry enough information about the spacetime and in particular the geometry behind the horizons. This information is encoded in the initial and final states.

The way this happens is instructive and reflects a number of subtle points about the holographic dictionary. Recall that because of the holographic conformal anomaly described in section 1.6 the theory depends on the specific boundary metric, not just its conformal class. In particular, the expectation value of the stress energy tensor changes anomalously under bulk diffeomorphisms that induce a boundary Weyl transformation [27, 23]. Now as mentioned earlier, one can choose coordinates such that the metric in any of the outer regions of the wormhole is exactly that of the BTZ black hole. In these coordinates the boundary metric is flat. According to the real-time gauge/gravity prescription, however, the Lorentzian solution should be matched in a smooth fashion to a corresponding Euclidean solution. Euclidean solutions that satisfy all matching conditions are provided by the handlebodies but these can never have a boundary metric that is globally flat (because the Euler number of the boundary Riemann surface is negative). One can arrange for an everywhere smooth matching by performing a bulk diffeomorphism on the Lorentzian side that induces an appropriate boundary Weyl transformation such that the Lorentzian boundary metric now matches with that of the handlebody. This has the effect that the expectation value of the stress energy tensor changes from its BTZ value to a new value, which is smooth as we cross from the Euclidean side to the Lorentzian side (as it should be). In other words, the initial state via the matching conditions dictates a specific bulk diffeomorphism on the outer regions of the Lorentzian solution and as a result the holographic data extracted using the solution in this coordinate system encode the information hidden behind the horizon.

Our results indicate that the dual state for a wormhole with n outer regions is an entangled state in a Hilbert space that is the direct product of n Hilbert spaces,

one for each component. A reasonable guess for this state is that it is the state obtained by the Euclidean path integral over the conformal boundary of half of the Euclidean space glued at the $t = 0$ surface of the Lorentzian wormhole. This is a Riemann surface with n boundaries and in the case of the handlebodies discussed above, it is precisely the Riemann surface that serves as the $t = 0$ slice of the wormhole. If one traces out all components but one, then the reduced description is given in terms of a mixed state in the remaining copy.

This chapter is organized as follows. In the next section we describe the wormhole spacetimes in detail and in section 5.3 and we discuss the handlebodies. In sections 5.4 and 5.5 we discuss holography for the handlebodies and the Lorentzian wormholes, respectively. After some general remarks in section 5.6 we conclude in section 5.7 with an outlook.

5.2 Lorentzian wormholes

In this section we describe the Lorentzian wormholes. We show how they can be obtained as quotients of a part of AdS_3 and discuss their physical properties. The material in this section summarizes discussions in [76, 77, 80, 81, 82]. We will occasionally use results from Teichmüller theory; more information on this topic can be found in [83, 84, 85, 82].

5.2.1 Wormholes as quotient spacetimes

The wormholes are obtained as follows. One starts with a Riemann surface S which is a quotient of the upper half plane H with respect to some discrete subgroup Γ of $SL(2, \mathbb{R})$. The upper half plane is then embedded into AdS_3 and the action of Γ is extended to AdS_3 entirely. After removing certain regions in AdS_3 that would lead to pathologies, one may take the quotient of the remainder with respect to Γ , which will give us the wormhole spacetime we are after. The topology of such a spacetime is $S \times \mathbb{R}$, with S the Riemann surface we started with and \mathbb{R} the time direction. The aim of this subsection is to discuss this procedure in more detail.

Riemann surfaces

Consider a Riemann surface S with $m > 0$ circular boundaries but no punctures². As follows from the uniformization theorem, such a Riemann surface can be de-

²Recall that a Riemann surface is a topological two-dimensional surface equipped with a complex structure. One can distinguish between punctures and circular boundaries precisely because of the complex structure.

scribed as a quotient of the upper half plane H by some discrete subgroup Γ of $PSL(2, \mathbb{R})$:

$$S = H/\Gamma, \tag{5.1}$$

where the action of

$$\begin{pmatrix} a & b \\ c & d \end{pmatrix} \in PSL(2, \mathbb{R}) \equiv SL(2, \mathbb{R})/\{\pm 1\} \tag{5.2}$$

on H is given by

$$z \mapsto \frac{az + b}{cz + d}. \tag{5.3}$$

Since these transformations act as isometries for the standard negatively curved metric on H ,

$$ds^2 = \frac{dzd\bar{z}}{\text{Im}(z)^2}, \tag{5.4}$$

this metric descends to a metric on S . Up to a constant rescaling, this is the unique hermitian metric of constant negative curvature on S (given the complex structure of S) and Γ is unique up to conjugation. We shall require absence of conical singularities on S , which means that the nontrivial elements of Γ cannot have fixed points in H . A simple analysis of the fixed points of (5.3) tells us that we should require that for all elements $\gamma \in \Gamma$ we have

$$|a + d| \geq 2. \tag{5.5}$$

Furthermore, absence of any punctures on S translates into $|a + d| > 2$ for all nontrivial γ . We then say that Γ consists of only *hyperbolic* elements (and the identity), and we call it a *Fuchsian group of the second kind*.

A particularly convenient way to visualize S as a quotient of H is to define a *fundamental domain* in H , basically a domain in H whose boundary in H consists of various segments that are pairwise identified by generators of Γ . For convenience we may take these segments to be geodesic segments, which are circular arcs in H . Two examples of a fundamental domain are sketched in figure 5.2.

From the theory of Fuchsian groups we obtain that the fixed points of such a group Γ form a nowhere dense subset of the conformal boundary ∂H of H , which is the real line plus a point at infinity. We will call this set the *limit set* and denote it as $\Lambda(\Gamma)$. Notice that $\Lambda(\Gamma)$ is invariant under the action of Γ .

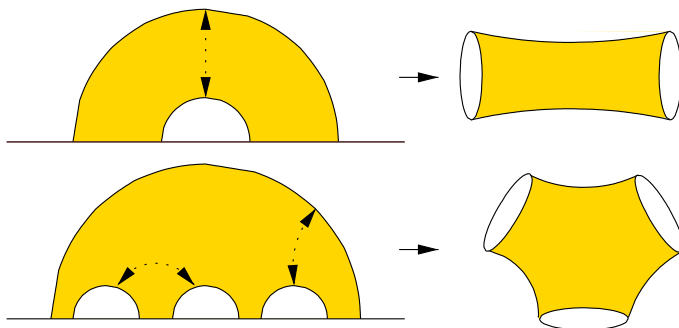


Figure 5.2: On the left we sketched two fundamental domains in H . The boundaries are pairwise glued together as indicated by the arrows. After the gluing we find the Riemann surfaces shown on the right.

AdS₃

To find the wormhole spacetime associated to S , we first fix some coordinate systems and conventions for AdS₃. We define AdS₃ as the surface

$$-U^2 - V^2 + X^2 + Y^2 = -1, \quad (5.6)$$

in $\mathbb{R}^{2,2}$, where the metric has the form

$$ds^2 = -dU^2 - dV^2 + dX^2 + dY^2, \quad (5.7)$$

and we have set the AdS radius $\ell^2 = 1$. By combining (U, V, X, Y) into a matrix,

$$\begin{pmatrix} V + X & Y + U \\ Y - U & V - X \end{pmatrix}, \quad (5.8)$$

we may identify the hyperboloid with the space of real unit determinant matrices, *i.e.* the group $SL(2, \mathbb{R})$. The connected component of the identity of the isometry group of AdS₃,

$$\text{Isom}_0(\text{AdS}_3) = (SL(2, \mathbb{R}) \times SL(2, \mathbb{R}))/\mathbb{Z}_2, \quad (5.9)$$

acts by left and right multiplication: if $(\gamma_1, \gamma_2) \in SL(2, \mathbb{R}) \times SL(2, \mathbb{R})$ then their action on AdS₃ is defined by

$$\begin{pmatrix} V + X & Y + U \\ Y - U & V - X \end{pmatrix} \mapsto \gamma_1 \begin{pmatrix} V + X & Y + U \\ Y - U & V - X \end{pmatrix} \gamma_2^T. \quad (5.10)$$

Taking the transpose of γ_2 is a convention which will turn out to be convenient below.

We may describe a patch in the hyperboloid with Poincaré coordinates (t, x, y) defined by

$$t = \frac{U}{V-X}, \quad x = \frac{Y}{V-X}, \quad y = \frac{1}{V-X}. \quad (5.11)$$

In these coordinates, the metric takes the form

$$ds^2 = \frac{-dt^2 + dx^2 + dy^2}{y^2}. \quad (5.12)$$

Although the Poincaré coordinate system may not cover the entire region of interest, the coordinate horizon at $y \rightarrow \infty$ will not be important in what follows.

Constructing wormholes

We can now construct a three-dimensional wormhole spacetime from the Riemann surface $S = H/\Gamma$. We begin by extending the action of the isometries of H to isometries on AdS_3 via the homomorphism:

$$PSL(2, \mathbb{R}) \hookrightarrow (SL(2, \mathbb{R}) \times SL(2, \mathbb{R}))/\mathbb{Z}_2, \quad (5.13)$$

which is given explicitly by $PSL(2, \mathbb{R}) \ni \gamma \mapsto (\gamma, \gamma) \in SL(2, \mathbb{R}) \times SL(2, \mathbb{R})$. One may check that elements of the form (γ, γ) leave the slice $U = 0$ invariant when they act on AdS_3 according to (5.10). Furthermore, their action on the slice $U = 0$ is exactly of the form (5.3) when we define $z = x + iy$ with (x, y) the Poincaré coordinates on this slice.

The image of Γ under this homomorphism is a discrete subgroup of $\text{Isom}_0(\text{AdS}_3)$ which is isomorphic to Γ and which we denote as $\hat{\Gamma}$. One may now try to take a quotient like $\text{AdS}_3/\hat{\Gamma}$, which clearly contains $S = H/\Gamma$ as the slice given by $U = 0$. However, away from the slice $U = 0$ this quotient turns out to have closed null or timelike curves. To get a spacetime free of pathologies we proceed as follows.

The embedding of H in AdS_3 as the slice $U = 0$ can be directly extended to an embedding of ∂H in the conformal boundary of AdS_3 . This extension maps the limit set $\Lambda(\Gamma)$ to a subset of the conformal boundary of AdS_3 , which we denote as $\Lambda(\hat{\Gamma})$. We then pass to the universal covering space of the hyperboloid and *remove* from it all points with a timelike or lightlike separation to $\Lambda(\hat{\Gamma})$ (after a standard conformal rescaling of the metric that brings the radial boundary to finite distance). Informally speaking, we are removing the filled forward and backward semi-lightcones emanating from every point in $\Lambda(\hat{\Gamma})$. We call the remainder $\widehat{\text{AdS}}_3$ which notably includes the original slice $U = 0$ entirely. The elements of $\hat{\Gamma}$ leave $\Lambda(\hat{\Gamma})$ invariant and, being isometries, they map lightcones to lightcones so they also leave $\widehat{\text{AdS}}_3$ invariant. Furthermore, the quotient

$$M = \widehat{\text{AdS}}_3/\hat{\Gamma} \quad (5.14)$$

is a spacetime that is free of closed timelike curves and conical singularities [80, 81] and contains $S = H/\Gamma$ as a hypersurface. These spacetimes are what we call the 2 + 1-dimensional wormholes.

5.2.2 Physical properties

We briefly discuss some physical properties of the wormholes. First of all, they are of course locally AdS₃ but, as was mentioned above, their global topology is of the form $S \times \mathbb{R}$ with S a surface with $m > 0$ circular boundaries and \mathbb{R} representing time. We sketched an example in figure 5.1, where S has genus 2 and has 2 boundary components. The wormholes can have an arbitrary number $m > 0$ cylindrical boundaries, and S can have arbitrary genus $g \geq 0$. There are two special cases: when $m = 2$ and $g = 0$ we obtain the eternal static BTZ black hole and the case $m = 1$, $g = 0$ is just AdS.

Except for the eternal BTZ black hole described already in [86], none of the wormholes have globally defined Killing vector fields since no such isometry of AdS₃ commutes with all the elements in Γ . On the other hand, all wormholes admit a discrete \mathbb{Z}_2 isometry, which acts as time reflection $U \leftrightarrow -U$ and therefore leaves the $U = 0$ slice invariant. The wormholes are not geodesically complete and begin with and end on locally Milne-type singularities. Furthermore, these singularities have associated black and white hole horizons (not drawn in figure 5.1).

Perhaps surprisingly, the m segments of the spacetime between the horizons and the conformal boundaries are *exactly* the same as for the BTZ black hole [76]. More precisely, we find that these segments can be covered by a (t, r, ϕ) coordinate system with the coordinate ranges $r > M$, $t \in \mathbb{R}$ and $\phi \sim \phi + 2\pi$, in which the metric is of the form

$$ds^2 = -(r^2 - M)dt^2 + \frac{dr^2}{r^2 - M} + r^2d\phi^2. \quad (5.15)$$

The mass M can be different for the m different boundaries, but it should always be strictly positive so we do not ‘pinch off’ the rest of the wormhole. We will call these m segments the *outer regions* of the wormhole, and what remains when we excise these segments we call the *inner region*. Notice that what we call the outer region is precisely the domain of outer communication [76]. What was called the ‘exterior region’ in [76] is obtained by keeping only the region outside of the future horizon, but we will never consider this region here. The fact that the nontrivial topology is hidden behind the horizons is in agreement with the general discussion of [87].

Depending on the genus of S , the geometry in the inner region is specified by a discrete number of parameters, namely the moduli of S . One may for example

think of these parameters as the elements (a_i, b_i, c_i, d_i) of a set $\{\gamma_i\}$ of generators of Γ . It will be important for what follows to notice that these parameters do not show up in the metric on the outer regions if we put the metric in the form (5.15). On the other hand, in chapter 6 we present a set of different coordinate systems that can be used to describe the wormholes as well. In these coordinate systems the coordinate ranges are natural and the metric features several parameters that are geometric (rather than abstract matrix elements). For example, some of the parameters are directly related to the lengths of certain cycles on the surface. As we explain in more detail in the next chapter, the combination of all parameters from the different charts that make up the surface can be used to completely describe the spacetime.³

It is straightforward to embed the wormholes into string theory, since the wormholes are locally just AdS_3 . For example, a wormhole times $S^3 \times T^4$ with a constant dilaton and three-form flux is an asymptotically locally AdS_3 solution of type IIB supergravity. However, these solutions are not supersymmetric.

5.3 Euclidean wormholes

In this section we describe ‘Euclidean wormholes’. These Euclidean spaces are *handlebodies* and one may think of them as closed Riemann surfaces filled in with three-dimensional hyperbolic space. They are a natural generalization of the Euclidean BTZ black hole, which is a solid torus [88]. These spaces were considered first in a holographic context in [79], where it was argued that they are natural Euclidean analogues of the Lorentzian wormholes, even though they are not obtained by analytic continuation of a globally defined time coordinate. We will see later that they are indeed suitable Euclidean counterparts of the Lorentzian wormholes, in the sense of the real-time gauge/gravity prescription of chapter 2, but we will also show that they are not the only possible Euclidean counterparts.

5.3.1 Construction

We will again describe the handlebodies via a quotient construction. Recall that Euclidean (unit radius) AdS_3 , denoted by H^3 , is defined as the hyperboloid

$$U^2 - V^2 + X^2 + Y^2 = -1, \quad (5.16)$$

³The parameters (a_i, b_i, c_i, d_i) are similar to the *Fricke* coordinates on the moduli space of S , whereas the metric we find in chapter 6 features parameters that are similar to *Fenchel-Nielsen* coordinates on the moduli space of S . These coordinate systems on the moduli or rather Teichmüller space of S are described in more detail in for example [83].

with $V > 0$ in $\mathbb{R}^{1,3}$ with the metric:

$$ds^2 = dU^2 - dV^2 + dX^2 + dY^2. \quad (5.17)$$

We may again combine (U, V, X, Y) into a matrix:

$$\begin{pmatrix} V + X & Y + iU \\ Y - iU & V - X \end{pmatrix} \quad (5.18)$$

which maps H^3 into the space of hermitian unit determinant matrices. An element γ of the connected component of the identity of the isometry group of H^3 ,

$$\text{Isom}_0(H^3) = PSL(2, \mathbb{C}), \quad (5.19)$$

acts on H^3 as

$$\begin{pmatrix} V + X & Y + iU \\ Y - iU & V - X \end{pmatrix} \mapsto \gamma \begin{pmatrix} V + X & Y + iU \\ Y - iU & V - X \end{pmatrix} \gamma^\dagger. \quad (5.20)$$

Notice that $PSL(2, \mathbb{C})$ maps the upper hyperboloid to itself.

We may again define Poincaré coordinates (τ, x, y) via

$$\tau = \frac{U}{V - X}, \quad x = \frac{Y}{V - X}, \quad y = \frac{1}{V - X}. \quad (5.21)$$

In these coordinates, the metric takes the form

$$ds^2 = \frac{d\tau^2 + dx^2 + dy^2}{y^2}. \quad (5.22)$$

This time there are no coordinate singularities and this metric covers all of H^3 .

To find the Euclidean analogue of the wormholes, we again start with the Riemann surface $S = H/\Gamma$. The action of Γ on H can again be extended to an action on H^3 entirely, this time via the trivial homomorphism

$$PSL(2, \mathbb{R}) \hookrightarrow PSL(2, \mathbb{C}), \quad (5.23)$$

(i.e. any element of $PSL(2, \mathbb{R})$ is also an element of $PSL(2, \mathbb{C})$). One may again check that real elements in $PSL(2, \mathbb{C})$ leave the slice $U = 0$ invariant when they act on H^3 according to (5.20). Furthermore, their action on the slice $U = 0$ is again of the form (5.3) if we define $z = x + iy$ with (x, y) the Poincaré coordinates on this slice.

After using this homomorphism to map Γ to $\hat{\Gamma}$ in $\text{Isom}_0(H^3)$, we can define the quotient

$$M_e = H^3/\hat{\Gamma}, \quad (5.24)$$

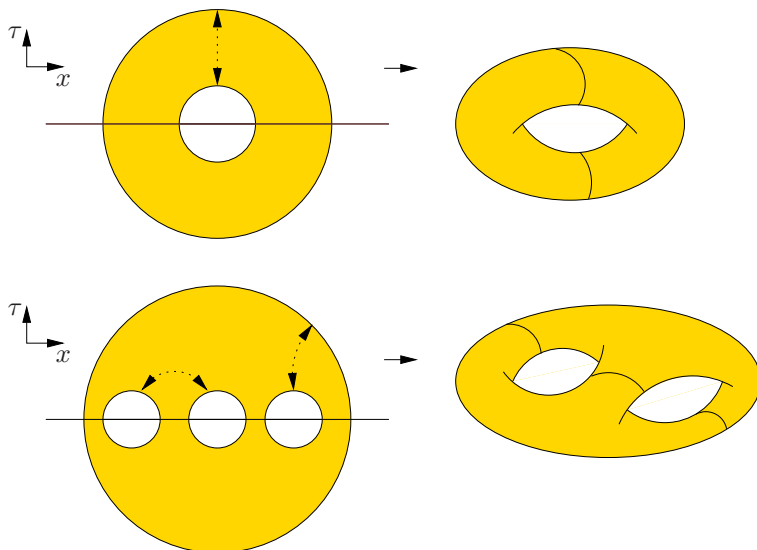


Figure 5.3: The Schottky double of the Riemann surfaces of figure 5.2 is constructed by gluing two copies of the fundamental domain to each other and identifying the boundaries. The line $\tau = 0$ is invariant and the Schottky double surface is symmetric under reflection in this line. The limit set $\Lambda(\hat{\Gamma})$ is a subset of the line $\tau = 0$ but is not shown here. It has to be removed from the (τ, x) plane before taking a quotient.

which now never leads to pathologies; M_e is a smooth and geodesically complete manifold. This quotient again contains $S = H/\Gamma$ as the $U = 0$ slice, and M_e also admits a \mathbb{Z}_2 isometry that leaves this surface invariant.

Let us now show why we call M_e a handlebody. We can extend the action of $\hat{\Gamma}$ to the conformal boundary of H^3 which is an S^2 . Consider an element γ of $\hat{\Gamma}$, *i.e.* a real element of $PSL(2, \mathbb{C})$, acting as (5.3) on the $U = 0$ slice. Its extension to H^3 entirely is found most easily by noticing that, according to (5.20), real elements of $\text{Isom}_0(H^3)$ leave slices of constant $U = \tau/y$ invariant and act on these slices exactly as on the slice $U = 0$. In the limit where $y \rightarrow 0$, we recover the action of γ on the conformal boundary, which is just the same as on the slice $U = 0$,

$$\gamma : w \mapsto \frac{aw + b}{cw + d}, \quad (5.25)$$

but this time with $w = x + i\tau$.

From (5.25) we find that the great circle $\tau = 0$ is invariant because a, b, c, d in (5.25) are all real. Just as in the Lorentzian case, this circle contains the limit set $\Lambda(\hat{\Gamma})$. After removing the limit set, the quotient of the remainder $S^2 \setminus \Lambda(\hat{\Gamma})$ with respect to $\hat{\Gamma}$ is a smooth manifold. As can be seen from figure 5.3, it consists

of two copies of S , one from the upper and one from the lower half plane, glued together along their m boundaries. This surface is called the *Schottky double* S_d of S . If S has genus g and m holes, then S_d has genus $2g + m - 1$ and no holes. Since S_d is just the conformal boundary of M_e , we may think of M_e as a filled S_d . This shows that M_e is indeed a handlebody.

A fundamental domain for M_e in H^3 is sketched in figure 5.4 and can be found by extending the circles on the boundary S^2 to hemispheres in H^3 . The fundamental domain for the original surface S is then embedded in this three-dimensional fundamental domain as the surface given by $\tau = 0$.

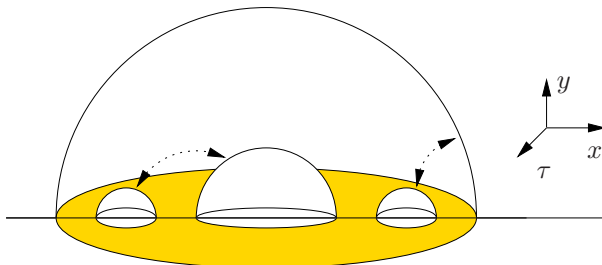


Figure 5.4: The extension of the fundamental domain for $\hat{\Gamma}$ from the S^2 to H^3 is bounded by a set of hemispheres that should be pairwise identified. We recover S as the surface given by $\tau = 0$.

5.4 Holographic interpretation of Euclidean wormholes

We discuss in this section the holographic interpretation of the Euclidean wormholes. Our discussion, which builds on [79, 89, 90, 82], is a fairly straightforward application of Euclidean holography. In the next section we will turn to Lorentzian wormholes, where things are more subtle.

Recall that the boundary S_d of the handlebody is a closed Riemann surface with $g > 1$ and therefore naturally has a metric of constant negative curvature. Below, following [89, 82], we holographically compute the one-point function of the stress energy tensor for this background metric.

The negative curvature metric on S_d is obtained by describing S_d as a quotient of H , that is $S_d = H/\Gamma_d$. Above we described S_d as a quotient of the conformal boundary S^2 of H^3 , with the limit set $\Lambda(\hat{\Gamma})$ removed, with respect to the group $\hat{\Gamma}$, that is $S_d = (S^2 \setminus \Lambda(\hat{\Gamma}))/\hat{\Gamma}$. As sketched in figure 5.5, this is just a different

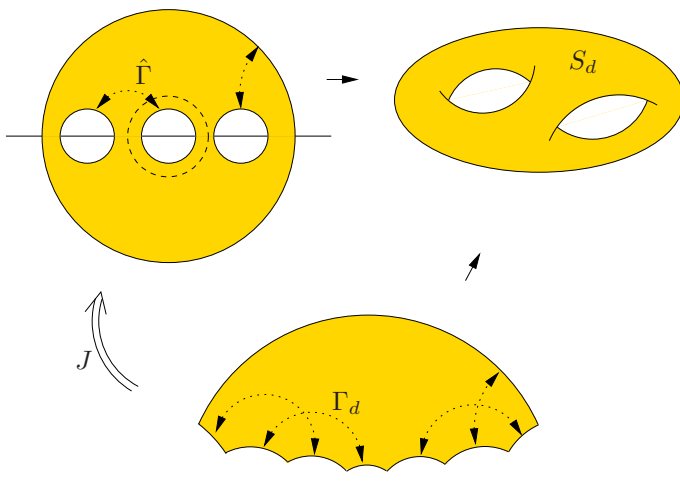


Figure 5.5: The Riemann surface S_d was originally obtained as $(S^2 \setminus \Lambda(\hat{\Gamma})) / \hat{\Gamma}$. However, like any closed Riemann surface with $g > 1$ it can also be described as H / Γ_d for some Γ_d for which we have drawn a fundamental domain in the bottom figure. J is a locally biholomorphic map interpolating between the two descriptions. The dashed circle is a homotopically nontrivial closed curve on S_d that can be contracted in the bulk.

description of the same Riemann surface. Therefore, there should be a locally biholomorphic map $J : H \rightarrow S^2$ between the two descriptions. Such a map should be compatible with the actions of Γ_d and Γ , in the sense that for every $\gamma_d \in \Gamma_d$ there should exist a $\gamma \in \hat{\Gamma}$ such that $J \circ \gamma_d = \gamma \circ J$. Now consider the case where γ is trivial for a nontrivial γ_d . Since γ_d corresponds to a nontrivial one-cycle on S_d , the image of this one-cycle under J must be a nontrivial closed curve on $S^2 \setminus \Lambda(\hat{\Gamma})$. The only way to do this is to let this curve encircle a nonempty subset of $\Lambda(\hat{\Gamma})$ on the S^2 , but such a one-cycle is contractible in the bulk manifold. For example, the dashed circle drawn within the fundamental domain of figure 5.5 can be continuously shrunk to a point by moving it inside the bulk, as can be seen from figure 5.4. Therefore, precisely those γ_d for which $J \circ \gamma_d = J$ correspond to contractible cycles in the bulk. The map J thus determines the filling of S_d : different maps J (up to composition with an element of $PSL(2, \mathbb{R})$ or $PSL(2, \mathbb{C})$) precisely correspond to the different fillings of S_d . It therefore suffices to know J in order to know which cycles of S_d are filled to give a handlebody and therefore to determine the Euclidean bulk geometry.

Since J is by construction locally biholomorphic, we can use the locally defined J^{-1} to pull back the metric (5.4) from H to $S^2 \setminus \Lambda(\Gamma)$. In Poincaré coordinates for H^3 defined in (5.21), the induced metric on the boundary S^2 was the flat metric

$ds_{(0)}^2 = dwd\bar{w}$ with $w = x + i\tau$. On the other hand, when we pull back the metric from H using J^{-1} , we find a metric on this S^2 which is of the form:

$$ds_{(0)}^2 = \left| \frac{dJ^{-1}}{dw} \right|^2 \frac{dw d\bar{w}}{\text{Im}(J^{-1}(w))^2} \equiv e^{2\sigma} dw d\bar{w}. \quad (5.26)$$

This metric is just a Weyl rescaling of the original metric:

$$dw d\bar{w} \mapsto e^{2\sigma} dw d\bar{w}, \quad (5.27)$$

where we note that σ becomes singular whenever $\text{Im}(J^{-1}(w))$ vanishes, which is precisely at the fixed point set $\Lambda(\hat{\Gamma})$ on S^2 .

We may now investigate what happens to the one-point function of the stress energy tensor. As we discussed in section 1.4.3 in the first chapter, the metric near the conformal boundary can always be put in the Fefferman-Graham form. For $d = 2$ the Fefferman-Graham expansion takes the specific form [78],

$$ds^2 = \frac{d\rho^2}{\rho^2} + \frac{1}{\rho^2} (g_{(0)ij} + \rho^2 g_{(2)ij} + \rho^4 g_{(4)ij}) dx^i dx^j, \quad g_{(4)ij} = \frac{1}{4} (g_{(2)ij} g_{(0)ij}^{-1} g_{(2)ij}). \quad (5.28)$$

In this coordinate system the one-point function of the stress energy tensor in the dual state is given by (1.169), which we repeat here as:

$$\langle T_{ij} \rangle = 2g_{(2)ij} + R_{(0)} g_{(0)ij}, \quad (5.29)$$

with $R_{(0)}$ the scalar curvature of $g_{(0)ij}$ and we set $16\pi G_N = 1$.

For the case at hand, starting with the bulk metric (5.22), we find that $ds_{(0)}^2 = dwd\bar{w}$ and $\langle T_{ij} \rangle_{g_{(0)}} = 0$. In section 1.4.3 we discussed how infinitesimal Weyl rescalings of the boundary metric follow from infinitesimal bulk diffeomorphisms. For the finite Weyl transformation in (5.27) the corresponding finite diffeomorphism has the effect of transforming $g_{(2)}$ such that [23]

$$\langle T_{ww} \rangle_{e^{2\sigma} g} = \langle T_{ww} \rangle_g + 2\partial_w^2 \sigma - 2(\partial_w \sigma)^2, \quad (5.30)$$

in agreement with CFT expectations. Since in our case

$$\sigma = \frac{1}{2} \ln(\partial_w J^{-1}) + \frac{1}{2} \ln(\overline{\partial_w J^{-1}}) - \ln\left(\frac{1}{2i}(J^{-1} - \bar{J}^{-1})\right), \quad (5.31)$$

we obtain directly that

$$\langle T_{ww} \rangle_{e^{2\sigma} g} = \frac{\partial_w^3 J^{-1}}{\partial_w J^{-1}} - \frac{3}{2} \left(\frac{\partial_w^2 J^{-1}}{\partial_w J^{-1}} \right) = S[J^{-1}](w), \quad (5.32)$$

with $S[f](w)$ the Schwarzian derivative of $f(w)$,

$$S[f] = \frac{f'''}{f'} - \frac{3}{2} \left(\frac{f''}{f'} \right)^2. \quad (5.33)$$

We therefore find that in the metric (5.26), the one-point function of the energy-momentum tensor is given by (5.32). This is already an encouraging result: we mentioned above that the bulk geometry is captured by J and here we find that the same J arises in the boundary energy-momentum tensor, which therefore provides the holographic encoding of the bulk geometry. However, the boundary metric (5.26) also depends on J which is not completely intuitive. This can be avoided by using J once more to pull back everything to H . If we use a complex coordinate z on H , so $w = J(z)$, then we find that:

$$\langle T_{zz} \rangle = -S[J] \quad ds_{(0)}^2 = \frac{dzd\bar{z}}{\text{Im}(z)^2}, \quad (5.34)$$

where we used that $(S[J^{-1}] \circ J)(dJ/dz)^2 = -S[J]$, which follows from [85]

$$S[f \circ g] = (S[f] \circ g)(dg/dz)^2 + S[g]. \quad (5.35)$$

This equation may be directly verified by using the chain rule for differentiation, which in our notation is written as $(f \circ g)' = (f' \circ g)g'$.

Equation (5.34) is the result we are after: if we describe the boundary S_d of the handlebody as the quotient H/Γ_d (corresponding to the bottom picture in figure 5.5), then the one-point function of the stress energy tensor in the constant negative curvature metric is given by minus the Schwarzian derivative of the map J to S^2 . If we now recall that J dictates which cycles in Γ_d are contractible in the bulk, namely precisely those for which $J \circ \gamma_d = J$, then this implies that $\langle T_{zz} \rangle$ indeed encodes the precise filling and therefore the bulk geometry.

Notice also that $S[J]$ has the right transformation properties under composition of J with $SL(2, \mathbb{R})$ from the right, under which it transforms covariantly, and with $SL(2, \mathbb{C})$ from the left, under which it is invariant. These transformation properties follow from (5.35) and the fact that $S[f] = 0$ if f is a Möbius transformation [85].

Finally, let us mention that the renormalized on-shell bulk gravity action has been computed in [79] and shown to be equal to the on-shell Liouville action on S_d , computed earlier in the mathematics literature [91]. Note also that the map J implicitly defines a solution to the Liouville equation.

5.4.1 Bulk interpretation and Teichmüller theory

We can make the holographic encoding of the spacetime a little more explicit. As mentioned above, we used the result from section 1.4.3 which states that from the bulk perspective the boundary Weyl rescaling is induced by a bulk diffeomorphism that preserves the Fefferman-Graham form of the metric but introduces a new

Fefferman-Graham radial coordinate ρ' . For the case at hand, the precise bulk diffeomorphism is given in [89, 82] and leads to the bulk metric

$$ds^2 = \frac{d\rho^2}{\rho^2} + \frac{(1 + \frac{1}{4}\rho^2)^2}{\rho^2} \frac{|dz + \mu_\rho d\bar{z}|^2}{\text{Im}(z)^2}, \quad (5.36)$$

with z again a coordinate on H and

$$\mu_\rho(z, \bar{z}) = -\frac{1}{2} \frac{\rho^2}{1 + \frac{1}{4}\rho^2} \left(\overline{S[J](z)} \right) \text{Im}(z)^2, \quad (5.37)$$

where the bar indicates complex conjugation and we dropped the primes on the new coordinates. Indeed, by expanding this metric in ρ^2 and using (5.29) we obtain again the result (5.34). It is noteworthy to mention that in the new coordinates the action of Γ leaves slices of constant ρ invariant, so its elements γ just act as $(\rho, z) \rightarrow (\rho, \gamma(z))$ with $\gamma(z)$ given by (5.3).

We expect these new coordinates to become ill-defined somewhere inside the handlebody since the contractible cycles shrink to zero length at a certain point. By inspection of (5.36), this only happens when $|S[J](z)| \text{Im}(z)^2 > \frac{1}{2}$. This bound on the Schwarzian derivative is familiar from Teichmüller theory as it figures prominently in the Ahlfors-Weil theorem concerning a local inverse of Bers' embedding of Teichmüller spaces [85] in the space of holomorphic quadratic differentials. The physical relevance of the bound is the following. When this bound is nowhere satisfied the coordinate system is nonsingular all the way to $\rho \rightarrow \infty$ where we recover another asymptotically AdS region. We then do not describe a wormhole but rather a spacetime with two disconnected boundaries which are simultaneously uniformized in the boundary S^2 , as expected from Teichmüller theory. These do not correspond to wormholes and we refer to [92] for more information as well as open questions regarding these spaces. For a handlebody there are no other asymptotic regions and we may therefore assume on physical grounds that the bound is everywhere satisfied. In that case, the coordinate system becomes degenerate at a surface given by

$$\rho^2 = \rho_c^2 \equiv \frac{1}{|S[J]| \text{Im}(z)^2 - \frac{1}{2}} \quad (5.38)$$

At the surface $\rho = \rho_c$, the metric is everywhere degenerate since $|\mu_{\rho_c}| = 1$. We then describe a point in the boundary of Teichmüller's compactification of the Teichmüller space [85]. It would be interesting to verify explicitly that the contractible cycles are indeed the degenerate cycles on this surface.

5.4.2 Non-handlebodies

The discussion so far was about Euclidean handlebodies, but these are not the only 3-manifolds that have a genus g Riemann surface as their conformal boundary. We

briefly discuss an example of such non-handlebody spacetimes in this subsection. A simple example can be constructed from the spacetimes described in [92]. These are obtained by starting from H^3 written in hyperbolic slicing and quotienting the boundary by a discrete subgroup Γ of H to obtain a compact, finite volume, genus $g > 1$ surface, Σ_g . This yields the metric with two boundaries,

$$ds^2 = dr^2 + \cosh^2(r) ds_{\Sigma_g}^2 \quad (5.39)$$

where $r \in (-\infty, \infty)$ and

$$ds_{\Sigma_g}^2 = \frac{dzd\bar{z}}{\text{Im}(z)^2} \quad (5.40)$$

is the constant negative curvature metric on Σ_g which has scalar curvature $R = -2$. To produce a manifold with a single boundary, one may try to quotient by $r \rightarrow -r$. This procedure however introduces a singularity at $r = 0$. The singularity can be avoided if the surface Σ_g has a fixed point free involution I , since then we can combine $r \rightarrow -r$ together with the action of I to obtain a smooth hyperbolic 3-manifold with conformal boundary the Riemann surface Σ_g . Such involutions are discussed, for example, in [93]. In this case the singularity at $r = 0$ is replaced by the smooth Riemann surface Σ_g/I . The resulting 3-manifold is a quotient of H^3 which has no contractible cycles so it is not a handlebody.

This 3-manifold has the same conformal boundary as the handlebody build from Σ_d but it has a different expectation value of the energy momentum tensor. Changing variable, $\rho = 2e^{-r}$, the metric becomes of the form (5.28) with:

$$g_{(0)ij} = 2g_{(2)ij} = ds_{\Sigma_g}^2. \quad (5.41)$$

We may then use (5.29) to obtain that:

$$\langle T_{ij} \rangle = -g_{(0)ij}. \quad (5.42)$$

We see that the one-point function of the energy-momentum tensor is notably different from that of a handlebody. However, we also observe that any involution that ‘ends’ the spacetime at $r = 0$ (with or without fixed points, orientation-reversing or orientation-preserving) results in the same one-point function, so the holographic one-point function of T_{ij} does not seem able to distinguish these geometries.

This is an interesting subtlety of the Euclidean dictionary due to global issues. Let us recall why we expect that locally, in the Euclidean setup, $g_{(0)ij}$ and $\langle T_{ij} \rangle$ uniquely fix a bulk solution (in any dimension). Intuitively, this is because the bulk equations of motion are second order differential equations and $g_{(0)ij}$ and $\langle T_{ij} \rangle$ provide the correct initial data. One can indeed show rigorously that given this data there exists a unique bulk solution in a thickening of the conformal boundary,

see [20] and references therein. Furthermore, one can show that $(g_{(0)ij}, T_{ij})$ are coordinates in the covariant phase space of the theory [30] and thus each such pair specifies a solution. In the case at hand this data indeed produces a unique metric for $r > 0$ but the way the spacetime is capped off at $r = 0$ depends on the fixed point free involution used. One can presumably distinguish the different spacetimes by using higher point functions and non-local observables, such as the expectation values of Wilson loops, *i.e.* minimal surfaces that end at a loop in the conformal boundary of the 3-manifold. It would be interesting to verify this explicitly.

5.5 Holographic interpretation of Lorentzian wormholes

We now move to discuss the holographic interpretation of the Lorentzian wormholes. We start by demonstrating in the next subsection that a direct adaptation of the analysis of the previous section leads to results where, in contrast with the Euclidean results, the spacetime geometry does not seem to be captured by the dual field theory on the Lorentzian side. We then demonstrate how the Lorentzian theory may capture the bulk geometry after all by using the real-time gauge/gravity prescription of chapter 2.

5.5.1 Naive computation

As we mentioned earlier, the metric in the outer regions can always be cast in the BTZ form (5.15). When using a new coordinate ρ defined via

$$r = \frac{\frac{M}{4}\rho^2 + 1}{\rho}, \quad (5.43)$$

the metric takes the form in (5.28) with

$$g_{(0)ij} = \eta_{ij}, \quad g_{(2)ij} = \frac{M}{2}\delta_{ij}, \quad g_{(4)ij} = \frac{M^2}{16}\eta_{ij}. \quad (5.44)$$

The one-point function of the stress energy tensor in the dual state can be computed from (5.29) yielding,

$$\langle T_{ij} \rangle = M\delta_{ij}. \quad (5.45)$$

On the other $(m-1)$ conformal boundaries, we obtain similar one-point functions (with different values of M) and all the other one-point functions vanish. Notice that we obtain no information whatsoever about the inner part of the geometry

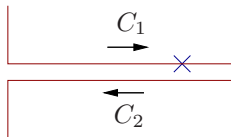


Figure 5.6: A contour in the complex time plane; the cross signifies the operator insertion.

and the Lorentzian one-point functions therefore seem to be insufficient to reconstruct the wormhole spacetime. One may however change this by a judicious choice of coordinates which is a natural consequence of the real-time gauge/gravity prescription.

5.5.2 Lorentzian gauge/gravity prescription

In this subsection, we prepare for the discussion below by highlighting some aspects about Lorentzian quantum field theory and the real-time gauge/gravity prescription of the previous chapters. We then apply the prescription to the wormholes in subsection 5.5.3.

States in field theory

The real-time gauge/gravity prescription of chapter 2 is based on the fact that *any* Lorentzian field theory path integral requires a specification of the initial and final states as well. Such a state $|\Psi\rangle$ may be specified via path integrals on a Euclidean space Y with a boundary and possible operator insertions away from this boundary. If we want to compute, say, $\langle\Psi|\mathcal{O}(t)|\Psi\rangle = \langle\Psi|e^{iHt}\mathcal{O}e^{-iHt}|\Psi\rangle$, we continue to path integrate along a Lorentzian segment with length t that is glued to the boundary of the Euclidean space, then insert the operator, and finally go *back* in time for a period t before we attach a second copy of the Euclidean space. For Euclidean spaces which are topologically $\mathbb{R} \times X$ with X a real space and \mathbb{R} representing Euclidean time, the overall field theory background manifold corresponds to a contour in the complex boundary time plane of the form sketched in figure 5.6 times a real space. Notice that extending the contour beyond the point t , say to a point $T > t$, amounts to an extra insertion of $e^{iH(T-t)}e^{-iH(T-t)} = \mathbf{1}$ which does not affect the correlation function. A similar story holds for higher-point correlation functions, but in those cases an operator ordering has to be specified. Although the contour may often be deformed to a simpler version, we emphasize that a procedure like the above is *always* necessary for Lorentzian quantum field theory.

Translation to gravity

In the Lorentzian gauge/gravity prescription of chapter 2, one incorporates the Euclidean segments for the path integral into the holographic description and ‘fills’ them with a bulk solution as well. For example, to the contour of figure 5.6 may correspond a bulk manifold consisting of two Lorentzian and two Euclidean segments. These segments are then glued to each other along spacelike hypersurfaces that should end on the corners of the boundary contour. The behavior of the fields at these hypersurfaces is then determined using *matching conditions* which guarantee the C^1 continuity of the fields. As we discussed in section 2.4, for the metric one imposes continuity of the induced metric h_{AB} and the extrinsic curvature K_{AB} with a factor of i :

$${}^L h_{AB} = {}^E h_{AB}, \quad {}^L K_{AB} = -i {}^E K_{AB}, \quad (5.46)$$

with the superscript indicating the Lorentzian or the Euclidean side and the extrinsic curvature on either side is defined using the outward pointing unit normal. There is also a *corner* matching condition⁴, which is defined at the intersection between S and the conformal (radial) boundary. It dictates that the inner product between the unit normal to S , denoted as n_μ , and the unit normal to the radial boundary, written as \hat{n}_μ , is continuous across the boundary (up to appropriate factors of i). For a Lorentzian-Euclidean gluing, using outward pointing unit normals, it becomes:

$$L(\hat{n}^\mu n_\mu) = i {}^E(\hat{n}^\mu n_\mu). \quad (5.47)$$

As discussed in section 2.2.1, all the matching conditions arise naturally from a saddle-point approximation. Although they are equivalent to analytic continuation in many simple cases, they do not rely on a globally defined time coordinate and are therefore more generally applicable.

This construction is an essential ingredient in the Lorentzian gauge/gravity dictionary. For example, it allows us to understand precisely how changing the initial and final states modifies the Lorentzian spacetime, gives the correct initial and final conditions for the bulk-boundary and bulk-bulk propagators, and also cancels surface terms from timelike infinity in the on-shell action, which would spoil a consistent dictionary and may also lead to additional infinities. Furthermore, the boundary correlators directly come in the in-in form as in quantum field theory.

⁴It is likely that this condition follows from the matching for the induced metric and the extrinsic curvature in (5.46), but in the absence of a general proof we treat it as an additional matching condition.

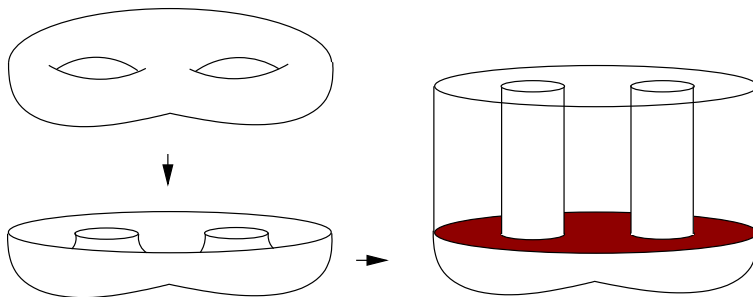


Figure 5.7: We take half of a genus two surface and attach Lorentzian cylinders to the boundary. This boundary manifold can be filled in with half a Euclidean handlebody plus a Lorentzian wormhole with spatial topology of a pair of pants. On the right, we shaded the matching surface between the Euclidean and the Lorentzian segment. It indeed has three boundaries and no handles.

5.5.3 Gauge/gravity duality for Lorentzian wormholes

Let us now apply the construction outlined in the previous subsection to the wormholes. To this end, we have to cut off the wormhole along some spatial bulk hypersurface and find a Euclidean space that we may glue to this hypersurface such that the matching conditions are satisfied.

Of course the field theory contour also has a backward-going segment and a final state. To fill this in, we have to cut off the wormhole along some final time slice as well and glue a second Lorentzian and Euclidean segment to this final surface. These second copies can be taken to be identical to the first ones, which correspond to taking the final and the initial state to be just the same. In section 3.4, we performed this procedure for the eternal BTZ black hole. As long as we do not switch on any perturbations, we may take the second Lorentzian and Euclidean segment to be completely identical to the first one. This also means that the matching conditions are trivially satisfied along the final gluing surface, so these do not have to be investigated separately. Therefore, it will be sufficient to focus on a single Euclidean-Lorentzian gluing below.

A candidate for the Euclidean space is half of the Euclidean handlebody M_e that we obtained in section 5.3. (It is not however the *only* candidate, as we will explicitly demonstrate in subsection 5.5.4.) Indeed, we may cut this handlebody and the wormhole spacetime in two halves along the surface S and glue them together along S . In the case S is a pair of pants (a surface of genus zero with three circular boundaries, so $g = 0$ and $m = 3$), the procedure is sketched in figure 5.7 and the filling of the full field theory contour, including the backward-going

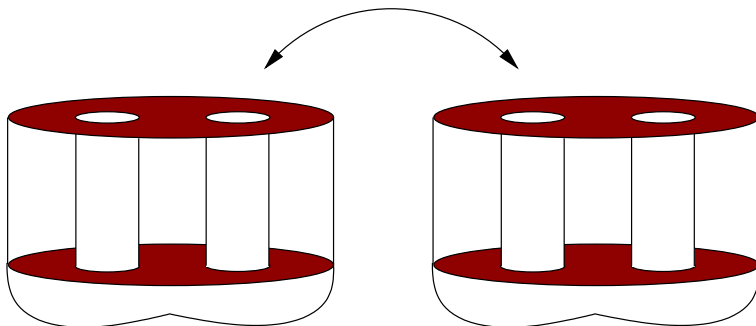


Figure 5.8: Analogous to figure 5.6, the full field theory contour has a forward- and a backward-going segment and two Euclidean segments to specify the initial and final state. Similarly, the full bulk spacetime consists of four segments as well. They should be glued along the matching surfaces which we shaded in this picture.

segment, is sketched in figure 5.8. Let us now verify that the matching conditions are satisfied at the shaded matching surface in figure 5.7. On both sides, the induced metric is locally just the unique negative curvature metric on S described as H/Γ , so it is the same metric indeed. Also, the extrinsic curvature vanishes completely on both sides because of the \mathbb{Z}_2 time-reversal symmetry. Therefore, the first and second matching conditions are satisfied indeed. Finally, the extra corner matching discussed in section 2.4 is also satisfied: in our case S intersects the conformal boundary orthogonally (again because of the \mathbb{Z}_2 symmetry) and the inner product $n^\mu \hat{n}_\mu$ thus vanishes both for M and for M_e . However, there is still a subtlety with the boundary metric which we now discuss.

If we use the BTZ coordinate system on the Lorentzian side, then the boundary metric on this side is flat. The boundary metric on the Euclidean side, however, can never be globally flat because S_d has negative Euler number. On the other hand, to match M and M_e , we should also take the boundary metric to be smooth (in the sense specified in section 2.4). This can be done by Weyl rescaling the Lorentzian boundary metric to a metric of constant negative curvature, as we discuss below. This makes the boundary metric analytic in the entire complexified coordinate space. In particular, the boundary metric is then smooth across the corner and the discrepancy between the boundary metrics on either side is removed.

Another possibility would be to Weyl rescale the metric on the Euclidean side such that it is flat in the vicinity of the gluing circles. Although the gluing is then smooth, the Euclidean boundary metric can then no longer be analytic since the curvature has to be nonzero at certain places. We shall not investigate this option here.

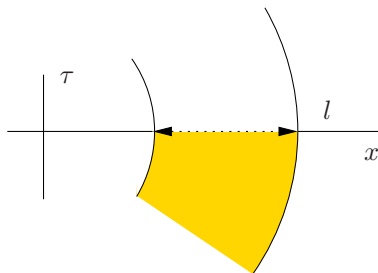


Figure 5.9: Part of a fundamental domain of S_d on S^2 . We will eventually replace the part with $\tau > 0$ with a Lorentzian wormhole. The single identification is given by $w \sim \lambda w$ and the line l is the entire positive x -axis.

Matching Euclidean and Lorentzian wormholes and $\langle T_{ij} \rangle$

We now discuss the consequences of the continuity of the boundary metric across the matching surface. As described above we match the initial $U = 0$ surface of the Lorentzian wormhole to half of the Euclidean handlebody. On the boundary of the spacetime, the Lorentzian cylinders are glued to the boundary of the Euclidean handlebody along the m circles that form the boundary of the $U = 0$ Riemann surface. These m circles lift to segments of the great circle given by $\tau = 0$ in the Poincaré coordinates (5.21) on the boundary S^2 of H^3 . Let us now focus on one of the m circles. After conjugation, we can always ensure that it lifts to the half-line l given by:

$$l : x > 0, \tau = 0 \quad (5.48)$$

on the S^2 . Its projection down to S_d is then given via the identification

$$w \sim \lambda w \quad (5.49)$$

with $w = x + i\tau$ and for some positive real $\lambda \neq 1$. The relevant part of the fundamental domain is then sketched in figure 5.9.

To find the boundary metric of constant curvature on this surface we again have to pass from the description of S_d as quotient of $(S^2 \setminus \Lambda(\hat{\Gamma}))$ to that of a quotient of H , for which we defined the map J in section 5.4. Using J^{-1} , we now map the half-line (5.48) to H , where we use the coordinate z . Although J^{-1} is multi-valued, we will need only one of the images of l in H . We can again use conjugation freedom to make sure that the image under consideration is the half-line:

$$l' : \text{Re}(z) = 0. \quad (5.50)$$

In H , the identification (5.49) becomes an isometry of $SL(2, \mathbb{R})$ that leaves l' invariant. Such an isometry is necessarily of the form:

$$z \sim \mu z, \quad (5.51)$$

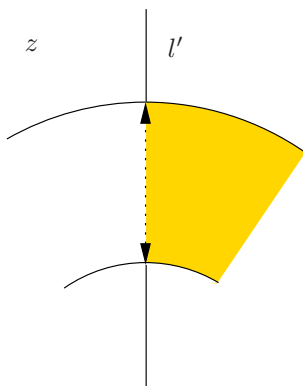


Figure 5.10: Under the locally defined map J^{-1} the domain in figure 5.9 maps to the sketched domain in H , where we use a coordinate z . The identification is given by $z \sim \mu z$. The line l' is the positive imaginary axis. We will replace the part $\text{Re}(z) < 0$ with a Lorentzian wormhole.

for some real $\mu \neq 1$ given implicitly by

$$J(\mu z) = \lambda J(z). \quad (5.52)$$

The construction in H is sketched in figure 5.10. Notice that $J(z)$ is an analytic map from the imaginary axis to the (positive) real axis, that is

$$\overline{J(iy)} = J(iy), \quad y > 0. \quad (5.53)$$

Notice also that the \mathbb{Z}_2 symmetry $w \leftrightarrow \bar{w}$ maps under J^{-1} to reflection in the imaginary axis, that is $z \leftrightarrow -\bar{z}$. (Again, as J^{-1} is multi-valued, it maps the original \mathbb{Z}_2 to many other reflections in H as well, but we do not need them here.)

We are now ready to attach a Lorentzian cylinder to the boundary. The procedure is sketched in figure 5.11. On H , this means that we cut away the half given by $\text{Re}(z) < 0$ and attach the universal covering of a Lorentzian cylinder to the gluing line $\text{Re}(z) = 0$. In the bulk, we can use the metric (5.36) with the matching surface given by $\text{Re}(z) = 0$, at least up to the point $\rho = \rho_c$. We now need to find a Lorentzian bulk metric that satisfies the matching conditions of section 2.2.1 when glued to this surface.

Both in the bulk and on the boundary, it is straightforward to obtain the explicit matching Lorentzian metric by analytic continuation. We first introduce a coordinate $z' = -iz$. In the z' plane the figure 5.10 is rotated clockwise by 90 degrees which slightly simplifies the matching below. In the coordinate z' the metric (5.36) becomes:

$$ds^2 = \frac{d\rho^2}{\rho^2} + \frac{(1 + \frac{1}{4}\rho^2)^2}{\rho^2} \frac{|dz' + \mu_\rho d\bar{z}'|^2}{\text{Re}(z')^2}, \quad (5.54)$$

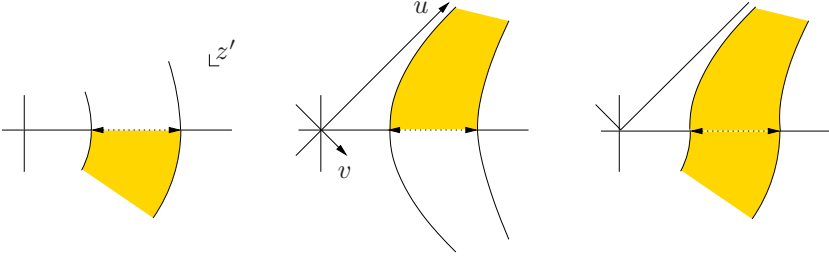


Figure 5.11: On the left, the Euclidean boundary geometry in the coordinate z' . In the center figure we sketched the Lorentzian boundary geometry and on the right the glued-together geometry.

where now

$$\mu_\rho(z', \bar{z}') = \frac{1}{2} \frac{\rho^2}{1 + \frac{1}{4}\rho^2} \left(S[\tilde{J}](z') \right) \text{Re}(z')^2, \quad \tilde{J}(z') = J(iz') \quad (5.55)$$

where we used that $S[J](iz') = -S[\tilde{J}](z')$, which follows from (5.35). The gluing takes place along the half-line $\text{Im}(z') = 0, \text{Re}(z') > 0$. We then replace $z' \rightarrow u$ and $\bar{z}' \rightarrow v$ to find the Lorentzian bulk metric:

$$ds^2 = \frac{d\rho^2}{\rho^2} + \frac{(1 + \frac{1}{4}\rho^2)^2}{\rho^2} \frac{(du + \mu_\rho(v)dv)(dv + \mu_\rho(u)du)}{\frac{1}{4}(u+v)^2}, \quad (5.56)$$

with

$$\mu_\rho(u) = \frac{1}{8} \frac{\rho^2}{1 + \frac{1}{4}\rho^2} \left(S[\tilde{J}](u) \right) (u+v)^2, \quad (5.57)$$

and a similar expression with $u \rightarrow v$. Note that $\tilde{J}(x)$ is real-analytic for $x > 0$ and monotonic, so $S[\tilde{J}](x)$ is real-analytic too. This Lorentzian metric is thus real and covers the bulk spacetime up to $\rho = \rho_c$. Since $z' \sim \mu z'$, the periodicity on the Lorentzian side is $(u, v) \sim \mu(u, v)$. The point $(u, v) = (0, 0)$ on the boundary is a fixed point of this identification and therefore we need to exclude the forward lightcone emanating from this point from the spacetime (the backward lightcone is already replaced by the Euclidean geometry). Since we also demanded $\text{Re}(z') > 0$, so $u + v > 0$, we need only the part of the Lorentzian boundary with $u > 0$ and $v > 0$.

On the boundary we find the metric:

$$ds_{(0)}^2 = \frac{dudv}{\frac{1}{4}(u+v)^2} \quad (5.58)$$

which has scalar curvature $R_{(0)} = -2$. Using once more (5.29) we obtain for the

one-point functions:

$$\langle T_{uu} \rangle = -S[\tilde{J}](u) \quad \langle T_{vv} \rangle = -S[\tilde{J}](v) \quad \langle T_{uv} \rangle = \frac{-1}{8(u+v)^2} \quad (5.59)$$

Notice that one expects that $T_i^i = \frac{c}{24\pi}R_{(0)}$ and we obtained here $T_i^i = -2$. Reinstating the factors of $16\pi G_N$, we find $c = 24\pi/(16\pi G_N) = 3/(2G_N)$ which is precisely the value of the central charge we found in (1.172).

Equation (5.59) is the main result of this section and demonstrates that the Lorentzian one-point function of the stress energy tensor as obtained from the metric (5.56) does contain information about the dual geometry that is hidden behind the horizons.

5.5.4 More fillings

In the previous section we glued a particular handlebody to the Lorentzian wormhole. There exist however a variety of handlebodies $\{M_e\}$ that all have a hypersurface S where the matching conditions are satisfied as we discuss now.

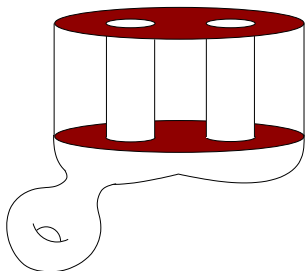


Figure 5.12: Adding a handle as indicated does not change the properties of the gluing surface or the Lorentzian spacetime.

In particular, one may attach an extra filled handle to M_e somewhere away from the matching surface to obtain a manifold M'_e with conformal boundary Σ with $\Sigma \neq S_d$. An example of this is sketched in figure 5.12. This procedure does not change any properties like the induced metric or the extrinsic curvature of the matching surface. Geometrically, this can be seen by going to the universal covering: one may add generators to $\hat{\Gamma}$ to obtain a group $\hat{\Gamma}'$ and as long as $M'_e = H^3/\hat{\Gamma}'$ has S as a surface of \mathbb{Z}_2 symmetry we may slice open M'_e along this surface and glue the Lorentzian wormhole $M_l = \widehat{\text{AdS}}_3/\hat{\Gamma}$ to it. For the boundary surface this procedure is sketched in figure 5.13. In the

figure we represented the addition of two generators to $\hat{\Gamma}$ by cutting out four circles out of the fundamental domain that are pairwise identified, all done in such a way that the original \mathbb{Z}_2 symmetry remains intact. Although we have not sketched it here, this procedure directly extends to the entire three-dimensional space: the \mathbb{Z}_2 symmetry is also present for the new handlebody and S is again the invariant surface given by $\tau = 0$.

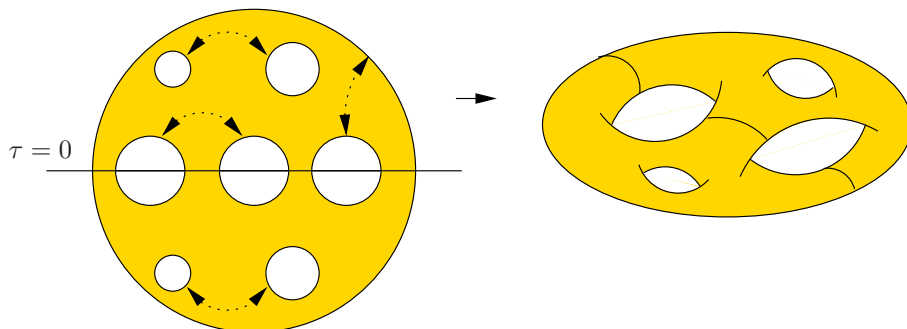


Figure 5.13: One may add generators to the Schottky group $\hat{\Gamma}$ without breaking the \mathbb{Z}_2 symmetry. We added here two generators to the surface described in figure 5.3. The resulting surface has two extra handles: one for the half corresponding to the initial state and another one for the final state.

We conclude that we can glue to the Lorentzian wormholes also half of M'_e . A similar analysis as in the previous section establishes that we can pick a coordinate system where the 1-point functions on the Lorentzian side capture the fact that the initial state is different than the one corresponding to M_e .

5.5.5 Two-point functions

To gain a better understanding of the dual state we discuss in this subsection the computation of the 2-point function for a scalar operator \mathcal{O} of dimension Δ . In the bulk it suffices to consider a free massive scalar field, as interaction terms contribute only to higher point functions. We glue a Euclidean handlebody at $t = 0$ and take the initial and final states to be the same. From the analysis in chapter 3 it follows that the different real-time correlators (time-ordered, Wightman, etc.) can be obtained by suitable analytic continuations of the Euclidean correlator in the handlebody geometry.

The two-point function of a scalar operator on the Euclidean plane is uniquely fixed by conformal invariance and takes the form:

$$\langle \mathcal{O}(\tau, x) \mathcal{O}(\hat{\tau}, \hat{x}) \rangle = \frac{1}{[(\tau - \hat{\tau})^2 + (x - \hat{x})^2]^\Delta}, \quad (5.60)$$

where we normalized the operators so that the coefficient in the numerator equals one. For the handlebody, we have to sum over the elements of the Schottky group $\hat{\Gamma}$, whose elements γ act as Möbius transformations on the boundary,

$$\gamma : \omega = x + i\tau \rightarrow \frac{a(x + i\tau) + b}{c(x + i\tau) + d}, \quad (5.61)$$

with real a, b, c, d and $ad - bc = 1$. This can also be written as

$$\gamma : (\tau, x) \rightarrow (\gamma_\tau, \gamma_x) \equiv \frac{1}{(cx + d)^2 + c^2\tau^2} \left(\tau, (ax + b)(cx + d) + ac\tau^2 \right). \quad (5.62)$$

Using the complex coordinate w on the boundary S^2 of H^3 , we obtain

$$\langle \mathcal{O}(w, \bar{w}) \mathcal{O}(w_1, \bar{w}_1) \rangle = \sum_{\gamma \in \hat{\Gamma}} \frac{1}{|cw + d|^{2\Delta} |\gamma_w - w_1|^{2\Delta}}. \quad (5.63)$$

where the boundary metric is locally $dwd\bar{w}$. We then Weyl transform to the metric (5.26) which is globally well-defined to find

$$\langle \mathcal{O}(w, \bar{w}) \mathcal{O}(w_1, \bar{w}_1) \rangle = \sum_{\gamma \in \hat{\Gamma}} \frac{e^{-\Delta\sigma(w, \bar{w})} e^{-\Delta\sigma(w_1, \bar{w}_1)}}{|cw + d|^{2\Delta} |\gamma_w - w_1|^{2\Delta}}, \quad ds^2 = e^{2\sigma(w, \bar{w})} dwd\bar{w}, \quad (5.64)$$

with

$$e^{2\sigma(w, \bar{w})} = \left| \frac{dJ^{-1}}{dw} \right|^2 \frac{1}{\text{Im}(J^{-1}(w))^2}. \quad (5.65)$$

We can now pull back to H , using $z = J^{-1}(w)$, to obtain

$$\langle \mathcal{O}(z, \bar{z}) \mathcal{O}(z_1, \bar{z}_1) \rangle = \sum_{\gamma \in \hat{\Gamma}} \frac{|J'(z)J'(z_1)|^\Delta (\text{Im}(z)\text{Im}(z_1))^\Delta}{|cJ(z) + d|^{2\Delta} |\gamma(J(z)) - J(z_1)|^{2\Delta}}, \quad (5.66)$$

and the metric is then just the standard metric on H given in (5.4). As before, we may assume the covering groups are such that $J(\lambda z) = \mu J(z)$. We then again introduce the coordinate $z' = -iz$ and the map $\tilde{J}(z') = J(iz') = J(z)$, replace $z' \rightarrow u$ and $\bar{z}' \rightarrow v$ to obtain the Lorentzian metric. We recall that in this case $\tilde{J}(x)$ is real-analytic for real positive x . More precisely, following similar steps as in chapter 3, one finds that the time-ordered correlator is obtained by replacing $z \rightarrow u - i\epsilon u$ and $\bar{z} \rightarrow v + i\epsilon v$, where the $i\epsilon$ insertions push the singularity everywhere away from the real-time contour. To avoid clutter we will however not write the $i\epsilon$ insertions explicitly below. The final answer is then

$$\langle T\mathcal{O}(u, v) \mathcal{O}(u_1, v_1) \rangle = \sum_{\gamma \in \hat{\Gamma}} \frac{2^{-2\Delta} (u + v)^\Delta (u_1 + v_1)^\Delta [\tilde{J}'(u)\tilde{J}'(v)\tilde{J}'(u_1)\tilde{J}'(v_1)]^{\Delta/2}}{(c\tilde{J}(u) + d)^\Delta (c\tilde{J}(v) + d)^\Delta (\gamma(\tilde{J}(u)) - \tilde{J}(u_1))^\Delta (\gamma(\tilde{J}(v)) - \tilde{J}(v_1))^\Delta} \quad (5.67)$$

in the metric

$$ds^2 = \frac{4dudv}{(u + v)^2}. \quad (5.68)$$

We will interpret (5.67) further in the next subsection.

Notice that at late times the correlator is dominated by the BTZ elements in $\hat{\Gamma}$. More precisely, if one defines coordinates⁵ $u = \exp(x + t)$, $v = \exp(x - t)$, then in the limit $t, t_1 \rightarrow \infty$ with $(t - t_1)$ fixed, all terms in (5.67) go to zero, except the ones with either $b = 0$ or $c = 0$. These are precisely the elements associated with the BTZ black hole. This may hint at some process of thermalization which corresponds to the presence of a horizon in the bulk.

5.5.6 State dual to wormholes

Let us now discuss what our results imply about the QFT state dual to the wormholes. Since there are m boundaries, the Hilbert space consists of a tensor product of m Hilbert spaces, one for each boundary component. From the fact that the wormholes are manifolds that interpolate between the m segments, we expect to find nonzero correlations between the m boundaries and the initial state to be an entangled state. Indeed, this is precisely what we find. To see this, suppose the initial state is separable, namely of a product form $|\alpha_1\rangle \otimes \cdots \otimes |\alpha_m\rangle$. Then the 1-point functions would necessarily take a factorizable form. More precisely, suppose the state was separable and consider the insertion of a stress energy tensor in, say, the first boundary component,

$$\begin{aligned} \langle T_{ij}(x_1) \rangle &= \langle \alpha_1 | \otimes \cdots \otimes \langle \alpha_m | T_{ij}(x_1) | \alpha_1 \rangle \otimes \cdots \otimes | \alpha_m \rangle \\ &= \langle \alpha_1 | T_{ij}(x_1) | \alpha_1 \rangle \prod_{k=2}^m |||\alpha_k|||^2 \end{aligned} \quad (5.69)$$

Now the naive 1-point function in (5.45) would support the view that the state is separable. Namely, in that case we could naively say that the state $|\alpha_1\rangle$ in the first copy depends only on the corresponding mass parameter M_1 and not on the other variables that determine the spacetime. One would then expect one- and higher-point functions of the energy momentum tensor in the first copy which up to an overall factor only depend on M_1 . The one-point functions (5.59) however are not of that form, as the Schwarzian $S[\tilde{J}]$ does not have such a factorizable form and does contain all the variables that determine the spacetime. These one-point functions therefore make the entangled nature of the state explicit.

Another check on the non-separability of the state is provided by the computation of the two-point function. An argument analogous to the one above implies that if the state is separable then the two-point function would have a factorizable form. The two-point function (5.67) however does not have this form, supporting the view that the dual state is an entangled state.

⁵In these coordinates the Lorentzian cylinder is $(t, x) \sim (t, x + \log \lambda)$.

A natural guess for the dual state is that it is the state obtained by a Euclidean path integral over a Riemann surface Σ with m circular boundaries. According to the reasoning of [39, 94], this surface Σ can be taken to be precisely the conformal boundary of one half of the Euclidean manifold M_e . This can be $\Sigma = S$, with S the surface of time reversal symmetry of the wormhole spacetime, for the case of the handlebodies of section 5.3, or $\Sigma \neq S$ if the initial state is obtained according to the discussion of the previous subsection.

If we now trace over all components but one, all wormholes with $m > 1$ can be thought of as been associated with a mixed state in the remaining copy. This mixed state would have a nonzero entropy and would then explain the presence of horizons. However from this viewpoint the $m = 1$ case would be special in that we only have a single copy of the CFT so there are no copies to trace out. These spacetimes were also analyzed in [95] which suggested that the dual state is in some respects similar to a thermal state. We leave a better understanding of this case for future work.

5.6 Remarks

In this section we discuss some general remarks concerning the wormhole spacetimes.

5.6.1 Other bulk spacetimes

The question we addressed in this chapter is what is the holographic interpretation of any given wormhole spacetime. One can also ask: given a geometry at infinity, how many different bulk spacetimes can one have? In general, all such saddle points contribute and should be taken into account, although typically one of the saddle points dominates at large N at any given regime. A well-known example is that associated with the Hawking-Page transition [96, 16]. In the case the boundary is $S^1 \times S^{d-1}$ and there are two possible (Euclidean) bulk manifolds corresponding to making contractible in the interior either S^1 or S^{d-1} , namely the Euclidean Schwarzschild AdS solution and thermal AdS. This question is usually addressed in Euclidean signature, but it is clearly also relevant in Lorentzian signature. In this context the question is now: given the conformal boundary of the complete Euclidean and Lorentzian pieces how many different bulk manifolds can one have?

Naively, one might think that for every Euclidean solution there would be a corresponding Lorentzian plus Euclidean solution, but this turns out not to be the

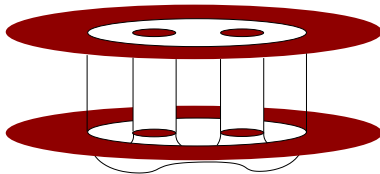


Figure 5.14: *The analogue of thermal AdS for the pair of pants wormhole. In this case three copies of Lorentzian AdS₃ are attached to the three boundaries of the pair of pants.*

case. This can be demonstrated with the case where the conformal boundary is a torus, $S^1 \times S^1$. As in the higher dimensional case, there are two solutions that correspond to either the first or the second circle being contractible in the interior (which correspond to thermal AdS and Euclidean BTZ), but there are now new possibilities obtained by considering a contractible cycle that is a linear combination of the above cycles [97]. These solutions are called the ‘ $SL(2, \mathbb{Z})$ family’ of black holes as they related to the Euclidean BTZ black hole by a modular transformation. In appendix 5.A we however show that none of these solutions can be used in the real-time gauge/gravity prescription as the Euclidean part associated with a vertical segment of the QFT contour. The reason is that the matching conditions force the bulk Lorentzian bulk metric to be complex. This results in a energy momentum tensor that does not satisfy the correct reality conditions.

For a higher genus Riemann surface there also exists a similar family of solutions [98] as well as the aforementioned non-handlebody solutions. As for the other fillings of handlebody-type, we expect that only the analogues of the BTZ and the thermal AdS would be relevant for holography of the Lorentzian wormholes. The analogue of thermal AdS is obtained by attaching m copies of empty Lorentzian AdS to the m boundary components of the handlebody. The case of a pair of pants wormhole is sketched in figure 5.14. For the non-handlebodies the corresponding Lorentzian solution remains to be investigated.

5.6.2 Rotating wormholes

In the previous sections we considered non-rotating wormholes. Rotating wormholes do exist [99, 100] and are obtained by taking a quotient with respect to a group generated by elements of the form $(\gamma_1, \gamma_2) \in SL(2, \mathbb{R}) \times \widehat{SL}(2, \mathbb{R})$ with $\gamma_1 \neq \gamma_2$. A similar region like $\widehat{\text{AdS}}_3$ exists such that the quotient $\widehat{\text{AdS}}_3/\Gamma$ is a good spacetime [80, 81] and the metric in the outer regions is isometric to the rotating BTZ metric [81]. The corresponding ‘Euclidean spaces’ for these wormholes, however, are not so straightforward. A prescription for obtaining them has been proposed in [101] and critically analyzed in [82]. From the holographic perspective,

the reality condition of the bulk fields, especially on the Euclidean caps, should be dictated by the standard reality condition of the dual QFT. In the case of the rotating BTZ we have demonstrated in section 3.5 that the matching conditions result in a complex metric on the Euclidean caps. It is likely that the same would be true here, namely the Euclidean solution that should be glued to the rotating Lorentzian wormhole would be complex.

5.7 Outlook

We have discussed the holographic interpretation of a class of 2+1-dimensional wormhole spacetimes. They are interesting toy models for the analysis of global issues in the real-time gauge/gravity correspondence. We have shown that the asymptotics of the complete solution that includes both the Lorentzian solution and the Euclidean caps completely characterize the geometry including the regions behind the horizons. This came about by a subtle interplay between global issues and the real-time gauge/gravity dictionary. In particular, the real-time gauge/gravity prescription requires gluing smoothly Euclidean solution to the Lorentzian solution at early and late times. This in turn can be used to fix the freedom for independent Weyl rescaling at different outer components and results in holographic data that contain information about the complete geometry.

In this way the Lorentzian CFT correlators can be made to encode in a very precise sense the parts of the geometry that lie behind the horizons. This presents a unique opportunity to study and settle classic questions and puzzles in black hole physics. The way the information is given to us, however, (i.e. in terms of CFT correlators) is very different from the way the black holes puzzles are usually formulated (e.g. using bulk local observers) and this presents the main obstacle in directly addressing these issues.

In this respect, one of the most interesting cases to further understand is that of spacetimes with $m = 1$ and $g > 0$. As discussed earlier, these spacetimes have only one outer region. A reasonable guess for the dual state would be the pure state obtained by performing the Euclidean path integral over the Riemann surface Σ that is the conformal boundary of the Euclidean 3-manifold that we glue to the Lorentzian spacetime at $t = 0$. However the fact that this is a pure state appears at odds with the presence of a bulk horizon. It would be interesting to clarify this and also check the identification of the state by computing in the CFT the expectation value of the stress energy tensor in this state and see if the results agree with our bulk computation.

We can suggest some possibilities for the resolution of this apparent paradox. Note

that all wormholes can be viewed as quotients of an open domain of BTZ, since the group Γ associated with them always contains a subgroup isomorphic to that of BTZ (namely \mathbb{Z}) and so one can take the quotient first with respect to this group, resulting in BTZ, and then with respect to the rest of the group elements (modulo issues related to the regions one needs to remove to avoid closed timelike curves that need to be investigated). Thus we find a state in the tensor product of two Hilbert spaces (associated with the two boundaries of BTZ) with certain correlations between the two components because of the final quotient. It would be interesting to make this more precise and understand whether it contains a certain entanglement which would result in an effective entropy when restricting to a subsystem.

One of the main reasons that black hole entropy has been so puzzling is that classically black holes appear to be unique (they have “no hair”) so their phase space is zero dimensional. In a typical quantum system the correspondence principle relates the quantum states to the classical phase space and the entropy of the system to the volume of phase space in Planck units. Thus since the phase space for black holes appears to be zero dimensional, they should not carry any entropy. As was discussed earlier, however, the outer region of the wormholes is isometric to the BTZ black hole. Thus one can view the ‘wormhole’ spacetimes with a single outer region as ‘BTZ hair’, where the ‘hair’ is essentially the non-trivial topology hidden behind the horizon. It is thus natural to ask whether this classical phase space can account for the entropy of the BTZ black hole upon quantization. In other words, these spacetimes would then be the semi-classical approximation of the underlying black hole microstates. This is similar in spirit to the fuzzball proposal (whose relation to holography was discussed extensively in the review [102]) although here the geometries counted contain horizons and singularities.

Let us outline how one would do such a computation, see also [103]. We have seen that these spacetimes are uniquely specified by a Riemann surface with one boundary and the mass of the BTZ black hole is determined by one of the moduli of the Riemann surface. Thus the classical phase space is the moduli space of Riemann surfaces of arbitrary genus with a single fixed modulus, corresponding to the length of the horizon (in other words the BTZ mass parameter), which is the only parameter accessible to an observer outside of the horizon. More precisely, if one uses the Fenchel-Nielsen coordinates on the Teichmüller space (described in detail in section 6.2) it becomes explicit that the restriction to a fixed BTZ mass amounts to considering a codimension one hypersurface in Teichmüller space. This hypersurface is invariant under the mapping class group and therefore directly descends to the moduli space. The complete phase space is then the union of these hypersurfaces for different genera. Classically, the volume of this phase space is infinite and one should proceed by geometric quantization. One can readily

compute the symplectic form on the covariant space following [104, 105, 106] and proceed to quantize. It would be interesting to carry out this computation. The explicit form of the metric derived in the next chapter may facilitate this.

5.A Eternal black holes and filled tori

In this appendix we discuss the genus 1 handlebodies. We show that the ‘ $SL(2, \mathbb{Z})$ family’ of black holes cannot be used in the real-time gauge/gravity prescription as the bulk filling of a vertical segment of the QFT contour because the matching conditions lead to a complex Lorentzian metric (and therefore $\langle T_{ij} \rangle$ does not satisfy the correct reality conditions, either).

Consider a Euclidean field theory on a torus with modular parameter $\tau = \tau_1 + i\tau_2$. Without loss of generality we can pick the circle given by $z \sim z + 1$ as the spatial circle along which we will cut open the Euclidean path integral and glue the Lorentzian solutions. More precisely, we will glue two Lorentzian cylinders to the lines $y = 0$ and $y = \tau_2/2$, where $z = x + iy$. As we discussed in section 3.5, τ_1 is then i times the angular momentum chemical potential, but since we are not interested in rotating black holes here we will set τ_1 to zero throughout this appendix (it is straightforward to generalize to $\tau_1 \neq 0$), so $\tau = i\tau_2$ is purely imaginary.

The torus so defined admits multiple bulk fillings, which are given by the specification of a contractible cycle $z \sim z + a\tau + b$ with (a, b) two relatively prime integers. For each of these fillings, one may obtain a complete Euclidean metric which is locally H^3 . After cutting the torus in half, we will glue a Lorentzian bulk solution to the bulk hypersurface ending on the lines $y = 0$ and $y = \tau_2/2$. This hypersurface has the shape of an annulus, except when $(a, b) = (0, 1)$, when it consists of two disks. In this case the matching Lorentzian solution is two segments of thermal AdS. Notice also that for $(a, b) = (1, 0)$ we obtain the rotating BTZ black hole. To find the matching Lorentzian solutions in the general case, we will first explicitly write down the Euclidean bulk metric. We then investigate how the Lorentzian metric is determined by the matching conditions.

Euclidean geometries

Let us give a brief review of the possible fillings of the torus. We will again use the Poincaré coordinates (τ, x, y) defined in (5.21) on H^3 , as well as the complex coordinate $w = x + i\tau$ on the boundary of H^3 . (Notice that the τ here is a coordinate and not the modular parameter of the torus. We henceforth exclusively use the coordinate w so no confusion should arise.) Any torus handlebody can be obtained as a quotient of H^3 by a cyclic group of identifications generated in

Poincaré coordinates by:

$$(w, y) \sim (e^{2\pi i\beta} w, |e^{2\pi i\beta}| y), \quad (5.70)$$

with $\beta = \beta_1 + i\beta_2$ a complex number.

Let us now compute the bulk metric when we use the complex boundary coordinate z which has the natural periodicity $z \sim z + 1 \sim z + \tau$. We can do so using the map J of section 5.4. In this case, J is a locally biholomorphic map from \mathbb{C} rather than H , since the universal covering of the torus is \mathbb{C} and not H . If the contractible cycle is given by (a, b) , the corresponding map $J : \mathbb{C} \rightarrow S^2$ is given by:

$$J : z \mapsto w = e^{\alpha z}, \quad (5.71)$$

with $\alpha = 2\pi i(a\tau + b)^{-1}$. The identifications $z \sim z + 1 \sim z + \tau$ become

$$w \sim we^{\alpha} \sim we^{\alpha\tau} \quad (5.72)$$

which implies

$$w \sim e^{\alpha(c\tau + d)} w. \quad (5.73)$$

Now, since one trivially has that $w \sim e^{\alpha(a\tau + b)} w$, it follows that the single identification (5.73) is equivalent to both identifications in (5.72) provided $ad - bc = 1$. Comparing (5.73) with (5.70), we then read off that

$$\beta = \frac{c\tau + d}{a\tau + b}. \quad (5.74)$$

Following the same steps as in section 5.4, we find that the bulk metric in the z coordinate becomes

$$ds^2 = \frac{d\rho^2}{\rho^2} + \frac{1}{\rho^2} |dz + \frac{\bar{\alpha}^2 \rho^2}{4} d\bar{z}|^2. \quad (5.75)$$

This metric is of the Fefferman-Graham form (5.28). It is valid for $\rho^4 < \alpha^2 \bar{\alpha}^2 / 16$. From (5.29) we can read off that the one-point function of the stress energy tensor is given by:

$$\langle T_{zz} \rangle = \frac{\alpha^2}{2}, \quad (5.76)$$

which is again $-S[J]$, just as we found for the higher genus handlebodies in section 5.4.

Lorentzian geometry

Let us now consider the continuation to the Lorentzian geometry. On the boundary we cut open the Euclidean geometry along the circles given by $y = 0$ and $y = \tau_2/2$. In every case except thermal AdS these circles are the boundary of a single

annular region in the bulk manifold. Locally the unique solution is simply given by analytic continuation. Using the boundary lightcone coordinates (u, v) , we find the Lorentzian metric,

$$ds^2 = \frac{d\rho^2}{\rho^2} + \frac{1}{\rho^2} \left(du + \frac{\bar{\alpha}^2}{4} \rho^2 dv \right) \left(dv + \frac{\alpha^2}{4} \rho^2 du \right). \quad (5.77)$$

The periodicity for the boundary coordinates is $(u, v) \sim (u + 1, v + 1)$, and (u, v) are real whereas ρ has the same range as above. This metric is however *complex* unless α^2 is real, which only happens if either $a = 0$ or $b = 0$. This is problematic both from the bulk and the holographic perspective. In particular, the expectation value of the dual stress energy tensor can again be computed using (5.29),

$$\langle T_{uu} \rangle = \frac{1}{2} \alpha^2, \quad \langle T_{vv} \rangle = \frac{1}{2} \bar{\alpha}^2, \quad (5.78)$$

and is complex, which cannot be the case for a hermitian operator.

Chapter 6

Coordinate systems for wormholes

In all of the previous literature as well as in the previous chapter the wormhole spacetimes of [76, 77] are described abstractly as quotients of a part of AdS_3 . While this presents no loss of information, this description is abstract and requires mastering prerequisite mathematical background in order to understand the properties of these spacetimes. One should contrast this with the case of the BTZ black hole [107, 86] where one has an explicit metric containing the physical parameters (the mass and angular momentum). The BTZ black hole also has an abstract representation as a quotient of AdS_3 but this has not been used as much as the explicit metric description. With the hope that a more concrete description of the wormholes would make them more readily accessible we derive in this chapter such an explicit description where all parameters that determine the spacetime appear explicitly in the metric.

6.1 Introduction and summary of results

We will see below how the wormholes can be described using a set of intuitive coordinate charts which taken together completely cover the spacetime. Each chart has the topology of a spacelike cylinder times a ‘time’ coordinate. The coordinate systems are chosen in such a way that coordinate ranges are natural and the structure of the spacetime appears explicitly in the metric. More precisely, we mentioned that a wormhole spacetime based on a Riemann surface of genus g

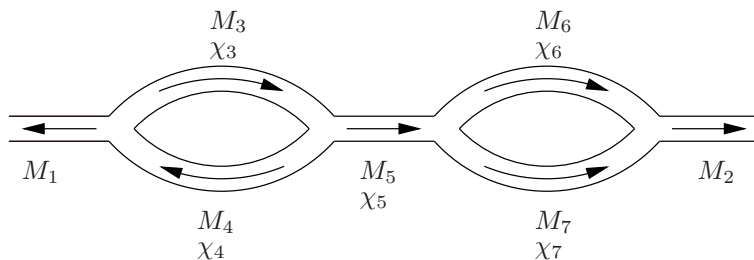


Figure 6.1: A fatgraph representing the wormhole spacetime sketched in figure 5.1.

with m circular boundaries is completely specified by $6g - 6 + 3m$ parameters and we will see below that all these parameters explicitly appear in the metric on the various charts.

The complete description of the spacetime can be summarized in an oriented trivalent fatgraph like the one in figure 6.1. This graph should have m outer edges (ends) and $3g - 3 + m$ inner edges. With every outer edge we associate one parameter M_k and with every inner edge two parameters M_i, χ_i , where $k=1, \dots, m$ and $i=m+1, \dots, 3g-3+2m$. This yields a total of $6g - 6 + 3m$ parameters, which is indeed the correct number of moduli¹. We now associate a coordinate chart to every edge of the fatgraph and every such chart has a canonical metric on it. The precise definition of the coordinate charts as well as the meaning of the orientation is given below. To complete the description we need to specify the transition functions in the overlap regions and these are also given below.

Thus, the spacetime is described by the graph and two different metrics, one for the outer charts and one for the inner charts. The metric in the k th outer chart takes the form:

$$ds_k^2 = \frac{\rho^2 + M_k}{\cosh^2(\sqrt{M_k}\tilde{\tau})} (-d\tilde{\tau}^2 + d\varphi^2) + \frac{d\rho^2}{\rho^2 + M_k}. \quad (6.1)$$

The corresponding $(\tilde{\tau}, \rho, \varphi)$ coordinate system has coordinate ranges,

$$\tilde{\tau} \in \mathbb{R}, \quad \varphi \sim \varphi + 2\pi, \quad \frac{\cosh(\sqrt{M_k}\tilde{\tau})\rho}{\sqrt{\rho^2 + M_k}} > Z_k, \quad (6.2)$$

where Z_k is defined explicitly in equation (6.88) below. These coordinates extend beyond the future and past horizons, which lie at

$$\rho = \sqrt{M_k} |\sinh(\sqrt{M_k}\tilde{\tau})|. \quad (6.3)$$

¹As we review in section 6.2, the parameters $\{M_I, \chi_i\}$ ($I = k, i$) are directly related to the Fenchel-Nielsen coordinates of the moduli space of the Riemann surface.

As discussed in section 5.2, if we restrict ourselves to the region outside of the horizons we may also put the metric in the static BTZ form,

$$ds_k^2 = -(r^2 - M_k)dt^2 + \frac{dr^2}{r^2 - M_k} + r^2 d\phi^2, \quad (6.4)$$

with coordinate ranges, $r > M_k$, $t \in \mathbb{R}$ and $\phi \sim \phi + 2\pi$. In these metrics M_k is the parameter of the corresponding outer edge. The metric in the i th inner chart is given by

$$ds_i^2 = \frac{1}{\cosh^2(t)} \left(-dt^2 + \frac{\mu_i^2 dr^2}{(\mu_i r + \nu_i)^2 + \cos^2(\chi_i)} + M_i(1 + (\mu_i r + \nu_i)^2) d\psi^2 - \frac{2\mu_i \sqrt{M_i} \sin(\chi_i)}{\sqrt{(\mu_i r + \nu_i)^2 + \cos^2(\chi_i)}} d\psi dr \right), \quad (6.5)$$

with coordinate ranges, $r \in [-1, 1]$, $\tau \in \mathbb{R}$ and $\psi \sim \psi + 2\pi$. This is a time-dependent metric of constant negative curvature which (as far as we know) has not appeared before in the literature. The parameters M_i and χ_i are the parameters associated with the i th inner edge. The parameters μ_i, ν_i on the other hand are functions of the M parameters, see the discussion in section 6.6.2. Note that both metrics (6.1) and (6.5) have an explicit $U(1)$ isometry, the transition functions however do not respect this symmetry and the entire spacetimes is not $U(1)$ symmetric.

The remainder of this chapter is structured as follows. In section 6.2 we review the Fenchel-Nielsen coordinates on the Teichmüller space of Riemann surfaces. We then define in section 6.3 the upper half plane H as a surface in three-dimensional Minkowski space and express some hyperbolic geometry results in this parametrization. Afterwards we consider the explicit construction of a building block of a Riemann surface, a so-called ‘pair of pants’, in section 6.4. In section 6.5 we define the domains on which the charts are defined and we prove that they cover the spacetime entirely. Finally in section 6.6 we introduce the definition of the coordinate systems and the related fatgraph description. We will also compute the coordinate ranges, the metric and the transition functions.

6.2 Fenchel-Nielsen coordinates

In this section we review the definition of the Fenchel-Nielsen coordinates on the Teichmüller space of Riemann surfaces of genus g with $m > 0$ circular boundaries (and no punctures). As we discussed in section 5.2, all such Riemann surfaces are quotients of the upper half plane, from which they all inherit a canonical metric of constant negative curvature.

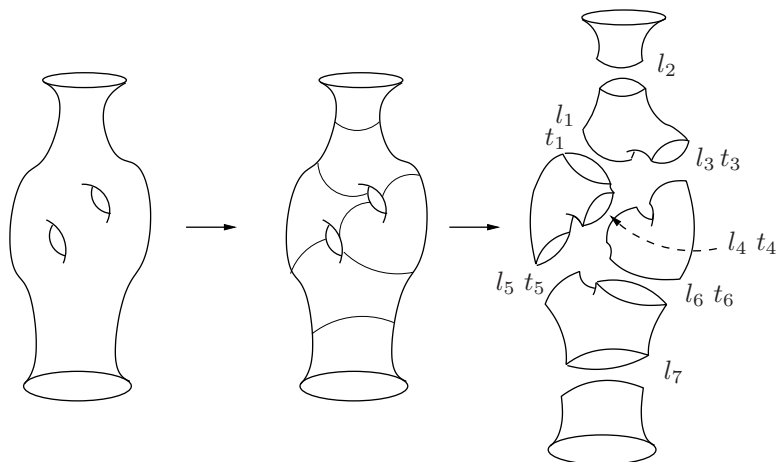


Figure 6.2: Defining Fenchel-Nielsen coordinates on a Riemann surface. We cut the Riemann surface into pairs of pants along simple closed geodesics and assign lengths l_i to all the edges of every pants plus a twisting parameter t_j for every gluing involving two pairs of pants.

It can be shown that in this metric there is precisely one smooth periodic geodesic corresponding to every nontrivial primitive loop on the surface. After a little counting one finds that one can pick a maximum of $3g - 3 + 2m$ of such periodic geodesics that do not intersect each other, see figure 6.2 for an example. We then *cut* the Riemann surface along these geodesics, *i.e.* we remove these geodesics from the surface. This leaves us with $2g - 2 + m$ disconnected so-called ‘pairs of pants’, that is Riemann surfaces of genus 0 with three circular boundary components, as well as m annuli. The annuli correspond to the regions on the Riemann surface between a periodic geodesic that is retractable into a boundary component and the boundary component itself.

The Fenchel-Nielsen coordinates are now based on the idea that we can reconstruct the complete Riemann surface from this collection of pairs of pants and annuli, provided we also specify how to glue these ‘building blocks’ together. Therefore, we can define coordinates on the Teichmüller space of Riemann surfaces of the given type by specifying enough data to first of all construct the pairs of pants and annuli that make up the original surface, plus some rules on how to glue them together.

Let us begin with the description of the individual pairs of pants and annuli. Using hyperbolic geometry we explain in section 6.4 how the pairs of pants are completely described by only three real moduli which one may take to be the strictly positive lengths of the periodic geodesics along which we made the cuts.

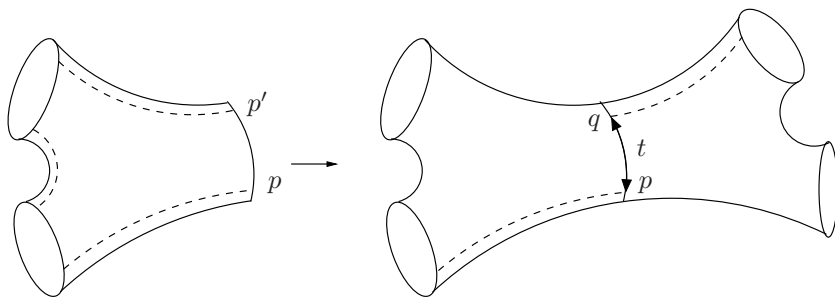


Figure 6.3: The twist parameter t is defined by the angle between two points p and q that lie at the intersection of the dashed geodesics with a boundary circle.

A similar statement is true for the annuli: these are completely specified by giving the length of the periodic geodesic as well. Since we cut along $3g - 3 + 2m$ periodic geodesics, we find that we can reconstruct the individual pairs of pants and annuli by the specification of precisely $3g - 3 + 2m$ strictly positive lengths.

Next, we have to specify the way in which the various components are glued together. More specifically, we have to specify the angle that the various components have to be twisted with before we perform the gluing. Notice that these angles are actually only relevant when we glue two pairs of pants together, since twisting an annulus is an isometry. The angles are defined as follows, see figure 6.3. On every pair of pants we may define three distinguished geodesics, namely the shortest non-intersecting geodesics that run from one boundary circle to another. A given boundary circle of the pants intersects with two of these geodesics, say at the points p and p' . (Figure 6.3 is drawn slightly distorted since these points actually lie diametrically opposite of each other. This follows from a reflection isometry of the pair of pants whose fixed points are precisely the three geodesics we just defined.) Following the same reasoning on the other pair of pants we find two more points, say q and q' , on this boundary circle. The twist parameter describing the gluing is now precisely the angle between, say, p and q on the boundary circle.²

Since we cut along $3g - 3 + 2m$ geodesics, we have as many gluings to perform. For precisely m of these we glue annuli to pairs of pants, which leaves us with $3g - 3 + m$ gluings between pairs of pants for which we need to specify an angle. Adding these to the $3g - 3 + 2m$ lengths precisely gives the required number of $6g - 6 + 3m$ parameters. Indeed, it can be shown that these lengths and angles provide good coordinates that cover the Teichmüller space of Riemann surfaces of

²A shift of 2π in the angles corresponds to an element of the mapping class group and therefore to two different points in Teichmüller space. Strictly speaking, therefore, these angles take values in \mathbb{R} in order to properly parametrize the Teichmüller space. We will be rather loose in this distinction.

the given type, which is therefore isomorphic to $(\mathbb{R}^+)^{3g-3+2m} \times \mathbb{R}^{3g-3+m}$. This is then the Fenchel-Nielsen description of the Teichmüller space.

6.3 The hyperbolic plane

This section gives a brief introduction to the geometry of the hyperbolic plane H . We present a number of results in hyperbolic geometry that will be used extensively in the next sections. We refer to [108] for the derivation of the results that are stated without proof below.

We will describe the hyperbolic plane H as the $U = 0$ slice of the AdS_3 hyperboloid given in equation (5.6). We therefore consider three-dimensional Minkowski space M^3 with coordinates (X, Y, V) and with an inner product between vectors $a = (a_X, a_Y, a_V)$ and $b = (b_X, b_Y, b_V)$ given as:

$$\langle a|b \rangle \equiv a_X b_X + a_Y b_Y - a_V b_V. \quad (6.6)$$

We define hyperbolic two-space H as the upper sheet of a hyperboloid:

$$H = \{w \in M^3 : \langle w|w \rangle = -1 \wedge w_z > 0\}. \quad (6.7)$$

As we described in section 5.2, the restriction of the Poincaré coordinates (5.11) on AdS_3 to this slice precisely maps it to the upper half plane with the metric (5.4).

We may also project H bijectively onto the unit disk Δ , defined as

$$\Delta = \{z \in \mathbb{C} : |z| < 1\}, \quad (6.8)$$

with the metric

$$ds^2 = \frac{dzd\bar{z}}{4(1 - |z|^2)^2}. \quad (6.9)$$

The map between H and Δ is stereographic projection through $(-1, 0, 0)$ onto the (X, Y) plane:

$$(X, Y, V) \mapsto \frac{X + iY}{V + 1} = z. \quad (6.10)$$

Most of the computations below will be performed using the embedding (6.7) of H into Minkowski space. The figures on the other hand will be based on the unit disk or upper half plane description.

Distances

The distance $d(w_1, w_2)$ obtained from the metric on H between two points $w_1, w_2 \in H$ is given by:

$$\cosh(d(w_1, w_2)) = -\langle w_1 | w_2 \rangle, \quad (6.11)$$

where indeed $-\langle w_1 | w_2 \rangle \geq 1$ on H .

Rays

Given a point p with $\langle p | p \rangle > 0$, we define the associated *spacelike ray* $[p]$ as the line from the origin through p :

$$[p] = \{\lambda p : \lambda \in \mathbb{R}\}. \quad (6.12)$$

With this definition, the homogenized inner product between two spacelike rays is given by:

$$\langle [p_1] | [p_2] \rangle \equiv \frac{|\langle p_1 | p_2 \rangle|}{\sqrt{\langle p_1 | p_1 \rangle \langle p_2 | p_2 \rangle}}, \quad (6.13)$$

where the right hand side can be calculated for any nonzero $p_1 \in [p_1]$ and $p_2 \in [p_2]$. Below we often use a similar notation where a property of rays is given in terms of a formula involving its elements. In such cases the corresponding formulas are invariant under $p_1 \mapsto \mu p_1$.

We define $\hat{p} \in [p]$ to be a unit vector associated to $[p]$, so

$$\langle \hat{p} | \hat{p} \rangle = 1. \quad (6.14)$$

Given $[p]$ this defines \hat{p} only up to a sign which we leave undefined for now.

Geodesics

Geodesics in H are given by the intersection of the hyperboloid with a plane through the origin. Such a plane is necessarily timelike and thus orthogonal to a spacelike ray: given any ray $[p]$, the geodesic in H associated to it is defined as:

$$C[p] = \{w \in H : \langle w | p \rangle = 0\}. \quad (6.15)$$

Both in the unit disk and in the upper half plane geodesics are circular arcs or straight lines whose endpoints are at a right angle with respect to the boundary of the plane. Examples of such geodesics are sketched in figure 6.4. We will need two lemma's concerning geodesics in H .

Lemma 6.3.1. *$C[p_1]$ and $C[p_2]$ are disjoint geodesics in H with disjoint endpoints if and only if $\langle [p_1] | [p_2] \rangle > 1$.*

Proof. Consider the line of intersection of the planes associated to $C[p_1]$ and $C[p_2]$. This line, which we call $[p_{12}]$, is spacelike if and only if the two geodesics are disjoint in H : if not so, then a $p_{12} \in [p_{12}]$ would lie in H or on its boundary and then the geodesics $C[p_1]$ and $C[p_2]$ would meet exactly at that point. So we need to verify that $[p_{12}]$, defined as:

$$\langle p_{12}|p_1 \rangle = \langle p_{12}|p_2 \rangle = 0 \quad (6.16)$$

is spacelike. Equation (6.16) solves to:

$$p_{12} \in \left[(p_{1y}p_{2z} - p_{1z}p_{2y}, p_{1x}p_{2z} - p_{1z}p_{2x}, -p_{1x}p_{2y} + p_{1y}p_{2x}) \right] \quad (6.17)$$

and one can use the invariance of the inner product under conjugation so that we can pick for example $p_1 = (1, 0, 0)$ and check directly that:

$$0 < \langle p_{12}|p_{12} \rangle \Leftrightarrow \langle [p_1]|[p_2] \rangle > 1 \quad (6.18)$$

provided p_2 is spacelike but this was part of the assumption. \square

Now, given any two completely disjoint geodesics $C[p_1]$ and $C[p_2]$, there exists a unique geodesic orthogonal to both of them, which from (6.16) is exactly $C[p_{12}]$. A straightforward calculation then shows that:

$$\cosh(D(C[p_1], C[p_2])) = \langle [p_1]|[p_2] \rangle \quad (6.19)$$

where D is the minimal distance in H between the two geodesics, so the distance measured along $C[p_{12}]$. Note finally that \hat{p}_1 and \hat{p}_2 both lie in and in fact form a basis for the plane associated to $C[p_{12}]$ (i.e. the plane orthogonal to $[p_{12}]$).

Consider now three geodesics in H . By definition, a *separating* geodesic divides H so that the other two geodesics lie on the opposite halves.

Lemma 6.3.2. *Suppose $C[p_1]$, $C[p_2]$ and $C[p_3]$ represent three non-separating geodesics in H that are disjoint and have disjoint endpoints. Then*

$$\langle p_1|p_2 \rangle \langle p_1|p_3 \rangle \langle p_2|p_3 \rangle < 0. \quad (6.20)$$

Proof. Another way of seeing non-separability is that for example the geodesic $C[p_{12}]$, joining $C[p_1]$ and $C[p_2]$, does not intersect $C[p_3]$. Translated into the same condition as in lemma 6.3.1, namely that the corresponding planes in M^3 intersect along a spacelike ray, this becomes:

$$\langle p_1|p_3 \rangle^2 + \langle p_2|p_3 \rangle^2 - 2\langle p_1|p_2 \rangle \langle p_1|p_3 \rangle \langle p_2|p_3 \rangle > 0 \quad (6.21)$$

and similar for cyclic permutations of the indices. Recalling the invariance under $p_i \mapsto \mu_i p_i$, we choose $p_i = \hat{p}_i$ and introduce new variables:

$$h_{12} \equiv \frac{\langle \hat{p}_1 | \hat{p}_3 \rangle \langle \hat{p}_2 | \hat{p}_3 \rangle}{\langle \hat{p}_1 | \hat{p}_2 \rangle}, \quad (6.22)$$

and similarly h_{13} and h_{23} . Now suppose that $\langle p_1 | p_2 \rangle \langle p_1 | p_3 \rangle \langle p_2 | p_3 \rangle > 0$. Since the sign of all h_{ij} is the same as that of $\langle p_1 | p_2 \rangle \langle p_1 | p_3 \rangle \langle p_2 | p_3 \rangle$, this means that all $h_{ij} > 0$ as well, and we can rewrite (6.21) as:

$$h_{13} + h_{23} - 2h_{13}h_{23} > 0, \quad (6.23)$$

but lemma 6.3.1 tells us that $\langle \hat{p}_i | \hat{p}_j \rangle^2 > 1$, translating into for example:

$$h_{13}h_{23} > 1 \quad (6.24)$$

and therefore either $h_{13} > 1$ or $h_{23} > 1$. Let us suppose, relabeling if necessary, that $h_{13} > 1$. Rewriting (6.23), however, as:

$$(1 - h_{23})h_{13} + (1 - h_{13})h_{23} > 0, \quad (6.25)$$

one deduces that then $h_{23} < 1$ and similarly (by permuting the indices) one obtains that $h_{12} < 1$. This falsifies $h_{12}h_{23} > 1$, which follows from a permutation of the indices of (6.24), so our assumption is false: we have $h_{ij} < 0$ and so $\langle p_1 | p_2 \rangle \langle p_1 | p_3 \rangle \langle p_2 | p_3 \rangle < 0$ necessarily. \square

Hypercycles

Finally we need the notion of *hypercycles*. These are defined as:

$$L(p) = \{w \in H : \langle w | p \rangle = -1\}, \quad (6.26)$$

for a point p with $\langle p | p \rangle > 0$. There is a natural map from hypercycles to geodesics: $L(p) \mapsto C[p]$. On the disk, this maps a hypercycle to the geodesic that has the same endpoints as the hypercycle. Some hypercycles and their associated geodesic are drawn in figure 6.4. Notice that hypercycles are also straight lines or circular arcs in the upper half plane or the unit disk, but they do not intersect the boundary at a right angle.

The distance $D(L(p), C[p])$ between any point on $L(p)$ and $C[p]$ is constant and given by

$$\sinh^2 (D(L(p), C[p])) = \frac{1}{\langle p | p \rangle} \quad (6.27)$$

as can be easily seen after conjugation so that for example $p = (\lambda, 0, 0)$.

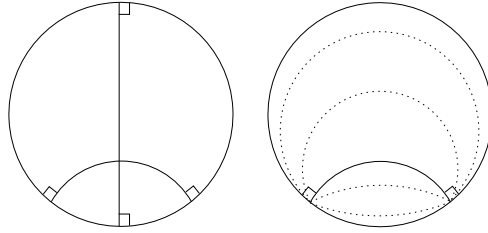


Figure 6.4: On the left, two geodesics in the unit disk. They are straight lines or circle segments whose ends are orthogonal to the boundary of the disk. On the right, four hypercycles (dotted) with their associated geodesic. In the hyperbolic metric, the distance between points on a hypercycle and the associated geodesic is constant.

Isometries

The connected component of the identity of the isometry group of H is the same as that of the subgroup of the isometries of M^3 that fixes the origin, which is $SO(2, 1) \simeq PSL(2, \mathbb{R})$. We explained in section 5.2 how it acts via Möbius transformations in the upper half plane description, see equation (5.3). In this chapter we need its action in the hyperboloid description (6.7). To this end we use the result [108] that every such an isometry is generated by two reflections in timelike planes through the origin in M^3 , so via reflections in geodesics in H . Given a geodesic $C[p]$, a reflection is defined as:

$$\eta_{[p]} : w \mapsto w - 2\hat{p}\langle w|\hat{p}\rangle \quad (6.28)$$

Both the embedding of H and the inner product (6.6) are invariant under this orientation-reversing map, so the composition of two reflections is an orientation-preserving isometry of H and:

$$\eta_{[p]} \circ \eta_{[p']} : H \rightarrow H \quad (6.29)$$

is an element of $\text{Isom}_0(H)$. Note the invariance $\hat{p} \leftrightarrow -\hat{p}$ in the definition of $\eta_{[p]}$ and also that $\eta_{[p]}$ leaves $C[p]$ pointwise fixed.

We will only use the *hyperbolic* elements of $\text{Isom}_0(H)$, which are by definition those isometries that have exactly two fixed points on the boundary of H . Consider such an isometry and call it γ . The unique geodesic in H connecting its fixed points is called the ‘axis’ of γ and is left invariant by this particular isometry. So if we denote the axis by $C[p]_\gamma$, then

$$\gamma(C[p]_\gamma) = C[p]_\gamma. \quad (6.30)$$

Since γ is an isometry and hence preserves distances, it follows that γ also leaves

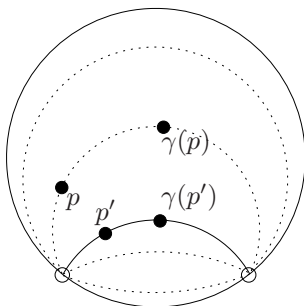


Figure 6.5: An isometry γ maps points along the flow lines from one fixed point towards the other. In this figure, the fixed points are the open circles. Two points p, p' and their image under γ are also drawn.

the corresponding hypercycles invariant and therefore

$$\gamma(L(p)) = L(p), \quad (6.31)$$

for all $p \in [p]_\gamma$, so for every hypercycle with the same endpoints as $C[p]$. This allows us to visualize the action of γ in H : repeated application of γ moves points along the hypercycles, more and more away from one fixed point and towards the other. That is why the fixed points are also called the ‘limit points’ of γ and the hypercycles its ‘flow lines’. Notice that γ is not uniquely specified by its invariant geodesic, since the distance with which γ moves points along the flow lines can vary. Also, note that γ^n , $n \in \mathbb{Z}$, so in particular γ^{-1} , have the same axis and flow lines as γ .

6.4 Construction of a pair of pants

In section 6.2 we reviewed how the Riemann surfaces relevant for the wormhole spacetimes can be constructed by gluing together ‘pairs of pants’, which are by definition Riemann surfaces with $g = 0$ and $m = 3$. In this section we review how such a pair of pants can be constructed as a quotient of H . We refer to [83] for more details.

Before we describe the explicit construction the following comment is in order. The pairs of pants used in the Fenchel-Nielsen decomposition of section 6.2 were bounded by a periodic geodesic and we glued semi-infinite annuli to the m ends that extended to a boundary of the complete Riemann surface. In this section we will actually describe ‘extended’ pairs of pants where such annuli are glued to all three boundary components. We will however also explicitly find the location

of the three periodic geodesics that are retractable into these three ends. It is therefore straightforward to remove these annuli and obtain an ‘amputated’ pair of pants which is used as a building block in the Fenchel-Nielsen decomposition of a more general Riemann surface.

6.4.1 Construction procedure

We mentioned in section 6.2 that a pair of pants is completely specified by the lengths of the three periodic geodesics homotopic to the three boundary components. For later convenience let us label these lengths as l_{12} , l_{13} and l_{23} . Given those lengths we construct a pair of pants using the following procedure, see figure 6.6.

We first specify an arbitrary geodesic $C[p_1]$, for example with $\hat{p}_1 = (1, 0, 0)$. Next, we specify a second geodesic $C[p_2]$ which is disjoint from $C[p_1]$ and chosen such that the hyperbolic distance between $C[p_2]$ and $C[p_1]$ equals $l_{12}/2$. Using equation (6.19) we find that this translates into the following condition for $[p_2]$:

$$\langle [p_1] | [p_2] \rangle = \cosh(l_{12}/2). \quad (6.32)$$

This equation determines $[p_2]$ only partially and its remainder can be fixed arbitrarily. In the example where $p_1 = (1, 0, 0)$ we can for example take $p_2 = (\cosh(l_{12}/2), 0, \sinh(l_{12}/2))$.

We then construct a third geodesic $C[p_3]$ which is at a distance $l_{13}/2$ from $C[p_1]$ and at a distance $l_{23}/2$ from $C[p_2]$. It should furthermore be defined so that none of the geodesics is separating and the three geodesics are ordered cyclically on the disk. These demands completely fix $C[p_3]$. In the example $[p_3]$ would be:

$$[p_3] = \left[(c_{13} \sinh(l_{12}/2), \sqrt{c_{12}^2 + c_{13}^2 + c_{23}^2 + 2c_{12}c_{13}c_{23} - 1}, c_{23} + c_{12}c_{13}) \right] \quad (6.33)$$

where we defined $c_{ij} = \cosh(l_{ij}/2)$.

The covering group Γ_P for the pair of pants is now generated by $\eta_{[1]} \circ \eta_{[2]}$ and $\eta_{[3]} \circ \eta_{[1]}$ with $\eta_{[i]}$ denoting reflection in $C[p_i]$. The pair of pants P is therefore defined as:

$$P = H/\Gamma_P. \quad (6.34)$$

Notice that P is indeed completely specified by the three lengths l_{ij} .

To visualize this quotient we may construct a fundamental domain for P in H . This is done by reflecting $C[p_3]$ and $C[p_2]$ in $C[p_1]$ using $\eta_{[1]}$, which using (6.28) is defined as:

$$\eta_{[1]} : w \mapsto w - 2\hat{p}_1 \langle w | \hat{p}_1 \rangle. \quad (6.35)$$

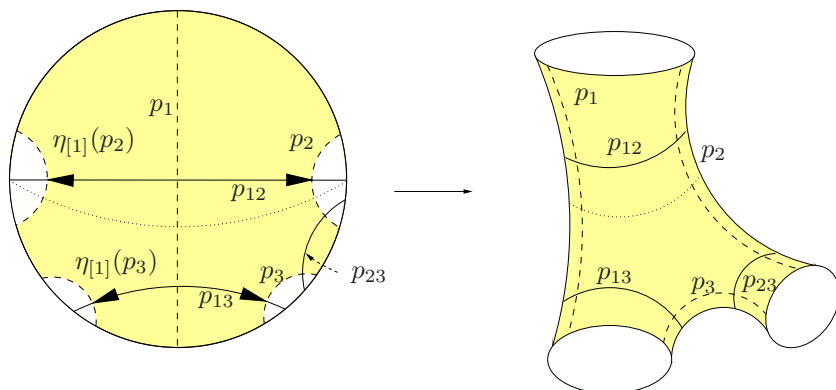


Figure 6.6: The fundamental domain for the complete pair of pants is shaded; each geodesic is indicated by a corresponding vector. Opposite edges of the domain are to be identified as prescribed by the arrows, yielding the pair of pants shown on the right. The dotted line is a hypercycle associated to the geodesic $C[p_{12}]$ and a flow line of $\eta_{[1]} \circ \eta_{[2]}$. It descends to a smooth closed curved on the pair of pants.

The domain bounded by $C[p_2]$, $C[p_3]$ and their reflected counterparts is then a fundamental domain for P since one may obtain P by gluing the appropriate edges together, see figure 6.6. In this figure the top arrows correspond to the generator $\eta_{[1]} \circ \eta_{[2]}$ and the bottom arrows correspond to $\eta_{[3]} \circ \eta_{[1]}$.

Let us denote the geodesic orthogonal to both $C[p_1]$ and $C[p_2]$ as $C[p_{12}]$. We similarly define $C[p_{13}]$ and $C[p_{23}]$. From direct computation it follows that $\eta_{[i]} \circ \eta_{[j]}$ maps $[p_{ij}]$ to itself and therefore $C[p_{ij}]$ is the axis of $\eta_{[i]} \circ \eta_{[j]}$. We sketched in figure 6.6 how the $C[p_{ij}]$ then descend to P as the periodic geodesics retractable into the boundary components of the pants. Their lengths on P are precisely the lengths l_{ij} from which P is constructed. To obtain an amputated pair of pants we have to cut off the surface along these geodesics. Notice furthermore that the geodesics $C[p_i]$ are precisely the shortest non-intersecting geodesics between the $C[p_{ij}]$ which we used in section 6.2 to define the Fenchel-Nielsen twist parameter. Finally, $\eta_{[1]}$ is the discrete isometry of P discussed in section 6.2 which leaves the $C[p_i]$ pointwise fixed.

Below we will need two more properties of the above construction. First of all, using the disjointness of the $C[p_i]$ and a hyperbolic triangle inequality one may directly find that $C[p_{12}]$ and $C[p_3]$ are disjoint and therefore, according to lemma 6.3.1,

$$\langle [p_{12}] | [p_3] \rangle > 1. \quad (6.36)$$

Similarly one obtains $\langle [p_{13}] | [p_3] \rangle > 1$ and $\langle [p_{23}] | [p_1] \rangle > 1$. Our second observation is based on the fact that for example p_1 and p_2 are both spacelike but not collinear

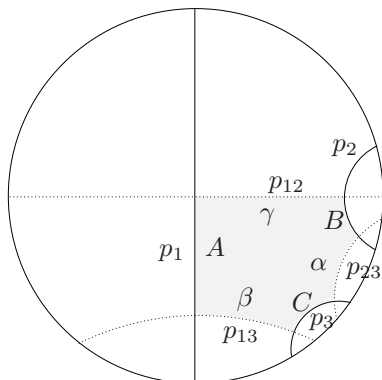


Figure 6.7: Each of the letters $\alpha, \beta, \gamma, A, B, C$ indicates a length of one side of the shaded hyperbolic hexagon.

and therefore span a two-dimensional plane in M^3 . Since p_{12} is orthogonal to this plane and therefore does not lie in the plane (because it is not lightlike), the set $\{\hat{p}_1, \hat{p}_2, \hat{p}_{12}\}$ forms a basis for M^3 . A similar argument again holds for $\{\hat{p}_1, \hat{p}_3, \hat{p}_{13}\}$ and $\{\hat{p}_2, \hat{p}_3, \hat{p}_{23}\}$.

Hyperbolic identities

In the construction of a pair of pants we found six geodesics associated to the spacelike rays $[p_1], [p_2], [p_3]$ and $[p_{12}], [p_{13}], [p_{23}]$. Recall that for each ray $[p]$ we defined in equation (6.14) a unit norm vector \hat{p} which was defined up to an overall sign. Let us now define:

$$\begin{aligned}
 \cosh(A) &= -\langle \hat{p}_{12} | \hat{p}_{13} \rangle \\
 \cosh(B) &= -\langle \hat{p}_{12} | \hat{p}_{23} \rangle \\
 \cosh(C) &= -\langle \hat{p}_{13} | \hat{p}_{23} \rangle \\
 \cosh(\alpha) &= -\langle \hat{p}_2 | \hat{p}_3 \rangle \\
 \cosh(\beta) &= -\langle \hat{p}_1 | \hat{p}_3 \rangle \\
 \cosh(\gamma) &= -\langle \hat{p}_1 | \hat{p}_2 \rangle,
 \end{aligned} \tag{6.37}$$

and fix the signs of the \hat{p}_i and \hat{p}_{ij} such that all the above inner products are negative. (The overall freedom to invert all the \hat{p}_i or all \hat{p}_{ij} together will be fixed below.) The variables $A, B, C, \alpha, \beta, \gamma$ are then all real and we define them to be positive. As shown in figure 6.7 these variables all correspond to specific geodesic lengths associated to the above construction of the pair of pants. For example, we find that $\gamma = l_{12}/2$.

By definition the geodesics $C[p_i]$ and $C[p_{ij}]$ intersect each other orthogonally and

therefore they bound a hyperbolic hexagon with all right angles, see figure 6.7. The usual [108] identity for such a hyperbolic hexagon is:

$$\frac{\sinh(A)}{\sinh(\alpha)} = \frac{\sinh(B)}{\sinh(\beta)} = \frac{\sinh(C)}{\sinh(\gamma)}. \quad (6.38)$$

Furthermore we find:

$$\begin{aligned} -\langle \hat{p}_1 | \hat{p}_{23} \rangle &= \sinh(\beta) \sinh(C) = \sinh(B) \sinh(\gamma) \\ -\langle \hat{p}_2 | \hat{p}_{13} \rangle &= \sinh(\gamma) \sinh(A) = \sinh(C) \sinh(\alpha) \\ -\langle \hat{p}_3 | \hat{p}_{12} \rangle &= \sinh(\alpha) \sinh(B) = \sinh(A) \sinh(\beta). \end{aligned} \quad (6.39)$$

This follows from the identity for a hyperbolic all-right pentagon [108], at least up to an overall sign which we fix by using the freedom to invert all the \hat{p}_i we mentioned above. From the above equations one may directly obtain that:

$$\frac{\sinh^2(A)}{\sinh^2(\alpha)} = \frac{\sinh^2(B)}{\sinh^2(\beta)} = \frac{\sinh^2(C)}{\sinh^2(\gamma)} = \frac{\cosh^2(\alpha) + \cosh^2(\beta) + \cosh^2(\gamma) + 2 \cosh(\alpha) \cosh(\beta) \cosh(\gamma) - 1}{\sinh^2(\alpha) \sinh^2(\beta) \sinh^2(\gamma)}$$

and therefore:

$$\begin{aligned} \cosh(A) &= \frac{\cosh(\beta) \cosh(\gamma) + \cosh(\alpha)}{\sinh(\beta) \sinh(\gamma)} \\ \cosh(B) &= \frac{\cosh(\alpha) \cosh(\gamma) + \cosh(\beta)}{\sinh(\alpha) \sinh(\gamma)} \\ \cosh(C) &= \frac{\cosh(\alpha) \cosh(\beta) + \cosh(\gamma)}{\sinh(\alpha) \sinh(\beta)}. \end{aligned} \quad (6.40)$$

These formulas will be used below.

6.5 Domains for the charts

In this section we will define the domains on which we will later define the coordinate charts for the wormholes. To this end we will perform the following steps. We first restrict ourselves to the $U = 0$ Riemann surface $S = H/\Gamma$ and give an intuitive description of the domains in subsection 6.5.1. The location of the domains in H is discussed afterwards in subsection 6.5.2. We then make the definition mathematically precise in subsection 6.5.3 and also compute the precise location of the domains as a function of the Fenchel-Nielsen parameters. In subsection 6.5.4 we prove that the domains indeed cover S entirely. Finally, we consider the extension of the domains to the entire spacetime in subsection 6.5.5.

6.5.1 Definition of the domains

The procedure to obtain the charts for the wormholes is sketched schematically in figure 6.8 and it is described in words as follows. Just as in the Fenchel-Nielsen description of S described in section 6.2, we begin by picking a maximal set of $3g - 3 + 2m$ primitive periodic geodesics. We now consider one geodesic and ‘thicken’ it, *i.e.* we define a small cylindrical neighborhood around the geodesic. More precisely, this neighborhood is defined such that its boundary circles are the flow lines or hypercycles discussed in section 6.3; we showed the image of one of these flowlines on a pants P in figure 6.6. When we now try to extend this thickening ever further we might eventually wrap another cycle and the cylinder will then start to overlap with itself. We then stop the thickening when the boundary flow lines just touch themselves, as indicated in figure 6.8. In the cases where the periodic geodesic we consider is retractable into a boundary component we extend the thickening on that end all the way to this boundary. Except for the BTZ black hole, the other end of the cylinder is then never extendable to another boundary component and pinches as usual.

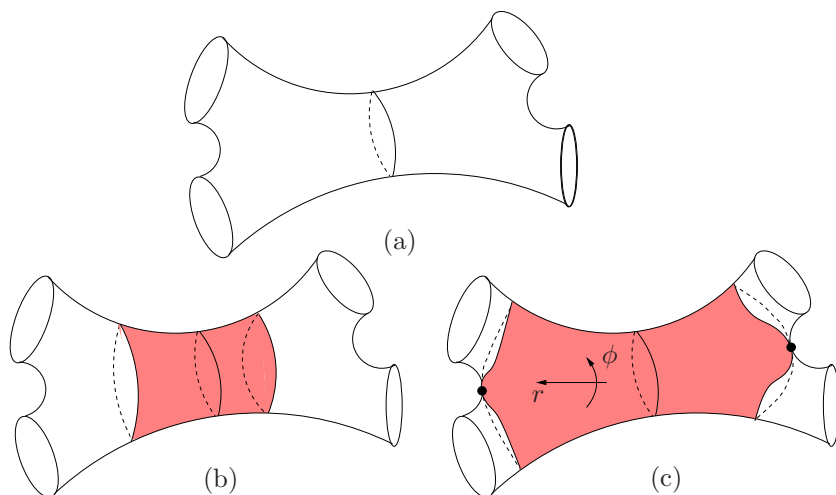


Figure 6.8: (a) Charts are defined around a closed periodic geodesic on the Riemann surface. (b) We begin by thickening this geodesic to obtain a cylinder. (c) We extend the cylinder as far as possible, until the bounding circles just touch, in this case on the black dots. We will eventually define coordinates (r, ϕ) as indicated, as well as a third time coordinate which is not shown.

Application of this procedure to all the $3g - 3 + 2m$ periodic geodesics on S results in a set consisting of just as many domains. These domains come in two different types, namely those where both boundary circles are pinched on S , which we

call ‘inner domains’, and those where precisely one end extends to a boundary component, which we call ‘outer domains’. An inner domain covers part of two pairs of pants, whereas an outer domain covers an annulus and part of a pair of pants. There are m outer domains and $3g - 3 + m$ inner domains.

We remark that the inner and outer domains we define here are not precisely the inner and outer regions we defined in the previous chapter. Namely, the inner and outer regions defined there were separated by the horizons, whereas the outer domains we define here do extend beyond the horizons. The inner domains that we define here never cross the horizons and therefore lie entirely in what we called the inner region in chapter 5.

Consider now a single pair of pants within S . It intersects with precisely three (inner or outer) domains which are defined around each of its boundary circles. Of course, the domains overlap with each other on the pants but more importantly we will show below that the *entire* pair of pants is covered by these three domains. Since the domains also cover the m annuli completely, it follows that the entire surface at $U = 0$ is covered by these domains. Below, we will use these domains as the $U = 0$ slice of analogously defined three-dimensional coordinate patches, which taken together cover the entire spacetime. We will then find a suitable coordinate system on these patches to complete our description of the wormholes.

6.5.2 Lift to the hyperbolic plane

In figure 6.9 we sketched the lift of the domains of figure 6.8 to the universal covering H . Let us label the periodic geodesic around which we define the chart as $C[p_{12}]$. Just as in figure 6.8 we suppose that on the complete surface S there is a pair of pants on either side of $C[p_{12}]$ and we therefore define an inner domain around it.

In figure 6.9a we give a fundamental domain for the two pairs of pants sketched in figure 6.8. The lower half of the disk is the same as in figure 6.6, but the pants is now amputated along $C[p_{12}]$ and the upper half of the disk contains the second pair of pants. Notice that we also sketched the two distinguished geodesics which end on $C[p_{12}]$ which we considered in figure 6.3. We label them as $C[p_1]$ on the lower pair of pants and $C[p'_1]$ on the upper pair of pants. The distance between their endpoints on $C[p_{12}]$ parametrizes a Fenchel-Nielsen angle as discussed in section 6.2.

In figure 6.9b we begin the ‘thickening’ of the geodesic $C[p_{12}]$. We define hypercycles $L(p_{12})$ and $L(p'_{12})$ associated to points $p_{12}, p'_{12} \in [p_{12}]$. The shaded domain in between these hypercycles will be covered by an inner chart. It descends to a

cylindrical region on S because of the gluing as indicated by the arrows.

Finally, in figure 6.9c we stop the thickening on both sides once the cylinder starts overlapping with itself. The resulting domain is then bounded by what we call the *critical hypercycles*; these are the hypercycles which just touch themselves on the quotient surface. We will denote them with $L(\tilde{p}_{12})$ and $L(\tilde{p}'_{12})$, as indicated in figure 6.9. Notice that the point where $L(\tilde{p}_{12})$ touches itself lies precisely on $C[p_3]$ (which was defined in figure 6.6) and similarly $L(\tilde{p}'_{12})$ lies on a corresponding $C[p'_3]$. This follows from the reflection symmetry in $C[p_1]$ but we will also give a computational proof below.

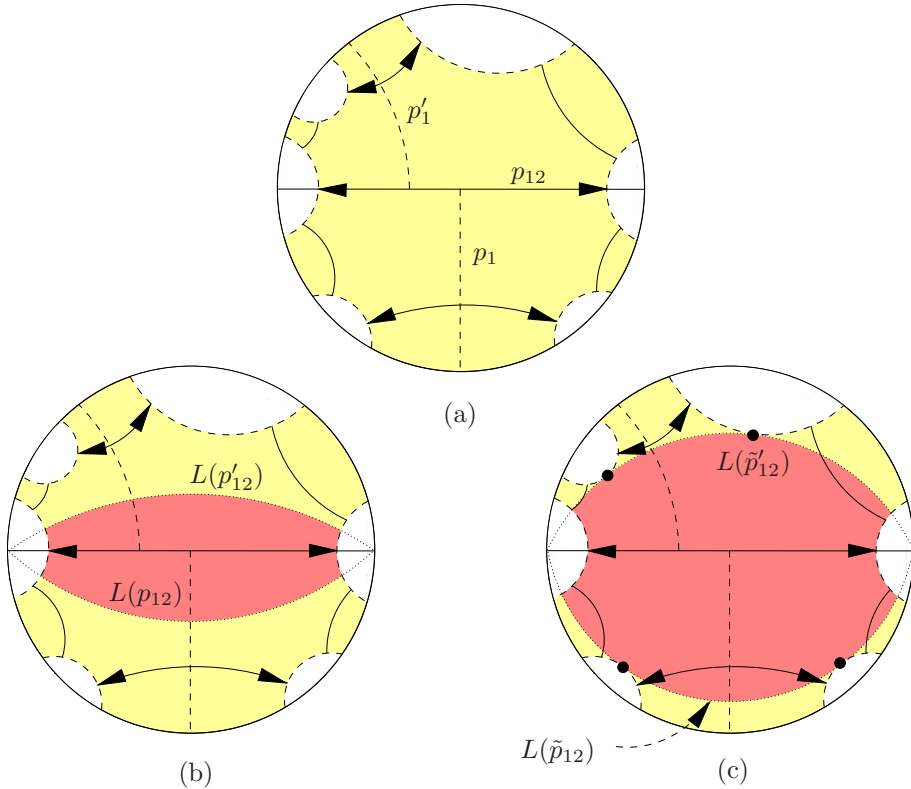


Figure 6.9: The lift to H of the construction of figure 6.8. (a) The shaded domain is a fundamental domain for the two pairs of pants in H and the edges should be identified as indicated by the arrows. (b) We define the cylindrical neighborhood as indicated. (c) The critical hypercycles just touch themselves once we glue the edges as indicated by the arrows.

6.5.3 Computation of the critical hypercycle

To define the coordinate systems below we need to know the location of the critical hypercycles as a function of the Fenchel-Nielsen parameters of S . From the above construction it should be clear that the location of for example the critical hypercycle $L(\tilde{p}_{12})$ depends only on the shape of the pair of pants on which it is defined and is independent of the shape of the adjacent pairs of pants or the twisting angles with which they are glued together. We therefore restrict ourselves to a single pair of pants P below, defined according to the procedure of section 6.4. The aim of this subsection is then to find a convenient expression for $L(\tilde{p}_{12})$ in terms of the Fenchel-Nielsen parameters l_{12} , l_{13} and l_{23} of P . Corresponding formulas for $L(\tilde{p}_{13})$ and $L(\tilde{p}_{23})$ can then be obtained using cyclic permutation of the indices.

Definition as an intersection

Consider a pants P as a quotient of H/Γ_P as described in section 6.4. We discussed in that section how the geodesics $C[p_{i,j}]$ descend onto the pants as closed periodic geodesics which are retractable into the three boundary components. Let us focus on the geodesic $C[p_{12}]$. The cyclic subgroup of Γ corresponding to this nontrivial loop on the pants is generated by $\eta_{[1]} \circ \eta_{[2]}$ and we shall denote it as $\langle \eta_{[1]} \circ \eta_{[2]} \rangle$. As we mentioned in 6.4, the nontrivial elements of this subgroup all have $C[p_{12}]$ as their axis since $\eta_{[1]} \circ \eta_{[2]}([p_{12}]) = [p_{12}]$. The corresponding flow lines are denoted $L(p_{12})$ for $p_{12} \in [p_{12}]$ and also descend to smooth circles on the pants, freely homotopic to $C[p_{12}]$ and lying at a constant distance from it.

We define a closed curve on P to be *simple* if it is not self-intersecting. Notice that $C[p_{12}]$ is simple and this implies that the image of $C[p_{12}]$ under any element of $\Gamma \setminus \langle \eta_{[1]} \circ \eta_{[2]} \rangle$ is completely disjoint from itself. However its associated hypercycles $L(p_{12})$ are not necessarily simple. Indeed we sketched in figure 6.8 how at a certain point the flow lines start intersecting with themselves. As mentioned above, we define the critical hypercycle $L(\tilde{p}_{12})$ to be the first flow line that is no longer simple. In H this implies that there must be another element $\gamma_c \in \Gamma \setminus \langle \eta_{[1]} \circ \eta_{[2]} \rangle$ for which the set:

$$\gamma_c(L(\tilde{p}_{12})) \cap L(\tilde{p}_{12}) \tag{6.41}$$

consists of exactly one point. However, from the topology of the pants we see that γ_c has to be $\eta_{[3]} \circ \eta_{[1]}$ and since $\eta_{[1]}$ leaves $L(\tilde{p}_{12})$ invariant we find that the precise condition becomes that

$$\eta_{[3]}(L(\tilde{p}_{12})) \cap L(\tilde{p}_{12}) \tag{6.42}$$

consists of a single point. We indicated this point and its reflection in $C[p_1]$ with black dots in figure 6.9.

Computation

According to the previous paragraph \tilde{p}_{12} is defined such that there exists precisely one $\hat{w} \in H$ which solves

$$\langle \hat{w} | \tilde{p}_{12} \rangle = \langle \hat{w} | \tilde{p}_{12} - 2\hat{p}_3 \langle \tilde{p}_{12} | \hat{p}_3 \rangle \rangle = -1 \quad (6.43)$$

Let us now compute both \tilde{p}_{12} and \hat{w} .

Lemma 6.5.1. *The critical flow line $L(\tilde{p}_{12})$ touches $C[p_3]$, so their intersection on H consists of exactly one point.*

Proof. Inner products are invariant under reflection and a reflection squares to the identity, so we find

$$\begin{aligned} 0 &= 1 + \langle \hat{w} | \eta_{[3]}(\tilde{p}_{12}) \rangle \\ &= 1 + \langle \eta_{[3]}(\hat{w}) | \eta_{[3]} \circ \eta_{[3]}(\tilde{p}_{12}) \rangle \\ &= 1 + \langle \eta_{[3]}(\hat{w}) | \tilde{p}_{12} \rangle \\ &= 1 + \langle \hat{w} | \tilde{p}_{12} \rangle - 2\langle \hat{p}_3 | \tilde{p}_{12} \rangle \langle \hat{w} | \hat{p}_3 \rangle \\ &= -2\langle \hat{p}_3 | \tilde{p}_{12} \rangle \langle \hat{w} | \hat{p}_3 \rangle. \end{aligned} \quad (6.44)$$

Now since $C[p_{12}]$ and $C[p_3]$ are disjoint we have $\langle [p_{12}] | [p_3] \rangle > 1$ and so in particular $\langle \tilde{p}_{12} | \hat{p}_3 \rangle \neq 0$. Hence

$$\langle \hat{w} | \hat{p}_3 \rangle = 0, \quad (6.45)$$

so indeed \hat{w} to (6.43) lies on $C[p_3]$. The converse also holds: if $\langle \hat{w} | \hat{p}_3 \rangle = 0$ and $\langle \hat{w} | \tilde{p}_{12} \rangle = -1$, then \hat{w} lies on the reflection under η_3 of $L(\tilde{p}_{12})$. This implies that $L(\tilde{p}_{12})$ touches $C[p_3]$ since if it would intersect $C[p_3]$ at two points, it would also intersect $L(\eta_{[3]}(\tilde{p}_{12}))$ twice and hence not be critical. \square

As we mentioned above the lemma can also be proved using the reflection symmetry in $C[p_1]$.

Notice that $\tilde{p}_{12} = \lambda \hat{p}_{12}$ for some nonzero λ so in order to find \tilde{p}_{12} it is sufficient to know its norm. This can be found by recalling that in section 6.4 we demonstrated that $\{\hat{p}_1, \hat{p}_2, \hat{p}_{12}\}$ form a basis of M^3 and we may therefore write $\hat{w} = a\hat{p}_1 + b\hat{p}_2 + c\hat{p}_{12}$. The condition (6.43) together with the above lemma then imply:

$$c\langle \hat{p}_{12} | \tilde{p}_{12} \rangle = -1, \quad (6.46)$$

as well as

$$a\langle \hat{p}_1 | \hat{p}_3 \rangle + b\langle \hat{p}_2 | \hat{p}_3 \rangle + c\langle \hat{p}_{12} | \hat{p}_3 \rangle = 0, \quad (6.47)$$

and since \hat{w} lies on H in M^3 we also have:

$$a^2 + b^2 + c^2 + 2ab\langle\hat{p}_1|\hat{p}_2\rangle = -1. \quad (6.48)$$

We find that there exists only one solution (a, b, c) whenever:

$$\langle\tilde{p}_{12}|\tilde{p}_{12}\rangle = \frac{1}{\langle\hat{p}_{12}|\hat{p}_3\rangle^2 - 1}. \quad (6.49)$$

This equals:

$$\langle\tilde{p}_{12}|\tilde{p}_{12}\rangle = \frac{\sinh^2(\gamma)}{\cosh^2(\alpha) + \cosh^2(\beta) + 2\cosh(\alpha)\cosh(\beta)\cosh(\gamma)}, \quad (6.50)$$

where we used the identities in section 6.4.1. Equation (6.50) is the formula we set out to find: it expresses the norm of \tilde{p}_{12} in terms of α , β and γ which according to the discussion below equation (6.37) are directly related to the lengths l_{ij} defining P . The solution for \hat{w} is given by:

$$\begin{aligned} a &= -c \frac{\sinh(\alpha)\sinh(B)[\cosh(\alpha)\cosh(\gamma) + \cosh(\beta)]}{\cosh^2(\alpha) + \cosh^2(\beta) + 2\cosh(\alpha)\cosh(\beta)\cosh(\gamma)} \\ b &= -c \frac{\sinh(\alpha)\sinh(B)[\cosh(\beta)\cosh(\gamma) + \cosh(\alpha)]}{\cosh^2(\alpha) + \cosh^2(\beta) + 2\cosh(\alpha)\cosh(\beta)\cosh(\gamma)} \\ c &= \frac{-1}{\langle\hat{p}_{12}|\tilde{p}_{12}\rangle}. \end{aligned} \quad (6.51)$$

Equation (6.49) actually defines \tilde{p}_{12} up to inversion but picking the solution with $\hat{w}_z > 0$ removes this freedom. The simple form of (6.49) also follows from the observation that the length between $C[p_{12}]$ and $L(\tilde{p}_{12})$ equals that between $C[p_{12}]$ and $C[p_3]$, which is just how the critical flow line is defined.

6.5.4 Covering of a pair of pants

In this subsection we demonstrate that the domains defined above cover the entire surface. To do so it suffices to prove that three domains can be used to cover a single pair of pants entirely, since one may then glue the pairs of pants together to obtain a covering of a more complicated Riemann surface.

The three domains on a single pair of pants P are bounded by critical hypercycles $L(\tilde{p}_{12})$, $L(\tilde{p}_{13})$ and $L(\tilde{p}_{23})$, with the latter two defined in a similar fashion as $L(\tilde{p}_{12})$ above. The domains lift to corresponding domains E_{ij} in H which are obtained as:

$$E_{ij} = \{w \in H : \langle w|\tilde{p}_{ij}\rangle < -1\}. \quad (6.52)$$

In section 6.4.1 we fixed the signs of the \hat{p}_i and the \hat{p}_{ij} so that all inner products in (6.37) are negative. The relative sign ambiguity between the \hat{p}_i and the \hat{p}_{ij} can then be fixed by setting $\langle \hat{p}_{ij} | \tilde{p}_{ij} \rangle > 0$; this means that all \hat{p}_{ij} as well as \hat{p}_2 and \hat{p}_3 point away from the (amputated) fundamental domain of P defined in figure 6.6. We can then define one half of the fundamental domain as:

$$D = \{w \in H : \langle w | \hat{p}_i \rangle < 0\}. \quad (6.53)$$

Notice that, depending on the overall sign of all the \hat{p}_i , D is the part of the shaded domain to the left or to the right of $C[p_1]$ in figure 6.6. We will now prove the following theorem.

Theorem 6.5.2. *For the domains D and the E_{ij} , the following holds:*

$$(E_{12} \cup E_{13} \cup E_{23}) \cap D = D \quad (6.54)$$

so D is covered by the three E_{ij} .

By the reflection symmetry in $C[p_1]$, it would follow from the theorem that the whole fundamental domain is covered. Since a fundamental domain with edges identified is equivalent to the original surface it follows that the pair of pants P is then indeed covered completely by the three charts.

Proof. Let us first consider the boundary of D . We will only prove the lemma below for the boundary component $C[p_3]$, but by cyclic permutation the lemma applies to $C[p_1]$ and $C[p_2]$ as well.

Lemma 6.5.3. *The line $C[p_3]$ is completely covered by the charts. Namely, the intersection point of $L(\tilde{p}_{12})$ with $C[p_3]$ is covered by both the chart bounded by $L(\tilde{p}_{13})$ and the chart bounded by $L(\tilde{p}_{13})$.*

Proof. Above, we found the unique point w on H where $L(\tilde{p}_{12})$ and $C[p_3]$ intersect; let us see whether it is covered by the chart bounded by $L(\tilde{p}_{13})$, so whether:

$$\langle w | \tilde{p}_{13} \rangle > -1. \quad (6.55)$$

After a little calculation, we have:

$$-\langle w | \tilde{p}_{13} \rangle = \frac{\cosh(\beta) \cosh(\gamma) + \cosh(\alpha)}{\cosh^2(\alpha) + \cosh^2(\beta) + 2 \cosh(\alpha) \cosh(\beta) \cosh(\gamma)} \frac{\langle \hat{p}_2 | \tilde{p}_{13} \rangle}{\langle \hat{p}_3 | \tilde{p}_{12} \rangle} \quad (6.56)$$

so $-\langle w | \tilde{p}_{13} \rangle < 1$ is certainly true if:

$$\left(\frac{\cosh(\beta) \cosh(\gamma) + \cosh(\alpha)}{\cosh^2(\alpha) + \cosh^2(\beta) + 2 \cosh(\alpha) \cosh(\beta) \cosh(\gamma)} \frac{\langle \hat{p}_2 | \tilde{p}_{13} \rangle}{\langle \hat{p}_3 | \tilde{p}_{12} \rangle} \right)^2 < 1 \quad (6.57)$$

but

$$\langle \hat{p}_3 | \tilde{p}_{12} \rangle = \langle \hat{p}_3 | \hat{p}_{12} \rangle \langle \hat{p}_{12} | \tilde{p}_{12} \rangle = -\sinh(A) \sinh(\beta) \langle \hat{p}_{12} | \tilde{p}_{12} \rangle \quad (6.58)$$

and substituting the expressions for the right hand side we found above, this simplifies to:

$$\begin{aligned} & (\cosh^2(\alpha)^2 + 2 \cosh(\alpha) \cosh(\beta) \cosh(\gamma)) \\ & \times (\cosh^2(\alpha) + \cosh^2(\beta) + \cosh^2(\gamma) + 2 \cosh(\alpha) \cosh(\beta) \cosh(\gamma)) > 0 \end{aligned} \quad (6.59)$$

which is obviously true and therefore w is trivially covered by E_{13} . Similarly, by permuting α, β, γ we find that w is also covered by E_{23} . But then the charts must cover $C[p_3]$ completely, since they overlap on (a neighborhood around) w and since both $L(\tilde{p}_{13})$ and $L(\tilde{p}_{23})$ intersect $C[p_3]$ only once. \square

Suppose now that the theorem is false so there would exist a small domain $F \subset D$ that is not covered by the E_{ij} . Consider the boundary of F . Since by the previous lemma the $C[p_i]$ are completely covered by the charts, no segment of any of the $C[p_i]$ can be part of the boundary of F . Also, clearly F cannot extend to ∂H and therefore F should be bounded by the critical flow lines only. Since the flow lines are circle segments, it follows that F is bounded by a segment of all three flow lines, i.e. F is a hyperbolic triangle. Consider now the segment of the boundary of F that is part of $L(\tilde{p}_{12})$: by the definition of F it is not covered by the two other charts. We conclude that if F exists then there is a part of $L(\tilde{p}_{12}) \cap D$ that is not covered by E_{13} and E_{23} .

Let us however take a closer look at the line segment $L(\tilde{p}_{12}) \cap D$. At the end lying at $C[p_1]$, we know we are in E_{13} (because of the above lemma) but outside of E_{23} (because $L(\tilde{p}_{23})$ only touches $C[p_1]$). If we now move towards \hat{w} on $C[p_3]$, we apparently cross $L(\tilde{p}_{23})$ an odd number of times, since we end up being also in E_{23} at \hat{w} . Similarly, we must have crossed $L(\tilde{p}_{13})$ exactly zero or an even number of times. After \hat{w} , moving further towards $C[p_2]$, the same happens: we cross $L(\tilde{p}_{13})$ an odd number of times and $L(\tilde{p}_{23})$ an even number of times. However, since the flow lines are circles, they intersect at most twice in H and by symmetry they can intersect at most once in D . (For example, the two intersection points of $L(\tilde{p}_{12})$ and $L(\tilde{p}_{13})$ lie on both sides of $C[p_1]$ because of the reflection symmetry in $C[p_1]$.) It follows that the aforementioned odd and even number of crossings are necessarily one and zero. So if we repeat our route along $L(\tilde{p}_{12}) \cap D$, we first meet $L(\tilde{p}_{23})$ exactly once, then w , and then $L(\tilde{p}_{13})$ exactly once.

However this order implies that we are already in E_{23} before we exit from E_{13} and we remain there all the way up to $C[p_2]$. Therefore $L(\tilde{p}_{12})$ is completely covered and our triangle F cannot exist; the theorem follows. \square

6.5.5 Extension to the spacetime

So far we have restricted ourselves to the Riemann surface at $U = 0$ of the spacetime. Let us now consider the extension of the domains to nonzero U . Recall that in the previous chapter we used the definition of AdS_3 as (the universal covering of) the quadric in $\mathbb{R}^{2,2}$ defined as:

$$\langle w|w \rangle - U^2 = -1. \quad (6.60)$$

In this notation w is again a vector in M^3 and $\langle \cdot, \cdot \rangle$ is the inner product on M^3 as defined in equation (6.6).

Geodesics extend straightforwardly to geodesic planes on AdS_3 , namely as the hyperplanes for which $\langle w|p \rangle = 0$ for some spacelike $p \in M^3$ and for all U . We will denote the associated hyperplanes also as $C[p]$. For hypercycles the extension to nonzero U can be done as follows. We define the extension of a hypercycle $L(p)$ as the domain in AdS_3 where

$$\langle w|p \rangle = -\sqrt{1 - U^2} \quad (6.61)$$

for all $|U| < 1$, and we denote the plane so defined also as $L(p)$. This extension is chosen such that critical hypercycles remain critical also for nonzero U . Indeed, by conjugating to a simple coordinate system one may explicitly check that (the extension of) $L(\tilde{p}_{12})$ touches $C[p_3]$ on any slice of constant U with $|U| < 1$. Notice that these extended hypercycles do not extend beyond the plane at $|U| = 1$. The same holds then for the inner charts as they are bounded by such planes.

6.6 Coordinate systems and fatgraph description

In the previous section we found three cylindrical domains that completely cover the pair of pants. On an extended pair of pants they would form three outer charts that cover the entire $U = 0$ space of the corresponding wormhole spacetime. We may however also amputate the pair of pants and glue the ends to other pairs of pants to construct a bigger Riemann surface. In that case we construct an inner chart by gluing together two such (amputated) domains, as indicated in figure 6.8.

In this section we will define and analyze appropriate coordinate systems on these domains. First of all, in subsection 6.6.1 we give the precise definition of the coordinates, fix the coordinate ranges to certain ‘natural’ values and compute the expressions for the metric. We will demonstrate in subsection 6.6.2 that the parameters appearing in the metric contain all the necessary information about the geometry of the spacetime. In subsection 6.6.3 we then use these parameters

to describe the spacetime in terms of a fatgraph as we already sketched in figure 6.1. Finally we give the transition functions between the charts in subsection 6.6.4.

6.6.1 Definition of the coordinate systems

In this subsection we will define the coordinate systems on the inner and outer domains.

Inner charts

Let us consider an inner chart defined around a periodic geodesic $C[p_{12}]$ as sketched in figure 6.9c. It is bounded by two critical hypercycles which we label as $L(\tilde{p}_{12})$ and $L(\tilde{p}'_{12})$. We use the above conventions for the signs of the inner products between the \hat{p}_i and \hat{p}_{ij} and in addition we require that $\langle \hat{p}_{12} | \tilde{p}_{12} \rangle > 0$.

Recall that $\{\hat{p}_1, \hat{p}_2, \hat{p}_{12}\}$ form a basis of M^3 . We may therefore parametrize a point (w, U) on AdS_3 using $\langle w | \hat{p}_1 \rangle, \langle w | \hat{p}_2 \rangle, \langle w | \hat{p}_{12} \rangle$ and U . The new coordinates (τ, r, ϕ) on an inner chart are then defined as follows:

$$\begin{aligned} \tanh(\tau) &= U \\ \mu r + \nu &= \frac{-\langle w | \hat{p}_{12} \rangle}{\sqrt{1 - U^2}} \\ e^{2\sqrt{M}(\phi - d)} &= \frac{\langle w | \hat{p}_1 \rangle + e^\gamma \langle w | \hat{p}_2 \rangle}{e^\gamma \langle w | \hat{p}_1 \rangle + \langle w | \hat{p}_2 \rangle}. \end{aligned} \tag{6.62}$$

We will shortly determine suitable values for the parameters μ, ν, \sqrt{M}, d . Notice that τ is a natural timelike coordinate and that the surfaces of constant τ and r are the extension to the entire spacetime of the flow lines of $\eta_{[1]} \circ \eta_{[2]}$. Indeed one may directly compute that $\eta_{[1]} \circ \eta_{[2]}$ in these coordinates takes the form

$$\eta_1 \circ \eta_2(\tau, r, \sqrt{M}(\phi - d)) = (\tau, r, \sqrt{M}(\phi - d) + 2\gamma). \tag{6.63}$$

If we define:

$$\sqrt{M} = \frac{2\gamma}{2\pi} = \frac{l_{12}}{2\pi}, \tag{6.64}$$

then we recover the natural periodicity $\phi \sim \phi + 2\pi$. Let us also require r to run from -1 to 1 so the critical hypercycles are at $|r| = 1$. If we pick $r = 1$ to correspond to the end defined by $L(\tilde{p}_{12})$ then we obtain:

$$\mu + \nu = \frac{1}{\langle \hat{p}_{12} | \tilde{p}_{12} \rangle}. \tag{6.65}$$

On the other side of the chart we similarly find:

$$-\mu + \nu = \frac{1}{\langle \hat{p}_{12} | \tilde{p}'_{12} \rangle}. \tag{6.66}$$

Equation (6.65) and (6.66) together fix μ and ν . Notice that $\langle \hat{p}_{12} | \hat{p}'_{12} \rangle < 0$ since we fixed \hat{p}_{12} so that $\langle \hat{p}_{12} | \tilde{p}_{12} \rangle > 0$ and $L(\hat{p}'_{12})$ lies on the other side of $C[p_{12}]$. This implies $\mu > 0$. Finally, we fix d so that the line $\phi = 0$ corresponds to $C[p_1]$ (which we recall is the geodesic orthogonal to both $C[p_{12}]$ and $C[p_{13}]$, see figure 6.9a). This implies that:

$$d = -\pi/2. \quad (6.67)$$

If we choose $C[p_2]$ instead of $C[p_1]$ to be $\phi = 0$, then we find $d = +\pi/2$, also implying that for $d = -\pi/2$, $C[p_2]$ lies at $\phi = -\pi$. The point \hat{w} on $L(\tilde{p}_{12})$ where this critical hypercycle pinches can then be shown to be given by:

$$\pm\phi = \frac{\pi}{2\gamma} \ln \left[\frac{e^\gamma \cosh(\alpha) + \cosh(\beta)}{\cosh(\alpha) + e^\gamma \cosh(\beta)} \right] - \frac{\pi}{2} \quad (6.68)$$

plus or minus any multiple of 2π .

Using (6.37) and (6.60) we may find the identity:

$$\langle w | \hat{p}_{12} \rangle^2 + 1 - U^2 = \frac{1}{\sinh^2(\gamma)} (\langle w | \hat{p}_2 \rangle + e^\gamma \langle w | \hat{p}_1 \rangle) (\langle w | \hat{p}_2 \rangle + e^{-\gamma} \langle w | \hat{p}_1 \rangle), \quad (6.69)$$

which can be used to find that the inverse transformation is given by:

$$\begin{aligned} U &= \tanh(\tau) \\ \langle w | \hat{p}_{12} \rangle &= -\frac{\mu r + \nu}{\cosh(\tau)} \\ \langle w | \hat{p}_1 \rangle &= \sinh(\sqrt{M}(\phi - d) - \gamma/2) \frac{\sqrt{(\mu r + \nu)^2 + 1}}{\cosh(\tau)} \\ \langle w | \hat{p}_2 \rangle &= -\sinh(\sqrt{M}(\phi - d) + \gamma/2) \frac{\sqrt{(\mu r + \nu)^2 + 1}}{\cosh(\tau)}. \end{aligned} \quad (6.70)$$

We will use this inverse transformation to define the transition functions below.

To find the metric in the new coordinates let us conjugate with an element of $SO(2, 1)$ to set $\hat{p}_{12} = (0, 1, 0)$. Furthermore, the vectors $\hat{p}_1 + e^\gamma \hat{p}_2$ and $\hat{p}_1 + e^{-\gamma} \hat{p}_2$ are both null, orthogonal to \hat{p}_{12} and have an inner product equal to $-2 \sinh^2(\gamma)$. We can therefore pick them to be $(1, 0, -1)$ and $\sinh^2(\gamma)(1, 0, 1)$, respectively. We then find that (6.62) simplifies and in the Poincaré coordinates introduced in (5.11) it becomes:

$$\tanh(\tau) = \frac{t}{y}, \quad \mu r + \nu = \frac{x}{\sqrt{y^2 - t^2}}, \quad e^{2\sqrt{M}(\phi - d')} = -t^2 + x^2 + y^2, \quad (6.71)$$

for some d' whose value we will not need here. Using the Poincaré metric (5.12) we find that the metric takes the form:

$$ds^2 = \frac{1}{\cosh^2(t)} \left(-dt^2 + \frac{\mu^2 dr^2}{(\mu r + \nu)^2 + 1} + M(1 + (\mu r + \nu)^2) d\phi^2 \right). \quad (6.72)$$

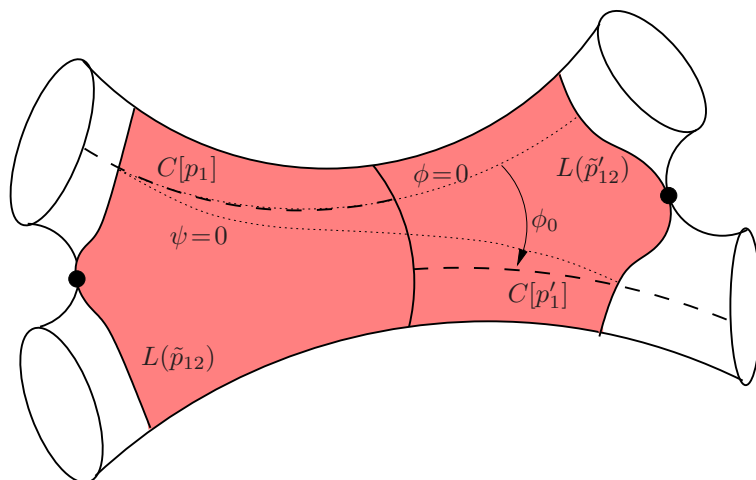


Figure 6.10: Definition of the twisted coordinate ψ . The line $\phi = 0$ coincides with $C[p_1]$ on one side but $C[p'_1]$ on the other side lies at $\phi = \phi_0$. We therefore define ψ such that at the two ends of the charts $\psi = 0$ coincides with $C[p_1]$ and $C[p'_1]$. As indicated these boundaries of the charts are defined by the critical hypercycles $L(\tilde{p}_{12})$ and $L(\tilde{p}'_{12})$.

In this coordinate system we therefore not only have natural coordinate ranges but the metric also features several parameters M, μ, ν which inform us about the geometry at least in this local patch. We can however introduce one more parameter which is related to the Fenchel-Nielsen twist described above.

Twisted inner charts

Our choice for d , using either $C[p_1]$ or $C[p_2]$, singles out one particular half of the domain since we might just as well have set $\phi = 0$ at $C[p'_1]$ or at $C[p'_2]$ (see for example figure 6.9a where only $C[p'_1]$ is sketched.) Furthermore, from the metric (6.72) we cannot read off the twisting parameter defined in section 6.2 that determines how the pants are glued together. These issues can be avoided by defining a ‘twisted’ coordinate ψ as we will now proceed to show. The procedure is sketched in figure 6.10.

First, suppose that we have an inner chart with μ, ν, \sqrt{M}, d defined as before. In particular, suppose that at the end where $r = 1$ we have the geodesic $C[p_1]$ at $\phi = 0$ and the geodesic $C[p_2]$ at $\phi = \pi$. On the other side, there is also a pants with a certain $C[p'_1]$ at, say, $\phi = \phi_0$. Then the geodesic $C[p'_2]$ lies at $\phi = \phi_0 + \pi$. We now introduce the twisted coordinate ψ as:

$$e^{\sqrt{M}\psi - d_t} = e^{\sqrt{M}\phi} \frac{\sin(\chi)(\mu r + \nu) + \sqrt{(\mu r + \nu)^2 + \cos^2(\chi)}}{\sqrt{(\mu r + \nu)^2 + 1}} \quad (6.73)$$

with μ, ν, \sqrt{M} (and d) as before, but with the new parameters d_t and χ defined via:

$$\begin{aligned} e^{-d_t} &= \frac{\sin(\chi)(\mu + \nu) + \sqrt{(\mu + \nu)^2 + \cos^2(\chi)}}{\sqrt{(\mu + \nu)^2 + 1}} \\ &= e^{c\phi_0} \frac{-\sin(\chi)(\mu - \nu) + \sqrt{(\mu - \nu)^2 + \cos^2(\chi)}}{\sqrt{(\mu - \nu)^2 + 1}}, \end{aligned} \quad (6.74)$$

from which it follows that the lines $\psi = 0$ and $\psi = \pi$ intersect the boundaries at $r = 1$ and $r = -1$ exactly at the four geodesics $C[p_1], C[p_2], C[p'_1], C[p'_2]$. (We do not need to explicitly solve for χ as a function of ϕ_0 , instead we simply take χ as the input parameter.)

Notice that ψ has again periodicity 2π . We already presented the metric in the twisted coordinate system in (6.5) and recall here that it takes the form:

$$\begin{aligned} ds^2 &= \frac{1}{\cosh^2(t)} \left(-dt^2 + \frac{\mu^2 dr^2}{(\mu r + \nu)^2 + \cos^2(\chi)} + M(1 + (\mu r + \nu)^2) d\psi^2 \right. \\ &\quad \left. - \frac{2\mu\sqrt{M}\sin(\chi)}{\sqrt{(\mu r + \nu)^2 + \cos^2(\chi)}} d\psi dr \right). \end{aligned} \quad (6.75)$$

We see that it features explicitly the twist parameter χ as well.

Notice that the parameters in the metric (6.75) contain all the information about the geometry that is covered by the chart. For example, one may easily find that the periodic geodesic around which we defined the chart lies at the point $r = -\nu/\mu$ and has length $2\pi\sqrt{M}$. The angle χ reflects the Fenchel-Nielsen twist between the pairs of pants and the parameters μ and ν are related to the shapes of these pairs of pants: for example, the distance between the periodic geodesic and the pinched hypercycle at $r = 1$ is

$$\left| \ln \left(\frac{\mu + \nu + \sqrt{(\mu + \nu)^2 + 1}}{\nu + \sqrt{\nu^2 + 1}} \right) \right|, \quad (6.76)$$

and the distance to the hypercycle at $r = -1$ has the same form with the replacement $\mu \rightarrow -\mu$.

Outer charts

Let us now consider the outer domains. We define appropriate coordinates $(\tilde{\tau}, \rho, \varphi)$ as:

$$\begin{aligned} \tanh(\sqrt{M}\tilde{\tau}) &= \frac{U}{\sqrt{\langle w|\hat{p}_{12}\rangle^2 + 1}} \\ \rho &= \sqrt{M}\langle w|\hat{p}_{12}\rangle \\ \exp\left(2\sqrt{M}(\varphi - f)\right) &= \frac{e^\gamma\langle w|\hat{p}_1\rangle + \langle w|\hat{p}_2\rangle}{\langle w|\hat{p}_1\rangle + e^\gamma\langle w|\hat{p}_2\rangle} \end{aligned} \quad (6.77)$$

with parameters f, \sqrt{M} . We see that we are now not restricted to $|U| < 1$. The inverse transformation is:

$$\begin{aligned} \langle w|\hat{p}_1\rangle &= -\sinh(\sqrt{M}(\varphi - f) + \gamma/2) \frac{\sqrt{M^{-1}\rho^2 + 1}}{\cosh(\sqrt{M}\tilde{\tau})} \\ \langle w|\hat{p}_2\rangle &= +\sinh(\sqrt{M}(\varphi - f) - \gamma/2) \frac{\sqrt{M^{-1}\rho^2 + 1}}{\cosh(\sqrt{M}\tilde{\tau})} \\ \langle w|\hat{p}_{12}\rangle &= \frac{\rho}{\sqrt{M}} \\ U &= \tanh(\sqrt{M}\tilde{\tau})\sqrt{M^{-1}\rho^2 + 1} \end{aligned} \quad (6.78)$$

Lines of constant $\tilde{\tau}$ and r are again flow lines of the isometry $\eta_{[1]} \circ \eta_{[2]}$. Furthermore, the periodicity $\phi \sim \phi + 2\pi$ can again be attained by choosing:

$$\sqrt{M} = \frac{2\gamma}{2\pi} = \frac{l_{12}}{2\pi}. \quad (6.79)$$

We also choose

$$f = \pi/2 \quad (6.80)$$

just like d for an inner chart: it implies that $\varphi = 0$ lies at $C[p_1]$. Note that this chart is defined on a single (extended) pair of pants and there is therefore no need to introduce a twisted parameter.

This chart also is bounded by some critical hypercycle $L(\tilde{p}_{12})$, so $\langle w|\tilde{p}_{12}\rangle > -\sqrt{1 - U^2}$, implying now the coordinate range:

$$\frac{\cosh(\sqrt{M}\tilde{\tau})\rho}{\sqrt{\rho^2 + M}} > \frac{-1}{\sqrt{1 + \langle \tilde{p}_{12}|\tilde{p}_{12}\rangle}} \quad (6.81)$$

After a suitable conjugation we find the new coordinates as a function of the Poincaré coordinates as:

$$\tanh(\sqrt{M}\tilde{\tau}) = \frac{t}{\sqrt{y^2 + x^2}}, \quad \rho = \sqrt{M} \frac{x}{y}, \quad e^{2\sqrt{M}(\varphi - h)} = -t^2 + x^2 + y^2, \quad (6.82)$$

from which we obtain that the metric in these coordinates becomes (6.1), which was:

$$ds^2 = \frac{\rho^2 + M}{\cosh^2(\sqrt{M}\tilde{\tau})}(-d\tilde{\tau}^2 + d\varphi^2) + \frac{d\rho^2}{\rho^2 + M}. \quad (6.83)$$

Notice that these coordinate systems extend beyond the future and past horizons, which lie at the surfaces $x = |t|$ or

$$\rho = \sqrt{M}|\sinh(\sqrt{M}\tilde{\tau})|. \quad (6.84)$$

The metric in the region outside of these horizons can be put back in BTZ form (5.15) by the coordinate transformation:

$$r^2 = \frac{\rho^2 + M}{\cosh^2(\sqrt{M}\tilde{\tau})}, \quad \tanh(\sqrt{M}t) = \sqrt{1 + M/\rho^2} \tanh(\sqrt{M}\tilde{\tau}), \quad \phi = \varphi. \quad (6.85)$$

Notice that the parameter M in (6.83) agrees with the BTZ mass M .

6.6.2 Parameters

The above charts can be combined to cover the wormhole spacetime completely. More specifically, for a wormhole of genus g and with m boundaries, we can cover the entire spacetime with $3g - 3 + m$ inner charts plus m outer charts. For every inner chart we have four parameters, M, μ, ν, χ , and for every outer chart we have a single parameter M . As we showed above, the angles χ and the parameters M are directly related to the Fenchel-Nielsen twists and length parameters associated to the periodic geodesics and should therefore completely determine the surface. Indeed we saw in (6.65) and in (6.66) how the remaining parameters μ and ν parameters can be expressed in terms of the Fenchel-Nielsen parameters of S .

In the new parametrization using the M and χ coordinates the precise relation takes the following form. Consider a single amputated pair of pants in the Fenchel-Nielsen decomposition of S . It is covered completely by using three different charts. Suppose now that chart number 3 is an inner chart (with parameters $\mu_3, \nu_3, M_3, \chi_3$) and that it is the half with $r > 0$ that lies on the pair of pants under consideration. Denote the M parameters in the other two charts as M_i with $i \in \{1, 2\}$. One then finds from (6.65) and (6.50) the relation:

$$\mu_3 + \nu_3 = \frac{\sqrt{C_1^2 + C_2^2 + 2C_1C_2C_3}}{\sinh(\pi\sqrt{M_3})}, \quad (6.86)$$

with $C_i = \cosh(\pi\sqrt{M_i})$. A similar relation can be found at the other side of chart number 3, which has $r < 0$ and lies on another pair of pants. Namely, using the

parameters M'_1 and M'_2 of the two other charts on that pair of pants we find:

$$-\mu_3 + \nu_3 = \frac{\sqrt{C'^2_1 + C'^2_2 + 2C'_1C'_2C'_3}}{\sinh(\pi\sqrt{M_3})}, \quad (6.87)$$

with $C'_i = \cosh(\pi\sqrt{M'_i})$. Using these formulas, we can determine all the μ, ν parameters in the inner charts if we are only given the M parameters in every chart. This reduces the number of independent parameters to two per inner chart and still one per outer chart, just as for the Fenchel-Nielsen description of the surface.

Finally, we notice that the coordinate range (6.81) may in a similar notation be written as follows:

$$\frac{\cosh(\sqrt{M_3}\tilde{\tau})\rho}{\sqrt{\rho^2 + M_3}} > -\sqrt{\frac{C^2_1 + C^2_2 + 2C_1C_2C_3}{C^2_1 + C^2_2 + C^2_3 + 2C_1C_2C_3 - 1}}, \quad (6.88)$$

where again the subscript indicates the chart under consideration and the coordinate range is then valid for chart number 3.

6.6.3 Fatgraph description

To completely specify the spacetime we need to specify both the parameters and the way the charts are glued together. This combinatorial data can be nicely summarized in an oriented trivalent fatgraph as shown in figure 6.1. (In the usual Fenchel-Nielsen description of the surface this combinatorial data is implicitly specified, for example by using a reference surface. The description given below, on the other hand, explicitly fixes the required combinatorial data and it is then no longer necessary to use a reference surface.)

The data in the fatgraph is translated to the coordinate systems as follows. Every edge represents a periodic geodesic and therefore a chart. Every vertex represents a pair of pants. The orientation of the edges indicates the direction of increasing r (and by convention always points outward for outer charts), and the ‘fattening’ is necessary to indicate how three charts come together on a pair of pants. If we add to this fatgraph two parameters M, χ for every interior edge of the graph and a single parameter M for every outer edge, then the wormhole spacetime is completely specified.

At this point we should note that there are two discrete ambiguities in the above definitions of the coordinates ψ and φ on the inner and outer charts that we have not yet dealt with. Although these ambiguities do not affect the metric or the coordinate ranges given above, they will affect the transition functions below and therefore they should be fixed.

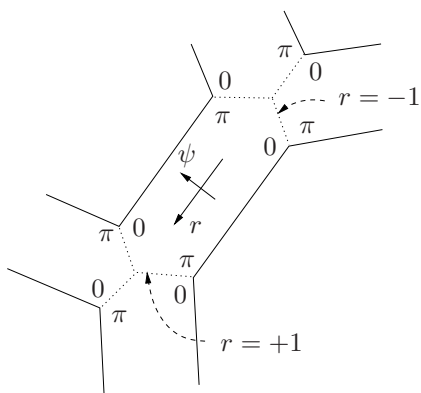


Figure 6.11: *Fixing the ambiguities in the definition of ψ and φ .*

at $\psi = \pi$ or $\varphi = \pi$. However the distinction between $C[p_1]$ and $C[p_2]$ is arbitrary at this point and this leads to an ambiguity as to which point should correspond to $\psi = 0$ and which one to $\psi = \pi$. This ambiguity can be fixed from the fatgraph. We first demand that at an overlap between two charts the point where $\psi = 0$ on one chart corresponds to $\psi = \pi$ on the other chart (and similarly for φ), as indicated in figure 6.11. Furthermore, for an inner chart we should alternately associate $\psi = 0$ and $\psi = \pi$ to the four corners of the corresponding edge in the fatgraph, which is indicated in figure 6.11 as well. This fixes the ambiguity up to an overall shift of ψ or φ with π in all charts at the same time, which is however irrelevant for the description of the manifold.

The first ambiguity involves the direction of increasing ψ and φ . With the fatgraph description this can be easily fixed by fixing the handedness of the (r, ψ) or (r, φ) coordinate system to be the same in every chart.

The second ambiguity is the fact that we have defined ψ or φ only up to an overall shift by π . To see this, recall that we decided that the point $\psi = 0$ or $\varphi = 0$ would correspond to the point on the boundary circle $L(\tilde{p}_{12})$ where it intersects $C[p_1]$ (as sketched in figure 6.10) and by the reflection isometry the point where it intersects $C[p_2]$ would then be

6.6.4 Transition functions

With all the ambiguities fixed, we may proceed to define transition functions on the overlap between two different charts. We will see below how these follow from a composition of the coordinate transformations (6.62) and (6.70).

An important subtlety is that we find different transition functions depending on the gluings and the orientations of the charts. For example, if we consider the vertex in figure 6.1 where we may go from chart 2 to chart 3 or chart 4, we find different transition functions because we turn ‘right’ at the vertex if we go to chart 3, whereas we turn ‘left’ if we go to chart 4. As another example, the transition functions between chart 2 and chart 3 (on both vertices) are different from those between chart 5 and chart 6 because (again on both vertices) the orientation of chart 3 and chart 6 are not the same. When we define the transition functions

below we will have to take into account these different possibilities.

In the transition functions we will not use the ‘twisted’ coordinate ψ defined in (6.73). Instead, we will use the coordinate ϕ which agrees with ψ at the bounding circle of the chart where we define the transition function. Of course, it is not hard to compose the transition functions with (6.73) and its inverse, or a similar function when the transition takes place at $r = -1$.

Transitions between two inner charts

The complete set of possibilities for the transitions between two inner charts is depicted in figure 6.12. As one may expect, the transition functions are *almost* the same for either one of these possibilities and it is convenient to give them in a general form with certain parameters ϵ , ϵ' , d and d' whose value depends on these possibilities and is given in the table in figure 6.12. Using these parameters, one finds the transition functions as follows.

Inner - inner

Let us consider the overlap of two inner charts on a single pair of pants. We will take them to be defined around the periodic geodesics $C[p_{12}]$ and $C[p_{13}]$, with primed coordinates corresponding to the latter geodesic. One may then compose the analogue of (6.62):

$$\begin{aligned} \tanh(t') &= U \\ \mu' r' + \nu' &= -\epsilon' \frac{\langle w | \hat{p}_{13} \rangle}{\sqrt{1 - U^2}} \\ e^{2\epsilon' \sqrt{M'}(\phi' - d') - \beta} &= \frac{e^\beta \langle w | \hat{p}_1 \rangle + \langle w | \hat{p}_3 \rangle}{\langle w | \hat{p}_1 \rangle + e^\beta \langle w | \hat{p}_3 \rangle} \end{aligned} \tag{6.89}$$

with the inverse transformation (6.70):

$$\begin{aligned} U &= \tanh(t) \\ \langle w | \hat{p}_{12} \rangle &= -\epsilon \frac{\mu r + \nu}{\cosh(t)} \\ \langle w | \hat{p}_1 \rangle &= \sinh(\epsilon \sqrt{M}(\phi - d)) \frac{\sqrt{(\mu r + \nu)^2 + 1}}{\cosh(t)} \\ \langle w | \hat{p}_2 \rangle &= -\sinh(\epsilon \sqrt{M}(\phi - d) + \gamma) \frac{\sqrt{(\mu r + \nu)^2 + 1}}{\cosh(t)} \end{aligned} \tag{6.90}$$

via the identities:

$$\begin{aligned}
 \langle w|p_3\rangle &= -\cosh(\beta)\langle w|p_1\rangle + \sinh(\beta)\left(-\sinh(A)\langle w|p_{12}\rangle\right. \\
 &\quad \left. + \frac{\cosh(A)}{\sinh(\gamma)}[\cosh(\gamma)\langle w|p_1\rangle + \langle w|p_2\rangle]\right) \\
 \langle w|p_{13}\rangle &= \frac{\sinh(A)}{\sinh(\gamma)}[\cosh(\gamma)\langle w|p_1\rangle + \langle w|p_2\rangle] - \langle w|p_{12}\rangle \cosh(A)
 \end{aligned} \tag{6.91}$$

to eventually find the transition functions:

$$\begin{aligned}
 t' &= t \\
 -\epsilon'(\mu'r' + \nu') &= \cosh(A)\epsilon(\mu r + \nu) - \sinh(A)\sqrt{(\mu r + \nu)^2 + 1} \cosh(\epsilon\sqrt{M}(\phi - d)) \\
 e^{2\epsilon'\sqrt{M'}(\phi' - d')} &= \frac{\epsilon(\mu r + \nu) - \sqrt{(\mu r + \nu)^2 + 1} \cosh(\epsilon\sqrt{M}(\phi - d) - g)}{\epsilon(\mu r + \nu) - \sqrt{(\mu r + \nu)^2 + 1} \cosh(\epsilon\sqrt{M}(\phi - d) + g)},
 \end{aligned} \tag{6.92}$$

where we defined:

$$\cosh(A) = \frac{\cosh(\pi\sqrt{M}) \cosh(\pi\sqrt{M'}) + \cosh(\pi\sqrt{M''})}{\sinh(\pi\sqrt{M}) \sinh(\pi\sqrt{M'})} \tag{6.93}$$

and

$$\sinh(A) \sinh(g) = 1. \tag{6.94}$$

Here M and M' denote mass parameters in the metric on the unprimed and the primed chart between which we define the transition functions, and M'' denotes the mass parameter from the metric of the third chart that joins this vertex. We therefore have to inspect the metric of all three charts at the vertex in order to obtain the transition functions between only two of these charts. The identities (6.91) can be found by expanding w in the basis $\{\hat{p}_1, \hat{p}_2, \hat{p}_{12}\}$ as well as in the basis $\{\hat{p}_1, \hat{p}_3, \hat{p}_{13}\}$ and using the hyperbolic identities presented in section 6.4.1.

Notice that the transition functions are not automatically periodic in ϕ or ϕ' ; they are in fact only valid for $\phi, \phi' \in [0, 2\pi)$. Of course, this is by no means a restriction as this is sufficient to cover the entire chart. The other boundaries of the domain of validity of the transition functions are obtained from the coordinate ranges $-1 < r < 1$ and $-1 < r' < 1$. For example, substituting $r' = 1$ in the second equation of (6.92) one finds an equality involving r and ϕ which defines the boundary of the domain of definition of the transition functions.

Transitions involving outer charts

If the transitions involve outer charts we need the $(\tilde{\tau}, \rho, \varphi)$ coordinate system. Since we always pick the ρ coordinate to increase towards the boundary there is no ambiguity on the orientation of this coordinate. We are however still left

	ϵ	ϵ'	d	d'
$1 \rightarrow 2$	-1	+1	0	π
$1 \rightarrow 3$	-1	+1	π	0
$2 \rightarrow 1$	+1	-1	π	0
$2 \rightarrow 3$	+1	+1	0	π
$3 \rightarrow 1$	+1	-1	0	π
$3 \rightarrow 2$	+1	+1	π	0
$4 \rightarrow 5$	-1	-1	π	0
$5 \rightarrow 4$	-1	-1	0	π

Figure 6.12: Possible transitions between inner charts. The transition functions are by definition always taken from unprimed to primed coordinate systems: for example, in the first line the unprimed coordinates in (6.92) are the coordinates in chart 1 and the primed coordinates are those of chart 2.

with the left/right ambiguity and correspondingly need the discrete parameter f associated to every outer chart. For the transition functions between two outer charts we then find in a similar fashion as before,

$$\begin{aligned}
 \rho' &= -\sqrt{\frac{M'}{M}} \left(\cosh(A)\rho + \sinh(A) \cosh(\sqrt{M}(\varphi - f)) \frac{\sqrt{\rho^2 + M}}{\cosh(\sqrt{M}\tilde{\tau})} \right) \\
 \sqrt{M} \tanh(\sqrt{M'}\tilde{\tau}') \sqrt{\rho'^2 + M'} &= \sqrt{M'} \tanh(\sqrt{M}\tilde{\tau}) \sqrt{\rho^2 + M} \\
 e^{2\sqrt{M'}(\varphi' - f')} &= \frac{\rho \cosh(\sqrt{M}\tilde{\tau}) + \sqrt{\rho^2 + M} \cosh(\sqrt{M}(\varphi - f) - g)}{\rho \cosh(\sqrt{M}\tilde{\tau}) + \sqrt{\rho^2 + M} \cosh(\sqrt{M}(\varphi - f) + g)},
 \end{aligned} \tag{6.95}$$

with the possible values of f and f' given in figure 6.13 and the same values of A and g as before. The transition function on the second line is slightly implicit but it is straightforward to plug in the solution for ρ' of the first line and then solve for $\tilde{\tau}'$.

Similarly, between an inner and an outer chart we find,

$$\begin{aligned}
 \rho' &= \frac{\sqrt{M'}}{\cosh(t)} \left(\cosh(A)\epsilon(\mu r + \nu) - \sinh(A) \sqrt{(\mu r + \nu)^2 + 1} \cosh(\epsilon\sqrt{M}(\phi - d)) \right) \\
 \tanh(\sqrt{M'}\tilde{\tau}') \sqrt{\rho'^2 + M'} &= \sqrt{M'} \tanh(t) \\
 e^{2\sqrt{M'}(\varphi' - f')} &= \frac{\epsilon(\mu r + \nu) - \sqrt{(\mu r + \nu)^2 + 1} \cosh(\epsilon\sqrt{M}(\phi - d) + g)}{\epsilon(\mu r + \nu) - \sqrt{(\mu r + \nu)^2 + 1} \cosh(\epsilon\sqrt{M}(\phi - d) - g)}
 \end{aligned} \tag{6.96}$$

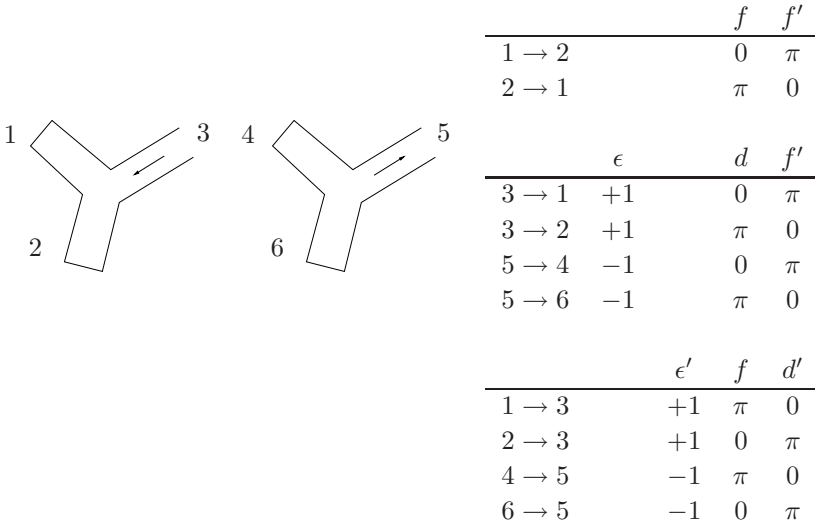


Figure 6.13: Possible transitions involving outer charts. In this picture the charts 1,2,4 and 6 are outer charts and the charts 3 and 5 are inner charts. Conventions are as in figure 6.12.

and conversely,

$$\sqrt{M} \tanh(t') = \tanh(\sqrt{M}\tilde{\tau})\sqrt{\rho^2 + M} \quad (6.97)$$

$$\frac{\epsilon'(\mu' r' + \nu')}{\cosh(t')} = \sqrt{\frac{1}{M}} \left(\cosh(A)\rho + \sinh(A) \cosh(\sqrt{M}(\varphi - f)) \frac{\sqrt{\rho^2 + M}}{\cosh(\sqrt{M}\tilde{\tau})} \right)$$

$$e^{2\epsilon'\sqrt{M'}(\phi' - d')} = \frac{\rho \cosh(\sqrt{M}\tilde{\tau}) + \sqrt{\rho^2 + M} \cosh(\sqrt{M}(\varphi - f) + g)}{\rho \cosh(\sqrt{M}\tilde{\tau}) + \sqrt{\rho^2 + M} \cosh(\sqrt{M}(\varphi - f) - g)}$$

Again, these transition functions are not obviously periodic in ϕ and φ are only valid in the interval $[0, 2\pi)$ and the other boundaries are again found by inserting the coordinate ranges $-1 < r < 1$ and (6.81) in the transition functions. One may again compose the transition functions with (6.73) and its inverse to obtain the transition functions for the twisted coordinate ψ on the inner charts.

Chapter 7

Topologically massive gravity

In this chapter we set up the holographic dictionary for a modified three-dimensional theory of gravity which is called *topologically massive gravity*. We will investigate the asymptotic structure of the solutions to the equation of motion and show the presence of leading and subleading logarithmic terms in the radial expansion. Just as in the examples presented in chapter 1 these inhomogeneous terms represent important structural properties of the boundary theory. We compute various two-point functions and demonstrate that these agree with expectations from a so-called *logarithmic CFT*.

7.1 Introduction

Although three-dimensional Einstein gravity is locally trivial, this is generally no longer the case once higher-derivative terms are added to the action. The addition of such terms provides the theory with propagating degrees of freedom, *i.e.* three-dimensional gravitons. The quantization of such theories therefore appears to give a richer structure than the Einstein theory, yielding potentially interesting toy models for higher-dimensional theories of quantum gravity.

Unfortunately, the addition of generic higher-derivative terms to the Einstein-Hilbert action often gives ghost-like excitations which render the theory unstable. Recently a renewed interest has been taken in the so-called topologically massive (cosmological) gravity [109, 110], or TMG for short. This theory consists of the

Einstein-Hilbert action with a negative cosmological constant plus a gravitational Chern-Simons term

$$S_{\text{cs}} = \frac{1}{32\pi G_N \mu} \int d^3x \sqrt{-G} \epsilon^{\lambda\mu\nu} \left(\Gamma_{\lambda\sigma}^\rho \partial_\mu \Gamma_{\rho\nu}^\sigma + \frac{2}{3} \Gamma_{\lambda\sigma}^\rho \Gamma_{\mu\tau}^\sigma \Gamma_{\nu\rho}^\tau \right). \quad (7.1)$$

Although adding a Chern-Simons term likely leads to instabilities for general values of the dimensionless parameter μ , it was argued in [111] that the theory becomes stable and *chiral* when $\mu = 1$. At that point, which we will call the “chiral point”, all the left-moving excitations of the theory would become pure gauge and one would effectively have a right-moving theory.

Other authors however found non-chiral modes at the chiral point, [112, 113, 114, 115, 116, 117, 118, 119] (see however also [120]). In particular in [113] a left-moving excitation of the linearized equations of motion was explicitly written down¹. From the transformation properties of the new mode of [113] under the (L_0, \bar{L}_0) operators one found a structure typical of a logarithmic conformal field theory (LCFT) and consequently it was claimed that the theory with $\mu = 1$ was dual to such a theory. Since LCFTs are not chiral (and not unitary either), this provided a further argument against the conjecture.

However, near the conformal boundary the new mode does not obey the same falloff conditions as the other modes. This has led to claims that one can ignore the new mode by imposing strict ‘Brown-Henneaux’ [33] boundary conditions: the new mode does not satisfy these so it then has to be discarded and the resulting theory could again be chiral [123]. In [118] a non-chiral mode of the linearized equations of motion, related to that of Grumiller and Johansson but satisfying the Brown-Henneaux boundary conditions, was found. However, [124] argued that this mode is not a linearization of a non-linear solution. This linearization instability was further discussed in [125]. On the other hand, in [126, 127] it was claimed that the Brown-Henneaux boundary conditions could be relaxed to incorporate the non-chiral mode without destroying the consistency of the theory. At first sight one seems to be free to choose either set of boundary conditions, supposedly leading to a different theory for each possibility [124].

The topologically massive theory admits solutions that are asymptotically AdS so one can use the AdS/CFT correspondence to analyze the theory. This is the viewpoint pursued in this chapter. One of the cornerstones of the AdS/CFT correspondence is that the boundary fields parameterizing the boundary conditions of the bulk fields are identified with the sources for the dual operators. It follows that the *leading* boundary behavior must be specified by unconstrained fields, whereas the *subleading* radial behavior of the fields is determined *dynamically* by

¹Solutions of the non-linear equations of motion exhibiting similar asymptotic form were presented earlier in [121, 122].

the equations of motion and should not be fixed by hand. Putting it differently, the subleading radial behavior is obtained by finding *the most general* asymptotic solution to the field equations given boundary data. For theories that admit asymptotically locally AdS solutions the most general asymptotic solution, which is sometimes called the ‘Fefferman-Graham expansion’, can always be found by solving *algebraic* equations. We saw this explicitly in the two examples discussed in section 1.5 and section 1.6 and refer to [31] for a general review. We would like to emphasize that the Fefferman-Graham expansion does *not* have a predetermined form, as is sometimes stated in the literature, but rather the form of the expansion is dynamically determined.

For theories that admit asymptotically (locally) AdS solutions conserved charges can always be defined as what would be the corresponding charges in a dual field theory. Such charges are guaranteed to be finite via the formalism of holographic renormalization which we reviewed in chapter 1. In particular, Ref. [30] provides a first principles proof that these holographic charges are the correct gravitational conserved charges for Asymptotically locally AdS spacetimes. One should contrast the logic here with what is usually done in other papers. The discussion there starts by selecting fall off conditions for all fields, for example the so-called Brown-Henneaux boundary conditions of [33], such that interesting known solutions (such as black holes etc.) are within the allowed class and then it is checked whether these boundary conditions lead to finite conserved charges. On the other hand, here we start by *deriving* the most general Asymptotically locally AdS boundary conditions. Finite conserved charges (which satisfy all expected properties) are then guaranteed by the general results of [30]. Note that the finite conserved charges are related to the 1-point function of the dual energy momentum tensor via the AdS/CFT dictionary. The next simplest quantities to compute are the 2-point functions of the dual operators. These are obtained from solutions of the linearized equations of motion with Dirichlet boundary conditions.

In this chapter we develop the AdS/CFT dictionary for topologically massive gravity. We obtain the most general asymptotic solutions that are Asymptotically locally AdS and compute the holographic one- and two-point functions of the theory at and away from the chiral point. One new feature in this case is that the field equations are third order in derivatives. Ordinarily higher derivative terms are treated as perturbative corrections to two derivative actions and as such they do not change the usual AdS/CFT set-up. In the case of TMG, however, we need to treat the Einstein and Chern-Simons terms on equal footing. The fact that the field equation is third order implies that there is an additional piece of boundary data to be specified. This means that we can fix both a boundary metric (or more precisely, a conformal class) and (part of) the extrinsic curvature. The boundary metric acts as a source for the boundary stress energy tensor, while the

field parametrizing the boundary condition for the extrinsic curvature is a source for a new operator. It turns out that this operator is irrelevant when $\mu > 1$ and it becomes the logarithmic partner of the stress energy tensor as $\mu \rightarrow 1$.

The asymptotic expansion at $\mu = 1$ contains the subleading log piece found earlier in [113]. The coefficient of this term corresponds to the 1-point function of the logarithmic partner of the energy momentum tensor. As this operator is obtained as a limit of an irrelevant operator, its source (as usual) should be treated perturbatively. This source, which is the above mentioned boundary condition for the extrinsic curvature, appears as the coefficient of a *leading order log* term in the solution to the linearized equations of motion (not to be confused with the subleading log of [113] which relates to the 1-point function of this operator). The results for the two-point functions at $\mu = 1$ completely agree with LCFT expectations and the results away from $\mu = 1$ smoothly limit to the $\mu = 1$ results. Bulk instabilities when $\mu \neq 1$ due to negative energy modes also neatly map to properties of the boundary theory, namely negative norm states and correspondingly negativity of the expectation value of the energy momentum tensor in these states.

The remainder of this chapter is structured as follows. After discussing some conventions and presenting the equations of motion, we point out in section 7.3 several aspects of the standard AdS/CFT dictionary which will be crucial in its application to TMG. In section 7.4 we analyze the asymptotic structure of the bulk solutions for $\mu = 1$. We compute the on-shell action, discuss its divergences and the holographic renormalization which enables us to concretely formulate the holographic dictionary. The holographic one point functions satisfy anomalous Ward identities whose interpretation is discussed in section 7.5. Section 7.6 concerns linearized analysis which is used to compute holographically one- and two-point functions for $\mu = 1$. We then repeat this analysis for general μ in section 7.7. We end with a short summary and an outlook. Various appendices contain computational details as well as a discussion of some relevant aspects of logarithmic CFTs.

7.2 Setup and equations of motion

The bulk part of the action has the form:

$$\begin{aligned}
 S = & \frac{1}{16\pi G_N} \int d^3x \sqrt{-G} (R - 2\Lambda) \\
 & + \frac{1}{32\pi G_N \mu} \int d^3x \sqrt{-G} \epsilon^{\lambda\mu\nu} \left(\Gamma_{\lambda\sigma}^{\rho} \partial_{\mu} \Gamma_{\rho\nu}^{\sigma} + \frac{2}{3} \Gamma_{\lambda\sigma}^{\rho} \Gamma_{\mu\tau}^{\sigma} \Gamma_{\nu\rho}^{\tau} \right),
 \end{aligned}
 \tag{7.2}$$

where we use the covariant ϵ -symbol such that $\sqrt{-G}\epsilon^{012} = 1$ with x^2 the radial direction denoted ρ below. We set $\Lambda = -1$ below. We use the following conventions for the curvatures:

$$R_{\mu\nu\rho}{}^\sigma = \partial_\nu\Gamma_{\mu\rho}^\sigma + \Gamma_{\mu\rho}^\lambda\Gamma_{\nu\lambda}^\sigma - (\mu \leftrightarrow \nu), \quad R_{\mu\rho} = R_{\mu\sigma\rho}{}^\sigma. \quad (7.3)$$

All Greek indices run over three dimensions, all Latin indices over two dimensions. In three dimensions the Weyl tensor vanishes identically, which means that:

$$R_{\mu\nu\rho\sigma} = G_{\mu\rho}R_{\sigma\nu} - G_{\nu\rho}R_{\sigma\mu} - \frac{1}{2}RG_{\mu\rho}G_{\sigma\nu} - (\rho \leftrightarrow \sigma). \quad (7.4)$$

The equation of motion derived from (7.2) becomes:

$$R_{\mu\nu} - \frac{1}{2}G_{\mu\nu}R - G_{\mu\nu} + \frac{1}{\mu}C_{\mu\nu} = 0, \quad (7.5)$$

with $C_{\mu\nu}$ the Cotton tensor:

$$C_{\mu\nu} = \epsilon_\mu{}^{\alpha\beta}\nabla_\alpha(R_{\beta\nu} - \frac{1}{4}RG_{\beta\nu}). \quad (7.6)$$

Using (7.4) we find that the Bianchi identity becomes:

$$C_{\mu\nu} - C_{\nu\mu} = 0. \quad (7.7)$$

The last term in the r.h.s. of (7.6) is totally antisymmetric in μ and ν and therefore merely subtracts the antisymmetric piece from the first term in the r.h.s. of (7.6). We alternatively have:

$$C_{\mu\nu} = \frac{1}{2}\left(\epsilon_\mu{}^{\rho\sigma}\nabla_\rho R_{\sigma\nu} + \epsilon_\nu{}^{\rho\sigma}\nabla_\rho R_{\sigma\mu}\right). \quad (7.8)$$

It is not hard to verify that

$$C_\mu{}^\mu = 0, \quad \nabla_\mu C^{\mu\nu} = 0. \quad (7.9)$$

Taking the trace of (7.5) we therefore find that:

$$R = -6, \quad (7.10)$$

independent of μ . Substituting this back, we find:

$$R_{\mu\nu} + 2G_{\mu\nu} + \frac{1}{\mu}\epsilon_\mu{}^{\rho\sigma}\nabla_\rho R_{\sigma\nu} = 0, \quad (7.11)$$

from which we also obtain that any solution to the Einstein equations has $R_{\mu\nu} = -2G_{\mu\nu}$ and is a solution to these equations as well.

7.3 Aspects of the AdS/CFT dictionary

In this section we review several aspects of the AdS/CFT dictionary that will be used below. In subsection 7.3.1 we discuss the asymptotic expansion of the bulk fields. We then consider the possibility of switching on sources for irrelevant operators in subsection 7.3.2 and finally discuss in subsection 7.3.3 how the dictionary should be modified in the presence of higher-derivative terms.

7.3.1 Asymptotic expansion of the bulk fields

In section 1.4 we discussed in detail the notion of AlAdS spacetimes and the corresponding structure in the asymptotic expansion of the solutions to the equations of motion. In particular, for a generic field the coefficients in a radial expansion are determined locally to very high order, as we explicitly demonstrated in the two examples of section 1.5 and section 1.6. The specific form of the subleading terms, including the radial power where the first subleading terms appears, depends however on the bulk theory under question and is not fixed a priori. For example, for Einstein gravity in $(d+1)$ dimensions we described in section 1.6 that in the Fefferman-Graham coordinate system:

$$ds^2 = \frac{dz^2}{z^2} + \frac{1}{z^2} g_{ij} dx^i dx^j \quad (7.12)$$

the corresponding expansion reads

$$g_{ij} = g_{(0)ij} + z^2 g_{(2)ij} + \dots + z^d (g_{(d)ij} + h_{(d)ij} \log(z)) + \dots \quad (7.13)$$

The fact that the subleading term starts at order z^2 is however specific to pure Einstein gravity. For example, $3d$ Einstein gravity coupled to matter can have the first subleading term appearing at order z , see [128] for an example. The logarithmic term $h_{(d)}$ appears in Einstein gravity when d is an even integer greater than 2. As we reviewed in section 1.6, this coefficient is given by the metric variation of the conformal anomaly. This fact immediately explains why there is no such coefficient in Einstein gravity when $d = 2$: in this case the conformal anomaly is given by a topological invariant and therefore its variation w.r.t. the metric vanishes. As soon as the bulk action contains additional fields the expansion will be modified accordingly [27, 64, 128, 65]. For example, the asymptotic solution for three dimensional Einstein gravity coupled to a free massless scalar field is of the form (7.13) with a non-zero $h_{(2)}$ coefficient, see equation (5.25) of [27]². Note

²Ref. [129], appendix E, contains an example of 3d gravity coupled to scalars with \log^2 terms in the asymptotic expansion.

that the log term found in [113] is precisely of this form. From this perspective the appearance of such a term in the asymptotic expansion of TMG is certainly not surprising.

What is however universal in this discussion is the structure of these expansions. The subleading coefficients are determined locally in terms of $g_{(0)}$ by solving asymptotically the field equations. This procedure leads to algebraic equations that can be readily solved. On the other hand, $g_{(d)}$ is not locally determined by $g_{(0)}$ but rather by global constraints like regularity of the bulk metric in the interior of M . This term is related to the 1-point function of T_{ij} .

To repeat, according to the standard AdS/CFT dictionary the allowed subleading terms in expansions like (7.13) (and similarly (1.72) in chapter 1) are determined by the equations of motion rather than fixed by hand. As long as the metric has the form (7.13) with a regular metric $g_{(0)}$, the AIAdS properties of (M, G) are unchanged.

7.3.2 Sources for irrelevant operators

As we explained in section 1.4, the fact that an asymptotically AdS metric becomes that of AdS near conformal infinity is dual to the statement that the boundary theory becomes conformal at high energies. Asymptotically AdS metrics describe relevant deformations of the CFT and/or vevs in the boundary theory.

On the other hand, one may also attempt to switch on sources for irrelevant operators. Such deformations are for example necessary to compute correlation functions of irrelevant operators, as these are obtained by functionally differentiating the on-shell action with respect to these sources. Switching on these sources spoils the conformal UV behavior of the field theory. Correspondingly, the bulk solutions will no longer be AIAdS and the usual AdS/CFT dictionary would break down. In particular, the usual counterterms no longer suffice to make the on-shell action finite, completely analogous to the nonrenormalizability of the field theory with such sources.

A consistent perturbative approach may however be set up by treating the sources for irrelevant operators as infinitesimal [27]. In the bulk, this means that one starts from an AIAdS solution and computes the bulk solution and the on-shell action to any given order n in the sources. This approximation allows for the computation of n -point functions of the irrelevant operator in any given state dual to the background AIAdS solution. We will see a concrete example worked out below.

7.3.3 Higher-derivative terms

Higher-derivative terms in the bulk action are usually treated perturbatively and in that case do not directly lead to a change in the setup described above. However, for TMG we cannot afford to treat these terms as perturbations as we want to study the complete theory around $\mu = 1$. The solution to the bulk equations of motion is then generally no longer fixed by the specification of Dirichlet data alone and some extra boundary data is needed; for example the z -derivatives of the metric g_{ij} at the boundary. Correspondingly, the on-shell action depends on these boundary data as well. We shall see below that this is precisely what happens for TMG.

Extending the usual AdS/CFT logic, we interpret the new boundary data as a new source for another operator in the field theory. Functionally differentiating the on-shell action with respect to this new boundary data then yields correlation functions of this new operator. To make contact with earlier results, notice that for TMG this operator creates the massive graviton states in the bulk and for $\mu = 1$ it creates the logarithmic solution found in [113]. One may say that these spaces have only a single operator insertion in the infinite past.

It turns out that this new operator is irrelevant for $\mu > 1$, as for $\mu \geq 1$ we find that switching on the corresponding source spoils the AlAdS properties of the spacetime. Following the discussion of the previous subsection, we therefore will have to treat the source as infinitesimal and approach the problem perturbatively to a given order in the source. This is precisely what we will do in section 7.6.2.

7.4 Asymptotic analysis for $\mu = 1$

In this section we return to TMG and carry out an asymptotic analysis of the equations of motion (7.5) in the Fefferman-Graham coordinate system. Note that because of (7.10) all conformally compact solutions of this theory are asymptotically locally AdS. However, not all solution of TMG are conformally compact. For example, the ‘warped’ solutions of [130] have a degenerate boundary metric, as is demonstrated in appendix 7.E, and thus they are not conformally compact. In this section we restrict to the AlAdS case. We compute the on-shell action, discuss the variational principle in detail and demonstrate how one holographically computes one-point functions in the CFT. As indicated in the previous section, we will find irrelevant operators and therefore the complete holographic renormalization of the on-shell action has to be done perturbatively. This is postponed until the next section, where we will renormalize the action to second order in the perturbations.

Although this and the next section focus on the case $\mu = 1$, μ is sometimes reinstated for later convenience.

7.4.1 Fefferman-Graham equations of motion

Following the discussion in section 1.4.3, we take the metric to be of the Fefferman-Graham form:

$$ds^2 = \frac{d\rho^2}{4\rho^2} + \frac{1}{\rho} g_{ij}(x, \rho) dx^i dx^j \quad (7.14)$$

where we defined $\rho = z^2$. As should be clear from section 1.4.3, this form of the metric is not an ansatz but it is a direct consequence of the AlAdS property of the spacetime. In other words, the metric of any AlAdS spacetime can be brought to this form near the conformal boundary. In this coordinate system the equations of motion (7.5) take the following form. For the component equations we find:

$$\begin{aligned} & -\frac{1}{2}\text{tr}(g^{-1}g'') + \frac{1}{4}\text{tr}(g^{-1}g'g^{-1}g') + \frac{1}{4\mu}\epsilon^{ij}\left(\nabla_i\nabla^k g'_{kj} + 2\rho(g''g^{-1}g')_{ji}\right) = 0, \\ & \left(\frac{1}{2}\text{tr}(g^{-1}g'') - \frac{1}{4}[\text{tr}(g^{-1}g')]^2\right)g_{ij} - g''_{ij} + \frac{1}{2}g'_{ij}\text{tr}(g^{-1}g') \\ & \quad + \frac{1}{\mu}\epsilon_i^k\left\{\frac{1}{4}\nabla_k\nabla^m g'_{mj} + \frac{1}{4}\nabla_j\nabla^m g'_{mk} - \frac{1}{2}\nabla_k\nabla_j[\text{tr}(g^{-1}g')] + 2\rho g'''_{jk} + \right. \\ & \quad \left. g''_{kj}\left[3 - \frac{3}{2}\rho\text{tr}(g^{-1}g')\right] + g'_{kj}\left(-\frac{3}{2}\text{tr}(g^{-1}g') + \frac{3}{4}\rho[\text{tr}(g^{-1}g')]^2\right) \right. \\ & \quad \left. - \frac{7}{2}\rho\text{tr}(g^{-1}g'') + \frac{7}{4}\rho\text{tr}(g^{-1}g'g^{-1}g')\right\} + i \leftrightarrow j = 0, \\ & (g^{kj} - \mu\epsilon^{kj})\nabla_k g'_{ij} - \nabla_i\left(\text{tr}(g^{-1}g') + \frac{1}{2}\rho\text{tr}(g^{-1}g'g^{-1}g') - \rho[\text{tr}(g^{-1}g')]^2\right) \\ & \quad + 2\rho\nabla^n\left(g''_{in} - \text{tr}(g^{-1}g')g'_{in}\right) + \rho(g^{-1}g')^k_i\nabla^l g'_{kl} = 0, \end{aligned} \quad (7.15)$$

whereas the trace equation $R = -6$ becomes:

$$-4\rho\text{tr}(g^{-1}g'') + 3\rho\text{tr}(g^{-1}g'g^{-1}g') - \rho[\text{tr}(g^{-1}g')]^2 + R(g) + 2\text{tr}(g^{-1}g') = 0. \quad (7.16)$$

A prime denotes a derivative with respect to ρ . The derivation of these equations is given in appendix 7.A.

7.4.2 Asymptotic solution

Rather than the usual asymptotic behavior $\lim_{\rho \rightarrow 0} g_{ij}(\rho, x^k) = g_{(0)ij}(x^k)$, the equations of motion for $\mu = 1$ also allow leading log asymptotics for g_{ij} . We therefore substitute the expansion

$$g_{ij} = b_{(0)ij} \log(\rho) + g_{(0)ij} + b_{(2)ij} \rho \log(\rho) + g_{(2)ij} + \dots \quad (7.17)$$

into the equations of motion. The subleading logarithmic term $b_{(2)ij}$ in this expansion is the mode considered in [113]. The leading logarithmic term $b_{(0)ij}$, on the other hand, changes the asymptotic structure of the spacetime and it is no longer AIAdS. Following the discussion in section 7.3.2, we will treat $b_{(0)ij}$ to be infinitesimal and work perturbatively in $b_{(0)ij}$. As we will be interested in two-point functions around a background with $b_{(0)ij} = 0$, it suffices to retain only terms linear in $b_{(0)ij}$ in the equations that follow.

Under these conditions we find:

$$\begin{aligned}
 g'_{ij} &= \frac{b_{(0)ij}}{\rho} + b_{(2)ij} \log(\rho) + b_{(2)ij} + g_{(2)ij} + \dots, \\
 g''_{ij} &= -\frac{b_{(0)ij}}{\rho^2} + \frac{b_{(2)ij}}{\rho} + \dots, \\
 g'''_{ij} &= \frac{2b_{(0)ij}}{\rho^3} - \frac{b_{(2)ij}}{\rho^2} + \dots, \\
 g^{ij} &= g_{(0)}^{ij} - b_{(0)}^{ij} \log(\rho) - b_{(2)}^{ij} \rho \log(\rho) - \rho g_{(2)}^{ij} + \mathcal{O}(b_{(0)}) + \dots,
 \end{aligned} \tag{7.18}$$

where in the last line indices are raised with $g_{(0)}$ and the $\mathcal{O}(b_{(0)})$ terms are of the form $b_{(2)k}^i b_{(0)}^{kj} \rho \log^2(\rho) + g_{(2)k}^i b_{(0)}^{kj} \rho \log(\rho)$, but will never be needed in what follows.

Substituting this expansion in the equations of motion (7.15) and (7.16), we find the following. To leading order we find both from the $(\rho\rho)$ equation as well as from the R equation that:

$$\text{tr}(b_{(0)}) = 0. \tag{7.19}$$

Notice that traces are now implicitly taken using $g_{(0)}$, that is $\text{tr}(b_{(0)}) \equiv g_{(0)}^{ij} b_{(0)ij}$. Also, in this subsection the ϵ -symbol and covariant derivatives are defined using $g_{(0)}$. From the (ij) equation we find that:

$$P_i^k b_{(0)kj} = 0, \tag{7.20}$$

where we define the projection operators:

$$P_i^k \equiv \frac{1}{2}(\delta_i^k + \epsilon_i^k), \quad \bar{P}_i^k \equiv \frac{1}{2}(\delta_i^k - \epsilon_i^k), \tag{7.21}$$

and we obtain no new constraint from the (ρi) equation at leading order.

At subleading order we encounter various log terms. From the R equation we find at order $\log^2(\rho)$ that

$$\text{tr}(b_{(2)} g_{(0)}^{-1} b_{(0)}) = 0 \tag{7.22}$$

and at order $\log(\rho)$ we then find:

$$-2\text{tr}(b_{(0)} g_{(0)}^{-1} g_{(2)}) + 2\text{tr}(b_{(2)}) + \tilde{R}[b_{(0)}] = 0, \tag{7.23}$$

with $\tilde{R}[b_{(0)}]$ the linearized curvature:

$$R[g] = R[g_{(0)}] + \log(\rho)\tilde{R}[b_{(0)}] + \dots, \quad (7.24)$$

which can be more explicitly written as:

$$\tilde{R}[b_{(0)}] = \nabla^i \nabla^j b_{(0)ij}, \quad (7.25)$$

where we used the properties of $b_{(0)ij}$ found at leading order. At subleading order in the $(\rho\rho)$ equation we again obtain (7.22) and (7.23). At order one in the R equation we obtain:

$$-2\text{tr}(b_{(2)}) + 2\text{tr}(g_{(2)}) + R[g_{(0)}] = 0. \quad (7.26)$$

For the (ij) equation the subleading terms at order $\log(\rho)/\rho$ give

$$(b_{(0)}g_{(0)}^{-1}b_{(2)})_{ij} + (b_{(2)}g_{(0)}^{-1}b_{(0)})_{ij} = 0, \quad (7.27)$$

and at order $1/\rho$ we obtain:

$$\bar{P}_i^k b_{(2)kj} = \frac{1}{2}(b_{(2)ij} - \epsilon_i^k b_{(2)kj}) = \mathcal{O}(b_{(0)ij}), \quad (7.28)$$

where the right-hand side is an expression linear in $b_{(0)ij}$ that we will not need below.

For the (ρi) equation, we find at subleading order that:

$$\bar{P}_i^k (\nabla^j g_{(2)jk} + \frac{1}{2} \nabla_k R[g_{(0)}]) = \nabla^l b_{(2)li} + \mathcal{O}(b_{(0)}). \quad (7.29)$$

We may apply (7.28) to rewrite schematically $b_{(2)ij} \rightarrow P_i^k b_{(2)kj} + \mathcal{O}(b_{(0)})$. Since P_i^k and \bar{P}_i^k are projection operators onto orthogonal subspaces we can split this equation into:

$$\bar{P}_i^k (\nabla^j g_{(2)jk} + \frac{1}{2} \nabla_k R[g_{(0)}]) = \mathcal{O}(b_{(0)}), \quad \nabla^l b_{(2)li} = \mathcal{O}(b_{(0)}). \quad (7.30)$$

If $b_{(0)ij} = 0$ then the first of these equations agrees with [131].

7.4.3 On-shell action

In this section we will write the on-shell action in Fefferman-Graham coordinates and analyze the divergences obtained by substituting the expansion (7.17).

We begin by computing the on-shell value of the Chern-Simons part of the action,

$$I_{\text{cs}} = \frac{1}{32\pi G_N \mu} \int d^3x \sqrt{-G} \epsilon^{\lambda\mu\nu} \left(\Gamma_{\lambda\sigma}^\rho \partial_\mu \Gamma_{\rho\nu}^\sigma + \frac{2}{3} \Gamma_{\lambda\sigma}^\rho \Gamma_{\mu\tau}^\sigma \Gamma_{\nu\rho}^\tau \right), \quad (7.31)$$

in Fefferman-Graham coordinates. Observing that the ϵ -symbol implies that only one of the indices λ , μ or ν can be the radial direction, we can directly write out the various terms. Using then (7.151) and (7.153) from appendix 7.A we find that many terms cancel due to the antisymmetry of ϵ^{ij} and we are left with:

$$\frac{1}{32\pi G_N \mu} \int d^3x \sqrt{-g} \epsilon^{ij} \left(2\rho (g' g^{-1} g'')_{ij} - \Gamma_{ib}^a \partial_\rho \Gamma_{aj}^b \right), \quad (7.32)$$

where the connection coefficients and ϵ tensor are now those associated with g_{ij} . Substituting (7.17), it is not hard to verify that this action is finite for $\rho_0 \rightarrow 0$ if $b_{(0)ij} = 0$, but there are log divergences if $b_{(0)ij}$ is nonzero.

For the Einstein-Hilbert action, the variational principle can be made well-defined for Dirichlet boundary conditions at a *finite* radial distance by the addition of the Gibbons-Hawking term [32]. In our conventions, this means that the Einstein part of the action is given by:

$$I_{\text{gr}} = \frac{1}{16\pi G_N} \int d^3x \sqrt{-G} (R - 2\Lambda) + \frac{1}{8\pi G_N} \int d^2x \sqrt{-\gamma} K, \quad (7.33)$$

where $\gamma_{ij} = g_{ij}/\rho$ is the induced metric on the cutoff surface $\rho = \rho_0$, which is kept fixed in the variational problem. Furthermore, K is the trace of the extrinsic curvature of this surface, which is defined using the outward pointing unit normal $n_\mu dx^\mu = -d\rho/(2\rho)$.

This variational problem becomes ill-posed as $\rho_0 \rightarrow 0$, since the induced metric γ diverges in this limit. What one should instead keep fixed is the conformal class of γ (or $g_{(0)}$ after taking into account the issues related to the conformal anomaly) [30]. This requires introducing additional boundary terms. These boundary terms not only make the variational problem well-posed but also make the on-shell action finite as $\rho_0 \rightarrow 0$. In particular, for the pure Einstein theory the counterterm action is

$$I_{\text{ct}} = \frac{1}{8\pi G_N} \int d^2x \sqrt{-\gamma} \left(-1 + \frac{1}{4} R[\gamma] \log(\rho_0) \right). \quad (7.34)$$

which directly follows from (1.164) with $d = 2$. Substituting the Fefferman-Graham form of the metric we find:

$$\begin{aligned} I_{\text{gr}} &= -\frac{1}{16\pi G_N} \int d^3x \frac{2}{\rho^2} \sqrt{-g} + \frac{1}{16\pi G_N} \int d^2x \frac{1}{\rho} \sqrt{-g} (4 - 2\rho \text{tr}(g^{-1} g')), \\ I_{\text{ct}} &= \frac{1}{8\pi G_N} \int d^2x \sqrt{-g} \left(-\frac{1}{\rho_0} + \frac{1}{4} R[g] \log(\rho_0) \right). \end{aligned} \quad (7.35)$$

We may now substitute the radial expansion (7.17) for g_{ij} and find the same behavior as for the Chern-Simons part: the action $I_{\text{gr}} + I_{\text{ct}}$ is finite when $b_{(0)ij} = 0$ but diverges otherwise.

We now define the following combined action:

$$I_c = I_{\text{gr}} + I_{\text{cs}} + I_{\text{ct}}, \quad (7.36)$$

which we emphasize is finite only as long as $b_{(0)ij}$ vanishes and needs to be supplemented with additional boundary counterterms otherwise. As we explained in section 7.3, this will be done perturbatively up to the required order in $b_{(0)ij}$. We will do an explicit analysis to second order in section 7.6, but first we discuss the variational principle and the computation of the one-point functions in general terms.

Variational principle

In this subsection we compute the variation of the combined action I_c defined in (7.36), which will be needed below in the holographic computation of boundary correlation functions.

First of all, according to (1.137) the variation of the Einstein-Hilbert action plus Gibbons-Hawking term has the form:

$$\delta I_{\text{gr}} = \int d^3x (\text{eom}) + \frac{1}{16\pi G_N} \int d^2x \sqrt{-\gamma} [\gamma^{ij} K - K^{ij}] \delta \gamma_{ij}, \quad (7.37)$$

and in Fefferman-Graham coordinates we find that:

$$\begin{aligned} \delta I_{\text{gr}} &= \int d^3x (\text{eom}) + \frac{1}{16\pi G_N} \int d^2x \sqrt{-g} \left(\frac{1}{\rho} g^{ij} + g'^{ij} - g^{ij} \text{tr}(g^{-1} g') \right) \delta g_{ij}, \\ \delta I_{\text{ct}} &= -\frac{1}{16\pi G_N} \frac{1}{\rho} \int d^2x \sqrt{-g} g^{ij} \delta g_{ij}. \end{aligned} \quad (7.38)$$

As for the Chern-Simons part, we find that

$$\delta I_{\text{cs}} = \frac{1}{32\pi G_N \mu} \int d^3x \sqrt{-G} \epsilon^{\lambda\mu\nu} C_{\lambda\sigma}^{\rho} R_{\nu\mu\rho}{}^{\sigma} + \frac{1}{32\pi G_N \mu} \int d^2x \sqrt{-\gamma} \epsilon^{\lambda\mu\nu} n_{\mu} \Gamma_{\lambda\sigma}^{\rho} C_{\nu\rho}^{\sigma}, \quad (7.39)$$

with

$$C_{\mu\nu}^{\lambda} = \delta \Gamma_{\mu\nu}^{\lambda} = \frac{1}{2} G^{\lambda\sigma} (\nabla_{\mu} \delta G_{\nu\sigma} + \nabla_{\nu} \delta G_{\mu\sigma} - \nabla_{\sigma} \delta G_{\mu\nu}) \quad (7.40)$$

and n_{μ} the outward pointing unit normal to the boundary and γ_{ij} the induced metric on the boundary. Integrating the bulk part once more by parts, we find:

$$\begin{aligned} \delta I_{\text{cs}} &= -\frac{1}{32\pi G_N \mu} \int d^3x \sqrt{-G} \epsilon^{\lambda\mu\nu} (\nabla_{\sigma} R_{\nu\mu}{}^{\rho\sigma}) \delta G_{\lambda\rho} \\ &\quad + \frac{1}{32\pi G_N \mu} \int d^2x \sqrt{-\gamma} \epsilon^{\lambda\mu\nu} (n_{\mu} \Gamma_{\lambda\sigma}^{\rho} C_{\nu\rho}^{\sigma} + n_{\sigma} R_{\nu\mu}{}^{\rho\sigma} \delta G_{\lambda\rho}) \end{aligned} \quad (7.41)$$

The first term eventually becomes the Cotton tensor in the equation of motion, using (7.4) and the Bianchi identity.

Substituting now once more the Fefferman-Graham metric (7.14), we find $n_\mu dx^\mu = -d\rho/(2\rho)$ and the surface terms can be rewritten to yield:

$$\begin{aligned} \delta I_{\text{cs}} = & \int d^3x (\text{eom}) + \frac{1}{16\pi G_N \mu} \int d^2x \sqrt{-g} \epsilon^{ij} \left(\frac{1}{2} \Gamma_{ik}^l \delta \Gamma_{jl}^k + (g' g^{-1} \delta g)_{ij} \right. \\ & \left. - \rho (g' g^{-1} \delta g')_{ij} + 2\rho (g'' g^{-1} \delta g)_{ij} - \rho (g' g^{-1} g' g^{-1} \delta g)_{ij} \right), \end{aligned} \quad (7.42)$$

with all covariant terms defined using g_{ij} . Notice that if $b_{(0)ij} = 0$ then all terms are finite in the limit where the radial cutoff $\rho_0 \rightarrow 0$, in agreement with the above analysis for the on-shell action.

Combining then (7.38) and (7.42), the variation of the combined action I_c defined in (7.36) is:

$$\begin{aligned} \delta I_c = & \frac{1}{16\pi G_N} \int d^2x \sqrt{-g} \left\{ g'_{ij} - g_{ij} \text{tr}(g^{-1} g') \right\} (g^{-1} (\delta g) g^{-1})^{ij} \\ & + \frac{1}{16\pi G_N \mu} \int d^2x \sqrt{-g} \left\{ \frac{1}{2} A_{ij} - 2\rho \epsilon_i^k [g''_{kj} - \frac{1}{2} (g' g^{-1} g')_{kj}] - \epsilon_i^k g'_{kj} \right\} (g^{-1} (\delta g) g^{-1})^{ij} \\ & + \frac{1}{16\pi G_N \mu} \int d^2x \sqrt{-g} \rho \epsilon_i^k g'_{kj} (g^{-1} (\delta g') g^{-1})^{ij}. \end{aligned} \quad (7.43)$$

where the term A_{ij} is a local term and is defined via:

$$\int d^2x \sqrt{-g} \epsilon^{ij} \Gamma_{ik}^l \delta \Gamma_{jl}^k = \int d^2x \sqrt{-g} A^{ij} \delta g_{ij}. \quad (7.44)$$

Explicitly, we find:

$$\begin{aligned} A_{ij} = & \frac{1}{4} \left[\epsilon^{kl} g_i^m g_{jn} + \epsilon_i^l g_j^m g_n^k - \epsilon_j^l g^{mk} g_{in} + (i \leftrightarrow j) \right] \nabla_k \Gamma_{lm}^n \\ = & \left[-\frac{1}{8} \epsilon_i^k \epsilon_j^l \epsilon^{mn} \nabla_l \partial_m g_{nk} + (i \leftrightarrow j) \right] + \frac{1}{4} \epsilon^{kl} \nabla_k \partial_l g_{ij}. \end{aligned} \quad (7.45)$$

Notice that the last term in (7.43) involves $\delta g'_{ij}$ and therefore changes the variational principle for this action. Although one may explicitly check that it vanishes if $b_{(0)ij} = 0$ and for $\rho_0 \rightarrow 0$ [132], this is no longer the case for nonzero $b_{(0)ij}$. As expected for a three-derivative bulk action, the on-shell action is a functional of both g_{ij} and g'_{ij} at the boundary and we can take functional derivatives with respect to both of them.

7.4.4 One-point functions

From the previous section it follows that there are two independent sources that should be specified at the conformal boundary, which are asymptotically related to

g_{ij} and g'_{ij} . According to the asymptotic solution (7.17) obtained in section 7.4.2 we can indeed independently specify both $b_{(0)ij}$ and $g_{(0)ij}$ and one can take these as the two boundary sources. These fields then source two operators which will be denoted t_{ij} and T_{ij} , respectively, with T_{ij} the usual energy-momentum tensor of the boundary theory. The standard AdS/CFT dictionary now dictates:

$$\langle T_{ij} \rangle = \frac{-4\pi}{\sqrt{-g_{(0)}}} \frac{\delta I}{\delta g_{(0)}^{ij}}, \quad \langle t_{ij} \rangle = \left(\frac{-4\pi}{\sqrt{-g_{(0)}}} \frac{\delta I}{\delta b_{(0)}^{ij}} \right)_L, \quad (7.46)$$

where the subscript ‘L’ means a projection onto the chiral traceless component,

$$(t_{ij})_L \equiv P_i^k (t_{kj} - \frac{1}{2} g_{kj} \text{tr}(t)), \quad (7.47)$$

whose origin is explained in the next paragraph. The signs and factors in (7.46) are explained in appendix 7.B. Notice that the on-shell action I on the right-hand sides of (7.46) coincides with I_c defined in (7.36) only to zeroth order in $b_{(0)ij}$, and as explained above additional boundary counterterms will be needed to render it finite to higher orders in $b_{(0)ij}$.

The projection onto the ‘L’ component originates as follows. Since $P_i^k b_{(0)kj} = \text{tr}(b_{(0)}) = 0$, $b_{(0)ij}$ has only a single nonvanishing component. We can therefore only take functional derivatives with respect to this component and we find that t_{ij} only has one component as well. For example, when we use lightcone coordinates and the boundary metric is flat, $g_{(0)ij} dx^i dx^j = dudv$, then in our conventions (see appendix 7.B) only $b_{(0)uu}$ is nonzero. Correspondingly, the only non-zero component of t_{ij} is t_{vv} and taking the ‘L’ piece projects onto this component.

To make contact with the regulated on-shell action which explicitly depends on g_{ij} and g'_{ij} , we observe that:

$$g_{(0)}^{ij} = \lim_{\rho \rightarrow 0} (g^{ij} + \rho \log(\rho) g'^{ij}), \quad b_{(0)ij} = \lim_{\rho \rightarrow 0} \rho g'^{ij}, \quad (7.48)$$

and therefore the one-point functions can be obtained concretely by computing:

$$\begin{aligned} \langle t_{ij} \rangle &= \lim_{\rho \rightarrow 0} \left(\frac{-4\pi}{\rho \sqrt{-g}} \frac{\delta I}{\delta g'^{ij}} + \log(\rho) \frac{4\pi}{\sqrt{-g}} \frac{\delta I}{\delta g^{ij}} \right)_L, \\ \langle T_{ij} \rangle &= \lim_{\rho \rightarrow 0} \frac{-4\pi}{\sqrt{-g}} \frac{\delta I}{\delta g^{ij}}, \end{aligned} \quad (7.49)$$

which are the main expressions that will be used in the following sections.

Explicit expressions for vanishing $b_{(0)ij}$

If we set $b_{(0)ij} = 0$ then the combined action I_c is finite on-shell. Although we then cannot take functional derivatives with respect to $b_{(0)ij}$, we can still compute

correlation functions involving the energy-momentum tensor by using the first equation in (7.46) with $I = I_c$. Explicitly, this means that we use (7.43) and substitute the expansion (7.17) with $b_{(0)ij} = 0$. This leads to the following one-point functions:

$$\begin{aligned}
 \langle T_{ij} \rangle &\equiv \lim_{\rho \rightarrow 0} \frac{-4\pi}{\sqrt{-g}} \frac{\delta I_c}{\delta g^{ij}} \\
 &= \frac{1}{4G_N} \left(g'_{ij} - g_{ij} \text{tr}(g^{-1}g') - \frac{1}{\mu} \left(\frac{1}{2} \epsilon_i^k g'_{kj} + \rho \epsilon_i^k g''_{kj} + (i \leftrightarrow j) \right) + \frac{1}{2\mu} A_{ij}[g_{ij}] \right) \\
 &= \frac{1}{4G_N} \left(g_{(2)ij} + \frac{1}{2} R[g_{(0)}] g_{(0)ij} - \frac{1}{2\mu} \left(\epsilon_i^k g_{(2)kj} + (i \leftrightarrow j) \right) - \frac{2}{\mu} b_{(2)ij} + \frac{1}{2\mu} A_{ij}[g_{(0)ij}] \right)
 \end{aligned} \tag{7.50}$$

where we defined ϵ_i^k using $g_{(0)}$ and also used the various properties of $b_{(2)ij}$ found above, in particular the condition $\epsilon_i^k b_{(2)kj} = b_{(2)ij}$ which ensured the absence of a logarithmic divergence. Notice that an extra sign arises because we functionally differentiate with respect to the inverse metric, whereas (7.43) uses a variation in the metric itself. The expression for the energy momentum tensor with $b_{(0)ij} = b_{(2)ij} = 0$ was also derived previously in [132]. The authors of [113] computed T_{ij} for non-zero $b_{(2)ij}$ and flat $g_{(0)}$. The result in equation (48) of [113] however is missing the $b_{(2)}$ term.

Using $g_{(0)}$ to raise indices and define covariant derivatives and using the above properties of $b_{(2)ij}$ and $g_{(2)ij}$, we find the following Ward identities:

$$\begin{aligned}
 \langle T_i^i \rangle &= \frac{1}{4G_N} \left(\frac{1}{2} R[g_{(0)}] + \frac{1}{2\mu} A_i^i[g_{(0)}] \right), \\
 \nabla^j \langle T_{ij} \rangle &= \frac{1}{4\mu G_N} \left(\frac{1}{4} \epsilon_{ij} \nabla^j R[g_{(0)}] + \frac{1}{2} \nabla^j A_{ij}[g_{(0)}] \right).
 \end{aligned} \tag{7.51}$$

These results agree with analogous computations in [131] and for $\mu \rightarrow \infty$ we also recover the results for Einstein gravity of section 1.6. We will discuss their interpretation in the next section.

Example: conserved charges for the BTZ black hole

The holographic energy momentum can be used to compute the conserved charges, namely the mass and the angular momentum, for the rotating BTZ black hole. The metric can be written in Fefferman-Graham coordinates as:

$$\begin{aligned}
 ds^2 &= \frac{d\rho^2}{4\rho^2} - \left[\frac{1}{\rho} - \frac{1}{2}(r_+^2 + r_-^2) + \frac{1}{4}(r_+^2 - r_-^2)^2 \rho \right] dt^2 \\
 &\quad + \left[\frac{1}{\rho} + \frac{1}{2}(r_+^2 + r_-^2) + \frac{1}{4}(r_+^2 - r_-^2)^2 \rho \right] d\phi^2 + 2r_+ r_- dt d\phi,
 \end{aligned} \tag{7.52}$$

from which we find the following one-point function (using $\epsilon_{t\phi} = -1$):

$$\begin{aligned}\langle T_{tt} \rangle &= \langle T_{\phi\phi} \rangle = \frac{1}{8G_N} (r_+^2 + r_-^2 + \frac{2}{\mu} r_+ r_-), \\ \langle T_{t\phi} \rangle &= \frac{1}{8G_N} (2r_+ r_- + \frac{1}{\mu} r_+^2 + r_-^2).\end{aligned}\tag{7.53}$$

Notice that our normalization of the energy-momentum tensor differs by a factor of 2π from that used in much of the AdS/CFT literature. We obtain the conserved charges:

$$\begin{aligned}M &= - \int d\phi T_t^t = \frac{\pi}{4G_N} [r_+^2 + r_-^2 + \frac{2}{\mu} r_+ r_-], \\ J &= - \int d\phi T_\phi^t = \frac{\pi}{4G_N} [2r_+ r_- + \frac{1}{\mu} (r_+^2 + r_-^2)].\end{aligned}\tag{7.54}$$

Up to the change in the overall normalization, these expressions agree with [133, 132] and in the Einstein case $\mu \rightarrow \infty$ they reduce to the usual expressions. In lightcone coordinates $u = t + \phi, v = -t + \phi$ we find that

$$\begin{aligned}\langle T_{uu} \rangle &= \frac{1}{G_N} \left((1 + \frac{1}{\mu})(r_+^2 + r_-^2) + 2(\frac{1}{\mu} + 1)r_+ r_- \right), \\ \langle T_{vv} \rangle &= \frac{1}{G_N} \left((1 - \frac{1}{\mu})(r_+^2 + r_-^2) + 2(\frac{1}{\mu} - 1)r_+ r_- \right).\end{aligned}\tag{7.55}$$

so when $\mu = 1$ only T_{uu} is nonzero.

7.5 Anomalies

In this section we will discuss and interpret the anomalous Ward identities (7.51). We will first consider the diffeomorphism anomaly and show that it agrees exactly with the expression expected from Wess-Zumino consistency conditions. We then discuss the Weyl anomaly and again find agreement with field theory expectations.

7.5.1 Diffeomorphism anomaly

The diffeomorphism Ward identity from (7.51) for $\mu = 1$ reads

$$\nabla^j \langle T_{ij} \rangle = \frac{1}{4G_N} \left(\frac{1}{4} \epsilon_i^k \nabla_k R[g_{(0)}] + \frac{1}{2} \nabla^j A_{ij}[g_{(0)}] \right).\tag{7.56}$$

The right-hand side is the diffeomorphism anomaly of the theory. A more explicit expression can be obtained following [134]. Consider a vector field ζ^i . Then,

under a diffeomorphism along ζ^i the metric change $\delta g_{ij} = \nabla_i \zeta_j + \nabla_j \zeta_i$ results in the following change in the connection coefficients:

$$\delta \Gamma_{ij}^k = \zeta^m \partial_m \Gamma_{ij}^k + (\partial_i \zeta^m) \Gamma_{mj}^k + (\partial_j \zeta^m) \Gamma_{im}^k - \Gamma_{ij}^m \partial_m \zeta^k + \partial_i \partial_j \zeta^k. \quad (7.57)$$

We may substitute this in (7.44) and find that:

$$\begin{aligned} & -2 \int d^2x \sqrt{-g} \zeta_j \nabla_i A^{ij} \\ &= \int d^2x \sqrt{-g} \epsilon^{ij} \Gamma_{ik}^l \left(\zeta^m \partial_m \Gamma_{jl}^k + (\partial_j \zeta^m) \Gamma_{ml}^k + (\partial_l \zeta^m) \Gamma_{jm}^k - \Gamma_{jl}^m \partial_m \zeta^k + \partial_j \partial_l \zeta^k \right) \\ &= \int d^2x \sqrt{-g} \left(-\zeta^m \Gamma_{mj}^i R \epsilon_i^j - (\partial_j \zeta^i) R \epsilon_i^j - (\partial_j \zeta^i) \epsilon^{kl} \partial_k \Gamma_{li}^j \right) \\ &= \int d^2x \sqrt{-g} \zeta^i \left(\epsilon_i^j \nabla_j R + \epsilon^{kl} \partial_j \partial_k \Gamma_{li}^j \right) \end{aligned} \quad (7.58)$$

where the first term on the third line comes from the grouping the first two terms on the second line; to find it we used that $\epsilon^{kl} \Gamma_{ki}^j \Gamma_{lj}^n \Gamma_{mn}^i = 0$ in two dimensions. Substituting the explicit expression for $\nabla^i A_{ij}$ obtained from (7.58) in (7.56) we obtain:

$$\nabla^j \langle T_{ij} \rangle = \frac{-1}{16G_N} \epsilon^{kl} \partial_j \partial_k \Gamma_{li}^j. \quad (7.59)$$

As explained in [134, 135], this is precisely the two-dimensional diffeomorphism anomaly that satisfies the Wess-Zumino consistency conditions. In particular, in this case the consistency condition requires that the anomaly under a diffeomorphism along ζ :

$$H_\zeta = \int d^2x \sqrt{-g} \zeta^i \nabla^j \langle T_{ij} \rangle, \quad (7.60)$$

satisfies

$$E_{\zeta_1} H_{\zeta_2} - E_{\zeta_2} H_{\zeta_1} = H_{[\zeta_2, \zeta_1]}, \quad (7.61)$$

where E_ζ denotes the action of a diffeomorphism with parameter ζ .

The consistent anomaly (7.59) is not covariant [134, 135] and therefore T_{ij} itself is not a covariant tensor either. One may try to remedy this by finding a symmetric local ‘improvement term’ Y_{ij} such that the new object \hat{T}_{ij} defined as:

$$\hat{T}_{ij} = T_{ij} + Y_{ij} \quad (7.62)$$

does transform as a tensor. This implies that $\nabla^i \hat{T}_{ij}$ is also covariant, resulting in a covariant diffeomorphism anomaly [134]. The covariant anomaly does not however satisfy the consistency conditions [135] and therefore \hat{T}_{ij} is not the variation of an effective action.

To better understand the form (7.56) of the diffeomorphism anomaly, we will now review the results summarized in [134].³ As we will see shortly, one may obtain the covariant and the consistent anomaly as well as the improvement term starting from a single polynomial $P(\mathbf{\Omega})$ of degree $d/2 + 1$ whose arguments are matrix-valued forms $\mathbf{\Omega}$. (In this section such forms are always written using bold face.) Although P generally depends on the theory at hand, in $d = 2$ we find that P should be quadratic, leaving us with the unique possibility:

$$P(\mathbf{\Omega}) = a \text{Tr}(\mathbf{\Omega} \wedge \mathbf{\Omega}), \quad (7.63)$$

with a so far arbitrary normalization factor a . We will also write $P(\mathbf{\Omega}_1, \mathbf{\Omega}_2) = a \text{Tr}(\mathbf{\Omega}_1 \wedge \mathbf{\Omega}_2)$. Following the usual conventions [134, 135], we view the connection coefficients Γ_{ij}^k as matrix-valued one-forms,

$$\mathbf{\Gamma} \equiv \Gamma_j^k = \Gamma_{ij}^k dx^i, \quad (7.64)$$

and the Riemann tensor as a matrix-valued two-form,

$$\mathbf{R} \equiv R_k^l = \frac{1}{2} R_{ijk}^l dx^i \wedge dx^j. \quad (7.65)$$

The consistent anomaly can be found by solving a set of descent equations which follow from the consistency condition, see [134]. Using a matrix-valued zero-form $\mathbf{v} = v_i^j = \partial_i \zeta^j$, the end result can be written as:

$$H_\zeta \equiv \int d^2 x \sqrt{-g} \zeta_i \nabla_j T^{ij} = \int P(d\mathbf{v}, \mathbf{\Gamma}). \quad (7.66)$$

With the above form of P this can be written more explicitly as:

$$\begin{aligned} \int d^2 x \sqrt{-g} \zeta_i \nabla_j T^{ij} &= -a \int \text{Tr}(d\mathbf{v} \wedge \mathbf{\Gamma}) \\ &= -a \int (\partial_k \partial_i \zeta^j) \Gamma_{lj}^i dx^k \wedge dx^l = -a \int d^2 x \sqrt{-g} \epsilon^{kl} (\partial_k \partial_i \zeta^j) \Gamma_{lj}^i. \end{aligned} \quad (7.67)$$

Similarly, the covariant anomaly is obtained in [134] as:

$$\begin{aligned} \int d^2 x \zeta_i \nabla_j \hat{T}^{ij} &= 2 \int P(\mathbf{M}, \mathbf{R}) = -a \int (\nabla_i \zeta^j) R_{klj}^i dx^k \wedge dx^l \\ &= -a \int \sqrt{-g} (\nabla_i z^j) \epsilon^{kl} R_{klj}^i = -a \int \sqrt{-g} (\nabla_i z^j) R \epsilon_j^i \end{aligned} \quad (7.68)$$

³Our conventions differ as follows. Our T_{ij} has an extra $1/\sqrt{-g}$ as opposed to the analogous object in [134]; indeed, in our case \hat{T}_{ij} is a tensor whereas in [134] it is a tensor density. The overall sign of the energy-momentum tensors is the same. The connection Γ_{ij}^k in [134] is defined with an extra minus sign, but the Riemann curvature has the same sign. Finally, we always use a covariant ϵ -symbol whereas this is not the case in [134].

where $\mathbf{M} = -\nabla_i \zeta^j$ is again a matrix-valued 0-form and R is the usual Ricci scalar. Finally, the improvement term Y_{ij} is given as:

$$\int d^2x \sqrt{-g} Y^{ij} \delta g_{ij} = 2 \int \text{Tr}(\delta \Gamma \wedge \mathbf{X}) \quad (7.69)$$

in terms of the variation of the connection and a matrix-valued one-form \mathbf{X} given again in terms of P . We refer to [134] for the exact expression for \mathbf{X} , which for $d = 2$ however reduces immediately to $\mathbf{X} = a\Gamma$. We therefore find:

$$\int d^2x \sqrt{-g} Y^{ij} \delta g_{ij} = 2a \int \sqrt{-g} \epsilon^{ij} (\delta \Gamma_{ik}^l) \Gamma_{jl}^k. \quad (7.70)$$

Let us now compare these results with our holographically computed expressions. Comparing (7.59) with (7.67) we find precise agreement provided that:

$$a = \frac{1}{16G_N}. \quad (7.71)$$

Furthermore, we are now able to understand our original expression (7.56). Namely, it is exactly of the form:

$$\nabla^i T_{ij} = \nabla^i \hat{T}_{ij} - \nabla^i Y_{ij}. \quad (7.72)$$

To see this, observe that the first term on the right-hand side of (7.56) agrees precisely with (7.68) and the second term is precisely $1/(8G_N)\nabla^i A_{ij}$ as can be seen by comparing (7.70) with (7.44). (This was recently noted in [136] as well.)

Notice that the energy-momentum tensor postulated in [131] does not include the term $\frac{1}{2}A_{ij}$ that we obtained in (7.50) from the variation of the on-shell supergravity action. The energy-momentum tensor of [131] is therefore precisely the tensor \hat{T}_{ij} defined above. In agreement with the above discussion, this \hat{T}_{ij} is not obtained from an on-shell action and the anomaly found there is precisely the covariant anomaly (7.68).

7.5.2 Weyl anomaly

For the Weyl anomaly we find from (7.51):

$$\langle T_i^i \rangle = \frac{1}{8G_N} \left(R[g_{(0)}] + A_i^i[g_{(0)}] \right). \quad (7.73)$$

We have already discussed that the extra term $A_i^i[g_{(0)}]$ can be removed by hand. We then obtain the trace of the covariant energy-momentum tensor:

$$\langle \hat{T}_i^i \rangle = \frac{1}{8G_N} R[g_{(0)}]. \quad (7.74)$$

On the other hand, in the conventions of this chapter we should have:

$$\langle \hat{T}_i^i \rangle = \frac{c_L + c_R}{24} R[g_{(0)}] \quad (7.75)$$

and therefore:

$$c_L + c_R = \frac{3}{G_N} \quad (7.76)$$

which agrees with the analysis in section 7.6.4 below.

7.6 Linearized analysis

In order to compute correlation functions involving the operator t_{ij} as well, we will proceed perturbatively. In this section we therefore consider small perturbations $\delta G_{\mu\nu} = H_{\mu\nu}$ around the AdS₃ background. We will first linearize the bulk equations of motion and solve these asymptotically in order to isolate the divergent pieces in the combined action I_c defined in (7.36). We then renormalize this action to second order in the fluctuations. Taking functional derivatives as in (7.49), we obtain finite expressions for the one-point functions of T_{ij} and t_{ij} in terms of the subleading coefficients in the radial expansion of the perturbations. Afterwards, we find the full linearized bulk solutions for H_{ij} so we can express these subleading pieces as nonlocal functionals of the sources $g_{(0)ij}$ and $b_{(0)ij}$. Finally, a second functional derivative then gives all boundary two-point functions involving T_{ij} and t_{ij} . At the end of this section we compare our results with those expected from a logarithmic CFT (LCFT) and find complete agreement.

7.6.1 Linearized equations of motion

We will now linearize the equations of section 7.4.1 around an empty AdS background solution. We work in Poincaré coordinates where the background metric $G_{\mu\nu}$ has the form

$$G_{\mu\nu} dx^\mu dx^\nu = \frac{d\rho^2}{4\rho^2} + \frac{1}{\rho} \eta_{ij} dx^i dx^j. \quad (7.77)$$

An earlier investigation of the linearized equations around this background can be found in [112, 116]. As we work in Fefferman-Graham coordinates, it is natural to pick a radial-axial gauge for the fluctuations as well. Thus we set $H_{\rho\rho} = H_{\rho i} = 0$ and define $h_{ij} \equiv \delta g_{ij} = H_{ij}/\rho$. We therefore substitute

$$g_{ij} = \eta_{ij} + h_{ij} \quad (7.78)$$

into the equations of motion (7.15). To leading order in h_{ij} we find:

$$\begin{aligned}
 & -\text{tr}(h'') + \frac{1}{2\mu}\epsilon^{ij}\partial_i\partial^m h'_{mj} = 0, \\
 & 2\rho\partial^k h''_{ik} + \partial^k h'_{ik} + \mu\epsilon^{jk}\partial_k h'_{ij} - \partial_i\text{tr}(h') = 0, \\
 & -h''_{ij} + \eta_{ij}\frac{1}{2}\text{tr}(h'') \\
 & \quad + \frac{1}{\mu}\epsilon_i{}^k\left[\frac{1}{4}\partial_k\partial^l h'_{lj} + \frac{1}{4}\partial_j\partial^l h'_{lk} - \frac{1}{2}\partial_k\partial_j\text{tr}(h') + 2\rho h''_{jk} + 3h''_{jk}\right] + (i \leftrightarrow j) = 0,
 \end{aligned} \tag{7.79}$$

and for the trace equation $R = -6$ we obtain:

$$-4\rho\text{tr}(h'') + \tilde{R}(h) + 2\text{tr}(h') = 0, \tag{7.80}$$

with $\tilde{R}[h]$ the linearized curvature of $\eta_{ij} + h_{ij}$, which can be explicitly written as

$$\tilde{R}[h] = \nabla^i\nabla^j h_{ij} - \nabla^i\nabla_i\text{tr}(h). \tag{7.81}$$

Notice that all covariant symbols and traces in the above equations are defined using the background metric η_{ij} .

We also obtained the linearized equations of motion in global coordinates, which can be found in appendix 7.C. The analysis in global coordinates would be useful should one want to compute directly⁴ the correlators of the CFT on $R \times S^1$ rather than R^2 .

7.6.2 Holographic renormalization

In this subsection we consider the holographic renormalization of the on-shell action. Since we work at the linearized level, we compute the on-shell action to second order in the perturbations around the Poincaré background. We isolate the divergences to that order and compute the necessary covariant counterterms to cancel these divergences.

Asymptotic analysis

We begin by substituting the asymptotic expansion for h_{ij} :

$$h_{ij} = b_{(0)ij}\log(\rho) + h_{(0)ij} + b_{(2)ij}\rho\log(\rho) + h_{(2)ij}\rho + \dots \tag{7.82}$$

⁴Alternatively, one can obtain the correlators on $R \times S^1$ from the ones on R^2 by using the fact that $R \times S^1$ is conformally related to R^2 . We mentioned in section 1.4 how Weyl transformations in the boundary theory can be implemented by specific bulk diffeomorphisms.

into the linearized equations of motion (7.79) and (7.80). We find from the linearization of the asymptotic analysis above that:

$$\begin{aligned}
 \text{tr}(b_{(0)}) &= 0, \\
 b_{ij} + \epsilon_i^k b_{kj} &= 0, \\
 \text{tr}(b_{(2)}) &= -\frac{1}{2}\tilde{R}[b_{(0)}] = -\frac{1}{2}\partial^i\partial^j b_{(0)ij}, \\
 \text{tr}(h_{(2)}) &= -\frac{1}{2}\tilde{R}[h_{(0)}] + \text{tr}(b_{(2)}), \\
 b_{(2)ij} - \epsilon_i^k b_{(2)kj} &= \frac{1}{2}\eta_{ij}\text{tr}(b_{(2)}) + \frac{1}{4}\epsilon_i^k(\partial_k\partial^l b_{(0)lj} + \partial_j\partial^l b_{(0)lk}), \\
 \partial^j\left(b_{(2)ij} - 3\epsilon_i^k b_{(2)kj} + 2\bar{P}_i^k h_{(2)kj} - 2\bar{P}_i^k \eta_{kj}(\text{tr}(h_{(2)}) + \text{tr}(b_{(2)}))\right) &= 0,
 \end{aligned} \tag{7.83}$$

where all covariant symbols and traces are defined using η_{ij} and $\tilde{R}[h]$ again denotes the linearized curvature of the metric $\eta_{ij} + h_{ij}$.

On-shell action and counterterms

The next step is to substitute the asymptotic expansion (7.82), together with the constraints (7.83), into the on-shell action (7.36). We then isolate the divergences and find the necessary counterterm action that makes the action finite to second order h_{ij} .

Expanding the on-shell action (7.36) in h_{ij} , we find that the first-order term vanishes, since it gives a term proportional to the bulk equations of motion plus the surface terms of (7.43), which vanish identically for the Poincaré background. At the second order we find:

$$I_2 = \frac{1}{32\pi G_N} \int d^2x \left(h'_{ij} - \eta_{ij}\text{tr}(h') - 2\rho\epsilon_i^k h''_{kj} - \epsilon_i^k h'_{kj} \right) h^{ij}. \tag{7.84}$$

Notice that there are no contributions from the A_{ij} -term for the Poincaré background, as can be seen easily from its definition (7.44). If we now substitute the expansion (7.82) and use the linearized equations of motion (7.83) then we find a logarithmic divergence of the form:

$$I_2 = \frac{1}{32\pi G_N} \int d^2x \left(\frac{1}{2}\text{tr}(h_{(0)})\tilde{R}[b_{(0)}] - 2b_{(2)ij}b_{(0)}^{ij} - \frac{1}{2}h_{(0)i}^k\partial^i\partial^j b_{(0)jk} \right) \log(\rho) + \dots \tag{7.85}$$

The next step in the holographic renormalization is to invert the series and rewrite the divergent terms in terms of h_{ij} plus finite corrections. This gives:

$$\begin{aligned}
 \log(\rho)b_{(0)ij} &= h_{ij} + \dots, \\
 h_{(0)ij} &= h_{ij} - \rho\log(\rho)h'_{ij} + \dots, \\
 \log(\rho)b_{(2)ij}b_{(0)}^{ij} &= \frac{1}{2}\rho h'_{ij}h'^{ij} + \dots,
 \end{aligned} \tag{7.86}$$

and we also have:

$$\text{tr}(h_{(0)})\tilde{R}[b_{(0)}] = 2h_{(0)i}^k \partial^i \partial^j b_{(0)jk} - h^{ij} \partial^k \partial_k b_{(0)ij}, \quad (7.87)$$

from which we find that this divergence is cancelled by adding the following counterterm action:

$$I_{2,\text{ct}} = \frac{1}{32\pi G_N} \int d^2x \left(\frac{1}{4} h^{ij} \partial^k \partial_k h_{ij} + \rho h'_{ij} h'^{ij} - \frac{1}{4} h_i^j \partial^i \partial^k h_{kj} \right). \quad (7.88)$$

This action can be written in a covariant form as follows. The background induced metric is written $\gamma_{ij} = \eta_{ij}/\rho$ and its deviation $h_{ij}/\rho = \sigma_{ij}$. The extrinsic curvature $K_i^j = -\delta_i^j + \rho g_i'^j$ and its deviation is $\tilde{K}_i^j[h] = \rho h_i'^j$. In this notation, the counterterm action becomes:

$$I_{2,\text{ct}} = \frac{1}{32\pi G_N} \int d^2x \sqrt{-\gamma} \left(\frac{1}{4} \sigma^{ij} \nabla^k \nabla_k \sigma_{ij} + \tilde{K}_{ij}[h] \tilde{K}^{ij}[h] - \frac{1}{4} \sigma_i^j \nabla^i \nabla^k \sigma_{kj} \right), \quad (7.89)$$

where indices are now raised and covariant derivatives and traces are defined using γ_{ij} .

Notice that the counterterm action involves the extrinsic curvature K_{ij} as well. Such a term would not be allowed in pure Einstein theory as it would lead to an incorrect variational principle. On the other hand, for TMG we already found that the variational principle is different. In particular, the higher-derivative terms allow for the specification of both γ_{ij} and K_{ij} at the boundary and therefore we are also allowed to use K_{ij} in the boundary counterterm action.

One-point functions

For the total action at this order $I_{2,\text{tot}} = I_2 + I_{2,\text{ct}}$ we find the variations:

$$\begin{aligned} \frac{\delta I_{2,\text{tot}}}{\delta h^{ij}} &= \frac{1}{16\pi G_N} \left(h'_{ij} - \eta_{ij} \text{tr}(h') - 2\rho \epsilon_i^k h''_{kj} - \epsilon_i^k h'_{kj} + \frac{1}{2} \tilde{A}_{ij}[h] \right. \\ &\quad \left. + \frac{1}{4} \partial^k \partial_k h_{ij} - \frac{1}{4} \partial_i \partial^k h_{kj} \right), \\ \frac{\delta I_{2,\text{tot}}}{\delta h'^{ij}} &= \frac{1}{16\pi G_N} \rho (\delta_i^k + \epsilon_i^k) h'_{kj}, \end{aligned} \quad (7.90)$$

with $\tilde{A}_{ij}[h]$ the linearization of A_{ij} as defined in (7.44):

$$\tilde{A}_{ij}[h] = \frac{1}{4} \epsilon_i^k (\partial_j \partial^l h_{kl} - \partial^l \partial_l h_{kj}) + (i \leftrightarrow j). \quad (7.91)$$

We now substitute the expansion (7.82) and find:

$$\begin{aligned}\frac{\delta I_{2,\text{tot}}}{\delta h^{ij}} &= \frac{1}{16\pi G_N} \left\{ b_{(2)ij} - 3\epsilon_i{}^k b_{(2)kj} + 2\bar{P}_i{}^k h_{(2)kj} + \eta_{ij} \left(\frac{1}{2} \tilde{R}[h_{(0)}] + \tilde{R}[b_{(0)}] \right) \right. \\ &\quad \left. + \frac{1}{2} \bar{P}_i{}^k \left(\partial^l \partial_l h_{(0)kj} - \partial_j \partial^l h_{(0)lk} \right) \right\}, \\ \frac{\delta I_{2,\text{tot}}}{\delta h^{ij}} &= \frac{\rho}{8\pi G_N} P_i{}^k \left(b_{(2)kj} \log(\rho) + b_{(2)kj} + h_{(2)kj} \right),\end{aligned}\tag{7.92}$$

where we dropped terms that vanish as $\rho \rightarrow 0$ and do not contribute below. In the above formulas symmetrization in i and j is implicit. When $b_{(0)ij} = 0$ we can compare the first of these expressions with (7.50) and we find that the additional counterterms only change the local terms.

Using (7.49) and taking into account an extra sign from the fact that $g^{ij} = \eta^{ij} - h^{ij}$, we obtain the following explicit expression for the one-point functions:

$$\begin{aligned}\langle T_{ij} \rangle &= \lim_{\rho \rightarrow 0} \frac{4\pi}{\sqrt{-\eta}} \frac{\delta I_{2,\text{tot}}}{\delta h^{ij}} \\ &= \frac{1}{4G_N} \left\{ b_{(2)ij} - 3\epsilon_i{}^k b_{(2)kj} + 2\bar{P}_i{}^k h_{(2)kj} + \eta_{ij} \left(\frac{1}{2} \tilde{R}[h_{(0)}] + \tilde{R}[b_{(0)}] \right) \right. \\ &\quad \left. + \frac{1}{2} \bar{P}_i{}^k \left(\partial^l \partial_l h_{(0)kj} - \partial_j \partial^l h_{(0)lk} \right) \right\}, \\ \langle t_{ij} \rangle &= \lim_{\rho \rightarrow 0} \left(\frac{-4\pi}{\rho\sqrt{-g}} \frac{\delta I}{\delta h^{ij}} - \log(\rho) \frac{4\pi}{\sqrt{-\eta}} \frac{\delta I}{\delta h^{ij}} \right)_L = \frac{1}{2G_N} \left(b_{(2)ij} + h_{(2)ij} \right)_L,\end{aligned}\tag{7.93}$$

where we note that the projection to the L -component in $\langle t_{ij} \rangle$ also removes (divergent) terms of the form $\eta_{ij}(\dots)$ or $\bar{P}_i{}^k(\dots)_{kj}$.

7.6.3 Exact solutions

In this subsection we solve the linearized equations of motion given in section 7.6.2. From the explicit solutions we find below, we can obtain the subleading terms $b_{(2)ij}$ and $h_{(2)ij}$ that enter in (7.93) as nonlocal functionals of $g_{(0)ij}$ and $b_{(0)ij}$. This will allow us to carry out the second functional differentiation required to obtain the two-point functions.

In explicitly solving the fluctuation equations it is convenient to Wick rotate and work in Euclidean signature; the procedure for analytic continuation is explained in detail in appendix 7.B. Concretely, one starts from the metric (7.77), introduces lightcone coordinates $u = t + x$, $v = -t + x$, and replaces $v \rightarrow z$, $u \rightarrow \bar{z}$ with (z, \bar{z}) complex boundary coordinates. The background metric then has the form:

$$ds^2 = \frac{d\rho^2}{4\rho^2} + \frac{1}{\rho} dz d\bar{z}.\tag{7.94}$$

We will employ the notation $\partial \equiv \partial_z$ and $\bar{\partial} \equiv \partial_{\bar{z}}$ below.

In these coordinates, the linearized equations of motion (7.79) and (7.80) become:

$$\begin{aligned}
 -\bar{\partial}(1 + \mu)h'_{z\bar{z}} + \partial(1 + \mu)h'_{\bar{z}z} + 2\rho(\partial h''_{z\bar{z}} + \bar{\partial}h''_{\bar{z}z}) &= 0 \\
 \partial(1 - \mu)h'_{z\bar{z}} - \bar{\partial}(1 - \mu)h'_{\bar{z}z} - 2\rho(\partial h''_{z\bar{z}} + \bar{\partial}h''_{\bar{z}z}) &= 0 \\
 -\bar{\partial}^2 h'_{z\bar{z}} + \bar{\partial}\partial h'_{\bar{z}z} + (3 + \mu)h''_{z\bar{z}} + 2\rho h_{z\bar{z}}^{(3)} &= 0 \\
 -\partial^2 h'_{z\bar{z}} + \bar{\partial}\partial h'_{\bar{z}z} + (3 - \mu)h''_{z\bar{z}} + 2\rho h_{z\bar{z}}^{(3)} &= 0 \\
 \partial^2 h'_{z\bar{z}} - \bar{\partial}^2 h'_{\bar{z}z} + 2\mu h''_{z\bar{z}} &= 0 \\
 \partial^2 h_{z\bar{z}} - 2\bar{\partial}\partial h_{z\bar{z}} + \bar{\partial}^2 h_{z\bar{z}} + 2h'_{z\bar{z}} - 4\rho h''_{z\bar{z}} &= 0,
 \end{aligned} \tag{7.95}$$

where again we have temporarily reinstated μ for later use. From these equations it is straightforward to verify that $h''_{z\bar{z}}$ satisfies a Bessel-like equation:

$$4\rho^2 h_{z\bar{z}}^{(4)} + 8\rho h_{z\bar{z}}^{(3)} + (4\rho\bar{\partial}\partial - \mu^2 + 1)h''_{z\bar{z}} = 0, \tag{7.96}$$

which has the general solution:

$$h''_{z\bar{z}} = \rho^{-1/2} K_\mu(q\sqrt{\rho})\alpha + \rho^{-1/2} I_\mu(q\sqrt{\rho})\beta, \tag{7.97}$$

with α and β arbitrary functions of u and v and we defined $q = \sqrt{-4\bar{\partial}\partial}$. Passing to momentum space, we have $q \geq 0$ and only K_μ is regular as $\rho \rightarrow \infty$ and we therefore set $\beta = 0$.

As a sidenote, in real time it is possible that $q < 0$ and then both solutions have a power-law divergence as $\rho \rightarrow \infty$. A solution that is regular at $\rho \rightarrow \infty$ can nevertheless be constructed from them using an infinite number of these modes [112, 116]; see also section 3.2 for an explicit example. Alternatively, one can solve the fluctuation equation using global coordinates. In any case, since we work in Euclidean signature such singular behavior for the individual modes is absent and there is no need to worry about these issues.

We can integrate (7.97) twice to find an explicit solution for $h_{z\bar{z}}$ which for general μ involves an integral of the hypergeometric functions ${}_1F_2$. Notice also that as $\mu \rightarrow \infty$ the linearized Einstein equations become $h''_{z\bar{z}} = 0$, so the radial dependence of the perturbation is linear in ρ . This correctly reproduces the linearization of the exact solution of the non-linear vacuum Einstein equation in three dimension in Fefferman-Graham coordinates given in [78], which has a Fefferman-Graham expansion that terminates at ρ^2 .

For the other components, the last two equations in (7.95) may be exploited to find that:

$$\begin{aligned}
 2\partial^2 h'_{z\bar{z}} &= 4\rho h_{z\bar{z}}^{(3)} + 2(1 - \mu)h''_{z\bar{z}} + 2\bar{\partial}\partial h'_{z\bar{z}}, \\
 2\bar{\partial}^2 h'_{\bar{z}z} &= 4\rho h_{z\bar{z}}^{(3)} + 2(1 + \mu)h''_{z\bar{z}} + 2\bar{\partial}\partial h'_{z\bar{z}},
 \end{aligned} \tag{7.98}$$

which allows us to completely solve the system.

Solutions for $\mu = 1$

In contrast to the case for general μ , for $\mu = 1$ one may use the modified Bessel equation:

$$\partial_x^2 \left(\sqrt{x} K_1(\sqrt{x}) \right) = \frac{1}{4\sqrt{x}} K_1(\sqrt{x}) \quad (7.99)$$

to integrate (7.97) twice giving:

$$h_{z\bar{z}} = B_{z\bar{z}} \partial^2 c_0 + c_1 \rho + c_2, \quad (7.100)$$

where c_i are integration constants which are arbitrary functions of \bar{z} and z and we defined

$$B_{z\bar{z}} \equiv -\frac{2\sqrt{\rho}}{q} K_1(q\sqrt{\rho}). \quad (7.101)$$

Notice that it is convenient to express $h''_{z\bar{z}}$ as:

$$h''_{z\bar{z}} = -\frac{1}{\rho} B_{z\bar{z}} \bar{\partial} \partial^3 c_0. \quad (7.102)$$

Integrating (7.98) then results in:

$$\begin{aligned} h_{\bar{z}\bar{z}} &= -B_{z\bar{z}} \partial \bar{\partial} c_0 - 2B'_{z\bar{z}} c_0 + \frac{\bar{\partial}}{\partial} c_1 \rho + c_3, \\ h_{zz} &= -B_{z\bar{z}} \frac{\partial^3}{\partial} c_0 + \frac{\partial}{\partial} c_1 \rho + c_4, \end{aligned} \quad (7.103)$$

and the last equation in (7.95) gives the constraint:

$$2c_1 + \bar{\partial}^2 c_4 + \partial^2 c_3 - 2\bar{\partial} \partial c_2 = 0, \quad (7.104)$$

i.e. c_1 is not an independent integration constant, but is determined in terms of the other integration constants.

Near the boundary $\rho \rightarrow 0$ we have the following expansion:

$$B_{z\bar{z}} = -\frac{2}{q^2} - \frac{\rho}{2}(2\gamma - 1) - \rho \log\left(\frac{q\sqrt{\rho}}{2}\right) - \frac{q^2 \rho^2}{8} \log\left(\frac{q\sqrt{\rho}}{2}\right) + \dots, \quad (7.105)$$

with γ the Euler-Mascheroni constant. Substitution in (7.103) then yields the expansions for the components:

$$\begin{aligned} h_{z\bar{z}} &= h_{(0)z\bar{z}} - \frac{1}{2} \rho \log(\rho) \partial^2 b_{(0)z\bar{z}} + \rho h_{(2)z\bar{z}} + \dots, \\ h_{\bar{z}\bar{z}} &= b_{(0)\bar{z}\bar{z}} \log(\rho) + h_{(0)\bar{z}\bar{z}} - \frac{1}{2} \rho \log(\rho) \bar{\partial} \partial b_{(0)\bar{z}\bar{z}} + \rho \left[\frac{\bar{\partial}}{\partial} h_{(2)\bar{z}\bar{z}} + \frac{4\gamma - 3}{2} \bar{\partial} \partial b_{(0)\bar{z}\bar{z}} \right] + \dots, \\ h_{zz} &= h_{(0)zz} + \frac{1}{2} \rho \log(\rho) \frac{\partial^3}{\partial} b_{(0)z\bar{z}} + \rho \left[(2\gamma - 1 + 2 \log\left(\frac{q}{2}\right)) \frac{\partial^3}{\partial} b_{(0)z\bar{z}} + \frac{\partial}{\partial} h_{(2)z\bar{z}} \right] + \dots, \end{aligned} \quad (7.106)$$

where the boundary sources $h_{(0)ij}$ and $b_{(0)\bar{z}\bar{z}}$ are given by the following combinations of the integration constants c_i :

$$\begin{aligned} h_{(0)z\bar{z}} &= c_2 - \frac{2}{q^2} \partial^2 c_0 & h_{(0)zz} &= c_4 - \frac{1}{2} \frac{\partial^2}{\partial^2} c_0 \\ h_{(0)\bar{z}\bar{z}} &= c_3 - \frac{1}{2} c_0 + 2\gamma c_0 + 2 \log\left(\frac{q}{2}\right) c_0 & b_{(0)\bar{z}\bar{z}} &= c_0. \end{aligned} \quad (7.107)$$

The normalizable mode is the combination:

$$h_{(2)z\bar{z}} = c_1 - \frac{2\gamma - 1}{2} \partial^2 c_0 - \log\left(\frac{q}{2}\right) \partial^2 c_0, \quad (7.108)$$

which using (7.104) is determined by the boundary sources via:

$$h_{(2)z\bar{z}} = -\frac{1}{2} \partial^2 h_{(0)\bar{z}\bar{z}} - \frac{1}{2} \bar{\partial}^2 h_{(0)zz} + \bar{\partial} \partial h_{(0)z\bar{z}} - \frac{1}{2} \partial^2 b_{(0)\bar{z}\bar{z}}. \quad (7.109)$$

This is indeed the linearized form of (7.26) and (7.23) combined. Notice also that the radial expansion (7.106) indeed shows the same asymptotic behavior as (7.17) in section 7.4.2.

7.6.4 Two-point functions

Substituting the solutions that we found above into the holographic one point functions (7.93), we find that:

$$\begin{aligned} \langle t_{zz} \rangle &= \frac{-1}{4G_N} \left((4\gamma - 1) \frac{\partial^3}{\partial} b_{(0)\bar{z}\bar{z}} + 4 \log\left(\frac{q}{2}\right) \frac{\partial^3}{\partial} b_{(0)\bar{z}\bar{z}} + 2 \frac{\partial}{\partial} h_{(2)z\bar{z}} \right), \\ \langle T_{z\bar{z}} \rangle &= \text{local}, \\ \langle T_{zz} \rangle &= -\frac{1}{4G_N} \left(\frac{\partial^3}{\partial} b_{(0)zz} + \text{local} \right), \\ \langle T_{\bar{z}\bar{z}} \rangle &= \frac{1}{2G_N} \left(\frac{\bar{\partial}}{\partial} h_{(2)z\bar{z}} + \text{local} \right), \end{aligned} \quad (7.110)$$

where the local pieces correspond to finite contact terms.

We now turn to the position space expressions for the two-point functions. These are obtained via the following functional differentiations:

$$\langle T_{ij} \dots \rangle = i \frac{4\pi}{\sqrt{-g_{(0)}}} \frac{\delta}{\delta g_{(0)}^{ij}} \langle \dots \rangle, \quad \langle t_{ij} \dots \rangle = i \frac{4\pi}{\sqrt{-g_{(0)}}} \frac{\delta}{\delta b_{(0)}^{ij}} \langle \dots \rangle, \quad (7.111)$$

where the prefactors are explained in appendix 7.B. Notice that in complex coordinates $ds^2 = dzd\bar{z}$ so $\sqrt{-g_{(0)}} = 1/2$ whilst in our case $g^{ij} = \eta^{ij} - h^{ij}$ and therefore

$$\frac{\delta}{\delta g^{ij}} = -\frac{\delta}{\delta h^{ij}} = -\eta_{ik} \eta_{jl} \frac{\delta}{\delta h_{kl}} \quad (7.112)$$

which in complex coordinates becomes:

$$\frac{\delta}{\delta g_{(0)}^{zz}} = -\frac{1}{4} \frac{\delta}{\delta h_{\bar{z}\bar{z}}}, \quad \frac{\delta}{\delta g_{(0)}^{\bar{z}\bar{z}}} = -\frac{1}{4} \frac{\delta}{\delta h_{zz}}. \quad (7.113)$$

Functionally differentiating the one point functions thus results in:

$$\begin{aligned} \langle t_{zz}(z, \bar{z}) t_{zz}(0) \rangle &= -\frac{2\pi i}{G_N} \left[\left(\gamma - \frac{1}{4} \right) + \log\left(\frac{q}{2}\right) \right] \frac{\partial^3}{\partial} \delta^2(z, \bar{z}) \\ \langle t_{zz}(z, \bar{z}) T_{zz}(0) \rangle &= -\frac{i\pi}{2G_N} \frac{\partial^3}{\partial} \delta^2(z, \bar{z}) \\ \langle T_{\bar{z}\bar{z}}(z, \bar{z}) T_{\bar{z}\bar{z}}(0) \rangle &= \frac{i\pi}{2G_N} \frac{\bar{\partial}^3}{\partial} \delta^2(z, \bar{z}) \end{aligned} \quad (7.114)$$

whilst $\langle t_{zz} T_{\bar{z}\bar{z}} \rangle = \langle T_{\bar{z}\bar{z}} T_{zz} \rangle = \langle T_{zz} T_{zz} \rangle = 0$ up to contact terms.

These expressions can be evaluated using the following set of identities. First notice that:

$$-2i\delta^2(z, \bar{z}) = \delta(x)\delta(\tau), \quad 4\partial\bar{\partial} = \partial_\tau^2 + \partial_x^2. \quad (7.115)$$

The former of these is obtained by requesting $\int d^2z \delta^2(z, \bar{z}) = 1$ and $\frac{1}{2} \int d^2z (\dots) = -i \int d^2x (\dots)$. We also need the following integral which is the two-dimensional analogue of (1.60) in section 1.3.3:

$$\frac{1}{4\pi^2} \int d\omega dk e^{i\omega\tau + ikx} \frac{1}{(\omega^2 + k^2)^{\alpha/2}} = \frac{1}{\pi} 2^{-\alpha} \frac{\Gamma(1 - \alpha/2)}{\Gamma(\alpha/2)} (\tau^2 + x^2)^{-1 + (\alpha/2)}. \quad (7.116)$$

Taking the limit $\alpha = 2$ on both sides gives the identity:

$$\frac{1}{\partial\bar{\partial}} \delta^2(z, \bar{z}) = \frac{2i}{\partial_\tau^2 + \partial_x^2} \delta^2(x, y) = \frac{i}{2\pi} \log(m^2(\tau^2 + x^2)) = \frac{i}{2\pi} \log(m^2|z|^2) \quad (7.117)$$

where we subtracted a contact term as in section 1.3.3 and m is a scale introduced in the process. By differentiating both sides in (7.116) with respect to α we also find:

$$\begin{aligned} \log(q) \frac{1}{\partial\bar{\partial}} \delta^2(z, \bar{z}) &= \log(q) \frac{2i}{\partial_\tau^2 + \partial_x^2} \delta^2(x, y) \\ &= -\frac{i}{8\pi} \log^2(m^2(\tau^2 + x^2)) = -\frac{i}{8\pi} \log^2(m^2|z|^2). \end{aligned} \quad (7.118)$$

Using these expressions the two-point functions become:

$$\begin{aligned} \langle t_{zz}(z, \bar{z}) t_{zz}(0) \rangle &= \frac{1}{4G_N} \partial^4 [B_m \log(m^2|z|^2) - \log^2(m^2|z|^2)] \\ &= \frac{1}{2G_N} \frac{-3B_m - 11 + 6 \log(m^2|z|^2)}{z^4}, \\ \langle t_{zz}(z, \bar{z}) T_{zz}(0) \rangle &= \frac{1}{4G_N} \partial^4 \log(m^2|z|^2) = \frac{-3/(2G_N)}{z^4}, \\ \langle T_{\bar{z}\bar{z}}(z, \bar{z}) T_{\bar{z}\bar{z}}(0) \rangle &= \frac{3/(2G_N)}{\bar{z}^4}, \end{aligned} \quad (7.119)$$

where B_m is a scale-dependent constant that can be changed by rescaling m in the first line. In fact, the entire non-logarithmic piece in the second line can also be removed from the correlation function by redefining $t \rightarrow t - (3B_m + 11)T_{zz}/6$. This transformation is familiar from logarithmic CFT as we review in appendix 7.D.

Comparison to logarithmic CFT

The expressions above agree with general expectations from a logarithmic CFT, see appendix 7.D for an introduction. The central charges can be computed as follows. From the two-point functions of $T_{\bar{z}\bar{z}}$ and T_{zz} , which should be of the form:

$$\langle T_{zz}T_{zz} \rangle = \frac{c_L}{2z^4}, \quad \langle T_{\bar{z}\bar{z}}T_{\bar{z}\bar{z}} \rangle = \frac{c_R}{2\bar{z}^4}, \quad (7.120)$$

we find that

$$c_L = 0, \quad c_R = \frac{3}{G_N}, \quad (7.121)$$

which agrees with [111]. As discussed in appendix 7.D two point functions of a logarithmic pair of operators (T, t) in a LCFT have the structure:

$$\begin{aligned} \langle T(z)T(0) \rangle &= 0; & \langle T(z)t(0,0) \rangle &= \frac{b}{2z^4}; \\ \langle t(z, \bar{z})t(0,0) \rangle &= \frac{-b \log(m^2|z|^2)}{z^4}. \end{aligned} \quad (7.122)$$

Note that by rescaling the operator t the coefficients of the non-zero two point functions can be changed; there is however a distinguished normalization of the operator in which the two point functions take this form, and the coefficient b is sometimes referred to as the new anomaly, see [137]. Comparing these expressions with (7.119) we see that our holographic two point functions indeed have the structure expected from a LCFT and the coefficient b is:

$$b = -\frac{3}{G_N}. \quad (7.123)$$

This value will be confirmed below in the analysis for general μ .

7.7 Linearized analysis for general μ

In this section we repeat the linearized analysis of section 7.6 for general μ around the Poincaré background. We define:

$$\lambda = \frac{1}{2}(\mu - 1), \quad \mu = 2\lambda + 1, \quad (7.124)$$

and we work around $\lambda = 0$.

7.7.1 Asymptotic analysis

The linearized equations of motion give the most general asymptotic form of the solution:

$$h_{ij} = h_{(-2\lambda)ij}\rho^{-\lambda} + h_{(0)ij} + h_{(2)ij}\rho + h_{(2-2\lambda)ij}\rho^{1-\lambda} + h_{(2+2\lambda)ij}\rho^{\lambda+1} + \dots, \quad (7.125)$$

with the conditions:

$$\begin{aligned} \text{tr}(h_{(-2\lambda)}) &= 0 & P_i^k h_{(-2\lambda)kj} &= 0 & \text{tr}(h_{(2)}) &= -\frac{1}{2}\tilde{R}[h_{(0)}] \\ \text{tr}(h_{(2-2\lambda)}) &= \frac{-\tilde{R}[h_{(-2\lambda)}]}{2(1-\lambda)(2\lambda+1)} & \text{tr}(h_{(2\lambda+2)}) &= 0 & \bar{P}_i^k h_{(2\lambda+2)kj} &= 0 \end{aligned} \quad (7.126)$$

as well as:

$$\begin{aligned} h_{(2-2\lambda)ij} + \frac{2\lambda-1}{2\lambda+1}\epsilon_i^k h_{(2-2\lambda)kj} \\ = \frac{1}{2}\eta_{ij}\text{tr}(h_{(2-2\lambda)}) + \frac{\epsilon_i^k(\partial_k\partial^l h_{(-2\lambda)lj} + \partial_j\partial^l h_{(-2\lambda)lk})}{4(1-\lambda)(2\lambda+1)}. \end{aligned} \quad (7.127)$$

Notice that for integer values of μ we see from the explicit solutions below that a logarithmic mode appears. In what follows we will consider only the case $0 < |\mu| < 2$ so $|\lambda| < \frac{1}{2}$, with $|\mu| = 1$ the special point discussed above, so such logarithmic modes are not required. It would be straightforward to generalize the linearized analysis to other values of λ , whilst for $\lambda < 0$ the corresponding dual operator is relevant and thus there is no obstruction to carrying out a full non-linear analysis of the system.

Substituting the expansions into the on-shell action, the second term in the expansion of the on-shell action I_2 was defined for $\mu = 1$ in (7.84) and now becomes:

$$I_{2,\lambda} = \frac{1}{32\pi G_N} \int d^2x \left(h'_{ij} - \eta_{ij}\text{tr}(h') - 2\rho\frac{1}{2\lambda+1}\epsilon_i^k h''_{kj} - \frac{1}{(2\lambda+1)}\epsilon_i^k h'_{kj} \right) h^{ij}. \quad (7.128)$$

Substituting (7.125), we find that this action is again divergent if $h_{(-2\lambda)}$ is nonzero and if $\lambda > 0$, with a leading piece of the form:

$$\begin{aligned} I_{2,\lambda} = \frac{1}{32\pi G_{N\mu}} \int d^2x \left(\frac{1}{2}\text{tr}(h_{(0)})\tilde{R}[h_{(-2\lambda)}] - 2\lambda h_{(2)ij} h_{(-2\lambda)}^{ij} \right. \\ \left. - \frac{1}{2}h_{(0)i}^k \partial^i \partial^j h_{(-2\lambda)jk} \right) \rho^{-\lambda} + \dots \end{aligned} \quad (7.129)$$

This term is cancelled precisely by adding $I_{2,\text{ct}}/(2\lambda+1)$, where $I_{2,\text{ct}}$ is the counterterm action for $\mu = 1$ defined in (7.88). For $\lambda < 0$ there is no divergence but the counterterm action is then finite as well and we will continue to include it.

The variation of the total action $I_{2,\lambda,\text{tot}} = I_{2,\lambda} + I_{2,\text{ct}}/(2\lambda + 1)$ is similar to (7.90):

$$\begin{aligned}\frac{\delta I_{2,\lambda,\text{tot}}}{\delta h^{ij}} &= \frac{1}{16\pi G_N} \left(h'_{ij} - \eta_{ij} \text{tr}(h') + \frac{1}{2\lambda + 1} \left[-2\rho \epsilon_i^k h''_{kj} - \epsilon_i^k h'_{kj} + \frac{1}{2} \tilde{A}_{ij}[h] \right. \right. \\ &\quad \left. \left. + \frac{1}{4} \partial^k \partial_k h_{ij} - \frac{1}{4} \partial_i \partial^k h_{kj} \right] \right), \quad (7.130) \\ \frac{\delta I_{2,\lambda,\text{tot}}}{\delta h'^{ij}} &= \frac{1}{16\pi G_N (2\lambda + 1)} \rho (\delta_i^k + \epsilon_i^k) h'_{kj}.\end{aligned}$$

To obtain the one-point functions we follow the same reasoning as in section 7.4.4. We have two independent variables, $h_{(0)ij}$ and $h_{(-2\lambda)ij}$, for which we define the corresponding CFT operators T_{ij} and X_{ij} , with T_{ij} again the energy-momentum tensor of the theory. To find their one-point functions, we first observe that:

$$h_{(0)}^{ij} = \lim_{\rho \rightarrow 0} (h^{ij} + \frac{1}{\lambda} h'^{ij} \rho) \quad h_{(-2\lambda)}^{ij} = \lim_{\rho \rightarrow 0} \left(-\frac{1}{\lambda} h'^{ij} \rho^{\lambda+1} \right) \quad (7.131)$$

where we note that indices are raised with η^{ij} . From these expressions we find:

$$\begin{aligned}\langle X_{ij} \rangle &\equiv \frac{-4\pi}{\sqrt{-g(0)}} \frac{\delta I_{2,\lambda,\text{tot}}}{\delta h_{(-2\lambda)}^{ij}} = \lim_{\rho \rightarrow 0} \left(\lambda \rho^{-1-\lambda} \frac{4\pi}{\sqrt{-g}} \frac{\delta I_{2,\lambda,\text{tot}}}{\delta h'^{ij}} - \rho^{-\lambda} \frac{4\pi}{\sqrt{-g}} \frac{\delta I_{2,\lambda,\text{tot}}}{\delta h^{ij}} \right)_L \\ \langle T_{ij} \rangle &\equiv \frac{4\pi}{\sqrt{-g(0)}} \frac{\delta I_{2,\lambda,\text{tot}}}{\delta h_{(0)}^{ij}} = \lim_{\rho \rightarrow 0} \frac{4\pi}{\sqrt{-g}} \frac{\delta I_{2,\lambda,\text{tot}}}{\delta h'^{ij}}, \quad (7.132)\end{aligned}$$

where the signs originate from the reasoning in appendix 7.B, plus an extra sign arising from the fact that $g^{ij} = \eta^{ij} - h^{ij}$. We inserted a factor of 4π in the definition of X_{ij} for later convenience. After substitution of (7.125) these expressions lead to the following finite one-point functions:

$$\begin{aligned}\langle T_{ij} \rangle &= \frac{1}{4G_N} \left\{ (\delta_i^k - \frac{1}{2\lambda + 1} \epsilon_i^k) h_{(2)kj} - \eta_{ij} \text{tr}(h_{(2)}) \right. \\ &\quad \left. + \frac{1}{2(2\lambda + 1)} \bar{P}_i^k \left(\partial^l \partial_l h_{(0)kj} - \partial_j \partial^l h_{(0)kl} \right) \right\}, \\ \langle X_{ij} \rangle &= \frac{\lambda(1 + \lambda)}{2G_N(2\lambda + 1)} (h_{(2+2\lambda)ij})_L.\end{aligned} \quad (7.133)$$

Symmetrization in i and j is again understood in these expressions.

7.7.2 Two-point functions

Just as in section 7.6.3, we can use the equations (7.97) and (7.98) (with the K_μ choice for the Bessel function) to find exact solutions to the linearized equations

of motion. Asymptotically, they behave as follows:

$$h_{z\bar{z}} = h_{(0)z\bar{z}} + \rho h_{(2)z\bar{z}} + \frac{1}{2(\lambda-1)(2\lambda+1)} \partial^2 h_{(-2\lambda)\bar{z}\bar{z}} \rho^{1-\lambda} + \dots, \quad (7.134)$$

$$h_{\bar{z}\bar{z}} = h_{(-2\lambda)\bar{z}\bar{z}} \rho^{-\lambda} + h_{(0)\bar{z}\bar{z}} + \frac{1}{2(\lambda-1)} \bar{\partial} \partial h_{(-2\lambda)\bar{z}\bar{z}} \rho^{1-\lambda} + \frac{\bar{\partial}}{\partial} h_{(2)z\bar{z}} \rho + \dots,$$

$$h_{zz} = h_{(0)zz} + \frac{\partial}{\partial} h_{(2)z\bar{z}} \rho + \frac{2^{-4\lambda+2} \lambda \Gamma(-2\lambda-1)}{(\lambda+1) \Gamma(2\lambda+1)} q^{4\lambda-2} \partial^4 h_{(-2\lambda)\bar{z}\bar{z}} \rho^{\lambda+1} + \dots,$$

with same trace condition as was given for $\mu = 1$ in (7.109),

$$h_{(2)z\bar{z}} = -\frac{1}{2} \partial^2 h_{(0)\bar{z}\bar{z}} - \frac{1}{2} \bar{\partial}^2 h_{(0)zz} + \bar{\partial} \partial h_{(0)z\bar{z}}, \quad (7.135)$$

and integration constants $h_{(0)\bar{z}\bar{z}}, h_{(0)zz}, h_{(0)z\bar{z}}$ and $h_{(-2\lambda)\bar{z}\bar{z}}$; these are as anticipated the sources for the dual operators.

We can substitute this solution in (7.133) to find the one-point functions:

$$\begin{aligned} \langle X_{zz} \rangle &= \frac{2^{-4\lambda+1} \lambda^2 \Gamma(-2\lambda-1)}{G_N \Gamma(2\lambda+2)} q^{4\lambda-2} \partial^4 h_{(-2\lambda)\bar{z}\bar{z}} \\ \langle T_{\bar{z}\bar{z}} \rangle &= \frac{2\lambda+2}{4G_N(2\lambda+1)} \frac{\bar{\partial}}{\partial} h_{(2)z\bar{z}} + \text{local} \\ \langle T_{z\bar{z}} \rangle &= \text{local} \\ \langle T_{zz} \rangle &= \frac{2\lambda}{4G_N(2\lambda+1)} \frac{\partial}{\partial} h_{(2)z\bar{z}}. \end{aligned} \quad (7.136)$$

From these expressions we obtain the following nonvanishing two-point functions:

$$\begin{aligned} \langle T_{\bar{z}\bar{z}}(z, \bar{z}) T_{\bar{z}\bar{z}}(0) \rangle &= \frac{i\pi}{2G_N} \frac{\lambda+1}{2\lambda+1} \frac{\bar{\partial}^3}{\partial} \delta^2(z, \bar{z}) = \frac{3}{2G_N} \frac{\lambda+1}{2\lambda+1} \frac{1}{\bar{z}^4}, \\ \langle T_{zz}(z, \bar{z}) T_{zz}(0) \rangle &= \frac{i\pi}{2G_N} \frac{\lambda}{2\lambda+1} \frac{\partial^3}{\bar{\partial}} \delta^2(z, \bar{z}) = \frac{3}{2G_N} \frac{\lambda}{2\lambda+1} \frac{1}{z^4}, \\ \langle X_{zz}(z, \bar{z}) X_{zz}(0) \rangle &= i \frac{4\pi}{\sqrt{-g(0)}} \frac{\delta}{\delta h_{(-2\lambda)}^{zz}(z, \bar{z})} \langle X(0) \rangle = 2\pi i \frac{\delta}{\delta h_{(-2\lambda)\bar{z}\bar{z}}(z, \bar{z})} \langle X_{zz}(0) \rangle \\ &= \frac{i\pi 2^{-4\lambda+2} \lambda^2 \Gamma(-2\lambda-1)}{G_N \Gamma(2\lambda+2)} q^{4\lambda-2} \partial^4 \delta^2(z, \bar{z}) \\ &= \frac{-1}{2G_N} \frac{\lambda(\lambda+1)(2\lambda+3)}{2\lambda+1} \frac{1}{z^{2\lambda+4} \bar{z}^{2\lambda}}, \end{aligned} \quad (7.137)$$

where the computation of the two-point function of the energy-momentum tensor is completely analogous to the previous section and we used the identity (7.116). Comparing now with (7.120) we read off that:

$$(c_L, c_R) = \frac{3}{G_N} \left(\frac{\lambda}{2\lambda+1}, \frac{\lambda+1}{2\lambda+1} \right) = \frac{3}{2G_N} \left(1 - \frac{1}{\mu}, 1 + \frac{1}{\mu} \right) \quad (7.138)$$

and from the last line in (7.137) we also find that X has weights $(h_L, h_R) = (2 + \lambda, \lambda) = \frac{1}{2}(\mu + 3, \mu - 1)$. Both expressions agree with [111].

The limit $\lambda \rightarrow 0$ and logarithmic CFT

As $\lambda \rightarrow 0$, we find that the $\langle TT \rangle$ -correlators return to the values given in section 7.6.4. On the other hand, the $\langle XX \rangle$ -correlator vanishes, but we also find that the definitions for X_{zz} and T_{zz} as given in (7.132) coincide in this limit (up to a sign). To remedy this we can introduce a new field,

$$t_{zz} = -\frac{1}{\lambda}X_{zz} - \frac{1}{\lambda}T_{zz}, \quad (7.139)$$

after which we can take $\lambda \rightarrow 0$ in (7.132) and obtain (7.49) (up to a sign from the fact that $g^{ij} = \eta^{ij} - h^{ij}$). We obtain for the nonzero two-point functions:

$$\begin{aligned} \langle t_{zz}(z, \bar{z})T_{zz}(0) \rangle &= -\frac{3}{2G_N} \frac{1}{2\lambda + 1} \frac{1}{z^4} = \frac{-3/(2G_N)}{z^4} + \dots \\ \langle t_{zz}(z, \bar{z})t_{zz}(0) \rangle &= \frac{B_m + 3/(G_N) \log(m^2|z|^2)}{z^4} + \dots \end{aligned} \quad (7.140)$$

where the dots represent terms that vanish as $\lambda \rightarrow 0$. These are exactly the same correlators as in section 7.6.4. The term B_m can again be removed by a redefinition of t_{zz} and from (7.140) we again see that $b = -3/G_N$.

In appendix 7.D we discuss the degeneration of a CFT to a logarithmic CFT as $c_L \rightarrow 0$ following Kogan and Nichols [138]. Their $c_L \rightarrow 0$ limit is precisely the same limit as taken here, i.e. the logarithmic partner of the stress energy tensor originates from another primary operator whose dimension approaches $(2, 0)$ in the $c_L \rightarrow 0$ limit. Given such a limiting procedure, the anomaly b is obtained by inverting the relation between λ (which is the right-moving weight of X) and c_L given above and using (7.204) in appendix 7.D. This results in $b = -\lim_{c_R \rightarrow 0} c_L/\lambda(c_L) = -3/G_N$ and thus agrees with (7.140). Note that there are other distinct approaches to taking a $c \rightarrow 0$ limit, see [139] for a review, but it is the Kogan-Nichols approach which is realized holographically here.

Energy computations

In Lorentzian signature and in global coordinates, the insertions of the operators X_{zz} , T_{zz} or $T_{\bar{z}\bar{z}}$ in the infinite past creates the massive, left-moving or right-moving graviton states discussed in [111]. In [111] the energy of these states was computed in the bulk and we are now able to give a CFT interpretation of their results.

For the states created by the operators $X_{zz}, T_{zz}, T_{\bar{z}\bar{z}}$, the equations (70)-(72) in [111] give energies of the form:

$$\begin{aligned} X_{zz} : \quad E_M &= \frac{-1}{8G_N} \left(\mu - \frac{1}{\mu}\right) (h_L + h_R) \left[\dots \right], \\ T_{zz} : \quad E_L &= \frac{-1}{4G_N} \left(-1 + \frac{1}{\mu}\right) \left[\dots \right], \\ T_{\bar{z}\bar{z}} : \quad E_R &= \frac{-1}{4G_N} \left(-1 - \frac{1}{\mu}\right) \left[\dots \right]. \end{aligned} \quad (7.141)$$

The expressions in square brackets are positive, but their exact value depends on the normalization of the solutions to the linearized equations of motion in [111] and is therefore arbitrary. We can thus only compare the overall sign of the energies (7.141) with our results. Notice that we put in an extra factor of the left- plus right-moving weight from each operator, which for T_{zz} and $T_{\bar{z}\bar{z}}$ are just factors of 2; in [111] such factors comes from a time derivative of the bulk modes and we will see similar factors appearing below.

Following the usual CFT logic, we may obtain the energies of a state by computing three-point functions. For example, for the massive mode we need to compute

$$\langle X_{zz} | T_{zz}(z) | X_{zz} \rangle, \quad (7.142)$$

with

$$|X_{zz}\rangle = X_{zz}(0,0)|0\rangle, \quad \langle X_{zz}| = \lim_{z, \bar{z} \rightarrow \infty} \langle 0 | X_{zz}(z, \bar{z}) z^{2\lambda+4} \bar{z}^{2\lambda}. \quad (7.143)$$

The usual Ward identity:

$$\langle X_{zz}(z_1) T_{zz}(z) X_{zz}(z_2) \rangle = \sum_{i \in \{1,2\}} \left(\frac{h_L}{(z - z_i)^2} + \frac{1}{z - z_i} \frac{\partial}{\partial z_i} \right) \langle X_{zz}(z_1) X_{zz}(z_2) \rangle \quad (7.144)$$

results in:

$$\langle X_{zz} | T_{zz}(z) | X_{zz} \rangle = \frac{C_X h_L}{z^2}, \quad (7.145)$$

where C_X is the normalization of the $\langle XX \rangle$ -correlator,

$$\langle X_{zz}(z, \bar{z}) X_{zz}(0) \rangle = \frac{C_X}{z^{4+2\lambda} \bar{z}^{2\lambda}}, \quad (7.146)$$

$$C_X = \frac{-1}{2G_N} \frac{\lambda(\lambda+1)(2\lambda+3)}{2\lambda+1} = \frac{-1}{8G_N} \left(\mu - \frac{1}{\mu}\right) (\mu+2).$$

Note that the magnitude (but not the sign) of C_X can change by changing the normalization of the operator X . This is the counterpart of the arbitrariness of

the quantities in the square brackets of (7.141) due to the normalization ambiguity of the solutions to the linearized equations.

By using the Virasoro algebra one may also obtain that:

$$\langle T_{zz}|T_{zz}(z)|T_{zz}\rangle = \langle 0|L_2 \sum_{m \in \mathbb{Z}} L_m z^{-m-2} L_{-2}|0\rangle = \frac{c_L}{z^2}, \quad (7.147)$$

with c_L the left-moving central charge defined in (7.138). The computation involving $T_{\bar{z}\bar{z}}$ is completely analogous, and of course the mixed three-point functions involving T_{zz} and $T_{\bar{z}\bar{z}}$ vanish. To transfer these results to the cylinder we use the conformal transformation:

$$z = \exp(iw), \quad (7.148)$$

whose Schwarzian derivative is $1/2$. We then find the following three-point functions on the cylinder:

$$\begin{aligned} \langle X_{ww}|T_{ww}(w) + T_{\bar{w}\bar{w}}(\bar{w}) - \frac{c_L + c_R}{24}|X_{ww}\rangle &= C_X(h_L + h_R) \\ &= \frac{-1}{8G_N} \left(\mu - \frac{1}{\mu}\right) (h_L + h_R)(\mu + 2), \\ \langle T_{ww}|T_{ww}(w) + T_{\bar{w}\bar{w}}(\bar{w}) - \frac{c_L + c_R}{24}|T_{ww}\rangle &= c_L = \frac{3}{2G_N} \left(1 - \frac{1}{\mu}\right), \\ \langle T_{\bar{w}\bar{w}}|T_{ww}(w) + T_{\bar{w}\bar{w}}(\bar{w}) - \frac{c_L + c_R}{24}|T_{\bar{w}\bar{w}}\rangle &= c_R = \frac{3}{2G_N} \left(1 + \frac{1}{\mu}\right). \end{aligned} \quad (7.149)$$

Let us now compare these results with [111]. Notice first of all that the zero-point of energy in that paper is that of global AdS, which is why we explicitly subtracted the Casimir energy in the above expressions. Comparing now (7.149) with (7.141) we indeed find the same structure and precisely the same signs. The computations are therefore in agreement.

Finally, notice that in a CFT one usually divides the expressions in (7.149) by the norm of the state (*e.g.* $\langle X_{zz}|X_{zz}\rangle$) to obtain energies that are precisely equal to the conformal weights of the operators creating the state. On the other hand, the energies computed using bulk methods as in [111] are the unnormalized energies of (7.149) and therefore extra signs may arise if a state has a negative norm. This explains the sign difference between the conformal weights and the energies found in [111].

7.8 Conclusions

By implementing the AdS/CFT dictionary for topologically massive gravity, we were able to provide further evidence for its duality at $\mu = 1$ to a logarithmic con-

formal field theory. The expressions for the two-point functions indicate problems with unitarity and positivity as we find zero-norm states at $\mu = 1$, negative-norm states at $\mu \neq 1$ and negative conformal weights at $\mu < 1$. It therefore seems problematic to consider the full TMG as a fundamental theory, but this duality could nonetheless have interesting applications to condensed matter systems. For example, $c = 0$ LCFTs arise in the description of critical systems with quenched disorder and in several other contexts.

One may try to restrict to the right-moving sector of the theory [124], which could yield a consistent chiral theory. In order for this sector to decouple a necessary requirement is that the $\langle t\bar{T}\bar{T} \rangle$ three-point function should vanish. This was shown to be the case in the discussion of [138], see their equation (42), and their analysis can be adapted to the case of interest, namely when only $c_L \rightarrow 0$, leading to the same result. This suggests that one can indeed truncate to the right-moving sector, but it would be interesting to extend our analysis and verify the vanishing of this 3-point function by a bulk computation.

One may also perform a holographic analysis for the ‘warped’ solutions found in [130]. The asymptotics in these cases are discussed in appendix 7.E and indicate qualitatively different UV behavior for the dual field theory; it would be interesting to extend the holographic setup to this class of solutions. A similar procedure could also be followed to analyze the ‘new massive gravity’ of [140] around AdS solutions. This would allow us to find out more about the possible dual CFTs.

7.A Derivation of the equations of motion

In this appendix we derive the equations of motion in Fefferman-Graham coordinates, where the metric has the form

$$ds^2 = \frac{d\rho^2}{4\rho^2} + \frac{1}{\rho} g_{ij}(x, \rho) dx^i dx^j. \quad (7.150)$$

In this section we raise indices using g^{ij} and the covariant derivative ∇_i and the two-dimensional antisymmetric tensor ϵ_{ij} are also defined using g_{ij} . In the metric (7.150) the nonzero connection coefficients are:

$$\Gamma_{\rho\rho}^{\rho} = -\frac{1}{\rho} \qquad \Gamma_{\rho j}^i = -\frac{1}{2\rho} g_j^i + \frac{1}{2} (g^{-1} g')_j^i \quad (7.151)$$

$$\Gamma_{ij}^{\rho} = 2g_{ij} - 2\rho g'_{ij} \qquad \Gamma_{jk}^i = \Gamma_{jk}^i(g), \quad (7.152)$$

where the index ρ now denotes the coordinate ρ and a prime denotes radial derivative. The curvature tensor becomes:

$$\begin{aligned}
 R_{\rho ij}{}^k(G) &= \frac{1}{2}g^{kl}(\nabla_l g'_{ij} - \nabla_j g'_{il}), \\
 R_{ij\rho}{}^\rho(G) &= -2\rho\left(g''_{ij} - \frac{1}{2}(g'g^{-1}g')_{ij}\right) - \frac{1}{\rho}g_{ij}, \\
 R_{ijk}{}^l(G) &= R_{ijk}{}^l(g) + \left(\frac{1}{\rho}g'_i g_{jk} + g'_j g'_{ik} + g^{ml}g_{ik}g'_{mj} + \rho g^{lm}g'_{im}g'_{jk} - (i \leftrightarrow j)\right),
 \end{aligned} \tag{7.153}$$

The Einstein part of the equation of motion, $R_{\mu\nu} + 2G'_{\mu\nu}$, is given by:

$$\begin{aligned}
 R_{\rho\rho}(G) + 2G_{\rho\rho} &= -\frac{1}{2}\text{tr}(g^{-1}g'') + \frac{1}{4}\text{tr}(g^{-1}g'g^{-1}g'), \\
 R_{i\rho}(G) + 2G_{i\rho} &= \frac{1}{2}\nabla^j g'_{ji} - \frac{1}{2}\nabla_i \text{tr}(g^{-1}g'), \\
 R_{ij}(G) + 2G_{ij} &= \frac{1}{2}R(g)g_{ij} + g_{ij}\text{tr}(g^{-1}g') \\
 &\quad + \rho[-2g''_{ij} - g'_{ij}\text{tr}(g^{-1}g') + 2(g'g^{-1}g')_{ij}],
 \end{aligned} \tag{7.154}$$

where we used that in two dimensions

$$R_{ijkl} = \frac{1}{2}R[g_{ik}g_{lj} - (l \leftrightarrow k)], \quad R_{ik} = \frac{1}{2}Rg_{ik}. \tag{7.155}$$

The trace equation $R = -6$ now becomes:

$$-4\rho\text{tr}(g^{-1}g'') + 3\rho\text{tr}(g^{-1}g'g^{-1}g') - \rho[\text{tr}(g^{-1}g')]^2 + R(g) + 2\text{tr}(g^{-1}g') = 0. \tag{7.156}$$

We use $\epsilon^{\rho ij} = 2\rho^2\epsilon^{ij}$ to relate the three- and two-dimensional ϵ -tensors. For the Cotton tensor $C_{\mu\nu}$ defined in (7.6) we then find:

$$\begin{aligned}
 C_{\rho\rho} &= \frac{1}{4}\epsilon^{ij}\left(\nabla_i\nabla^k g'_{kj} + 2\rho(g''g^{-1}g')_{ji}\right), \\
 C_{\rho i} &= \frac{1}{2}\epsilon^{jk}\left(\frac{1}{2}g_{ik}\nabla_j R - 2\rho\nabla_j g''_{ik} - \rho\text{tr}(g^{-1}g')\nabla_j g'_{ik} + 2\rho\nabla_j(g'g^{-1}g')_{ik} \right. \\
 &\quad \left. - (g_{ij} - \rho g'_{ij})\nabla^l g'_{lk}\right), \\
 C_{i\rho} &= \epsilon_i^k\left(-\rho\nabla^l g'_{lk} - \frac{1}{4}\rho\nabla_k\text{tr}(g^{-1}g'g^{-1}g') + \frac{1}{2}\rho(g^{-1}g')^j_k\nabla^l g'_{lj} + \rho(g^{-1}g')^j_i\nabla^l g'_{jk} \right. \\
 &\quad \left. + \frac{1}{2}\nabla_k\text{tr}(g^{-1}g') - \frac{1}{2}\nabla^j g'_{jk}\right), \\
 C_{ij} &= 2\rho\epsilon_i^k\left(g_{jk}\left[-\frac{1}{2}R' - \frac{1}{4\rho}R - \frac{1}{2\rho}\text{tr}(g^{-1}g') + \frac{1}{2}\text{tr}(g^{-1}g'g^{-1}g')\right] - \frac{1}{4}Rg'_{jk} \right. \\
 &\quad + \frac{1}{2}\nabla_k\nabla^m g'_{mj} - \frac{1}{2}\nabla_k\nabla_j[\text{tr}(g^{-1}g')] + 2\rho g'''_{jk} + g''_{kj}[3 + \rho\text{tr}(g^{-1}g')] \\
 &\quad + g'_{kj}[\text{tr}(g^{-1}g') + \rho(\text{tr}(g^{-1}g'))' - \rho\text{tr}(g^{-1}g'')] + \frac{1}{2}\rho\text{tr}(g^{-1}g'g^{-1}g') \\
 &\quad + (g'g^{-1}g')_{kj}\left[-3 - \frac{1}{2}\rho\text{tr}(g^{-1}g')\right] - 3\rho(g''g^{-1}g')_{kj} - 2\rho(g'g^{-1}g'')_{kj} \\
 &\quad \left. + 3\rho(g'g^{-1}g'g^{-1}g')_{kj}\right). \tag{7.157}
 \end{aligned}$$

With these expressions we indeed find that $C_\mu^\mu = 0$, $C_{\rho i} = C_{i\rho}$ and $C_{ij} = C_{ji}$. To verify this we used the Cayley-Hamilton identity,

$$\frac{1}{2}g_{jl}\left([\text{tr}(g^{-1}g')]^2 - \text{tr}(g^{-1}g'g^{-1}g')\right) + (g'g^{-1}g')_{jl} - g'_{jl}\text{tr}(g^{-1}g') = 0, \tag{7.158}$$

the radial derivative of the two-dimensional Ricci tensor,

$$R'_{ik} = \frac{1}{2}\left(\nabla^l\nabla_i g'_{kl} + \nabla^l\nabla_k g'_{il} - \nabla^a\nabla_a g'_{ik} - \nabla_i\nabla_k\text{tr}(g^{-1}g')\right), \tag{7.159}$$

as well as the identity for the two-dimensional ϵ -symbol,

$$\epsilon_{ij}\epsilon_{kl} = -g_{ik}g_{jl} + g_{il}g_{jk}. \tag{7.160}$$

As C_{ij} is symmetric, we can also rewrite it as $\frac{1}{2}(C_{ij} + C_{ji})$ which allows us to drop the term proportional to $\epsilon_i^k g_{kj}$. This, the expression for R given in (7.156), and further application of the Cayley-Hamilton theorem eventually give:

$$\begin{aligned}
 C_{ij} &= \rho\epsilon_i^k\left(\frac{1}{2}\nabla_k\nabla^m g'_{mj} - \frac{1}{2}\nabla_k\nabla_j[\text{tr}(g^{-1}g')] + 2\rho g'''_{jk} + g''_{kj}\left[3 + \rho\text{tr}(g^{-1}g')\right] \right. \\
 &\quad + g'_{kj}\left[-\frac{3}{2}\text{tr}(g^{-1}g') + \frac{3}{4}\rho[\text{tr}(g^{-1}g')]^2 - \rho\text{tr}(g^{-1}g'') + \frac{7}{4}\rho\text{tr}(g^{-1}g'g^{-1}g')\right] \\
 &\quad \left. - 3\rho(g''g^{-1}g')_{kj} - 2\rho(g'g^{-1}g'')_{kj}\right) + i \leftrightarrow j. \tag{7.161}
 \end{aligned}$$

Combining the above expressions (7.154) and (7.157) leads to the full equations of motion which are given by:

$$\begin{aligned}
 & -\frac{1}{2}\text{tr}(g^{-1}g'') + \frac{1}{4}\text{tr}(g^{-1}g'g^{-1}g') + \frac{1}{4\mu}\epsilon^{ij}\left(\nabla_i\nabla^k g'_{kj} + 2\rho(g''g^{-1}g')_{ji}\right) = 0, \\
 & \frac{1}{2}\nabla^j g'_{ji} - \frac{1}{2}\nabla_i\text{tr}(g^{-1}g') + \frac{1}{2\mu}\epsilon^{jk}\left(\frac{1}{2}g_{ik}\nabla_j R + g_{ik}\nabla^l g'_{lj} \right. \\
 & \quad \left. + \rho\left[-2\nabla_j g''_{ik} - \text{tr}(g^{-1}g')\nabla_j g'_{ik} + 2\nabla_j(g'g^{-1}g')_{ik} + g' a_{ij}\nabla^l g'_{lk}\right]\right) = 0, \\
 & \left(\text{tr}(g^{-1}g'') - \frac{3}{4}\text{tr}(g^{-1}g'g^{-1}g') + \frac{1}{4}[\text{tr}(g^{-1}g')]^2\right)g_{ij} \\
 & \quad - g''_{ij} - \frac{1}{2}g'_{ij}\text{tr}(g^{-1}g') + (g'g^{-1}g')_{ij} \\
 & \quad + \frac{1}{\mu}\epsilon_i{}^k\left(\frac{1}{2}\nabla_k\nabla^m g'_{mj} - \frac{1}{2}\nabla_k\nabla_j[\text{tr}(g^{-1}g')]\right) \\
 & \quad + 2\rho g''_{jk} + g''_{kj}\left[3 + \rho\text{tr}(g^{-1}g')\right] - 3\rho(g''g^{-1}g')_{kj} - 2\rho(g'g^{-1}g'')_{kj} \\
 & \quad + g'_{kj}\left[-\frac{3}{2}\text{tr}(g^{-1}g') + \frac{3}{4}\rho[\text{tr}(g^{-1}g')]^2 - \rho\text{tr}(g^{-1}g'') + \frac{7}{4}\rho\text{tr}(g^{-1}g'g^{-1}g')\right]) \\
 & \quad + i \leftrightarrow j = 0,
 \end{aligned} \tag{7.162}$$

where we emphasize that the symmetrization in the last equation concerns all the terms. We can use the $(\rho\rho)$ equation of motion to simplify the (ij) equation of motion to:

$$\begin{aligned}
 & \left(\frac{1}{2}\text{tr}(g^{-1}g'') - \frac{1}{2}\text{tr}(g^{-1}g'g^{-1}g') + \frac{1}{4}[\text{tr}(g^{-1}g')]^2\right)g_{ij} \\
 & \quad - g''_{ij} - \frac{1}{2}g'_{ij}\text{tr}(g^{-1}g') + (g'g^{-1}g')_{ij} \\
 & \quad + \frac{1}{\mu}\epsilon_i{}^k\left(\frac{1}{4}\nabla_k\nabla^m g'_{mj} + \frac{1}{4}\nabla_j\nabla^m g'_{mk} - \frac{1}{2}\nabla_k\nabla_j[\text{tr}(g^{-1}g')]\right) \\
 & \quad + 2\rho g''_{jk} + g''_{kj}\left[3 + \rho\text{tr}(g^{-1}g')\right] - \frac{5}{2}\rho(g''g^{-1}g')_{kj} - \frac{5}{2}\rho(g'g^{-1}g'')_{kj} \\
 & \quad + g'_{kj}\left[-\frac{3}{2}\text{tr}(g^{-1}g') + \frac{3}{4}\rho[\text{tr}(g^{-1}g')]^2 - \rho\text{tr}(g^{-1}g'') + \frac{7}{4}\rho\text{tr}(g^{-1}g'g^{-1}g')\right]) \\
 & \quad + i \leftrightarrow j = 0.
 \end{aligned} \tag{7.163}$$

If we use the first radial derivative of (7.158) we can simplify this further to:

$$\begin{aligned}
 & \left(\frac{1}{2} \text{tr}(g^{-1}g'') - \frac{1}{4} [\text{tr}(g^{-1}g')]^2 \right) g_{ij} - g''_{ij} + \frac{1}{2} g'_{ij} \text{tr}(g^{-1}g') \\
 & + \frac{1}{\mu} \epsilon_i^k \left(\frac{1}{4} \nabla_k \nabla^m g'_{mj} + \frac{1}{4} \nabla_j \nabla^m g'_{mk} - \frac{1}{2} \nabla_k \nabla_j [\text{tr}(g^{-1}g')] \right) \\
 & + 2\rho g'''_{jk} + g''_{kj} \left[3 - \frac{3}{2} \rho \text{tr}(g^{-1}g') \right] \\
 & + g'_{kj} \left[-\frac{3}{2} \text{tr}(g^{-1}g') + \frac{3}{4} \rho [\text{tr}(g^{-1}g')]^2 - \frac{7}{2} \rho \text{tr}(g^{-1}g'') + \frac{7}{4} \rho \text{tr}(g^{-1}g'g^{-1}g') \right] \\
 & + i \leftrightarrow j = 0.
 \end{aligned} \tag{7.164}$$

We can use the equation of motion to rewrite the Riemann tensor as:

$$R_{\alpha\beta\gamma\delta}[G] = G_{\alpha\delta}G_{\beta\gamma} - G_{\alpha\gamma}G_{\beta\delta} - \left(\left[\frac{1}{\mu} G_{\alpha\gamma} C_{\beta\delta} - (\alpha \leftrightarrow \beta) \right] - (\gamma \leftrightarrow \delta) \right), \tag{7.165}$$

Using then (7.153) for the Riemann tensor in Fefferman-Graham coordinates we obtain:

$$\begin{aligned}
 & -2g''_{ij} + (g'g^{-1}g')_{ij} + \frac{4}{\mu} g_{ij} C_{\rho\rho} + \frac{1}{\mu\rho} C_{ij} = 0, \\
 & \frac{1}{2} \left(\nabla_k g'_{ij} - \nabla_j g'_{ik} \right) = \frac{1}{\mu} (g_{ij} C_{\rho k} - g_{ik} C_{\rho j}), \\
 & \frac{1}{2} \left(g_{ik} g_{jl} - g_{il} g_{jk} \right) \left(-2\text{tr}(g^{-1}g') + \rho [\text{tr}(g^{-1}g')]^2 - \rho \text{tr}(g^{-1}g'g^{-1}g') \right) \\
 & + \left(g_{jl} g'_{ik} + g_{ik} g'_{jl} + \rho g'_{il} g'_{jk} - (i \leftrightarrow j) \right) = 0.
 \end{aligned} \tag{7.166}$$

Taking the trace $g^{ik} R_{ijkl}$ of the last equation results again in the Cayley-Hamilton identity (7.158). This is also the equation that one obtains from the first equation by eliminating C_{ij} and $C_{\rho\rho}$ using the equations of motion. On the other hand, the second of these equations can alternatively be written as:

$$\begin{aligned}
 & (g^{kj} - \mu \epsilon^{kj}) \nabla_k g'_{ij} - \nabla_i \left(\text{tr}(g^{-1}g') + \frac{1}{2} \rho \text{tr}(g^{-1}g'g^{-1}g') - \rho [\text{tr}(g^{-1}g')]^2 \right) \\
 & + 2\rho \nabla^n \left(g'_{in} - \text{tr}(g^{-1}g') g'_{in} \right) + \rho (g^{-1}g')^k_i \nabla^l g'_{kl} = 0.
 \end{aligned} \tag{7.167}$$

7.B Wick rotation

Given a Lorentzian theory, the most straightforward way to find the corresponding action in Euclidean signature is to use a complex diffeomorphism:

$$t = -i\tau. \tag{7.168}$$

After this diffeomorphism (or a similar one using a different coordinate system) the metric generally becomes positive definite and one has to be careful about the definition of the square root in the metric determinant. As we explained in section 2.4, the signs work out correctly if we define $\sqrt{-1} = -i$. As in any coordinate system, the antisymmetric tensor is still defined such that $\sqrt{-G}\epsilon^{012} = 1$ with x^0 now the τ -direction. Because of the volume element the ϵ -tensor is now complex and to comply with standard notation we make this explicit by writing $-i\epsilon^{\lambda\mu\nu} = \hat{\epsilon}^{\lambda\mu\nu}$, where $\hat{\epsilon}^{\lambda\mu\nu}$ is the standard antisymmetric tensor in Euclidean coordinates which is defined such that $\sqrt{G}\hat{\epsilon}^{012} = 1$.

As for the action of the theory, we find that the diffeomorphism results in $iS_L \rightarrow -S_E$ with S_E the standard Euclidean action. In our case, (7.2) becomes:

$$iS_L = -\frac{1}{16\pi G_N} \int d^3x \sqrt{G}(-R + 2\Lambda) + \frac{i}{32\pi G_N \mu} \int d^3x \sqrt{G} \hat{\epsilon}^{\lambda\mu\nu} \left(\Gamma_{\lambda\sigma}^\rho \partial_\mu \Gamma_{\rho\nu}^\sigma + \frac{2}{3} \Gamma_{\lambda\sigma}^\rho \Gamma_{\mu\tau}^\sigma \Gamma_{\nu\rho}^\tau \right). \quad (7.169)$$

Notice that the implicit metric determinant present in the ϵ -symbol cancels the one in the volume element and there is no sign change for the Chern-Simons term. From this action, we see that a convenient way to determine the Euclidean equations of motion is to replace everywhere

$$\epsilon^{\lambda\mu\nu} \rightarrow i\hat{\epsilon}^{\lambda\mu\nu}, \quad \epsilon^{ij} \rightarrow i\hat{\epsilon}^{ij}. \quad (7.170)$$

With these replacements the equations of motion become complex, and so do the linearized solutions we find in the main text, but this is not a problem as we discussed more extensively in section 3.5.

When using component equations, the conversion between Euclidean and Lorentzian signature is most easily done by introducing lightcone coordinates on the Lorentzian side:

$$u = x + t, \quad v = x - t. \quad (7.171)$$

In these coordinates the metric becomes:

$$ds^2 = dudv \quad (7.172)$$

and we fix the sign of the ϵ -tensor such that $\epsilon_{uv} = -\frac{1}{2}$. The passage to Euclidean signature is then implemented by defining complex coordinates:

$$z = x + i\tau, \quad \bar{z} = x - i\tau, \quad (7.173)$$

after which the metric $ds^2 = d\tau^2 + dx^2$ becomes:

$$ds^2 = dzd\bar{z}. \quad (7.174)$$

The metric determinant in complex coordinates becomes negative again and therefore $\tilde{\epsilon}^{ij}$ is complex and ϵ^{ij} is real. We deduce that the component equations in Euclidean signature can be obtained by the simple replacement

$$v \rightarrow z, \quad u \rightarrow \bar{z}, \quad (7.175)$$

in the Lorentzian equations of motion, without any modification of the ϵ -tensor.

Incidentally, notice that the operators:

$$P_i^k = \frac{1}{2}(\delta_i^k + \epsilon_i^k), \quad \bar{P}_i^k = \frac{1}{2}(\delta_i^k - \epsilon_i^k), \quad (7.176)$$

take the following form in lightcone coordinates:

$$\begin{pmatrix} P_u^u & P_u^v \\ P_v^u & P_v^v \end{pmatrix} = \begin{pmatrix} 0 & 0 \\ 0 & 1 \end{pmatrix} \quad \begin{pmatrix} \bar{P}_u^u & \bar{P}_u^v \\ \bar{P}_v^u & \bar{P}_v^v \end{pmatrix} = \begin{pmatrix} 1 & 0 \\ 0 & 0 \end{pmatrix} \quad (7.177)$$

so that, if for example $P_i^k b_{(0)kj} = 0$ and $b_{(0)i}^i = 0$ then only the $b_{(0)uu}$ component can be nonzero. From the above reasoning it follows that these operators take the same form in complex coordinates and therefore only $b_{(0)\bar{z}\bar{z}}$ can be nonzero.

Signs in correlation functions

Our conventions are such that on a Euclidean background metric g_{ij} the energy-momentum tensor is defined as:

$$T_{E,ij} = \frac{4\pi}{\sqrt{g}} \frac{\delta S_E}{\delta g^{ij}}. \quad (7.178)$$

Notice that we functionally differentiate with respect to the inverse metric. By comparing with (1.28) we find that the normalization in this chapter differs by a factor 2π with respect to chapter 1. When we analytically continue back to Lorentzian signature, the definition on the right-hand side changes. Namely, from the above discussion it follows that $S_E = -iS_L$ and $\sqrt{g} = i\sqrt{-g}$, so in Lorentzian signature

$$T_{L,ij} = -\frac{4\pi}{\sqrt{-g}} \frac{\delta S_L}{\delta g^{ij}}. \quad (7.179)$$

In terms of the generating functional of connected correlation functions, $W = \log(Z)$, we find that:

$$T_{E,ij} = -\frac{4\pi}{\sqrt{g}} \frac{\delta W_E}{\delta g^{ij}}, \quad T_{L,ij} = i \frac{4\pi}{\sqrt{-g}} \frac{\delta W_L}{\delta g^{ij}}. \quad (7.180)$$

These expressions lead to the following identity that we use in the main text:

$$\langle T_{ij} \dots \rangle_g = i \frac{4\pi}{\sqrt{-g}} \frac{\delta}{\delta g^{ij}} \langle \dots \rangle_g \quad (7.181)$$

where $\langle \dots \rangle_g$ is an arbitrary correlator in the background metric g_{ij} . Notice that this expression holds irrespective of the signature of the metric, provided we define the square root as above.

Now for general correlation functions of an operator \mathcal{O} , we customarily define the source-operator coupling in Euclidean signature as:

$$- \int d^2x \sqrt{-g} \phi_E \cdot \mathcal{O}_E, \quad (7.182)$$

with ϕ_E the Euclidean source and the dot denoting various possible index contractions. Using once more the above conventions, we find that in Lorentzian signature the coupling becomes:

$$-i \int d^2x \sqrt{-g} \phi_L \cdot \mathcal{O}_L, \quad (7.183)$$

and therefore

$$\langle \mathcal{O}_E \rangle = -\frac{1}{\sqrt{g}} \frac{\delta W_E}{\delta \phi_E}, \quad \langle \mathcal{O}_L \rangle = i \frac{1}{\sqrt{-g}} \frac{\delta W_L}{\delta \phi_L}. \quad (7.184)$$

This results in the general expression in terms of correlation functions:

$$\langle \mathcal{O} \dots \rangle_\phi = i \frac{1}{\sqrt{-g}} \frac{\delta}{\delta \phi} \langle \dots \rangle_\phi. \quad (7.185)$$

In the context of AdS/CFT, $W_E \sim -S_E$ and $W_L \sim iS_L$ with S_E and S_L the Euclidean and the Lorentzian on-shell bulk action, respectively. This leads to:

$$\langle \mathcal{O}_E \rangle = \frac{1}{\sqrt{g}} \frac{\delta S_E}{\delta \phi_E}, \quad \langle \mathcal{O}_L \rangle = -\frac{1}{\sqrt{-g}} \frac{\delta S_L}{\delta \phi_L}. \quad (7.186)$$

On the other hand, for the energy-momentum tensor one may directly use the formulas (7.178) and (7.179), where now S_L and S_E are the on-shell bulk action. It was shown in chapter 2 that these expressions, with in particular the above choice of signs, lead to continuous holographic expressions for the one-point functions. For example, in the case of three-dimensional Einstein gravity one finds from equation (1.169) that in the conventions of this chapter:

$$\langle T_{ij} \rangle = \frac{1}{4G_N} (g_{(2)ij} + \frac{1}{2} g_{(0)ij} R[g_{(0)}]), \quad (7.187)$$

which we demonstrated in 2.4 to be independent of the metric signature. In this expression $g_{(0)ij}$ and $g_{(2)ij}$ the leading and subleading terms in the Fefferman-Graham expansion (7.17). Similarly, for a scalar operator \mathcal{O} dual to a bulk scalar field Φ one finds the expressions (1.117) which according to the discussion in 2.3 holds again both in Lorentzian and in Euclidean signature.

7.C Linearized equations of motion in global coordinates

In this appendix we will present the linearized equations in global coordinates. The usual metric

$$ds^2 = -\cosh^2(r)dt^2 + \sinh^2(r)d\phi^2 + dr^2 \quad (7.188)$$

can be put in the Fefferman-Graham form (7.14) by defining

$$\rho = 4e^{-2r}, \quad (7.189)$$

after which we obtain:

$$ds^2 = -\frac{1}{\rho}\left(1 + \frac{1}{2}\rho + \frac{1}{16}\rho^2\right)dt^2 + \frac{1}{\rho}\left(1 - \frac{1}{2}\rho + \frac{1}{16}\rho^2\right)d\phi^2 + \frac{d\rho^2}{4\rho^2}. \quad (7.190)$$

These coordinates cover all of AdS and are thus global coordinates. Notice that $\partial_k g_{ij} = 0$ and therefore $\Gamma_{ij}^k[g] = 0$ (which of course does *not* imply that $\delta\Gamma_{ij}^k$ vanishes in the linearized equations). We also find that:

$$(g'g^{-1}g')_{ij} = 2g''_{ij}; \quad g''_{ij} - \frac{1}{2}\text{tr}(g^{-1}g')g'_{ij} = f(\rho)g_{ij}; \quad \text{tr}(g^{-1}g') = -2\rho f(\rho), \quad (7.191)$$

with

$$f(\rho) = \frac{2}{16 - \rho^2}, \quad (7.192)$$

which we use to simplify the formulas below. In the expressions below traces are implicitly taken with the aid of g^{-1} , that is we write $\text{tr}(g')$ where before we wrote $\text{tr}(g^{-1}g')$.

The linearized (ij) equation of motion (7.164) becomes:

$$\begin{aligned} & -h''_{ij} - \rho f(\rho)h'_{ij} + f(\rho)h_{ij} + \frac{1}{2}g'_{ij} \left[\text{tr}(h') - \text{tr}(g'g^{-1}h) \right] \\ & + g_{ij} \left[\frac{1}{2}\text{tr}(h'') - \frac{1}{2}\text{tr}(hg^{-1}g'') + \rho f(\rho)(\text{tr}(h') - \text{tr}(g'g^{-1}h)) \right] \\ & + \frac{1}{\mu}\epsilon_i^k \left[\frac{1}{4}\partial_k \partial^l h'_{lj} - \frac{1}{4}(g^{-1}g')_j^c [\partial_k \partial^l h_{lc} - \frac{1}{2}\partial_k \partial_c \text{tr}(h)] + (j \leftrightarrow k) \right] \\ & + \frac{1}{\mu}\epsilon_i^k \left[\frac{1}{4}\partial_k \partial_j \text{tr}(g'g^{-1}h) - \frac{1}{2}\partial_k \partial_j \text{tr}(h') + 2\rho h'''_{jk} \right. \\ & \quad \left. + 3(1 + \rho^2 f(\rho))[h''_{jk} + \rho f(\rho)h'_{jk} - f(\rho)h_{kj}] \right] \\ & + \frac{1}{\mu}\epsilon_i^k g'_{jk} \left[-\frac{3}{2}(1 + \rho^2 f(\rho))[\text{tr}(h') - \text{tr}(hg^{-1}g')] \right. \\ & \quad \left. - \frac{7}{2}\rho[\text{tr}(h'') + \text{tr}(hg^{-1}g'') - \text{tr}(h'g^{-1}g')] \right] + (i \leftrightarrow j) = 0, \quad (7.193) \end{aligned}$$

The linearized version of the (ρi) equation given in (7.167) becomes:

$$\begin{aligned}
 & 2\rho\partial^k h''_{ik} + (1 + 4\rho^2 f(\rho))\partial^k h'_{ik} + \mu\epsilon^{jk}\partial_k h'_{ij} - \frac{1}{2}\mu\epsilon^{jk}(g^{-1}g')^l_j(\partial_k h_{il} + \partial_i h_{kl} - \partial_l h_{ik}) \\
 & - \partial_i \left[\rho\text{tr}(h'g^{-1}g') + [1 + 4\rho^2 f(\rho)]\text{tr}(h') - \left[\frac{1}{2} + 2\rho^2 f(\rho) \right]\text{tr}(g'g^{-1}h) - \rho\text{tr}(g''g^{-1}h) \right] \\
 & + (g^{-1}g')^k_i \left[\rho\partial^l h'_{kl} - 2\rho\partial_k \text{tr}(h') - \frac{3}{2}\rho\partial_k \text{tr}(hg^{-1}g') \right. \\
 & \quad \left. - [1 + 4\rho^2 f(\rho)][\partial^l h_{kl} - \frac{1}{2}\partial_k \text{tr}(h)] \right] \\
 & - 2\rho(g^{-1}g'')^k_i [2\partial^l h_{kl} - \partial_k \text{tr}(h)] = 0
 \end{aligned} \tag{7.194}$$

and the $(\rho\rho)$ equation results in:

$$\begin{aligned}
 & -\text{tr}(h'') + \text{tr}(h'g^{-1}g') - \text{tr}(hg^{-1}g'') + \frac{1}{2\mu}\epsilon^{ij} \left[\partial_i \partial^m h'_{mj} \right. \\
 & \quad \left. - (g^{-1}g')^c_j (\partial_i \partial^m h_{mc} - \frac{1}{2}\partial_i \partial_c \text{tr}(h)) + 2\rho(h'g^{-1}g'')_{ij} \right. \\
 & \quad \left. - 2\rho(g'g^{-1}hg^{-1}g'')_{ij} + 2\rho(g'g^{-1}h'')_{ij} \right] = 0.
 \end{aligned} \tag{7.195}$$

7.D Some results from LCFT

A logarithmic conformal field theory (LCFT) is a conformal field theory in which logarithmic structure arises in the operator product expansion. Such logarithmic structure arises when there are fields with degenerate scaling dimensions having a Jordan block structure; in any logarithmic conformal field theory one of these degenerate fields becomes a zero norm state coupled to a logarithmic partner. In what follows we will be interested in the simplest situation, in which two operators become degenerate and form a logarithmic pair, denoted by (C, D) . If the operator C becomes a zero norm state, the two point functions for this logarithmic pair have the structure:

$$\begin{aligned}
 \langle C(z, \bar{z})C(0) \rangle &= 0; & \langle C(z, \bar{z})D(0, 0) \rangle &= \frac{b_D}{z^{2h_L} \bar{z}^{2h_R}}; \\
 \langle D(z, \bar{z})D(0, 0) \rangle &= \frac{1}{z^{2h_L} \bar{z}^{2h_R}} [-b_D \log m^2 |z|^2 + B_D],
 \end{aligned} \tag{7.196}$$

where the conformal weights of both operators are (h_L, h_R) . The constant B_D may be removed by the redefinition $D \rightarrow D - B_D C/b_D$ but b_D has an invariant meaning and is a characteristic of the LCFT. One can easily generalize these formulas to the case when there are n degenerate fields and the Jordan cell is given by an $n \times n$ matrix, in which case the maximal power of the logarithm will be $\log^n |z|$.

In the current context we are interested in the case where the conformal field theory becomes logarithmic as $c_L \rightarrow 0$ and one of the logarithmic pair is the holomorphic stress energy tensor. There are several distinct approaches to taking such limits, see [139] for a review, but the limit relevant for us was discussed in Kogan and Nichols [138]. The following is a slightly modified version of the discussion in that paper, in which we take the limit $c_L \rightarrow 0$ only in the holomorphic sector.

Consider a conformal field theory with central charges (c_L, c_R) and holomorphic and anti-holomorphic stress energy tensors $(T(z), \bar{T}(\bar{z}))$ respectively, such that

$$\langle T(z)T(0) \rangle = \frac{c_L}{2z^4}; \quad \langle \bar{T}(\bar{z})\bar{T}(0) \rangle = \frac{c_R}{2\bar{z}^4}. \quad (7.197)$$

Let $V(z, \bar{z})$ be a primary field of dimensions (h_L, h_R) , normalized as

$$\langle V(z, \bar{z})V(0, 0) \rangle = \frac{A}{z^{2h_L} \bar{z}^{2h_R}}. \quad (7.198)$$

If T is the only $h_L = 2$ field present (and \bar{T} is the only $h_R = 2$ field), then the OPE for $V(z, \bar{z})$ is of the form

$$V(z, \bar{z})V(0, 0) \sim \frac{A}{z^{2h_L} \bar{z}^{2h_R}} \left[1 + \frac{2h_L}{c_L} z^2 T(0) + \frac{2h_R}{c_R} \bar{z}^2 \bar{T}(0) + \dots \right] \quad (7.199)$$

where the ellipses denote operators of higher dimension.

Consider now the limit $c_L \rightarrow 0$ with c_R finite: if A remains finite in this limit then the OPE is not well-defined. Suppose that as c_L approaches zero then there is another field X with dimension $(2 + \lambda, \lambda)$ which approaches $(2, 0)$; suppose also that its normalization is such that this field contributes to the OPE as

$$V(z, \bar{z})V(0, 0) \sim \frac{A}{z^{2h_L} \bar{z}^{2h_R}} \left[1 + \frac{2h_L}{c_L} z^2 T(0) + \frac{2h_R}{c_R} z^{2+\lambda} \bar{z}^\lambda X(0, 0) + \dots \right]. \quad (7.200)$$

Let the two-point function of X be given by:

$$\langle X(z, \bar{z})X(0, 0) \rangle = \frac{B(\lambda)}{z^{4+2\lambda} \bar{z}^{2\lambda}}, \quad (7.201)$$

whilst $\langle T(z_1)X(z_2, \bar{z}_2) \rangle$ vanishes as they have different dimensions. Now let us define a new field $t(z, \bar{z})$ via

$$t = -\frac{1}{\lambda} T - \frac{1}{\lambda} X. \quad (7.202)$$

In this way the OPE (7.200) is rendered well-defined as $c_L \rightarrow 0$:

$$V(z, \bar{z})V(0, 0) \sim \frac{A}{z^{2h_L} \bar{z}^{2h_R}} \left[1 + \frac{2h_L}{b} z^2 [t(0, 0) + T(0) \log(m^2 |z|^2)] + \dots \right], \quad (7.203)$$

provided the parameter b , defined as

$$b \equiv - \lim_{c_L \rightarrow 0} \frac{c_L}{\lambda(c_L)} = - \frac{1}{\lambda'(0)}, \quad (7.204)$$

is finite. As $c_L \rightarrow 0$ the two point functions of the pair (T, t) become:

$$\begin{aligned} \langle T(z)T(0) \rangle &= 0; & \langle T(z)t(0,0) \rangle &= \frac{b}{2z^4}; \\ \langle t(z, \bar{z})t(0,0) \rangle &= \frac{1}{z^4} \lim_{c_L \rightarrow 0} \left[-\frac{b}{2\lambda} + \frac{B}{\lambda^2} - 2\lambda B \log(m^2|z^2|) + \dots \right]. \end{aligned} \quad (7.205)$$

For this to be well-defined as $c_L \rightarrow 0$,

$$B(c_L) = \frac{b\lambda}{2} + B_m\lambda^2 + \mathcal{O}(\lambda^3), \quad (7.206)$$

and therefore

$$\langle t(z, \bar{z})t(0,0) \rangle = \frac{B_m - b \log(m^2|z|^2)}{z^4}. \quad (7.207)$$

The logarithmic pair (T, t) thus indeed has the anticipated two-point function structure given in (7.196). We are interested in the case where $c_R \neq 0$, and thus there is no such degeneration in the anti-holomorphic sector. Note that

$$\langle \bar{T}(\bar{z})t(0,0) \rangle = 0. \quad (7.208)$$

Recall that the constant B_m can be changed by a redefinition of t ; choosing $t \rightarrow t - B_m T/b$ removes the non-logarithmic term in the two point function (7.207).

7.E Warped AdS

The metric of global AdS₃ can be written in ‘warped’ form as:

$$ds^2 = -\cosh^2(\sigma)d\tau^2 + \frac{1}{4}d\sigma^2 + (du + \sinh(\sigma)d\tau)^2 \quad (7.209)$$

We can define:

$$z = 2e^{-\sigma/2} \quad \sigma = 2 \log(z/2) \quad (7.210)$$

after which the metric becomes:

$$ds^2 = \frac{dz^2}{z^2} - d\tau^2 + du^2 + \left(\frac{4}{z^2} - \frac{z^2}{4}\right)dud\tau. \quad (7.211)$$

In this coordinate system it is manifest that this metric is conformally compact. Namely, z can be used as the defining function: in agreement with the discussion in section 7.3, z has a single zero at $z = 0$ and the metric:

$$z^2 ds^2 = dz^2 + 4dud\tau + \dots \quad (7.212)$$

is a non-degenerate three-dimensional metric that extends smoothly to $z = 0$.

On the other hand, the metric of spacelike warped AdS can be written as:

$$ds^2 = \left(-\cosh^2(\sigma)(\nu^2 + 3) + 4\nu^2 \sinh^2(\sigma) \right) d\tau^2 + \frac{d\sigma^2}{\nu^2 + 3} + 4\nu^2 du^2 + 8\nu^2 \sinh(\sigma) dud\tau, \quad (7.213)$$

with $\nu = \mu/3$. After the coordinate transformation:

$$\sigma = -\sqrt{\nu^2 + 3} \log(z) \quad (7.214)$$

it becomes asymptotically of the form:

$$ds^2 = \frac{dz^2}{z^2} + 3(\nu^2 - 1)z^{-2\sqrt{\nu^2+3}}d\tau^2 + 8\nu^2z^{-\sqrt{\nu^2+3}}dud\tau + \dots \quad (7.215)$$

As $z \rightarrow 0$, we find that the terms have a different pole structure and therefore this metric cannot be made regular by multiplication with the usual defining function z , unless $\nu^2 = 1$ (which is AdS). Furthermore, the leading term in the induced metric at slices of constant z is proportional to $d\tau^2$ and so it is degenerate. Thus the spacetime with metric (7.213) is not conformally compact. Notice that the same conclusion holds for any spacetime whose metric asymptotes to (7.213).

For timelike warped AdS the metric has the form:

$$ds^2 = \left(\cosh^2(\sigma)(\nu^2 + 3) - 4\nu^2 \sinh^2(\sigma) \right) du^2 + \frac{d\sigma^2}{\nu^2 + 3} - 4\nu^2 d\tau^2 - 8\nu^2 \sinh(\sigma) dud\tau. \quad (7.216)$$

This is just spacelike warped AdS with the replacement $\tau \rightarrow iu$ and $u \rightarrow i\tau$ and we can immediately draw the same conclusions as for spacelike warped AdS.

For null warped AdS the metric is given by:

$$ds^2 = \frac{dz^2}{z^2} + \frac{dudv}{z^2} \pm \frac{du^2}{z^4}, \quad (7.217)$$

which is a solution of TMG with $\mu = 3$ or $\nu = 1$. We again find a different pole structure for the different terms, as well as a singular leading-order term in the induced metric on slices of constant z . Again, no good defining function exists that makes the three-dimensional metric regular on the slice $z = 0$ and this manifold is not conformally compact.

Bibliography

- [1] K. Skenderis and B. C. van Rees, “Real-time gauge/gravity duality,” *Phys. Rev. Lett.* **101** (2008) 081601, arXiv:0805.0150 [hep-th].
- [2] K. Skenderis and B. C. van Rees, “Real-time gauge/gravity duality: Prescription, Renormalization and Examples,” *JHEP* **05** (2009) 085, arXiv:0812.2909 [hep-th].
- [3] B. C. van Rees, “Real-time gauge/gravity duality and ingoing boundary conditions,” *Nucl. Phys. Proc. Suppl.* **192-193** (2009) 193–196, arXiv:0902.4010 [hep-th].
- [4] K. Skenderis and B. C. van Rees, “Holography and wormholes in 2+1 dimensions,” *Com. Math. Phys. (to appear)* (2009) , arXiv:0912.2090 [hep-th].
- [5] K. Skenderis, M. Taylor, and B. C. van Rees, “Topologically Massive Gravity and the AdS/CFT Correspondence,” *JHEP* **09** (2009) 045, arXiv:0906.4926 [hep-th].
- [6] K. Skenderis, M. Taylor, and B. C. van Rees, “AdS boundary conditions and the Topologically Massive Gravity/CFT correspondence,” *AIP Conference Proceedings* **1196** (2009) 266–275, arXiv:0909.5617 [hep-th].
- [7] G. 't Hooft, “Dimensional reduction in quantum gravity,” arXiv:gr-qc/9310026.
- [8] L. Susskind, “The World as a hologram,” *J. Math. Phys.* **36** (1995) 6377–6396, arXiv:hep-th/9409089.
- [9] J. M. Maldacena, “The large N limit of superconformal field theories and supergravity,” *Adv. Theor. Math. Phys.* **2** (1998) 231–252, hep-th/9711200.

- [10] O. Aharony, S. S. Gubser, J. M. Maldacena, H. Ooguri, and Y. Oz, “Large N field theories, string theory and gravity,” *Phys. Rept.* **323** (2000) 183–386, arXiv:hep-th/9905111.
- [11] E. D’Hoker and D. Z. Freedman, “Supersymmetric gauge theories and the AdS/CFT correspondence,” arXiv:hep-th/0201253.
- [12] N. Seiberg, “Supersymmetry and Nonperturbative beta Functions,” *Phys. Lett.* **B206** (1988) 75.
- [13] G. ’t Hooft, “A planar diagram theory for strong interactions,” *Nucl. Phys.* **B72** (1974) 461.
- [14] H. J. Kim, L. J. Romans, and P. van Nieuwenhuizen, “The Mass Spectrum of Chiral N=2 D=10 Supergravity on S⁵,” *Phys. Rev.* **D32** (1985) 389.
- [15] S. S. Gubser, I. R. Klebanov, and A. M. Polyakov, “Gauge theory correlators from non-critical string theory,” *Phys. Lett.* **B428** (1998) 105–114, hep-th/9802109.
- [16] E. Witten, “Anti-de Sitter space and holography,” *Adv. Theor. Math. Phys.* **2** (1998) 253–291, hep-th/9802150.
- [17] P. Di Francesco, P. Mathieu, and D. Senechal, “Conformal field theory,” New York, USA: Springer (1997) 890 p.
- [18] H. Osborn, “Implications of conformal invariance for quantum field theories in $d > 2$,” arXiv:hep-th/9312176.
- [19] C. R. Graham, “Volume and area renormalizations for conformally compact Einstein metrics,” arXiv:math/9909042.
- [20] M. T. Anderson, “Geometric aspects of the AdS/CFT correspondence,” hep-th/0403087.
- [21] C. Fefferman and C. Graham, “Conformal Invariants,” *Elie Cartan et les Mathématiques d’aujourd’hui (Asterisque 95)* (1985) .
- [22] C. Imbimbo, A. Schwimmer, S. Theisen, and S. Yankielowicz, “Diffeomorphisms and holographic anomalies,” *Class. Quant. Grav.* **17** (2000) 1129–1138, arXiv:hep-th/9910267.
- [23] K. Skenderis, “Asymptotically Anti-de Sitter spacetimes and their stress energy tensor,” *Int. J. Mod. Phys.* **A16** (2001) 740–749, hep-th/0010138.
- [24] M. Henningson and K. Skenderis, “The holographic Weyl anomaly,” *JHEP* **07** (1998) 023, arXiv:hep-th/9806087.

- [25] M. Henningson and K. Skenderis, “Holography and the Weyl anomaly,” *Fortsch. Phys.* **48** (2000) 125–128, arXiv:hep-th/9812032.
- [26] V. Balasubramanian and P. Kraus, “A stress tensor for Anti-de Sitter gravity,” *Commun. Math. Phys.* **208** (1999) 413–428, arXiv:hep-th/9902121.
- [27] S. de Haro, S. N. Solodukhin, and K. Skenderis, “Holographic reconstruction of spacetime and renormalization in the AdS/CFT correspondence,” *Commun. Math. Phys.* **217** (2001) 595–622, arXiv:hep-th/0002230.
- [28] J. de Boer, E. P. Verlinde, and H. L. Verlinde, “On the holographic renormalization group,” *JHEP* **08** (2000) 003, arXiv:hep-th/9912012.
- [29] I. Papadimitriou and K. Skenderis, “AdS / CFT correspondence and geometry,” *Proceedings Strasbourg 2003, AdS/CFT correspondence, ed. O. Biquard* 73, hep-th/0404176.
- [30] I. Papadimitriou and K. Skenderis, “Thermodynamics of asymptotically locally AdS spacetimes,” *JHEP* **08** (2005) 004, hep-th/0505190.
- [31] K. Skenderis, “Lecture notes on holographic renormalization,” *Class. Quant. Grav.* **19** (2002) 5849–5876, hep-th/0209067.
- [32] R. M. Wald, *General Relativity*. The University of Chicago Press, 1984.
- [33] J. D. Brown and M. Henneaux, “Central Charges in the Canonical Realization of Asymptotic Symmetries: An Example from Three-Dimensional Gravity,” *Commun. Math. Phys.* **104** (1986) 207–226.
- [34] D. T. Son and A. O. Starinets, “Viscosity, Black Holes, and Quantum Field Theory,” *Ann. Rev. Nucl. Part. Sci.* **57** (2007) 95–118, arXiv:0704.0240 [hep-th].
- [35] S. Sachdev, “Condensed matter and AdS/CFT,” arXiv:1002.2947 [hep-th].
- [36] S. A. Hartnoll, “Lectures on holographic methods for condensed matter physics,” *Class. Quant. Grav.* **26** (2009) 224002, arXiv:0903.3246 [hep-th].
- [37] V. Balasubramanian, P. Kraus, and A. E. Lawrence, “Bulk vs. boundary dynamics in Anti-de Sitter spacetime,” *Phys. Rev.* **D59** (1999) 046003, hep-th/9805171.
- [38] V. Balasubramanian, P. Kraus, A. E. Lawrence, and S. P. Trivedi, “Holographic probes of Anti-de Sitter space-times,” *Phys. Rev.* **D59** (1999) 104021, hep-th/9808017.

-
- [39] J. M. Maldacena, “Eternal black holes in Anti-de-Sitter,” *JHEP* **04** (2003) 021, hep-th/0106112.
- [40] D. T. Son and A. O. Starinets, “Minkowski-space correlators in AdS/CFT correspondence: Recipe and applications,” *JHEP* **09** (2002) 042, hep-th/0205051.
- [41] C. P. Herzog and D. T. Son, “Schwinger-Keldysh propagators from AdS/CFT correspondence,” *JHEP* **03** (2003) 046, hep-th/0212072.
- [42] Y. Satoh and J. Troost, “On time-dependent AdS/CFT,” *JHEP* **01** (2003) 027, hep-th/0212089.
- [43] P. Kraus, H. Ooguri, and S. Shenker, “Inside the horizon with AdS/CFT,” *Phys. Rev.* **D67** (2003) 124022, hep-th/0212277.
- [44] D. Marolf, “States and boundary terms: Subtleties of Lorentzian AdS/CFT,” *JHEP* **05** (2005) 042, hep-th/0412032.
- [45] G. Festuccia and H. Liu, “Excursions beyond the horizon: Black hole singularities in Yang-Mills theories. I,” *JHEP* **04** (2006) 044, arXiv:hep-th/0506202.
- [46] A. Lawrence and A. Sever, “Holography and renormalization in Lorentzian signature,” *JHEP* **10** (2006) 013, arXiv:hep-th/0606022.
- [47] N. Iqbal and H. Liu, “Universality of the hydrodynamic limit in AdS/CFT and the membrane paradigm,” arXiv:0809.3808 [hep-th].
- [48] M. E. Peskin and D. V. Schroeder, “An Introduction to quantum field theory,”. Reading, USA: Addison-Wesley (1995) 842 p.
- [49] S. Weinberg, “The Quantum theory of fields. Vol. 1: Foundations,”. Cambridge, UK: Univ. Pr. (1995) 609 p.
- [50] A. Smilga, “Lectures on quantum chromodynamics,”. Singapore, Singapore: World Scientific (2001) 322 p.
- [51] N. P. Landsman and C. G. van Weert, “Real and Imaginary Time Field Theory at Finite Temperature and Density,” *Phys. Rept.* **145** (1987) 141.
- [52] J. S. Schwinger, “Brownian motion of a quantum oscillator,” *J. Math. Phys.* **2** (1961) 407–432.
- [53] P. M. Bakshi and K. T. Mahanthappa, “Expectation value formalism in quantum field theory. 1,” *J. Math. Phys.* **4** (1963) 1–11.
- [54] P. M. Bakshi and K. T. Mahanthappa, “Expectation value formalism in quantum field theory. 2,” *J. Math. Phys.* **4** (1963) 12–16.

- [55] L. V. Keldysh, “Diagram technique for nonequilibrium processes,” *Zh. Eksp. Teor. Fiz.* **47** (1964) 1515–1527 [*Sov. Phys. JETP* **20** (1965) 1018].
- [56] J. B. Hartle and S. W. Hawking, “Wave Function of the Universe,” *Phys. Rev.* **D28** (1983) 2960–2975.
- [57] J. J. Halliwell and J. B. Hartle, “Integration Contours for the No Boundary Wave Function of the Universe,” *Phys. Rev.* **D41** (1990) 1815.
- [58] G. Hayward, “Gravitational action for space-times with nonsmooth boundaries,” *Phys. Rev.* **D47** (1993) 3275–3280.
- [59] S. W. Hawking and C. J. Hunter, “The Gravitational Hamiltonian in the Presence of Non- Orthogonal Boundaries,” *Class. Quant. Grav.* **13** (1996) 2735–2752, arXiv:gr-qc/9603050.
- [60] J. D. Brown, S. R. Lau, and J. York, “Action and Energy of the Gravitational Field,” arXiv:gr-qc/0010024.
- [61] J. B. Hartle, “Ground state wave function of linearized gravity,” *Phys. Rev.* **D29** (1984) 2730–2737.
- [62] R. F. Streater and A. S. Wightman, “PCT, spin and statistics, and all that,”. Redwood City, USA: Addison-Wesley (1989) 207 p. (Advanced book classics).
- [63] D. Birmingham, I. Sachs, and S. N. Solodukhin, “Relaxation in conformal field theory, Hawking-Page transition, and quasinormal/normal modes,” *Phys. Rev.* **D67** (2003) 104026, arXiv:hep-th/0212308.
- [64] M. Bianchi, D. Z. Freedman, and K. Skenderis, “How to go with an RG flow,” *JHEP* **08** (2001) 041, arXiv:hep-th/0105276.
- [65] M. Bianchi, D. Z. Freedman, and K. Skenderis, “Holographic renormalization,” *Nucl. Phys.* **B631** (2002) 159–194, arXiv:hep-th/0112119.
- [66] G. Mack and I. T. Todorov, “Conformal-invariant green functions without ultraviolet divergences,” *Phys. Rev.* **D6** (1973) 1764–1787.
- [67] W. G. Unruh, “Notes on black hole evaporation,” *Phys. Rev.* **D14** (1976) 870.
- [68] N. Birrel and P. Davies, *Quantum Fields in Curved Space*. Cambridge University Press, 1982.
- [69] E. Keski-Vakkuri, “Bulk and boundary dynamics in BTZ black holes,” *Phys. Rev.* **D59** (1999) 104001, hep-th/9808037.

- [70] M. Bañados, C. Teitelboim, and J. Zanelli, “The black hole in three-dimensional space-time,” *Phys. Rev. Lett.* **69** (1992) 1849–1851, hep-th/9204099.
- [71] M. Bañados, M. Henneaux, C. Teitelboim, and J. Zanelli, “Geometry of the 2+1 black hole,” *Phys. Rev. D* **48** (1993) 1506–1525, gr-qc/9302012.
- [72] B. Carter, “Hamilton-Jacobi and Schrodinger separable solutions of Einstein’s equations,” *Commun. Math. Phys.* **10** (1968) 280.
- [73] S. W. Hawking, C. J. Hunter, and M. Taylor, “Rotation and the AdS/CFT correspondence,” *Phys. Rev.* **D59** (1999) 064005, arXiv:hep-th/9811056.
- [74] G. W. Gibbons, H. Lu, D. N. Page, and C. N. Pope, “Rotating black holes in higher dimensions with a cosmological constant,” *Phys. Rev. Lett.* **93** (2004) 171102, arXiv:hep-th/0409155.
- [75] J. B. Hartle and S. W. Hawking, “Path Integral Derivation of Black Hole Radiance,” *Phys. Rev.* **D13** (1976) 2188–2203.
- [76] S. Aminneborg, I. Bengtsson, D. Brill, S. Holst, and P. Peldan, “Black holes and wormholes in 2+1 dimensions,” *Class. Quant. Grav.* **15** (1998) 627–644, gr-qc/9707036.
- [77] D. Brill, “Black holes and wormholes in 2+1 dimensions,” gr-qc/9904083.
- [78] K. Skenderis and S. N. Solodukhin, “Quantum effective action from the AdS/CFT correspondence,” *Phys. Lett.* **B472** (2000) 316–322, hep-th/9910023.
- [79] K. Krasnov, “Holography and Riemann surfaces,” *Adv. Theor. Math. Phys.* **4** (2000) 929–979, arXiv:hep-th/0005106.
- [80] T. Barbot, “Causal properties of AdS-isometry groups. I: Causal actions and limit sets,” math.gt/0509552.
- [81] T. Barbot, “Causal properties of AdS-isometry groups. II: BTZ multi black-holes,” math.gt/0510065.
- [82] B. van Rees, “Wormholes in 2+1 dimensions.” Master’s thesis, <http://staff.science.uva.nl/~brees>, June, 2006.
- [83] Y. Imayoshi and M. Taniguchi, *An Introduction to Teichmüller Spaces*. Springer-Verlag, 1992.
- [84] O. Lehto, *Univalent Functions and Teichmüller Spaces*. Springer-Verlag, 1986.

- [85] S. Nag, *The Complex Analytic Theory of Teichmüller spaces*. John Wiley & Sons, 1988.
- [86] M. Banados, M. Henneaux, C. Teitelboim, and J. Zanelli, “Geometry of the (2+1) black hole,” *Phys. Rev.* **D48** (1993) 1506–1525, arXiv:gr-qc/9302012.
- [87] G. J. Galloway, K. Schleich, D. M. Witt, and E. Woolgar, “Topological censorship and higher genus black holes,” *Phys. Rev.* **D60** (1999) 104039, gr-qc/9902061.
- [88] S. Carlip and C. Teitelboim, “Aspects of black hole quantum mechanics and thermodynamics in (2+1)-dimensions,” *Phys. Rev.* **D51** (1995) 622–631, gr-qc/9405070.
- [89] K. Krasnov, “On holomorphic factorization in asymptotically AdS 3D gravity,” *Class. Quant. Grav.* **20** (2003) 4015–4042, hep-th/0109198.
- [90] K. Krasnov, “Black Hole Thermodynamics and Riemann Surfaces,” *Class. Quant. Grav.* **20** (2003) 2235–2250, arXiv:gr-qc/0302073.
- [91] L. Takhtajan and P. Zograf, “On uniformization of Riemann surfaces and the Weyl-Peterson metric on Teichmüller and Schottky spaces,” *Math. USSR Sbornik* **60** (1988) 297–313.
- [92] J. M. Maldacena and L. Maoz, “Wormholes in AdS,” *JHEP* **02** (2004) 053, arXiv:hep-th/0401024.
- [93] H. Parlier, “Fixed point free involutions on Riemann surfaces,” *Israel J. Math.* **166** (2008) 297–311, arXiv:math.DG/0504109.
- [94] B. Freivogel *et al.*, “Inflation in AdS/CFT,” *JHEP* **03** (2006) 007, arXiv:hep-th/0510046.
- [95] J. Louko and D. Marolf, “Single-exterior black holes and the AdS-CFT conjecture,” *Phys. Rev.* **D59** (1999) 066002, arXiv:hep-th/9808081.
- [96] S. W. Hawking and D. N. Page, “Thermodynamics of black holes in anti-de Sitter space,” *Commun. Math. Phys.* **87** (1983) 577.
- [97] J. M. Maldacena and A. Strominger, “AdS(3) black holes and a stringy exclusion principle,” *JHEP* **12** (1998) 005, hep-th/9804085.
- [98] X. Yin, “Partition Functions of Three-Dimensional Pure Gravity,” arXiv:0710.2129 [hep-th].
- [99] S. Aminneborg, I. Bengtsson, and S. Holst, “A spinning Anti-de Sitter wormhole,” *Class. Quant. Grav.* **16** (1999) 363–382, gr-qc/9805028.

- [100] D. Brill, “2+1-dimensional black holes with momentum and angular momentum,” *Annalen Phys.* **9** (2000) 217–226, gr-qc/9912079.
- [101] K. Krasnov, “Analytic continuation for asymptotically AdS 3D gravity,” *Class. Quant. Grav.* **19** (2002) 2399–2424, arXiv:gr-qc/0111049.
- [102] K. Skenderis and M. Taylor, “The fuzzball proposal for black holes,” *Phys. Rept.* **467** (2008) 117–171, arXiv:0804.0552 [hep-th].
- [103] A. Maloney *to appear* .
- [104] C. Crnkovic and E. Witten, “Covariant description of canonical formalism in geometrical theories,”. Print-86-1309 (Princeton).
- [105] C. Crnkovic, “Symplectic geometry and (super)Poincare algebra in geometrical theories,” *Nucl. Phys.* **B288** (1987) 419.
- [106] J. Lee and R. M. Wald, “Local symmetries and constraints,” *J. Math. Phys.* **31** (1990) 725–743.
- [107] M. Banados, C. Teitelboim, and J. Zanelli, “The Black hole in three-dimensional space-time,” *Phys. Rev. Lett.* **69** (1992) 1849–1851, arXiv:hep-th/9204099.
- [108] W. P. Thurston, *The Geometry and Topology of Three-Manifolds*. Princeton University Press, 1980. Lecture notes, <http://www.msri.org/publications/books/gt3m/>.
- [109] S. Deser, R. Jackiw, and S. Templeton, “Three-Dimensional Massive Gauge Theories,” *Phys. Rev. Lett.* **48** (1982) 975–978.
- [110] S. Deser, R. Jackiw, and S. Templeton, “Topologically massive gauge theories,” *Ann. Phys.* **140** (1982) 372–411.
- [111] W. Li, W. Song, and A. Strominger, “Chiral Gravity in Three Dimensions,” *JHEP* **04** (2008) 082, arXiv:0801.4566 [hep-th].
- [112] S. Carlip, S. Deser, A. Waldron, and D. K. Wise, “Cosmological Topologically Massive Gravitons and Photons,” *Class. Quant. Grav.* **26** (2009) 075008, arXiv:0803.3998 [hep-th].
- [113] D. Grumiller and N. Johansson, “Instability in cosmological topologically massive gravity at the chiral point,” *JHEP* **07** (2008) 134, arXiv:0805.2610 [hep-th].
- [114] M.-i. Park, “Constraint Dynamics and Gravitons in Three Dimensions,” *JHEP* **09** (2008) 084, arXiv:0805.4328 [hep-th].

- [115] D. Grumiller, R. Jackiw, and N. Johansson, “Canonical analysis of cosmological topologically massive gravity at the chiral point,” arXiv:0806.4185 [hep-th].
- [116] S. Carlip, S. Deser, A. Waldron, and D. K. Wise, “Topologically Massive AdS Gravity,” *Phys. Lett.* **B666** (2008) 272–276, arXiv:0807.0486 [hep-th].
- [117] S. Carlip, “The Constraint Algebra of Topologically Massive AdS Gravity,” *JHEP* **10** (2008) 078, arXiv:0807.4152 [hep-th].
- [118] G. Giribet, M. Kleban, and M. Porrati, “Topologically Massive Gravity at the Chiral Point is Not Chiral,” *JHEP* **10** (2008) 045, arXiv:0807.4703 [hep-th].
- [119] M. Blagojevic and B. Cvetkovic, “Canonical structure of topologically massive gravity with a cosmological constant,” arXiv:0812.4742 [gr-qc].
- [120] W. Li, W. Song, and A. Strominger, “Comment on ‘Cosmological Topological Massive Gravitons and Photons’,” arXiv:0805.3101 [hep-th].
- [121] E. Ayon-Beato and M. Hassaine, “pp waves of conformal gravity with self-interacting source,” *Ann. Phys.* **317** (2005) 175–181, arXiv:hep-th/0409150.
- [122] E. Ayon-Beato and M. Hassaine, “Exploring AdS waves via nonminimal coupling,” *Phys. Rev.* **D73** (2006) 104001, arXiv:hep-th/0512074.
- [123] A. Strominger, “A Simple Proof of the Chiral Gravity Conjecture,” arXiv:0808.0506 [hep-th].
- [124] A. Maloney, W. Song, and A. Strominger, “Chiral Gravity, Log Gravity and Extremal CFT,” arXiv:0903.4573 [hep-th].
- [125] S. Carlip, “Chiral Topologically Massive Gravity and Extremal B-F Scalars,” arXiv:0906.2384 [hep-th].
- [126] D. Grumiller and N. Johansson, “Consistent boundary conditions for cosmological topologically massive gravity at the chiral point,” *Int. J. Mod. Phys.* **D17** (2009) 2367–2372, arXiv:0808.2575 [hep-th].
- [127] M. Henneaux, C. Martinez, and R. Troncoso, “Asymptotically anti-de Sitter spacetimes in topologically massive gravity,” arXiv:0901.2874 [hep-th].
- [128] M. Berg and H. Samtleben, “An exact holographic RG flow between 2d conformal fixed points,” *JHEP* **05** (2002) 006, arXiv:hep-th/0112154.

- [129] I. Kanitscheider, K. Skenderis, and M. Taylor, “Holographic anatomy of fuzzballs,” *JHEP* **04** (2007) 023, arXiv:hep-th/0611171.
- [130] D. Anninos, W. Li, M. Padi, W. Song, and A. Strominger, “Warped AdS₃ Black Holes,” *JHEP* **03** (2009) 130, arXiv:0807.3040 [hep-th].
- [131] S. N. Solodukhin, “Holography with Gravitational Chern-Simons Term,” *Phys. Rev.* **D74** (2006) 024015, arXiv:hep-th/0509148.
- [132] P. Kraus and F. Larsen, “Holographic gravitational anomalies,” *JHEP* **01** (2006) 022, arXiv:hep-th/0508218.
- [133] K. A. Moussa, G. Clement, and C. Leygnac, “The black holes of topologically massive gravity,” *Class. Quant. Grav.* **20** (2003) L277–L283, arXiv:gr-qc/0303042.
- [134] W. A. Bardeen and B. Zumino, “Consistent and Covariant Anomalies in Gauge and Gravitational Theories,” *Nucl. Phys.* **B244** (1984) 421.
- [135] L. Alvarez-Gaume and P. H. Ginsparg, “The Structure of Gauge and Gravitational Anomalies,” *Ann. Phys.* **161** (1985) 423.
- [136] K. Hotta, Y. Hyakutake, T. Kubota, T. Nishinaka, and H. Tanida, “Left-Right Asymmetric Holographic RG Flow with Gravitational Chern-Simons Term,” arXiv:0906.1255 [hep-th].
- [137] V. Gurarie and A. W. W. Ludwig, “Conformal field theory at central charge $c = 0$ and two-dimensional critical systems with quenched disorder,” arXiv:hep-th/0409105.
- [138] I. I. Kogan and A. Nichols, “Stress energy tensor in $c = 0$ logarithmic conformal field theory,” arXiv:hep-th/0203207.
- [139] M. Flohr and A. Muller-Lohmann, “Notes on non-trivial and logarithmic CFTs with $c = 0$,” *J. Stat. Mech.* **0604** (2006) P002, arXiv:hep-th/0510096.
- [140] E. A. Bergshoeff, O. Hohm, and P. K. Townsend, “Massive Gravity in Three Dimensions,” *Phys. Rev. Lett.* **102** (2009) 201301, arXiv:0901.1766 [hep-th].

Summary

In this chapter we sketch an overview of the line of research to which this thesis belongs. We begin with a brief overview of our current knowledge of the elementary particles which can be summarized in a quantum field theory called the *standard model*. Afterwards we discuss the incompleteness of the standard model, in particular we discuss the absence of a proper description of gravity. In the third section below we eventually explain how string theory may possibly complete the standard model into a theory that would correctly describe gravity. Afterwards we discuss the so-called ‘gauge/gravity dualities’, the research direction within string theory to which this thesis belongs. Finally we summarize the results of this thesis.

The standard model

In 1900 Max Planck presented a formula for the temperature-dependence of electromagnetic radiation. The most remarkable property of Planck’s formula was that it contained a new constant, h , whose value is currently determined to be around $6,63 \cdot 10^{-34} Js$. It was soon realized that h was a new fundamental constant of nature around which a radically new theory, called quantum mechanics, had to be developed in order to correctly describe the behavior of particles at short distances. Using quantum mechanics one may for example describe the electron’s orbits in an atom and compute the associated absorption spectrum.

The development of quantum mechanics was however not the only revolution taking place at the beginning of the twentieth century. In 1905 another fundamental constant of nature, namely the speed of light c , featured prominently in a paper by Einstein. According to his special theory of relativity there is no absolute way to measure time or distance, rather their definitions depend on the observer’s own velocity. The speed of light makes it possible to unify distances and times in a single concept, called the *spacetime*.

Measurable effects of special relativity only occur when particles move close to the speed of light. These effects are however not incorporated by quantum mecha-

tics, which therefore gives incorrect results for example when trying to describe electrons moving close to the speed of light. Improving quantum mechanics to incorporate relativistic effects however turned out to be remarkably difficult. The resulting framework is called *quantum field theory* and its development required the efforts of several generations of physicists. Furthermore, quantum field theory is still not fully understood, although we nowadays have sufficient understanding to properly use quantum field theory to predict with very high accuracy the outcome of certain particle accelerator experiments.

A quantum field theory describes the quantum-mechanical behavior of an arbitrary set of particles moving at high velocities. In nature we however observe a very concrete set of *elementary particles* which form the fundamental constituents of all other matter. The specific quantum field theory describing these elementary particles is called the *standard model*. The particles in the standard model are six types of *quarks*, six types of *leptons* and the *Higgs boson*. The quarks are called up, down, charm, strange, top and bottom. The leptons are called the electron, the muon and the tau-particle plus three different neutrino particles. The Higgs boson has not been observed yet but is necessary for consistency of the standard model. According to the standard model all known matter can be obtained by combining these constituents, for example a proton would roughly speaking consist of two up quarks and a single down quark.

In the standard model there are also three different *forces* that act on these elementary particles: the strong nuclear force, the weak nuclear force and the more well-known electromagnetic force. These forces are modelled by so-called *force-carrying particles*. For example, the electromagnetic force between two electrons is modelled by the exchange of *photons*. The force-carrying particles replace the usual description in terms of for example electromagnetic fields, which is no longer tenable because of the quantum-mechanical behavior of the particles at short distances. The particles used to model the strong nuclear force are called *gluons*, whereas those modelling the weak nuclear force are the so-called *W-* and *Z-bosons*. There are eight gluons in nature, two W-bosons and a single Z-boson.

Incompleteness

Besides Planck (in 1918) more than 60 nobel prizes have been awarded for contributions to the development of first quantum mechanics and then quantum field theory and the standard model. The standard model represents our most fundamental knowledge of the workings of nature which certainly makes it a model to be proud of. Present-day theoretical physicists are however also relieved that the standard model is necessarily *incomplete* and more fundamental physics remains to be discovered. Important experimental evidence in this direction are the scale

of electroweak symmetry breaking as well as dark matter which essentially point towards new particles that are yet to be discovered. In the future we may find such particles using for example particle accelerator experiments and we may then add these to the standard model. In this way it is plausible that this procedure results in a more complete quantum field theory which incorporates these new particles.

Another incompleteness of the standard model is the fact that there exists yet another force, namely gravity, which is not yet described by the standard model. Let us now explain how this is conceptually a much larger problem.

First of all there exists of course an accurate description of gravity at large distances, namely Einstein's classical theory of general relativity. According to general relativity the spacetime which already featured in special relativity is actually *curved*. General relativity successfully describes a vast array of astrophysical and cosmological phenomena. At very small distances we however do not know how to properly describe gravity; although the *special* theory of relativity was eventually united with quantum mechanics into quantum field theory, there appears to be no easy way to do the same for the *general* theory of relativity. This is because quantum field theory dictates that one should replace the gravitational field with a force-carrying particle (just like the electromagnetic field was replaced with a photon) which in this case is called the *graviton*. However when we perform computations with a quantum field theory that has gravitons then we obtain certain mathematical problems which point towards the fact that this cannot be a fundamental description of nature. Because of these issues quantum field theory and gravity cannot be united on a fundamental level: in a world where quantum field theory would be exactly valid there is no place for gravity and vice versa. Nevertheless to describe events happening in our world one needs to use both theories and therefore neither theory can be exactly true! The challenge is then to find a correct and mathematically consistent *quantum theory of gravity*, which because of the aforementioned problems has to surpass the concept of a quantum field theory.

Unfortunately there are very few experimental results available to assist us in addressing this challenge. The experimental success of the standard model (so of a quantum field theory without gravity) for example demonstrates that the effects of gravity on the results of particle-accelerator experiments is completely negligible. This is consistent with a simple order-of-magnitude estimate: if we assume that general relativity remains valid at very short distances then we can for example estimate that the gravitational attraction between two electrons is 10^{42} times smaller than the repulsive electric force. This is hopelessly beyond our current experimental abilities: the electric force is for example known with a relative precision of about 10^{10} . (This order-of-magnitude analysis uses however the *classical* theory of general relativity which we know cannot be consistent at

small distances. This makes the analysis inherently unreliable and in reality there is so far no consistent theoretical approximation of the effects of gravity at small distances.)

String theory

The fundamental idea of string theory is to replace the elementary particles with small one-dimensional strings. This indeed surpasses the usual quantum field theory which considers all particles to be point particles. Furthermore this assumption makes it possible to overcome the aforementioned mathematical problems and to consistently describe the interactions with gravitons. String theory thus seems to fulfill all the basic requirements for a quantum theory of gravity. Our current comprehension of string theory is however still incomplete and understanding string theory better is the main motivation behind much present-day research.

Although string theory seems to be a consistent theory of quantum gravity it has so far been quite difficult to also obtain a *realistic* version of such a theory. Although depending largely on the precise type of string theory used, one generically seems to obtain far more and rather different elementary particles than the aforementioned particles of the standard model. It is however not impossible that we eventually find a specific type of string theory which does result in a realistic particle spectrum. The search for such a string theory is another point of focus in much present-day research.

Nevertheless string theory remains a useful concept which gives us unique insights in the inner workings of a quantum theory of gravity. An example of such an insight is the description of black holes in string theory. Black holes cannot be accurately described by general relativity since according to this theory the gravitational force would pull matter together to zero size. At small distances however quantum effects become important and therefore a quantum theory of gravity like string theory should be used to accurately describe black holes. String theory has already given us important insights into this ‘microscopic’ structure of black holes but this also remains an active area of ongoing research.

The gauge/gravity dualities

The research presented in this thesis concerns the so-called ‘gauge/gravity dualities’. These dualities propose a radically new picture of quantum gravity: they postulate that quantum theories of gravity may alternatively be described in terms of an ‘ordinary’ quantum field theory without gravity, but this quantum field theory is defined in one spacetime dimension *less* than the original gravitational theory. This is called the ‘holographic principle’ as it is just like a hologram which contains all the necessary information to reconstruct a three-dimensional image from

the data on a two-dimensional surface. The fact that a quantum field theory in d dimensions (for arbitrary d) can be used to completely describe quantum gravity in $d + 1$ dimensions is very counterintuitive and the implications of this idea are still not completely understood.

To obtain a concrete realization of such a gauge/gravity duality one needs to make the relation between the quantum field theory and the quantum theory of gravity more precise. This amounts to the development of a *dictionary* which translates quantities between the two theories. Using this dictionary we for example know how to describe objects like black holes in terms of the lower-dimensional quantum field theory. The dictionary can actually also be used the other way and this turns out to be quite practical as well, since it allows one to use relatively simple computations in general relativity to obtain so far notoriously difficult results in the quantum field theory.

So far the dictionary had been developed in great detail for equilibrium cases like for example the so-called eternal black holes, which are present in the spacetime for all times. For non-equilibrium situations, for example the holographic description of gravitational collapse of a star to a black hole, the dictionary was however not yet complete. In chapter 2 we give a detailed dictionary for these dynamical situations, which not only allows us to apply the duality to several new cases but also allows us to gain insights in the structure of the quantum theory of gravity. To test this new dictionary we worked out a number of relatively simple examples in chapter 3. According to our dictionary several quantities in the quantum field theory should be obtained by performing some very specific computations in the quantum gravity theory. We perform these computations in a number of concrete cases for which the quantum field theory answer is known and indeed find complete agreement with expectations. In chapter 4 we briefly describe the relation between our dictionary and another prescription from the literature which applies to certain special cases.

For certain spacetimes it is difficult to precisely understand the workings of the holographic principle since naively some information is hidden ‘too deeply’ in the spacetime. This is for example the case for so-called *wormholes* which are spacetimes that are roughly speaking comparable to black holes. If the gauge/gravity duality holds exactly then *all* the information about the spacetime should be stored in the quantum field theory, so in particular also the information which is deeply hidden. Using our new dictionary we can describe the details of the duality in detail for these wormhole spacetimes and verify its validity. This is the subject of chapter 5, where we demonstrate that at least for the wormhole spacetimes no information can possibly be hidden too deeply in the spacetime. In chapter 6 we give an alternative representation of the wormhole spacetimes which may be useful

for future research.

The success of holography in string theory has led to several attempts at a generalization of this approach. In particular one often tries to apply holography to theories of gravity in only two spatial dimensions (rather than the usual three dimensions). These theories are ‘toy models’ for the real world where computations simplify and therefore new insights might be gained more easily. One may for example apply the usual dictionary to such lower-dimensional theories to investigate whether this would result in a consistent quantum theory without reference to string theory. We apply this idea to a specific two-dimensional theory of gravity called *topologically massive gravity*, which is a slight variation of the usual general theory of relativity. The results we obtain for a possible dual quantum field theory are however inconsistent with the basic requirements for a ‘good’ quantum field theory. It therefore seems that topologically massive gravity is not a suitable toy model for quantum gravity and we would need a more complete theory like string theory to obtain consistent results.

Samenvatting

In dit hoofdstuk geven we een overzicht van de lijn van onderzoek waar dit proefschrift deel van uitmaakt. We beginnen met een kort overzicht van onze huidige kennis van de elementaire deeltjes, samengevat in een zogeheten kwantumveldentheorie die het *standaardmodel* genoemd wordt. Daarna bespreken we de onvolledigheid van het standaardmodel, in het bijzonder het ontbreken van een goede beschrijving van de zwaartekracht. Vervolgens leggen we uit hoe de snaartheorie een mogelijke completering van het standaardmodel kan geven die de zwaartekracht wel correct kan beschrijven. Daarna bespreken we de zogenaamde ‘gauge/gravity dualiteiten’, een onderwerp in de snaartheorie waarnaar momenteel veel onderzoek plaatsvindt. Aan het einde van dit hoofdstuk vatten we de resultaten van dit proefschrift samen en leggen we uit hoe die onze kennis over deze dualiteiten vergroten.

Het standaardmodel

In 1900 presenteerde Max Planck een formule voor de temperatuurafhankelijkheid van elektromagnetische straling. Het meest opmerkelijke aan de formule van Planck was het feit dat deze formule een geheel nieuwe constante bevatte, h , waarvan de waarde tegenwoordig bepaald is op $6,63 \cdot 10^{-34} Js$. Het bleek al snel dat h een nieuwe fundamentele natuurconstante was waaromheen een volledig nieuwe theorie ontwikkeld diende te worden om correct het gedrag van deeltjes op kleine afstanden te beschrijven, de zogeheten kwantummechanica. Met de kwantummechanica worden bijvoorbeeld de elektronenbanen in een atoom beschreven en kan het bijbehorende lijnspectrum van een atoom worden uitgerekend.

De kwantummechanica was echter niet de enige revolutie aan het begin van de twintigste eeuw. In 1905 stond een andere fundamentele natuurconstante, de lichtsnelheid c , centraal in een paper van Einstein. Volgens zijn speciale relativiteitstheorie bestaat er geen absolute manier om tijd of afstand te definiëren, maar hangen deze definities af van de snelheid waarmee men beweegt. De lichtsnel-

heid maakt het mogelijk om afstanden en tijden te combineren in één concept, de *ruimtetijd*.

De effecten van de speciale relativiteitstheorie worden pas merkbaar als deeltjes zich met snelheden dichtbij de lichtsnelheid bewegen. Deze effecten worden echter helemaal niet meegenomen in de kwantummechanica van Planck en zijn tijdgenoten, zodat die verkeerde voorspellingen geeft voor bijvoorbeeld elektronen die met ongeveer de lichtsnelheid bewegen. Het verbeteren van de kwantummechanica tot een ‘relativistische kwantummechanica’ bleek echter lastig. Het resulterende framework wordt de *kwantumveldentheorie* genoemd; de ontwikkelingen ervan vergde de inspanningen van meerdere generaties fysici en de theorie is nog altijd niet volledig doorgrond. De kwantumveldentheorie is echter voldoende begrepen om zeer precies de uitkomsten van bijvoorbeeld deeltjesversnellerexperimenten te beschrijven.

Een kwantumveldentheorie is een abstracte theorie die het kwantummechanische gedrag beschrijft van willekeurige deeltjes die met hoge snelheden bewegen. In de natuur zien we echter een heel concreet aantal *elementaire deeltjes* waar alle andere materie uit is opgebouwd. De specifieke kwantumveldentheorie voor deze elementaire deeltjes heet het *standaardmodel*. De deeltjes in het standaardmodel zijn zes typen *quarks*, zes typen *leptonen* en het *Higgs boson*. De quarks hebben elk een eigen naam: ze heten up, down, charm, strange, top en bottom. De leptonen zijn het elektron, het muon en het tau-deeltje alsmede drie verschillende neutrino-deeltjes. Het Higgs boson is nog niet geobserveerd maar is nodig voor de consistentie van het standaardmodel. Volgens het standaardmodel vormen deze deeltjes samen de bouwstenen van alle materie om ons heen: zo bestaat een proton bijvoorbeeld grofweg uit een samenstelling twee up quarks en één down quark.

In het standaardmodel zijn er bovendien drie verschillende krachten werkzaam op de elementaire deeltjes: de sterke kernkracht, de zwakke kernkracht en de meer bekende elektromagnetische kracht. Deze krachten worden gemodelleerd door zogenaamde *krachtendragende deeltjes*. Zo wordt de elektromagnetische kracht tussen bijvoorbeeld twee elektronen beschreven door de uitwisseling van *fotonen*. Het model in termen van krachtendragende deeltjes vervangt de bekende beschrijving door middel van bijvoorbeeld een elektromagnetisch veld en zo’n vervanging is noodzakelijk vanwege het kwantummechanische gedrag van de deeltjes op hele kleine afstanden. De deeltjes waarmee de sterke kernkracht gemodelleerd wordt heten *gluonen* en de zwakke kernkracht wordt gemodelleerd door de zogeheten *W- en Z-bosonen*. Er zijn acht gluonen, twee W-bosonen en één Z-boson.

Onvolledigheden

Na Planck (in 1918) zijn er meer dan 60 nobelprijzen uitgereikt voor bijdragen aan de ontwikkeling van eerst de kwantummechanica en later kwantumveldentheorie en het standaardmodel. Het is dan ook een model dat onze meest fundamentele kennis van de natuur representeert en daar mag men best trots op zijn. Tot grote opluchting van de huidige generatie theoretisch natuurkundigen is het standaardmodel echter ook *incompleet* en ligt er nog veel meer onontdekte fundamentele natuurkunde in het verschiet. Belangrijke experimentele aanwijzingen daarvoor zijn de schaal van elektrozwakke symmetriebreking en ook donkere materie, die in essentie wijzen op het bestaan van nieuwe, nog onontdekte elementaire deeltjes. Deze deeltjes kunnen wellicht in de toekomst gevonden worden, bijvoorbeeld in experimenten met deeltjesversnellers, en zullen dan moeten worden toegevoegd aan het standaardmodel. Het is dan plausibel dat we op die manier een meer complete kwantumveldentheorie verkrijgen die deze deeltjes incorporeert.

Een andere incompleetheid van het standaardmodel is het feit dat er nog een kracht bestaat, namelijk de zwaartekracht, die ook niet door het standaardmodel wordt beschreven. Zoals we nu zullen uitleggen is dit conceptueel een veel groter probleem.

Om te beginnen hebben we op zich al een accurate beschrijving van hoe de zwaartekracht werkt op grote afstanden, namelijk in termen van Einstein's klassieke algemene relativiteitstheorie. Deze theorie stelt dat de ruimtetijd uit de speciale relativiteitstheorie in werkelijkheid *gekromd* is en geeft daarmee een succesvolle beschrijving van allerlei astrofysische en kosmische fenomenen. Op hele kleine afstanden weten we echter niet hoe de zwaartekracht beschreven moet worden. Hoewel de *speciale* relativiteitstheorie en de kwantummechanica verenigd konden worden in de kwantumveldentheorie blijkt dat er niet zomaar een eenvoudige manier te bestaan om hetzelfde te doen voor de *algemene* relativiteitstheorie. Volgens de kwantumveldentheorie moet men namelijk het gravitationele veld vervangen door een krachtdragend deeltje (net als het elektromagnetische veld vervangen werd door het foton) dat in dit geval een *graviton* wordt genoemd. Als we echter gaan rekenen met een kwantumveldentheorie met een graviton dan vinden we allerlei mathematische problemen die laten zien dat dit geen fundamentele beschrijving van de natuur kan zijn. Door die problemen zijn kwantumveldentheorie en zwaartekracht fundamenteel onverenigbaar: in een wereld waarin kwantumveldentheorie exact geldig is kan er geen zwaartekracht zijn en vice versa. Toch leven wij in een wereld waarin wij zowel kwantumveldentheorie als algemene relativiteitstheorie succesvol gebruiken om experimenten te beschrijven en daarom is het noodzakelijk dat geen van beiden exact geldig zijn! De uitdaging is daarom om een correcte en mathematisch consistente *kwantumtheorie van de zwaartekracht* te

vinden. Vanwege de bovengenoemde problemen zal die voorbij moeten gaan aan de huidige kwantumveldentheorie.

Er zijn helaas bijzonder weinig experimentele resultaten beschikbaar die behulpzaam zouden kunnen zijn in het vinden van een dergelijke theorie. Het experimentele succes van het standaardmodel (dus van een kwantumveldentheorie zonder zwaartekracht) bijvoorbeeld toont aan dat het effect van de zwaartekracht op de resultaten van experimenten met deeltjesversnellers totaal verwaarloosbaar is. Dit is consistent met een simpele theoretische orde-van-grootte analyse: als we aannemen dat de algemene relativiteitstheorie geldig blijft tot op hele kleine afstanden kunnen we schatten dat de aantrekkende zwaartekracht tussen bijvoorbeeld twee elektronen een factor 10^{42} kleiner dan de afstotende elektrische kracht. Dat is inderdaad vele malen kleiner dan tot nu toe meetbaar: de elektrische kracht is bijvoorbeeld bekend met een relatieve precisie van ongeveer 10^{10} . (Deze orde-van-grootte analyse gebruikt echter de *klassieke* algemene relativiteitstheorie waarvan wij weten dat zij niet consistent is op kleine afstanden. De analyse is daarmee inherent onbetrouwbaar en in werkelijkheid is er momenteel geen consistente theoretische afschatting van de effecten van de zwaartekracht op kleine afstanden.)

Snaartheorie

Het idee van de snaartheorie is dat de elementaire deeltjes eigenlijk hele kleine uitgestrekte snaartjes zijn. Het gaat daarmee voorbij aan de kwantumveldentheorie, waarin de deeltjes altijd als puntdeeltjes beschreven worden. Bovendien maakt deze aanname het mogelijk om een consistente wisselwerking met gravitonen te beschrijven en daarmee lijkt de snaartheorie alle benodigde ingrediënten te bevatten voor een kwantumtheorie van de zwaartekracht. De snaartheorie is momenteel echter nog geen volledige theorie en het precies begrijpen wat de snaartheorie nu precies inhoudt is iets waar momenteel veel onderzoek naar gedaan wordt.

Hoewel de snaartheorie een consistente theorie van de kwantumzwaartekracht lijkt te zijn is het moeilijk gebleken om ook een *realistische* versie van een dergelijke theorie te verkrijgen. Afhankelijk van de precieze versie van de snaartheorie die men hanteert blijkt de snaartheorie namelijk vaak veel meer en ook heel andere deeltjes te voorspellen dan de hierboven genoemde deeltjes van het standaardmodel. Het is echter niet uitgesloten dat er een versie van de snaartheorie bestaat met een realistisch deeltjesspectrum en hier wordt momenteel dan ook hard naar gezocht.

Niettemin is de snaartheorie wel een theorie die ons diverse inzichten kan geven in hoe een kwantumtheorie van de zwaartekracht eruit ziet. Een mooi voorbeeld hiervan is de beschrijving van zwarte gaten in de snaartheorie. In de algemene relativiteitstheorie kunnen zwarte gaten niet goed beschreven worden omdat de

materie door de gravitationele aantrekkingskracht zo sterk wordt samengeperst dat de energiedichtheden oneindig zouden worden. Op zulke kleine schalen worden kwantumeffecten echter belangrijk en daarom zal een kwantumtheorie van de zwaartekracht zoals de snaartheorie gebruikt moeten worden. De snaartheorie heeft ons al diverse belangrijke inzichten gegeven in de ‘microscopische’ structuur van zwarte gaten, maar ook dit blijft nog een bron van veel onderzoek.

De gauge/gravity dualiteiten

In dit proefschrift worden de zogeheten ‘gauge/gravity dualiteiten’ binnen de snaartheorie bestudeerd. Deze dualiteiten stellen een volledig nieuw beeld van de kwantumzwaartekracht voor: zij postuleren dat er een alternatieve beschrijving bestaat van de kwantumtheorie van de zwaartekracht in termen van een ‘gewone’ kwantumveldentheorie zonder zwaartekracht, maar deze kwantumveldentheorie leeft dan wel in één ruimtetijd dimensie *minder* dan de oorspronkelijke zwaartekracht. Dit is het ‘holografisch principe’: net zoals een hologram alle informatie bevat om een drie-dimensionaal beeld te reconstrueren aan de hand van gegevens op een twee-dimensionaal vlak, zo kan een kwantumveldentheorie in d dimensies (voor willekeurige d) gebruikt worden om kwantumzwaartekracht te beschrijven in $d + 1$ dimensies. Dit is zeer tegenintuïtief en het is dan ook nog lang niet uitgekristalliseerd wat de implicaties van het holografisch principe voor de kwantumtheorie van de zwaartekracht precies zijn.

Om de dualiteiten concreet te maken moet nog wel de relatie tussen de kwantumveldentheorie en de kwantumtheorie van de zwaartekracht precies gemaakt worden. Zo’n dualiteit komt daarom met een zogeheten ‘dictionary’ dat grootheden tussen de twee theorieën vertaalt. Gebruik makend van dit dictionary weten we bijvoorbeeld in principe hoe we objecten als zwarte gaten moeten beschrijven in termen van de kwantumveldentheorie. Het dictionary kan echter ook de andere kant op gebruikt worden en dit is een interessante spinoff van de dualiteiten: door middel van relatief eenvoudige berekeningen in de algemene relativiteitstheorie (zoals we weten is dat op grote afstanden een voldoende goede benadering van de kwantumtheorie) blijken we vrij simpel resultaten te kunnen verkrijgen over de kwantumveldentheorie die tot dan toe allerlei onmogelijk ingewikkelde berekeningen vereisten.

Het dictionary was tot op heden in groot detail ontwikkeld voor de gevallen waarin sprake is van een evenwichtssituatie. Een voorbeeld van zo’n situatie is bijvoorbeeld een zogeheten eeuwig zwart gat dat zich voor altijd in de ruimtetijd bevindt. Voor niet-evenwichtssituaties, bijvoorbeeld de holografische beschrijving van de ineenstorting van een ster die leidt tot de vorming van een zwart gat, was het dictionary echter nog niet volledig ontwikkeld. In hoofdstuk 2 geven we een gede-

tailleerd dictionary voor dit soort dynamische situaties. Dit stelt ons in staat om de dualiteit toe te passen in nieuwe situaties maar levert ons ook interessante inzichten op in de structuur van de theorie van de kwantumzwaartekracht. Om ons nieuwe dictionary te testen hebben we een aantal relatief eenvoudige voorbeelden uitgewerkt in hoofdstuk 3. Volgens ons dictionary moeten bepaalde grootheden in de kwantumveldentheorie gegeven worden door de uitkomst van heel specifieke berekeningen in de kwantumtheorie van de zwaartekracht. We doen deze berekeningen voor een aantal gevallen waarvan we de uitkomst in de kwantumveldentheorie al weten en vinden inderdaad dat ons dictionary de verwachte antwoorden geeft. In hoofdstuk 4 beschrijven we kort hoe een andere prescriptie uit de literatuur, geldig voor een subklasse van deze gevallen, ook volgt uit de toepassing van ons algemene dictionary.

Voor sommige ruimtetijden is het lastig om te zien hoe het holografisch principe precies werkt omdat informatie ‘te diep’ in de ruimtetijd verstopt lijkt te zitten. Dit lijkt bijvoorbeeld het geval te zijn bij *wormgaten*, ruimtetijden die vergelijkbaar zijn met zwarte gaten. Als de dualiteit exact geldig zou zijn dan zou echter *alle* informatie over de ruimtetijd in de kwantumveldentheorie opgeslagen moeten worden, ook de erg diep verstopte informatie. Met ons nieuwe dictionary kunnen we ook de werking van de dualiteit voor wormgaten in detail beschrijven en controleren of die nog steeds geldig is. Dit doen we in hoofdstuk 5 en het blijkt inderdaad dat in ieder geval voor deze klasse van ruimtetijden informatie nooit te diep verstopt kan zitten. Hoofdstuk 6 geeft een alternatieve beschrijving van de wormgaten die nuttig kan zijn voor verder onderzoek.

Door het succes van de holografische benadering van de snaartheorie heeft men geprobeerd dit concept te veralgemeniseren. In het bijzonder wordt de holografische benadering vaak toegepast op theorieën van de zwaartekracht in slechts twee ruimtelijke dimensies (in plaats van de gebruikelijke drie). Dit is een ‘toy model’ waarin we de kwantumeffecten van de zwaartekracht makkelijker kunnen bestuderen omdat veel berekeningen vereenvoudigen. Hierdoor het makkelijker wordt om nieuwe inzichten te verkrijgen. Men kan bijvoorbeeld het gebruikelijke ‘dictionary’ toepassen op zulke lager-dimensionale theorieën om te zien of men wellicht op die manier een consistente kwantumtheorie kan formuleren zonder gebruik te maken van de snaartheorie. In hoofdstuk 7 passen we dit idee toe in een bepaalde tweedimensionale theorie van de zwaartekracht, *topologically massive gravity*, die een variatie is op de gebruikelijke algemene relativiteitstheorie. De resultaten die we zo verkrijgen voor de duale kwantumveldentheorie (in één ruimtelijke dimensie) voldoen echter niet aan de basisvereisten voor een goede kwantumveldentheorie en daarmee bewijzen we dat dit model eigenlijk ongeschikt is als toy model. Het lijkt erop dat een meer complete theorie zoals de snaartheorie nodig is om consistente resultaten op te leveren.

Acknowledgements

First and foremost it is a great pleasure to thank my advisor Kostas Skenderis. I am very happy with the opportunity you gave me to further develop myself as a Ph.D. student. You guided me in many ways and in particular towards a number of interesting projects where we were able to obtain solid results. I am especially grateful for the fact that you were virtually always available, not only for scientific discussions but also for example during the postdoc application process. In the same spirit I would also very much like to thank Marika Taylor for her guidance during our collaboration in the second half of my Ph.D.

I would also like to acknowledge all the other members of the ITFA for their company and for all the numerous scientific and non-scientific conversations we had together. Special thanks to Erik Verlinde for being my promotor and for Robbert Dijkgraaf for financially supporting my research. I would like to thank Yocklang and Bianca who provided ample support and always friendly company. Furthermore I would like to acknowledge my fellow volunteers of the ITF/WZI social clubs for the nice time we had while organizing a nice time for others.

My office mates Liza, Sheer and Marco were often the first available people to whom I could enthusiastically ventilate my newly acquired insights, both right and wrong. I am glad to have always found a listening ear and thoroughly enjoyed the discussions with all of you.

Away from work I am grateful for having enjoyed the company of many people. First of all let me thank jaarclub Scalpel for the many borrels, dinners and week-ends in Friesland we spent together. Similarly I would like to acknowledge my other friends from Delft, especially those who joined me on trips to Stavanger or to Cornwall. I thoroughly enjoyed an occasional concert performance made possible by Ingmar. I also happily remember the time spent in De Roeter, Kriterion or Brouwerij 't IJ with all the new friends I made in Amsterdam and I would like to thank all of you for your company. In the final years of my Ph.D. I very much enjoyed the dinners and barbecues at Alexanderplein or in the parks with so many

people but especially with Alessia, Fendy, Richard, Yenny, Marco, and, sometimes at least, a few shooting stars.

Out of all these events I am especially happy to have attended a specific dinner in Utrecht in the fall of 2009, which among many other things led me to visit a small, picturesque restaurant in the polders of the Waal. I was fortunate enough that the one person accompanying me there was willing to see me a few more times afterwards. Josien, thank you for simply everything.

Finally I would like to thank my four big brothers and my parents for their constant and unconditional support. I greatly appreciate the fact that my parents are always available, be it for sharing my good and bad experiences, for advice about the larger and the smaller things in life or simply for enjoying a coffee in Warmond. The stability they provide in this way continues to influence my life in a very positive manner and in a way this is the main foundation of this thesis. For this reason I would like to deeply thank my parents, again but never enough.